STRUCTURE AND BONDING 127

Series Editor D. M. P. Mingos
Volume Editor T. E. Albrecht-Schmitt

Organometallic and Coordination Chemistry of the Actinides

Springer

127
Structure and Bonding

Series Editor: D. M. P. Mingos

Structure and Bonding
Series Editor: D. M. P. Mingos

Recently Published and Forthcoming Volumes

Contemporary Metal Boron Chemistry I
Volume Editors: Marder, T. B., Lin, Z.
Vol. 130, 2008

Recognition of Anions
Volume Editor: Vilar, R.
Vol. 129, 2008

Liquid Crystalline Functional Assemblies and Their Supramolecular Structures
Volume Editor: Kato, T.
Vol. 128, 2008

Organometallic and Coordination Chemistry of the Actinides
Volume Editor: Albrecht-Schmitt, T. E.
Vol. 127, 2008

Halogen Bonding
Fundamentals and Applications
Volume Editors: Metrangolo, P., Resnati, G.
Vol. 126, 2008

High Energy Density Materials
Volume Editor: Klapötke, T. H.
Vol. 125, 2007

Ferro- and Antiferroelectricity
Volume Editors: Dalal, N. S., Bussmann-Holder, A.
Vol. 124, 2007

Photofunctional Transition Metal Complexes
Volume Editor: V. W. W. Yam
Vol. 123, 2007

Single-Molecule Magnets and Related Phenomena
Volume Editor: Winpenny, R.
Vol. 122, 2006

Non-Covalent Multi-Porphyrin Assemblies
Synthesis and Properties
Volume Editor: Alessio, E.
Vol. 121, 2006

Recent Developments in Mercury Science
Volume Editor: Atwood, David A.
Vol. 120, 2006

Layered Double Hydroxides
Volume Editors: Duan, X., Evans, D. G.
Vol. 119, 2005

Semiconductor Nanocrystals and Silicate Nanoparticles
Volume Editors: Peng, X., Mingos, D. M. P.
Vol. 118, 2005

Magnetic Functions Beyond the Spin-Hamiltonian
Volume Editor: Mingos, D. M. P.
Vol. 117, 2005

Intermolecular Forces and Clusters II
Volume Editor: Wales, D. J.
Vol. 116, 2005

Intermolecular Forces and Clusters I
Volume Editor: Wales, D. J.
Vol. 115, 2005

Superconductivity in Complex Systems
Volume Editors: Müller, K. A., Bussmann-Holder, A.
Vol. 114, 2005

Principles and Applications of Density Functional Theory in Inorganic Chemistry II
Volume Editors:
Kaltsoyannis, N., McGrady, J. E.
Vol. 113, 2004

Organometallic and Coordination Chemistry of the Actinides

Volume Editor: Thomas E. Albrecht-Schmitt

With contributions by

S. C. Bart · F. G. N. Cloke · M. S. Eisen · K. Meyer
M. Sharma · O. T. Summerscales

Springer

The series *Structure and Bonding* publishes critical reviews on topics of research concerned with chemical structure and bonding. The scope of the series spans the entire Periodic Table. It focuses attention on new and developing areas of modern structural and theoretical chemistry such as nanostructures, molecular electronics, designed molecular solids, surfaces, metal clusters and supramolecular structures. Physical and spectroscopic techniques used to determine, examine and model structures fall within the purview of Structure and Bonding to the extent that the focus is on the scientific results obtained and not on specialist information concerning the techniques themselves. Issues associated with the development of bonding models and generalizations that illuminate the reactivity pathways and rates of chemical processes are also relevant.
As a rule, contributions are specially commissioned. The editors and publishers will, however, always be pleased to receive suggestions and supplementary information. Papers are accepted for *Structure and Bonding* in English.
In references *Structure and Bonding* is abbeviated *Struct Bond* and is cited as a journal.

Springer WWW home page: springer.com
Visit the Struct Bond content at springerlink.com

ISBN 978-3-540-77836-3 ISBN 978-3-540-77837-0 (eBook)
DOI 10.1007/978-3-540-77837-0

Structure and Bonding ISSN 0081-5993

Library of Congress Control Number: 2008921238

Cover design: WMXDesign GmbH, Heidelberg
Typesetting and Production: le-tex publishing services oHG, Leipzig

Printed on acid-free paper

9 8 7 6 5 4 3 2 1 0

springer.com

Series Editor

Prof. D. Michael P. Mingos

Principal
St. Edmund Hall
Oxford OX1 4AR, UK
michael.mingos@st-edmund-hall.oxford.ac.uk

Volume Editor

Prof. Dr. Thomas E. Albrecht-Schmitt

University of Auburn
Department Chemistry
Auburn, AL 36849, USA
albreth@auburn.edu

Editorial Board

Structure and Bonding
Also Available Electronically

For all customers who have a standing order to Structure and Bonding, we offer the electronic version via SpringerLink free of charge. Please contact your librarian who can receive a password or free access to the full articles by registering at:

springerlink.com

If you do not have a subscription, you can still view the tables of contents of the volumes and the abstract of each article by going to the SpringerLink Homepage, clicking on "Browse by Online Libraries", then "Chemical Sciences", and finally choose Structure and Bonding.

You will find information about the

- Editorial Board
- Aims and Scope
- Instructions for Authors
- Sample Contribution

at springer.com using the search function.

Color figures are published in full color within the electronic version on SpringerLink.

Preface

This volume reviews recent developments in the fields of organometallic and coordination chemistry of the actinides, and in particular uranium. Actinide chemistry in general has recently been rejuvenated with demonstrations of unprecedented structures, reactivity, and physical properties. While organouranium chemistry can be traced back to the Manhattan Project, most of these efforts were unsuccessful. However, by the mid-1950s the first uranium cyclopentadienyl (Cp) complexes were being reported, e.g. tricyclopentadienyl uranium(IV) chloride, $(C_5H_5)_3UCl$. The late 1960s heralded the synthesis and structural elucidation of "uranocene," bis(cyclooctatetraenyl)uranium(IV), $U(C_8H_8)_2$, an expanded-ring sandwich compound that provided tantalizing evidence that 5f orbitals might be involved in bonding. One of the chapters in this volume details the expansion of this kind of work to include mixed sandwich U(III) cyclooctatetraene and pentalene complexes. As discussed by several of the authors, the availability of easily prepared mid-valent starting materials has been one of the primary factors involved in reinvigorating this field. Of particular interest to many readers will be the binding of small molecules by both organometallic and coordination compounds of uranium. Some of the holy grails of this chemistry include the activation of dinitrogen, carbon monoxide, and carbon dioxide. Various aspects of this work can be found in all three chapters, but are detailed in particular by O.T. Summerscales and F.G.N. Cloke.

The origins of coordination compounds of uranium are difficult to define precisely because the definition of what constitutes a coordination compound versus a purely inorganic compound can be difficult to differentiate. However, the coordination chemistry of uranium is very old, dating back to at least the early 1800s. There is tremendous diversity in the type of ligands that have been found to form stable complexes with uranium. Recent work has focused on highly tailored ligand sets to yield specific physico-chemical responses. This work has included the development of uranium complexes that specifically bind small molecules such as carbon dioxide. In addition, heterometallic 3d-5f systems are now being developed to explore magnetic interactions. It is important not to overlook early pioneering efforts by T.J. Marks and co-workers, who among other key discoveries found that uranyl cations can template the formation of superphthalocyanines. S.C. Bart and K. Meyer's chapter details

more recent advances in the coordination chemistry of uranium in mid- to high oxidation states.

One of the most exciting and active areas of actinide research involves the development of novel catalysts. Thorium and uranium metallocene complexes have been shown to react in highly specific manners that in some cases parallel those of early transition metals, and in others the reactions are unique to the actinides. M. Sharma and M.S. Eisen's chapter details metallocene organoactinide chemistry with a special focus on novel reaction pathways that have in some cases been deduced from thermochemical studies.

In summary, the publication of this volume is a strong indicator of the substantial activity currently taking place in the organometallic and coordination chemistries of the actinides. The future promises to hold many more surprises.

Auburn, December 2007 Thomas E. Albrecht-Schmitt

Contents

Struct Bond (2008) 127: 1–85
DOI 10.1007/430_2008_082

Published online: 10 April 2008

Metallocene Organoactinide Complexes

Manab Sharma · Moris S. Eisen (✉)

Schulich Faculty of Chemistry, Institute of Catalysis Science and Technology, Technion – Israel Institute of Technology, Technion City, 32000 Haifa, Israel
chmoris@tx.technion.ac.il

Abstract During the last decade, the chemistry of d^0/f^n actinides has flourished reaching a high level of sophistication. Compared to the early or late transition-metal complexes and lanthanides, the actinides sometimes exhibit parallel but mostly complementary activities for similar organic processes, and sometimes even challenge the activities of the transition metals. A rapid increase in the numbers of reports in the Cambridge database also reflects their current importance. In view of the above, in this particular review we have provided an overview and updated information about the preparation and properties of the major classes of actinide complexes containing different cyclopentadienyl ligands and having the oxidation states (+3 and +4).

Keywords Metallocene complexes · Organoactinides · Sterically induced reduction (SIR)

Abbreviations

Cp	Cyclopentadienyl, η^5-C_5H_5
Cp′	η^5-$C(CH_3)_3C_5H_4$
$Cp^{\neq}$	η^5-$(CH_3)C_5H_4$
Cp^{ϕ}	η^5-$\{Si(CH_3)_3\}C_5H_4$
Cp″	η^5-1,3-$\{Si(CH_3)_3\}_2C_5H_3$
$Cp^{\#}$	η^5-1,3-$\{C(CH_3)_3\}_2C_5H_3$
Cp^*	η^5-$(CH_3)_5C_5$
Cp‴	$(CH_3)_4C_5$
COT	η-C_8H_8

THF	Tetrahydrofuran
DMSO	Dimethylsulfoxide
tmeda	$Me_2NCH_2CH_2NMe_2$
pmdeta	$(Me_2NCH_2CH_2)_2NMe$
HMPA	$OP(NMe_2)_3$
dddt	5,6-Dihydro-1,4-dithiin-2,3-dithiolate
bipy	2,2′-Bipyridine
terpy	2,2′:6′,2″-Terpyridine
py	Pyridine

1 Introduction

Organometallic chemistry has attracted much attention in recent years because of the structural novelty, reactivity, and catalytic applications. This interesting area of chemistry is building a bridge between organic and inorganic chemistry that involves a direct metal-to-carbon bond formation. With the advances of analytical techniques, researchers are able to investigate the chemistry to a much deeper level and, therefore, this subject is in the limelight of coordination chemistry. Since the preparation of ferrocene, the first metallic complex containing a π-bonding ligand, $(\eta^5\text{-}C_5H_5)_2Fe$ [1], organometallic chemistry has traveled a long way from the early transition metals to the chemistry of electrophilic d^0/f^n actinides complexes. In fact, the first well-characterized organoactinide complex, Cp_3UCl, was synthesized by Reynolds and Wilkinson [2] shortly after the synthesis of ferrocene. Actinides are relatively large in size, which facilitates high coordination numbers. The availability of 5*f* valance orbitals make them chemically and coordinatively different from the *d*-block elements. The interests of researchers have been stimulated by the effective employment of the 5*f* and 6*d* orbitals in chemical bonding. Again, in comparison to the lanthanides, actinides are much more prone to complex formation as the 5*f* orbitals have a greater spatial extension relative to the 7*s* and 7*p* orbitals than the 4*f* orbitals have relative to the 6*s* and 6*p* [3]. Unlike the early or late transition-metal complexes and lanthanides, the actinides exhibit parallel but mostly different reactivities for similar organic processes, sometimes challenging the activities of transition metals and shedding light on their unique reactivities. Most developments in the non-aqueous chemistry of the actinides have involved the use of thorium and uranium, both due to their lower specific activity, and to the apparent chemical similarity to group IV metals in organometallic transformations. At present, among these, the coordination chemistry of uranium is drawing extra attention, which is evident from the statistical data of crystal structures in the Cambridge structural database. The compounds of uranium and thorium that have been crystallographically characterized during 2003 to 2007

are almost 1.3 times more than those reported during the previous 5 years (Fig. 1), whereas all the molecular complexes of the 3*d* transition metals and *f* elements increased by a factor of around 1.5 times [4]:

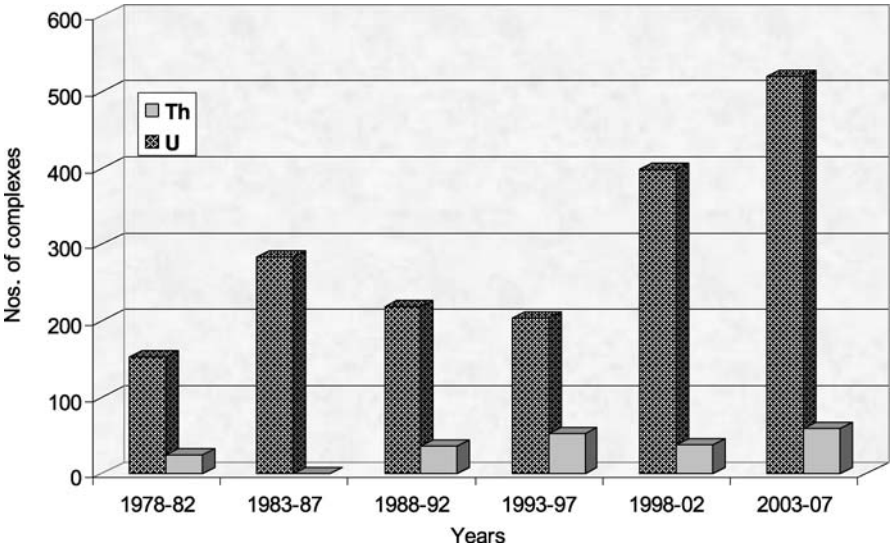

Fig. 1 Number of thorium and uranium complexes crystallographically characterized from 1978 to 2007

The electronic states of the actinides are also interesting as the energies of the 5*f*, 6*d*, 7*s* and 7*p* orbitals are very close to each other over a range of atomic number (especially U to Am) [3, 5] and might be responsible for a broad spectrum of oxidation states. Uranium has further demonstrated the ability to access a wide range of oxidation states (III to VI) in organic solvents, providing for greater flexibility in affecting chemical transformations.

During the 1960s, the main technological interest in organoactinide chemistry lay in its potential for application in isotope separation processes [5], but at present the advancement of sophistication has put impetus on the interest of actinide chemistry towards the stoichiometric and catalytic transformations, particularly in comparison to *d*-transition metal analogs. In many instances the regio- and chemo-selectivities displayed by organoactinides are complementary to those observed for other transition-metal complexes. The reactivity of organoactinide complexes lies in their ability to perform bond-breaking and bond-forming reactions of distinct functional groups. Steric and electronic factors play key roles in such processes. While discussing the steric effect, Xing-Fu suggested that the stability of a complex is governed by the sum of the ligand cone angles [6–8]. According to this model, highly coordinative "oversaturated" complexes will display low stability. An additional model for steric environments has been proposed by Pires de Matos [9]. This

model assumes pure ionic bonding, and is based on cone angles defining the term "steric coordination number".

A more important and unique approach to the reactivity of organo-5*f*-complexes regards the utilization of thermochemical studies. The knowledge of the metal–ligand bond enthalpies is of fundamental importance for the estimation of new reaction pathways [10–17]. In addition, neutral organoactinides have been shown to follow activation via a four-center transition state (Eq. 1) due to the high-energy orbital impediment to undergo oxidative addition and reductive elimination. Such a transition state allows the predictions of new actinide reactivities, when taking into account the negative entropies of activation [18]:

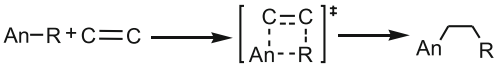

(1)

Several general review articles [19–41] dealing mostly with the synthesis of new actinide complexes confirm the broad and rapidly expanding scope of this field. Those reviews dealt with the structure, stability, and reactivates of complexes with cyclopentadienyl, dienyls (pentadienyl, cyclohexadienyl, indenyl, phospholyl), cyclooctatetraenyl, arene ligands, hydrocarbyls, and hydrides ligands.

In this particular review we will provide an overview of the preparation and properties of the major classes of actinide complexes containing different cyclopentadienyl ligands. Discussions are classified on the basis of formal oxidation states and we are confining our discussions only to the oxidation states III and IV.

2
Synthesis and Reactivity of Actinide Complexes

The rapid growth of the organoactinide chemistry is intimately coupled with the use of the π-coordinating cyclopentadienyl (Cp) or modified Cp ligands. Since the first report of the complex $(Cp)_3UCl$ by Wilkinson [2], followed by Fischer's report of cyclopentadienyl compound of U and Th [42], a plethora of Cp actinide complexes have been synthesized. The most interesting part of this chemistry is that it is possible to coordinate one, two, three, or four Cp ligands in an η^5-coordination mode [43–48] and that it has the ability to stabilize a wide variety of oxidation states and coordination environments [3].

2.1
Trivalent Actinide Cp Complexes

Among the bis-, tris- or tetrakis-Cp complexes, a overwhelming number of homoleptic tris-Cp (or modified Cp) complexes of the type $(\eta^5\text{-}C_5H_5)_3An$

(An = actinide) has been reported. During the period of 1960s to 1970s a spurt of activity concerning the primary investigation of trivalent organoactinides was observed, after that there was a dormant period till 1987 when Cramer, Gilje, and coworkers uncovered a rich chemistry in the reactions of Cp_3UCl with lithiated phosphoylides and related molecules [49, 50]. The reaction of $UC1_3$, with Cp-, or the reduction of Cp_3UX in the presence of neutral Lewis bases (L), was shown to produce a variety of U(III) complexes Cp_3UL [50, 51]. Later, it has been reported that these ligands support most members of the actinide series from thorium to californium to form complexes of the type $(\eta^5\text{-}C_5H_5)_3An$ (An = actinide). These complexes exhibit a wide variety of novel structures and reactivities, including uranium–carbon multiple bonding.

A number of synthetic routes have been reported to generate these species and their tetrahydrofuran (THF) adducts, including direct metathesis with alkali metal salts [50, 52–55], or transmetallation with $Be(\eta^5\text{-}C_5H_5)_2$ or $Mg(\eta^5\text{-}C_5H_5)_2$ [56–62]. In addition, the trivalent compounds may be obtained from chemical [53] or photochemical [63, 64] reduction of suitable tetravalent actinide precursors [51, 65–67]. Examples of these preparations are given in Eqs. 2–5:

$$2AnCl_3 + 3M(C_5H_5)_2 \longrightarrow (\eta^5\text{-}C_5H_5)_3An + 3MCl_2$$

An = Pu, Am, Cm, Bk, Cf; M = Be
An = Pu; M = Mg (2)

$$(\eta^5\text{-}C_5H_5)_3UCH(CH_3)_2 \xrightarrow{h\upsilon,\ C_6H_6} (\eta^5\text{-}C_5H_5)_3U\text{-}H + CH_2{=}CHCH_3$$

$$\downarrow + (\eta^5\text{-}C_5H_5)_3UCH(CH_3)_2$$

$$(\eta^5\text{-}C_5H_5)_3U + CH_3CH_2CH_3 \quad (3)$$

$$Cs_2PuCl_6 + Mg(C_5H_5)_2 \xrightarrow{THF} (Cp)_3Pu + \text{by products} \quad (4)$$

$$UCl_3{\cdot}nTHF + 3Na(C_5H_5) \xrightarrow{THF} (Cp)_3U(THF) + 3NaCl$$

$Cp = \eta^5\text{-}C_5H_5$ (5)

Le Marechal and coworkers [68] showed a new method for the preparation of $Cp_3U(THF)$ by the treatment of Cp_3UCl with sodium amalgam, Na/Hg, in the presence of 18-crown-6-ether and NaH (Eq. 6):

$$(Cp)_3UCl + Na/Hg \xrightarrow[18\text{-crown-6-ether}]{THF} (Cp)_3U(THF)$$

$Cp = \eta^5\text{-}C_5H_5$ (6)

Table 1 NMR data of actinide complexes

Compound	Chemical shifts in C_6D_6 (ppm)	Refs.
$(MeC_5H_4)_3U{\cdot}THF$	–11.62 (6H), –13.99 (4H), –14.39 (6H), –15.61 (9H), –31.06 (4H)	[72]
$(MeSiC_5H_4)_3U$	–19.2 (2H), –18.7 (9H), 9.2 (2H)	[72]
$(Me_3CC_5H_4)_3U$	–21.0 (9H), –24.2 (2H), 9.04 (2H)	[73]
$[1,3\text{-}(Me_3Si)_2(C_5H_3)]_3U$	20.8 (s, 1H, CH–Cp′), –4.8 (s, 2H, CH–Cp′), –9.3 (s, 18H, $SiMe_3$–Cp′)	[75]
$[(C_5Me_4H)_3U]$	7.4, –35.5 (s, 6H each, CH_3–Cp′), –5.0 (s, 1H, CH–Cp′)	[74]
$(Me_5C_5)_3U$	–0.93	[85]

They also reported the successful synthesis of $[Cp_3UCl][Na(18\text{-crown-6})]$, and $[(Cp_3U)_2(\mu\text{-}H)][Na(THF)_2]$ (Cp = η^5-C_5H_5) by following the same procedure.

The solubility of the parent tris(cyclopentadienyl)actinide, Cp_3An, complexes is limited in non-polar media, presumably due to oligomerization through bridging cyclopentadienyl ligands. Therefore, the synthesis of the most soluble iodine starting material, AnI_3L_4 (An = U, Np, Pu; L = THF, pyridine, DMSO) [69], perhaps can be considered as the major useful development of the actinide coordination chemistry. These species, generated from actinide metals and halide sources in coordinating solvents, are readily soluble in organic solvents, and serve as convenient precursors to a variety of trivalent actinide species [70]. Later, the hurdle of solubility was attended by a number of researchers by synthesizing a variety of substituted-tris-Cp ligand complexes (Table 1). A wide spectrum of synthetic routes have been proposed for these precursors [71–75] (Eqs. 7–11):

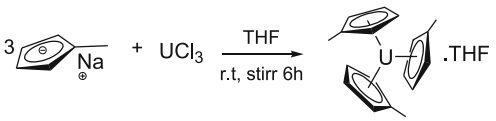

(7)

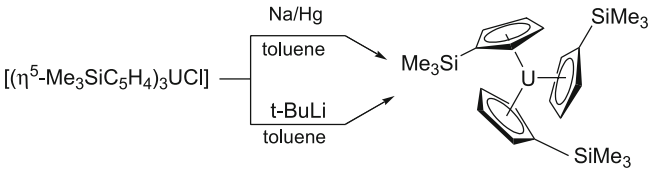

(8)

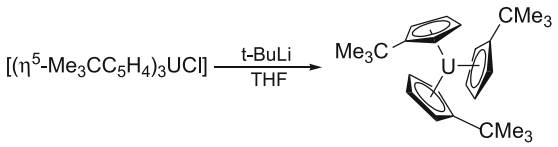

(9)

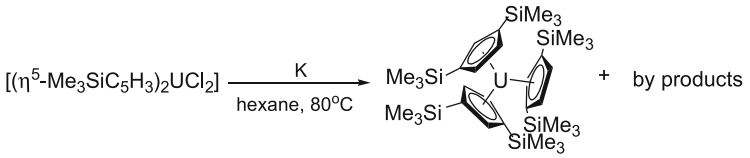

(10)

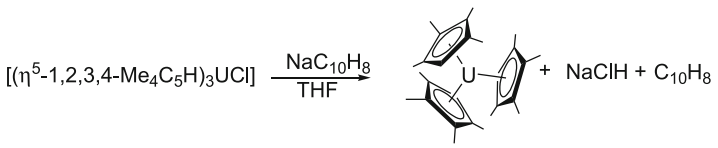

(11)

Until 1999 the only reported single crystalline compound of thorium(III)-Cp was $[ThCp''_3]\{Cp'' = \eta^5\text{-}C_5H_3(SiMe_3)_2\text{-}1,3\}$. In 1986, Blake and co-worker [76] reported the synthesis of dark blue crystalline complex $[ThCp''_3]$

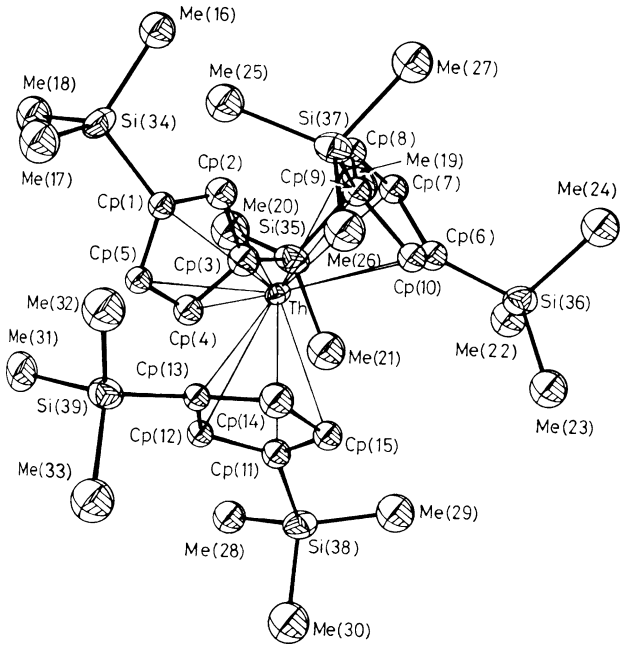

Fig. 2 Crystal structure of $[\eta^5\text{-}(Me_3Si)_2C_5H_3]_3Th$ [76]. Reproduced with permission from the Royal Society of Chemistry

(Fig. 2) by the reduction of $[Cp''_2ThCl_2]$ in toluene with sodium–potassium alloy along with metallic Th as the byproduct. Later a preferred route was reported [77] (Scheme 1) for the synthesis of this complex by using $[Cp_3ThCl]$ as the precursor, which could control the production of Th byproducts.

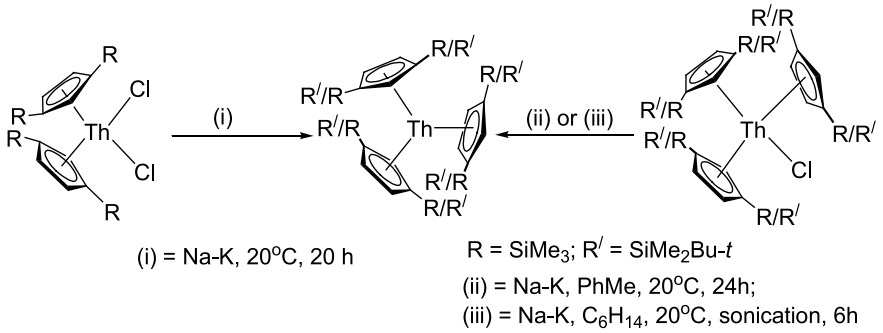

Scheme 1 Synthetic routes of $[Th\{C_5H_4(R/R')\}_3]$; R = $SiMe_3$; R' = $SiMe_2Bu$-*t* [76, 77]

Most of the base-free tris(cyclopentadienyl)thorium complexes crystallize in a pseudotrigonal planar structure, with averaged (ligand centroid)–Th–(ligand centroid) angles near 120°, and average Th–C_{ring} distances of 2.80(2) Å. One of the most investigated aspects of actinide–cyclopentadienyl chemistry is the nature of the bonding between the metal and the ligands [78]. Experimental studies of tris(cyclopentadienyl)actinide complexes, including ^{237}Np Mössbauer studies of $(\eta^5\text{-}C_5H_5)_3Np$ [51] and infrared and absorption spectroscopic studies of plutonium, americium, and curium analogs [57, 79, 80] suggest that the bonding is somewhat more covalent than that of lanthanide analogs, but the interaction between the metal and the cyclopentadienyl ring is still principally ionic. Theoretical treatments have suggested that the 6*d* orbitals are chiefly involved in interactions with ligand-based orbitals. While the 5*f* orbital energy drops across the series, creating an energy match with ligand-based orbitals, spatial overlap is poor, precluding strong metal–ligand bonding [44]. Thorium lies early in the actinide series and the relatively high energy of the 5*f* orbitals (before the increasing effective nuclear charge across the series drops the energy of these orbitals) has lead to speculation that a Th(III) compound could in fact demonstrate a $6d^1$ ground state. In support of this, Kot and coworkers [81] have reported the observation of an EPR spectrum with *g* values close to 2 at room temperature.

Although in actinide and lanthanide chemistry the use of permethylated cyclopentadienyl $(C_5Me_5^-)$ species as ligand is quite common, for a decade it was thought that the molecules of formula $[M(C_5Me_5)_3]$ will be sterically too crowded to exist as the cone angle of $(C_5Me_5^-)$ was thought to be more larger than the 120° necessary for $[M(C_5Me_5)_3]$ complexes [82–84]. However, the synthesis of $[U(C_5Me_5)_3]$ by Evans et al. [85] opened the door to a new era

of cyclopentadienyl-actinide chemistry. The complex $(\eta^5\text{-}C_5Me_5)_3U$ was prepared by the reaction of a trivalent hydride complex with tetramethylfulvene (Scheme 2) and, in fact, a direct metathesis route has not yet proven successful. The discovery of two or three electron reductivity of this complex had stimulated researchers to develop better synthetic routes.

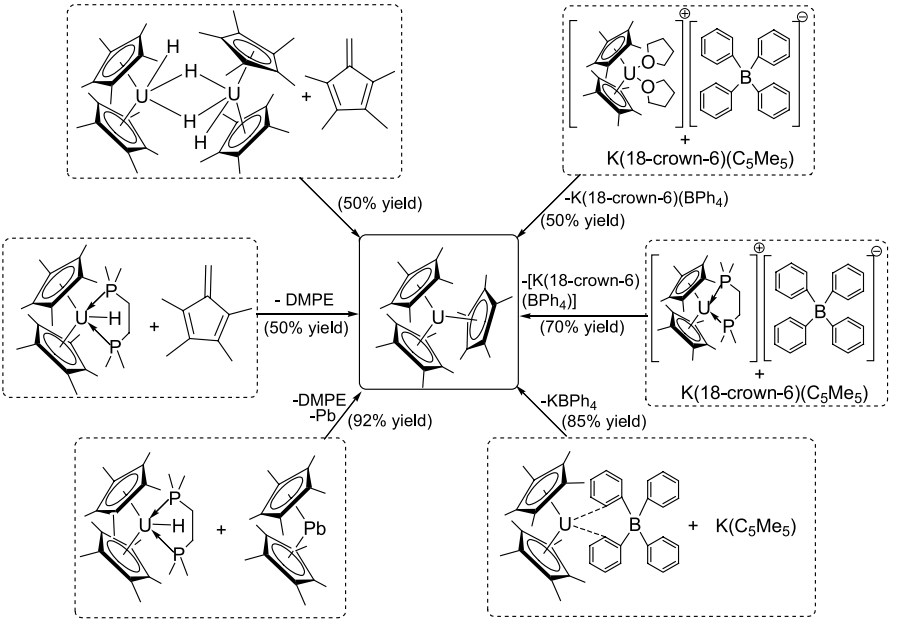

Scheme 2 Multiple synthetic routes of $[(Me_5C_5)_3U]$ [85, 86]

Evans [86] and coworker have developed a modified pathway for the synthesis of Cp^*_3U with improved yield up to 92% (Scheme 3). The molecular structure of the complex is shown in Fig. 3. The average $U\text{–}C_{ring}$ bond distance in this compound (2.858(3) Å) is much larger than in other crystallographically characterized U(III) pentamethylcyclopentadienyl complexes (ca. 2.77 Å), suggesting a significant degree of steric crowding.

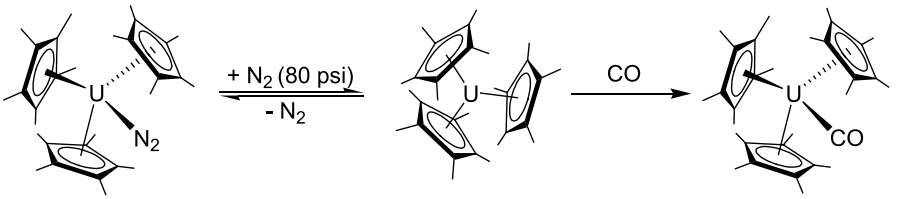

Scheme 3 Sterically crowded U(III) complexes [95, 96]

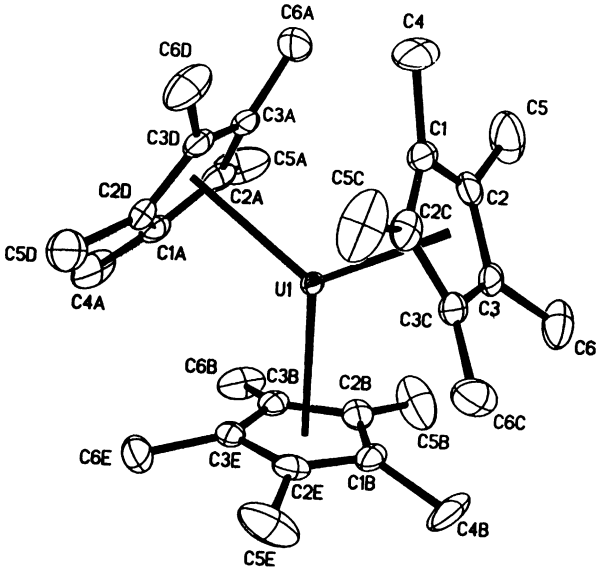

Fig. 3 Crystal structure of $(\eta^5\text{-}C_5Me_5)_3U$ [85]. Reproduced with permission

2.2
Sterically Induced Reduction

The synthesis of $Cp^*{}_3U\{Cp^* = \eta^5\text{-}C_5Me_5\}$ carved a new path for the researchers to go one step ahead in the electrochemical studies of organoactinide complexes. The reduction reaction involving more than two electrons are not common for metal complexes containing just one metal. However, the synthesis of complexes of the type $Cp^*{}_3M$ led to the development of "sterically induced reduction" (SIR) chemistry in which sterically crowded complexes of redox inactive metals act as reductants [87, 88]. Evans et al. showed that the sterically induced reduction couple, U(III)/U(IV), can act as a multielectron reductant [89]. As an example, $Cp^*{}_3U$ reacts as a three-electron reductant with 1,3,5,7-C_8H_8, (Eq. 12) in which one electron arises from U(III) (Eq. 13) and two result from two $C_5Me_5^-/C_5Me_5$ half reactions (Eq. 14) presumably via SIR. This phenomenon was further corroborated by the stepwise reduction of phenyl halide with $Cp^*{}_3U$ (Eq. 15):

$$2(C_5Me_5)_3U + 3\,C_8H_8 \xrightarrow[-2(C_5Me_5)_2]{} [(C_5Me_5)(C_8H_8)U]_2(\mu\text{-}C_8H_8) \tag{12}$$

$$U^{3+} \longrightarrow U^{4+} + e^- \tag{13}$$

$$(C_5Me_5)^- \longrightarrow {}^1/_2(C_5Me_5)_2 + e^- \tag{14}$$

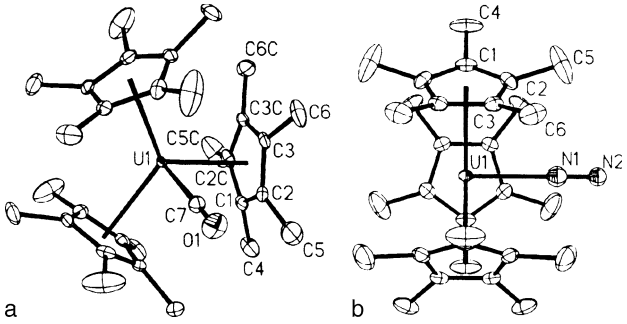

Fig. 4 Crystal structure of **a** $(\eta^5\text{-}C_5Me_5)_3U(CO)$ [95] and **b** $(\eta^5\text{-}C_5Me_5)_3U(N_2)$ [96]. Reprinted with permission from [95, 96]; © (2003) American Chemical Society

$$(C_5Me_5)_3U + 2\,C_6H_5Cl \xrightarrow[-2(C_5Me_5)_2 \\ -\,H_5C_6\text{-}C_6H_5]{} [(C_5Me_5)_2UCl_2] \qquad (15)$$

Sterically hindered metal centers for the class of compounds of the type $(\eta^5\text{-}C_5Me_5)_3M$ have unusually long metal ligand bonds. Although long metal ligand distances are known in *f*-element complexes containing agostic interactions [90], they generally involve only one or two interactions and the rest of the bonds are normal and predictable based on ionic radii [91–93]. In contrast, in the molecule $(\eta^5\text{-}C_5Me_5)_3U$ all the metal–ligand bonds were longer than the conventional distance [94]. This phenomenon further induced researchers to investigate the reaction chemistry of the $(\eta^5\text{-}C_5Me_5)_3U$ moiety. The reaction of $(\eta^5\text{-}C_5Me_5)_3U$ with CO produced the sterically more crowded U(III) complex $Cp^*_3U(CO)$ [95]. With N_2 [96] it afforded the monometallic complex $Cp^*_3U(\eta^1\text{-}N_2)$ (Fig. 4), demonstrating that end-on nitrogen coordination is possible for *f*-elements (Scheme 3)(vide supra). In fact, this is the first monometallic *f*-element complex of N_2 of any kind because it is most commonly found as $M_2(\mu\text{-}\eta^2\text{:}\eta^2\text{-}N_2)$ moieties involving $(N_2)^{-2}$ [97–103]. The binding of N_2 in $Cp^*_3U(\eta^1\text{-}N_2)$ was found to be reversible, i.e., it releases N_2 when the pressure was lowered to 1 atm in a solution of C_6D_6, quantitatively regenerating the parent complex (Scheme 3). In contrast, a solution of $Cp^*_3U(CO)$ was found to be stable for hours under Ar or vacuum.

The discovery of the SIR phenomenon for this kind of complex opened the window for the multi-electron reduction system. The complex Cp^*_3U shows a reductive coupling of acetylene [104] and reductive cleavage of azobenzene [105] (Scheme 4), two- and four-electron processes, respectively.

These U(IV) and U(VI) complexes can also be obtained from $[(\eta^5\text{-}C_5Me_5)_2U][(\mu\text{-}Ph)_2BPh_2]$, where $[BPh_4]^-$ acts as a one-electron reductant (Scheme 4) [104]. On the other hand the reaction of $(\eta^5\text{-}C_5Me_5)_3U$ and cyclooctatetraene giving $[\{U(\eta^5\text{-}C_5Me_5)(C_8H_8)\}_2(\mu\text{-}C_8H_8)]$ is accomplished through one U(III)/U(IV) and two $(C_5Me_5)^-/C_5Me_5$ couples [89].

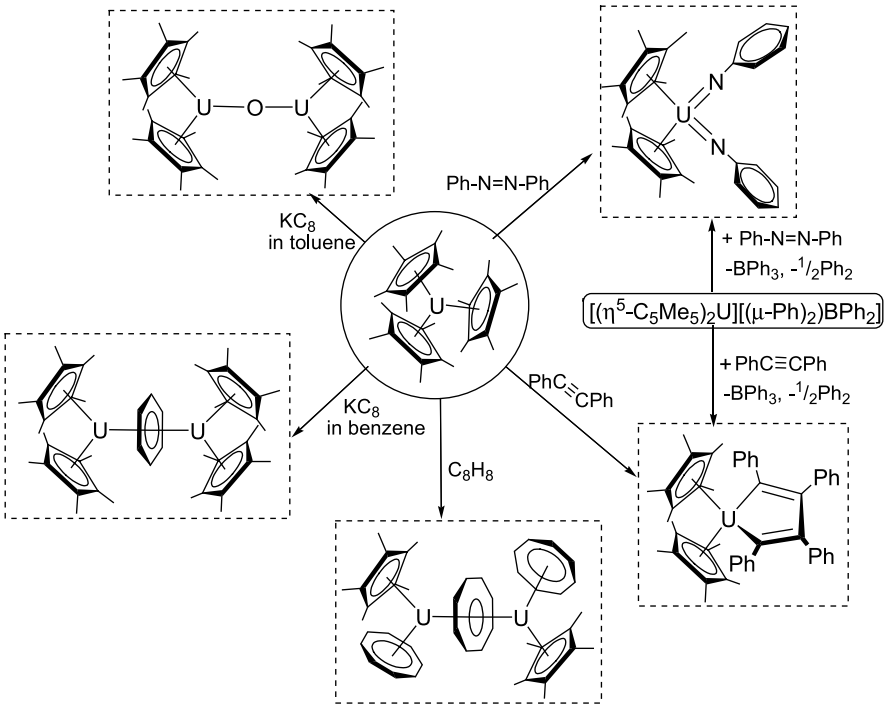

Scheme 4 Sterically induced reduction chemistry of $[(Me_5C_5)_3U]$ [89, 104–107]

With KC_8 in benzene it gave $[\{U(\eta^5\text{-}C_5Me_5)_2\}_2(\mu\text{-}\eta^6\text{:}\eta^6\text{-}C_6H_6)]$ [106], which itself proved to be also quite interesting in the area of multi-electron reduction chemistry, as shown by its reaction with azobenzene in which it functions as an eight-electron reductant [104]. Thus, it is clear that the complex $(\eta^5\text{-}C_5Me_5)U$ shows quite an interesting two- to four-electron reduction chemistry in a similar way to that of the com-

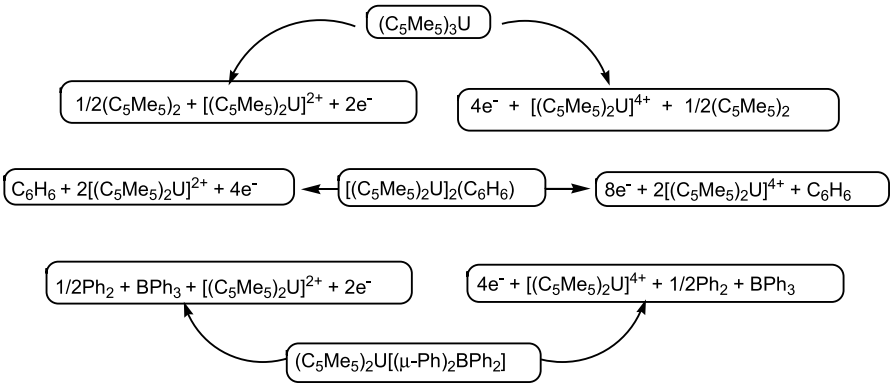

Scheme 5 Multielectron oxidation/reduction couple of SIR uranium system [104]

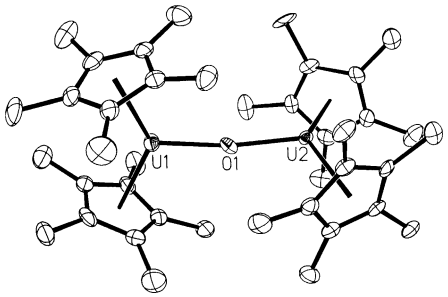

Fig. 5 Crystal structure of $[(\eta^5\text{-}C_5Me_5)_2U]_2(\mu\text{-}O)$ [107]. Reprinted with permission from Elsevier

plexes $[(\eta^5\text{-}C_5Me_5)_2U][(\mu\text{-}Ph)_2BPh_2]$ and $[\{U(\eta^5\text{-}C_5Me_5)_2\}_2(\mu\text{-}\eta^6\text{:}\eta^6\text{-}C_6H_6)]$ (Scheme 5).

Another most interesting and unusual result has been reported regarding the formation of an U(III) oxide complex, $[(Cp^*)_2U]_2(\mu\text{-}O)$ (Fig. 5) obtained by the $(\eta^5\text{-}C_5Me_5)_3U$ reduction system (Scheme 4) [107]. This has been claimed to be the first molecular trivalent uranium oxide so far reported. The complex was isolated from a reaction of $(\eta^5\text{-}C_5Me_5)_3U$ with KC_8 in toluene. Probably this is the first example of an SIR process in which the $C_5Me_5^{-1}$ reduction precedes the U(III) electron transfer.

Further investigating the SIR, Evans et al. [106] reported that $[(Cp^*)_2U]_2(\mu\text{-}\eta^6\text{:}\eta^6\text{-}C_6H_6)$ functions as a six-electron reductant in its reaction with three equivalents of cyclooctatetraene to form $[(Cp^*)(C_8H_8)U]_2(\mu\text{-}\eta^3\text{:}\eta^3\text{-}C_8H_8)$, $(C_5Me_5)_2$, and benzene (Eq. 16):

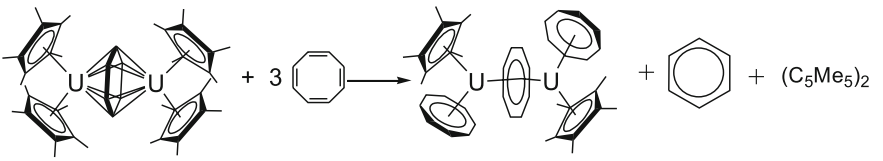

(16)

This multi-electron transformation can be formally attributed to three different sources: two electrons from two U(III)/U(IV) reaction, two electrons from sterically induced reduction by two $(C_5Me_5)^{1-}/(C_5Me_5)$ ligands, and two electrons from a bridging $(C_6H_6)^{2-}/(C_6H_6)$ process.

Apart from these SIR processes, there are few other examples where the U(III) center undergoes one- or two-electron oxidation. It was found that alkyl halides can also be oxidized by U(III) to generate equimolar mixtures of U(IV)–R and U(IV)–X as shown in Eq. 17 [108]:

$$2\,[(\eta^5\text{-}C_5H_5)_3U(THF)] + R\text{-}X \longrightarrow [(\eta^5\text{-}C_5H_5)_3U\text{-}R] + [(\eta^5\text{-}C_5H_5)_3U\text{-}X] \qquad (17)$$

There are few examples on the oxidation of the U(III) center to give corresponding U(IV) complexes. Stults et al. [73] showed that unlike the cerium metallocene, the uranium metallocene $(MeC_5H_4)_3U(THF)$ behaves quite differently with alcohols and thiols. It forms the U(IV) complex of the type $[(MeC_5H_4)_3UER]$, where ER is OMe, $OCHMe_2$, OPh, or $SCHMe_2$. The different type of reaction shown by cerium and uranium metallocenes towards alcohols and thiols most likely reflects the case of oxidizing uranium: the U(IV)/U(III) couple is -0.63 V in aqueous acid whereas the Ce(IV)/Ce(III) is $+1.74$ V [73]. Even the uranium complex with the more crowded substituent on the cyclopentadiene, i.e, $(Me_3CC_5H_4)_3U$, also undergoes a similar type of reaction with thiophenol (Eq. 18) to give $(Me_3CC_5H_4)_3USPh$:

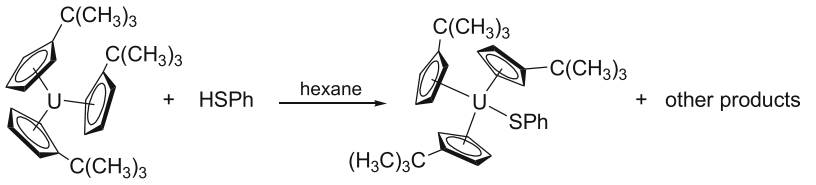

(18)

2.3 Displacement of $(C_5Me_5)^{1-}$ Ligands

Significant steric hindrance and the longer M–C bond in complexes of the type $(C_5Me_5)_3M$ induced another type of reaction, i.e., $(C_5Me_5)^{1-}$ substitution reaction from the metal center [106]. Removal of $(C_5Me_5)^{1-}$ is very reasonable due to the steric crowding in these long bonded organometallics. The loss of $(C_5Me_5)^{1-}$ anions from $(C_5Me_5)_3M$ complexes by η^1-alkyl or SIR pathways is well known [94], but the removal of $(C_5Me_5)^{1-}$ rings from *f* element complexes by ionic metathesis is not a common reaction.

The synthesis of $[(Cp^*)_2U]_2[(\mu\text{-}\eta^6\text{:}\eta^6\text{-}C_6H_6)]$ provides an example of the $(C_5Me_5)^{1-}$ displacement from the $(Cp^*)_3U$ moiety. Initially the complex $[(Cp^*)_2U]_2[(\mu\text{-}\eta^6\text{:}\eta^6\text{-}C_6H_6)]$ was obtained as a byproduct in the synthesis of $(Cp^*)_3U$ from $[(Cp^*)_2U][(\mu\text{-}Ph_2)BPh_2]$ [86], but it could have been synthesized directly from $(C_5Me_5)_3U$ [106] (Scheme 4) (vide supra). In an another synthetic route, it was also synthesized from $[(Cp^*)_2U][(\mu\text{-}Ph_2)BPh_2]$, the precursor to $(C_5Me_5)_3U$, in combination with K/18-crown-6/benzene as shown in Eq. 19:

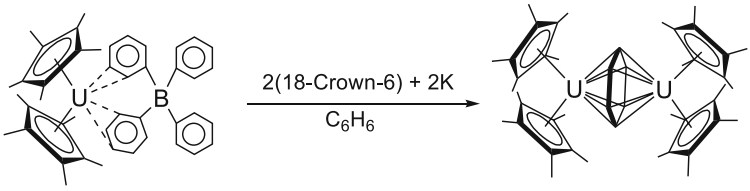

(19)

The complex $[(C_5Me_5)_2U]_2[(\mu\text{-}\eta^6\text{:}\eta^6\text{-}C_6H_6)]$ was structurally characterized as a bimetallic species in which an arene ring is sandwiched between two $[(C_5Me_5)_2U]$ moieties. The U–U distance was found to be 4.396 Å, and the $(C_5Me_5)^{1-}$ rings arranged tetrahedrally around the U–C_6H_6–U core. In a similar manner, the amide analog, $\{[(Me_3Si)_2N](C_5Me_5)U\}_2[(\mu\text{-}\eta^6\text{:}\eta^6\text{-}C_6H_6)]$, was synthesized by displacement of two $(C_5Me_5)^{1-}$ moieties from $[(C_5Me_5)_2U]_2[(\mu\text{-}\eta^6\text{:}\eta^6\text{-}C_6H_6)]$ when it reacts with two equivalents of $KN(SiMe_3)_2$ (Eq. 20). The comparison of the crystallographic data (Table 2) of these two complexes revealed that the average U–C(C_5Me_5) bond distances in $\{[(Me_3Si)_2N](C_5Me_5)U\}_2[(\mu\text{-}\eta^6\text{:}\eta^6\text{-}C_6H_6)]$ is shorter than that of $[(C_5Me_5)_2U]_2[(\mu\text{-}\eta^6\text{:}\eta^6\text{-}C_6H_6)]$ as well as the angle (C_5Me_5 ring centroid)–U –(C_6H_6 ring centroid) in the former is smaller than the latter (Table 2). Thus, incorporation of the $(Me_3Si)_2N$ ligand into the coordination sphere reduced the steric constrain around the metal centers. In $\{[(Me_3Si)_2N](C_5Me_5)U\}_2[(\mu\text{-}\eta^6\text{:}\eta^6\text{-}C_6H_6)]$ (Fig. 6), the two C_5Me_5 ring centroid, the two N-donor sites took a square plane arrangement rather than the sterically more compact tetrahedral arrangement of the four rings as in $[(C_5Me_5)_2U]_2[(\mu\text{-}\eta^6\text{:}\eta^6\text{-}C_6H_6)]$ [106]:

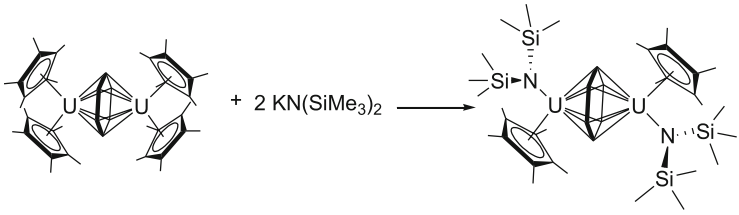

(20)

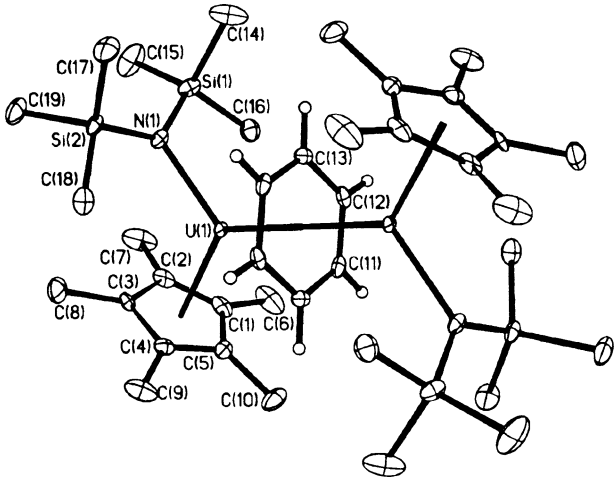

Fig. 6 Crystal structure of $[(Me_3Si)_2NCp^*U]_2(\mu\text{-}\eta^6\text{:}\eta^6\text{-}C_6H_6)$ [106]. Reprinted with permission from [106]; © (2004) American Chemical Society

Table 2 Comparison of bond length (Å) and bond angle (°) of $[(C_5Me_5)_2U]_2$ (μ-η^6:η^6-C_6H_6) and $\{[(Me_3Si)_2N](C_5Me_5)U\}_2$($\mu$-$\eta^6$:$\eta^6$-$C_6H_6$)[106]

$[(C_5Me_5)_2U]_2$(μ-η^6:η^6-C_6H_6)		$\{[(Me_3Si)_2N](C_5Me_5)U\}_2$($\mu$-$\eta^6$:$\eta^6$-$C_6H_6$)			
Parameters	Bond distance (Å)	Bond angle (°)	Parameters	Bond distance (Å)	Bond angle (°)
U(1)–U(2)	4.396		U(1)–U(2)	4.219	
U(1)–Cp1 [a]	2.567		U(1)–Cp1 [a]	2.506	
U(1)–Cp2 [a]	2.583		U(1)–Bz [a]	2.146	
U(1)–Bz [a]	2.194		U(1)–N(1)	2.306	
U(1)–Cp1 [b]	2.835		U(1)–Cp1 [b]	2.781	
U(1)–Cp2 [b]	2.852		U(1)–Bz [b]	2.540	
U(1)–Bz [b]	2.621		Cp1 [a]–U(1)–Bz [a]		130.9
Cp1 [a]–U(1)–Cp2 [a]		121.1	Cp1 [a]–U(1)–N		111.2
Cp1 [a]–U(1)–Bz [a]		118.9	Bz [a]–U(1)–N		117.8
Cp2 [a]–U(1)–Bz [a]		119.8			

Bz benzene
[a] Centroid
[b] Average

While investigating the nature of bonding in these complexes, Evans et al. reported [106] an arene exchange reaction in which a bridged xylene complex was formed by the reaction of $(C_5Me_5)_3U$, KC_8 and *p*-xylene as shown in Eq. 21:

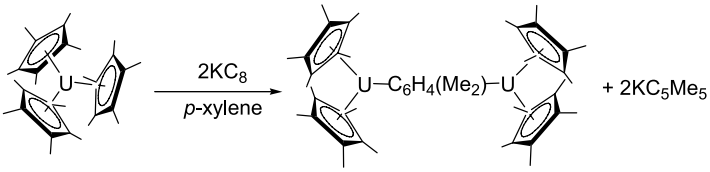

(21)

The synthesis of $(C_5Me_5)_2U[N(SiMe_3)_2]$ by the addition of $KN(SiMe_3)_2$ to a solution of $(C_5Me_5)_3U$ in C_6D_6 provides an excellent example of an ionic metathesis reaction [106] (Scheme 6). $(Cp^*)_2U[N(SiMe_3)_2]$ has been previously synthesized by addition of $M[N(SiMe_3)_2]$ $(M = Na, K)$ to $[(Cp^*)_2UCl]_3$ [109, 110] or $(Cp^*)_2UMe_2K$ [86]. It can also be obtained from $KN(SiMe_3)_2$ and $[(Cp^*)_2U][(\mu\text{-}Ph_2)BPh_2]$, a complex that is an excellent reagent for ionic metathesis reactions because it contains the $[(Cp^*)_2U]^+$ cation loosely ligated by bridging η^2-arenes of the $(BPh_4)^{1-}$ anion [106].

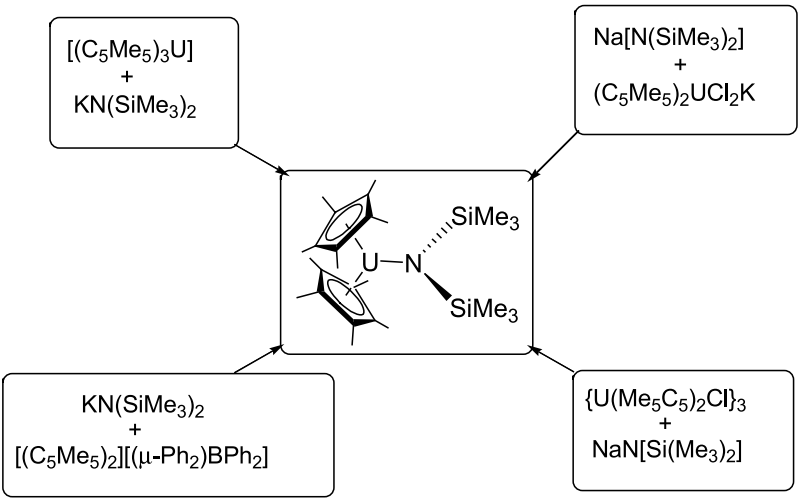

Scheme 6 Synthetic routes for $[(C_5Me_5)_2U][N(SiMe_3)_2]$ [86, 106, 109]

Manriquez et al. [109] showed an example of unusual chemistry of the uranium pentamethylcyclopentadienyl complex. It was found to form a tetrameric $\{U[\eta^5\text{-}(CH_3)_5C_5]_2Cl\}_3$ unit, which was synthesized by different

procedures as shown in the following reactions (Eqs. 22–25):

$$3\,U[(Me)_5C_5]_2(R)Cl + {}^3/_2H_2\ (1\ atm) \xrightarrow[25^oC]{\text{toluene}} \{U[(Me)_5C_5]_2)Cl\}_3 + 3RH$$

$$R = Me,\ CH_2Si(Me)_3 \qquad (22)$$

$$3\,U[(Me)_5C_5]_2Cl_2 + 3\,Li(t\text{-}C_4H_9) \xrightarrow[-78^oC]{\text{ether}} \{U[(Me)_5C_5]_2)Cl\}_3 + 3LiCl + \text{Organic products} \qquad (23)$$

$${}^3/_2\,\{U[(Me)_5C_5]_2H_2\} + 3\,U[(Me)_5C_5]_2Cl_2 \longrightarrow \{U[(Me)_5C_5]_2)Cl\}_3 + 3H_2 \qquad (24)$$

$$U[(Me)_5C_5]_2Cl_2 \xrightarrow{Na\ /\ Hg} \{U[(Me)_5C_5]_2)Cl\}_3 + NaCl \qquad (25)$$

The structural analysis shows that the crystals composed of discrete trinuclear $\{[\eta^5\text{-}(CH_3)_5C_5]U(\mu_2\text{-}Cl)\}_3$ molecules (Fig. 7) in which each U(III) ion adopts the familiar pseudotetrahedral "bent sandwich" configuration. The bridging Cl^- ligands serve to generate the planar (to within 0.02 Å) six-atom $(–U–CI–)_3$ ring.

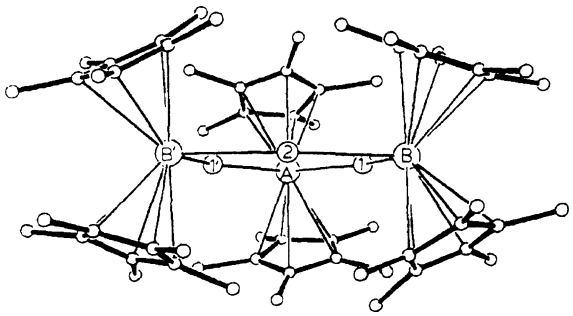

Fig. 7 Perspective drawing of the $\{U[\eta^5\text{-}(CH_3)_5C_5]_2Cl\}_3$ molecule [109]. Reprinted with permission from [109]; © (1979) American Chemical Society

The complex $\{[\eta^5\text{-}(CH_3)_5C_5]U(\mu_2\text{-}Cl)\}_3$ is insoluble in hydrocarbon solvents, but readily dissolves in the presence of Lewis base donors to form the corresponding adducts (Scheme 7) [109]. Once the solubility problem was solved, the chemistry of this molecule was investigated in various reactions, like alkylation with the sterically bulky lithium reagent, preparation of organouranium(III) amide, and reductive coupling of alkyne as shown in Scheme 7.

Apart from these persubstituted Cp-ligand complexes, mono- and disubstituted Cp-ligand complexes are also in the race to achieve the milestone. The *f*-elements, when they form complexes with a variety of cyclopentadienyl ligands, possess an extensive organometallic chemistry that includes,

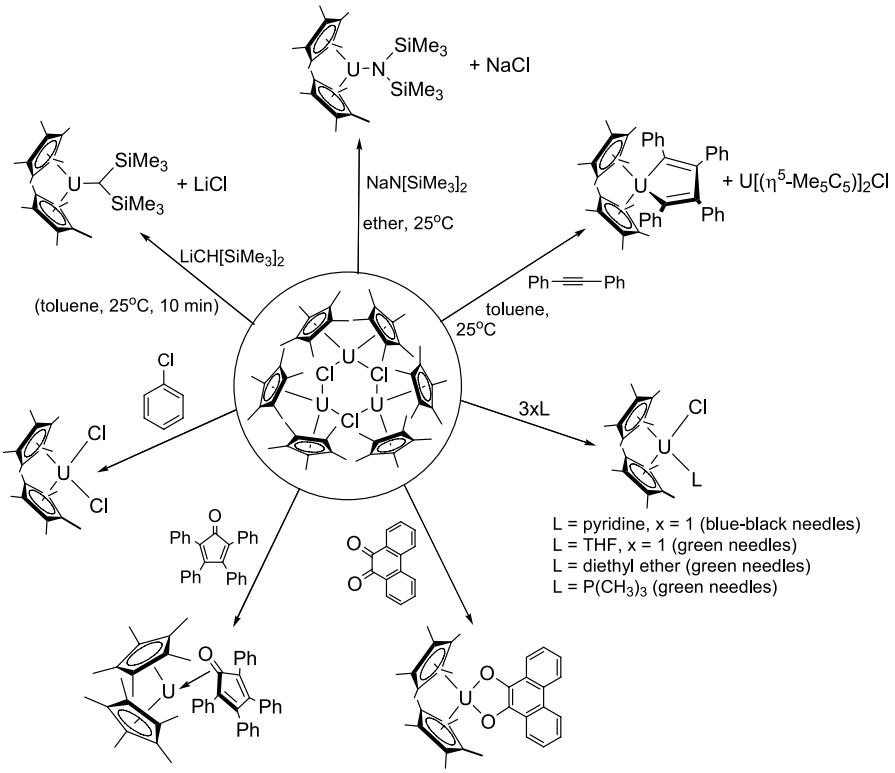

Scheme 7 Reaction chemistry of $\{(\eta^5\text{-}Me_5C_5)_2U(\mu_2\text{-}Cl)\}_3$ [109]

among other interesting features, metal-to-carbon bonding, metal-to-X atom σ-bond formation, Lewis base adduct formation, ligand reductive coupling etc., all of them with unique features. The tris(cyclopentadienyl)actinide complexes sheds light on the nature of metal orbital participation in chemical bonding. Actinide metals generally are acidic and coordinate to Lewis bases. Therefore, to understand these unique features, the chemistry of these mono- or di-substituted cyclopentadienyl complexes have been studied extensively. As previously discussed, many of the tris(cyclopentadienyl)actinide complexes can be isolated as THF adducts directly from reactions carried out in that solvent. Trivalent uranium metallocenes form compounds of the type $(RC_5H_4)_3U(L)$ where R is either H or CH_3 and L is a Lewis base such as tetrahydrofuran [111], tetrahydrothiophene [112], 4-dimethylaminopyridine [113], trimethylphosphine [114], or 1,2-bis-(dimethylphosphino)-ethane [115]. All of these molecules may be described as four-coordinate complexes of trivalent uranium (defining the midpoint of the cyclopentadienyl ring centroid as occupying one coordination position) with a distorted tetrahedral stereochemistry.

2.4 Bridging Complexes

During the 1980s, Zalkin and coworkers synthesized a variety of complexes to profoundly study the coordination chemistry of tetra- and trivalent uranium complexes with a variety of mono-, or bidentate ligands. A phosphorus bridge uranium complex $[U(C_5H_5)_3]_2\{(CH_3)_2PCH_2CH_2P(CH_3)_2\}$ was synthesized (Eq. 26) [115] in which the P–P ligand did not act as a bidentate chelating ligand but indeed formed a bridge in a monodetate fashion between two trivalent U units (Fig. 8):

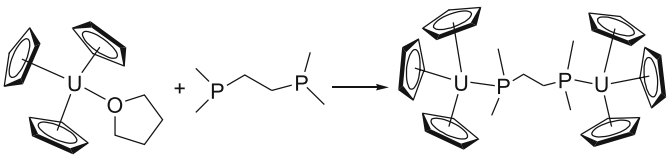

(26)

Therefore, the geometry of the complex is quite unusual with respect to the type of the ligand. The reason for this structural change is presumably the steric hindrance around the metal center. The coordination geometry around each uranium atom is quite similar to that in $(CH_3C_5H_4)_3U\{P(CH_3)_3\}$ (vide infra) [114]. The average U–P bond distance in $[U(C_5H_5)_3]_2\{(CH_3)_2PCH_2CH_2P(CH_3)_2\}$ is 3.022(2) Å, which is almost same as that found in $(CH_3C_5H_4)_3U\{P(CH_3)_3\}$ (2.972(6) Å).

Another U(III) bridging complex, $[Li(tmeda)_2] \cdot [Li(tmeda)]_2[\mu\text{-}MeC_5H_4][(MeC_5H_4)U]_2[\mu\text{-}Me]$, was obtained by the addition of one molar equivalent of methyllithium to $(C_5H_4Me)_3U(THF)$ in diethyl ether in the presence of one molar equivalent of $Me_2NCH_2CH_2NMe_2$ (tmeda) at $-30\,^{\circ}C$ [116]. The crystal structure of the complex reveals that it contains one molecule each of $Li(tmeda)_2$ and $[Li(tmeda)]_2[\mu\text{-}MeC_5H_4]$, and two molecules of $[(MeC_5H_4)_3U]_2[\mu\text{-}Me]$. The geometry of the anion has an U–C–U angle of

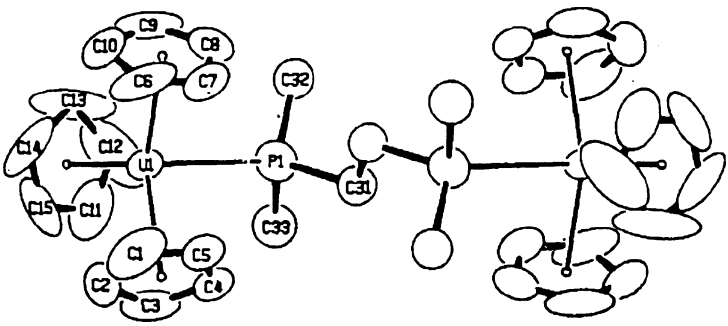

Fig. 8 Molecular structure of $[U(C_5H_5)_3]_2\{(CH_3)_2PCH_2CH_2P(CH_3)_2\}$ [115]. Reprinted with permission from IUCr Journals, http://journals.iucr.org

176.9° and U–C distances of 2.71(3) and 2.74(2) Å. The U–C (bridging) distance is long relative to $Cp_3U(n\text{-Bu})$ [117] with 2.43(2) Å and $[Cp_3U(n\text{-Bu})]^-$ with 2.56(1) Å [118], as expected due to bridging. The bonding was explained with the help of the D_{3h} symmetry methyl anion, which was formed from *s*- and two *p*-orbitals giving a sp^2-hybridized set that contains six electrons for the C–H bonds and an unhybridized *p*-orbital with its two electrons that can be used in bonding with the σ-orbitals on the Lewis acid $(MeC_5H_4)_3U$.

A series of halide bridge U(III) complexes of the type $[Cp''_2U(\mu\text{-X})]_n$ (where Cp″ = 1,3-$(SiMe_3)_2C_5H_3$; X = F, Cl, Br or I) have been synthesized [119] by the reduction of corresponding U(IV) halides, $[Cp''_2UX_2]$ (X = F, Cl, Br or I) with Na/Hg in toluene. The complexes were fully characterized analytically and single crystal analysis showed that Cl and Br form dimeric bridging compounds. In contrast, chlorine formed a trimeric bridge complex when it contained the ligand η^5-$(CH_3)_5C_5$ (vide supra) [109]. This implies that $(SiMe_3)_2C_5H_3$ is sterically more demanding than $(CH_3)_5C_5$. However, when the two structures $[Cp''_2U(\mu\text{-Cl})]_2$ and $[Cp^*_2U(\mu\text{-Cl})]_3$ were compared, it was found that the average U–C(Cp) distance is equivalent (2.78(2) Å and 2.77(1) Å, respectively), whereas the U–Cl bond distance in the former (2.810(4) Å) was found to be significantly shorter than in the latter (2.900(2) Å). This may be due to weak U–Cl interaction in the latter, caused by the wider U–Cl–U angle of 154.9(1)° compared to that of the former 101.5(1)°. Investigating in this series, chlorine was found to form another bridging complex, $[(Cp^{\#})_4U_2(\mu\text{-Cl})_2]$ (where $Cp^{\#}$ = 1,3-$(Me_3C)_2C_5H_3$) [120], which was produce by the reaction of K[1,3-$(Me_3C)_2C_5H_3$] and UCl_3 in THF (Eq. 27):

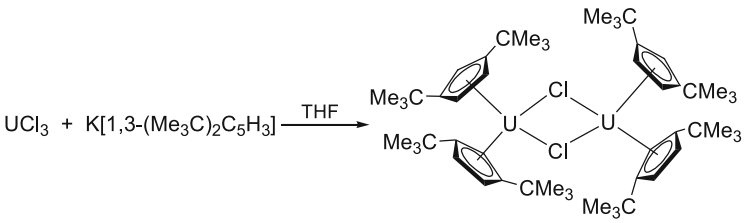

(27)

The complex was also fully characterized by single crystal X-ray crystallography (Fig. 9) and found to have a similar structure to that of the $[(Cp'')_4U_2(\mu\text{-Cl})_2]$. The average U–C distance of 2.79 Å and U–Cp (centroid) distance of 2.51 Å are not significantly different from those values in other trivalent uranium metallocenes.

The reaction of $(\eta^5\text{-}C_5H_5)_3U(THF)$ with dioxygen produces the bridged bimetallic complex $[(\eta^5\text{-}C_5H_5)_3U]_2(\mu\text{-O})$ [121]. The analogous μ-sulfido complex was produced by the reaction of $(\eta^5\text{-}C_5H_5)_3UCl$ with freshly prepared K_2S.

A number of the dimeric complexes of the class $\{[\eta^5\text{-}1,3\text{-}R_2C_5H_3]_2U(\mu\text{-X})\}_2$ (R = Me_3Si or Me_3C) were structurally characterized [122] and found

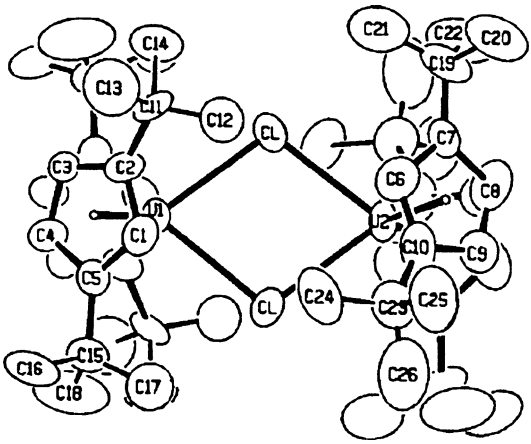

Fig. 9 The complex structure of $[1,3\text{-}(Me_3C)_2C_5H_3]_4U_2(\mu\text{-}Cl)_2$ [120]. Reprinted with permission from IUCr Journals, http://journals.iucr.org

that they exist as dimers also in solution [123, 124]. These were found to react with Lewis bases to yield monomeric mono- or bis-ligand adducts [125–127].

In continuation to the exploration of bridging uranium complexes, Blake et al. reported a newer type of bimetallic bridging complex [128] of uranium with alkali metals of the type $[UCp''_2(\mu\text{-}Cl)_2M(THF)_2]$ (where M = Li(**1**), Na(**2**)), $[UCp''_2(\mu\text{-}Cl)_2M(tmeda)]$ (where M = Li(**3**), Na(**4**)), $[UCp''_2(\mu\text{-}Cl)_2Li(pmdeta)]$ (**5**), $[UCp''_2(\mu\text{-}Cl)_2Li(THF)_2]$ (**6**) and $[PPh_4][UCp''Cl X]$ (where X = Cl(**7**), Br(**8**); $Cp'' = \eta^5\text{-}(C_5H_3)\text{–}(SiMe_3)_2\text{-}1,3$; THF =

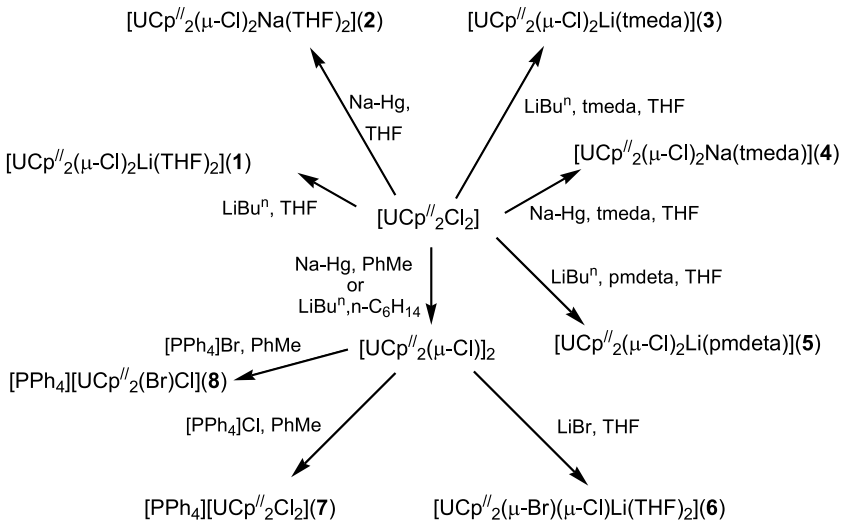

Scheme 8 Synthetic routes for complexes **1**–**8** [128]

tetrahydrofuran; tmeda = $(Me_2NCH_2)_2$; and pmdeta = $(Me_2NCH_2CH_2)_2NMe$). The complexes **1–5** were prepared by the reduction of $[Cp''UCl_2]$ with *n*-butyllithium or sodium amalgam in the presence of the appropriate neutral ligand, and **6–8** were prepared from $[Cp''_2U(\mu\text{-}Cl)]_2$ [128] (Scheme 8). The single crystal X-ray structure of the complex $[UCp''_2(\mu\text{-}Cl)_2Li(pmdeta)]$ was found to be very interesting and quite unique in nature because the Li center had a trigonal bipyramidal environment around it, with one Cl-ligand axial and the other equatorial. The crystal structure of the complex $[UCp''_2(\mu\text{-}Cl)_2Li(THF)_2]$ has also been reported [129].

On investigating the reactivity of chalcogen donor ligands towards $(Cp^{\neq})_3U(THF)$ (where $Cp^{\neq} = \eta^5\text{-}MeC_5H_4$), it was found that SCO, $SPPh_3$, $SePPh_3$, and $TeP(n\text{-}Bu)_3$ form bridging complexes of the type $[(Cp^{\neq})_3U]_2(\mu\text{-}E)$ (where E = S, Se, Te) (Scheme 9) [130]. The complex $[(Cp^{\neq})_3U]_2(\mu\text{-}S)$ was characterized structurally (Fig. 10) and it was found that the two $(Cp^{\neq})_3U$ units bridging by the S atom have a U–S–U bond angle of 164.9(4)°. The average U–S distance of 2.60(1) Å supports the π-bonding explanation for the bridging-sulfido geometry [130]. The averaged U–C (ring) distance of 2.71±0.06 Å and the average ring centroid–U–ring centroid angle, 116(2)°

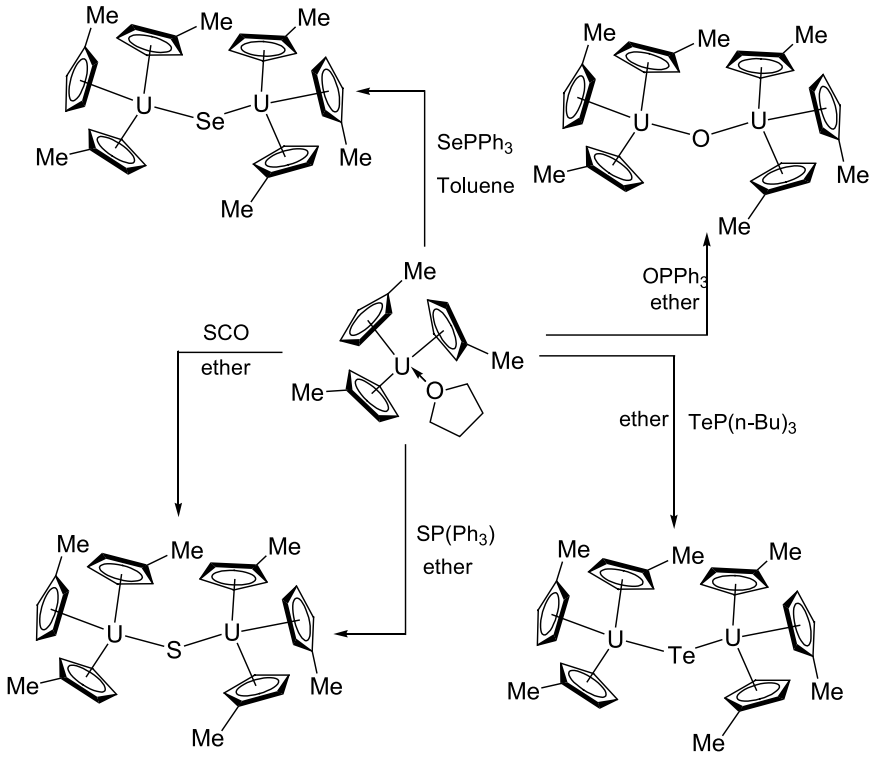

Scheme 9 Synthesis of chalcogen bridged uranium(IV) complexes [130]

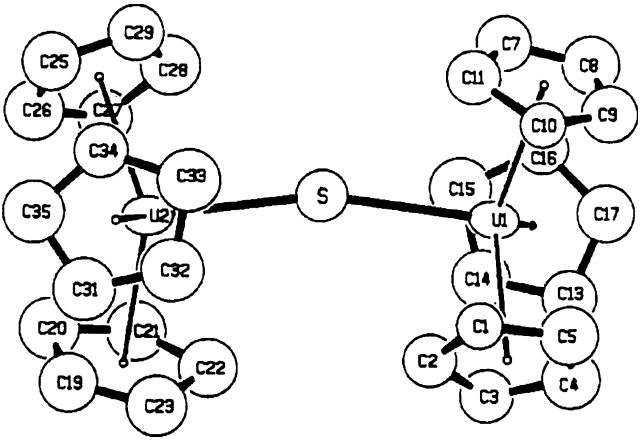

Fig. 10 Molecular structure of complexes $[(MeC_5H_4)_3U]_2(\mu\text{-}S)$ [130]. Reprinted with permission from [130]; © (1986) American Chemical Society

is well within the range of complexes of the type $Cp_3U^{IV}X$ [111, 112, 114, 131, 132]. The linearity of the U–S–U bond angle was explained by assuming the bonding in this complex primarily as electrostatic, and the repulsive interaction between the $(MeC_5H_4)_3U$ groups.

An analogous bridging oxo complex was generated by the reaction of $(Cp^{\phi})_3U$ (where $Cp^{\phi} = \eta^5\text{-}C_5H_4SiMe_3$) with CO_2 or N_2O (Eq. 28) [133]:

$$[(\eta^5\text{-}C_5H_4SiMe_3)_3U] + CO_2 / N_2O \longrightarrow [(\eta^5\text{-}C_5H_4SiMe_3)_3U\text{-}O\text{-}U(\eta^5\text{-}C_5H_4SiMe_3)_3] \quad (28)$$

The oxo bridged complexes $\{(Cp^{\phi})_3U\}_2(\mu\text{-}O)$ and $\{(Cp^{\phi})_2U(\mu\text{-}O)\}_3$ were also obtained simultaneously when $[(Cp^{\phi})_3U(OH)]$ was heated in toluene in the presence of an equivalent amount of $[(Cp^{\phi})_3UH]$. Under the same reaction conditions, thermolysis of $[(Cp^{\phi})_3U(OH)]$ was found to afford only $\{(Cp^{\phi})_2U(\mu\text{-}O)\}_3$ with the elimination of $C_5H_4SiMe_3$ (trimethylsilylcyclopentadiene) [134, 135].

In a comparative reactivity study of Ce(III) and U(III) complexes with pyrazine, Ephritikhine and coworkers reported [136] that $[Ce(C_5H_4R)_3]$ forms a Lewis base type of adduct $[Ce(C_5H_4R)_3(pyz)]$ while $[U(C_5H_4R)_3]$ oxidized to form dimeric complex $[U(C_5H_4R)_3]_2(\mu\text{-pyz})$, (where R = *t*-Bu, $SiMe_3$; pyz = pyrazine) (Eq. 29):

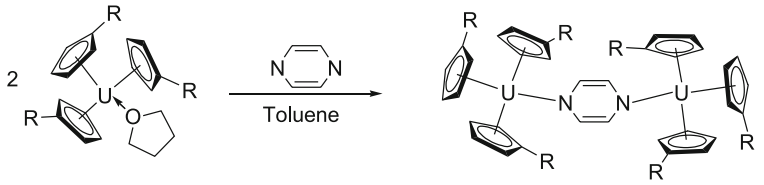

(29)

2.5
Affinity Towards Lewis Bases

As a part of the study on how steric and electronic factors influence the coordinative affinity of a given Lewis base towards trivalent uranium, a number of complexes were synthesized. The affinity of PMe_3 was determined by synthesizing the complex $[(C_5H_4Me)_3U(PMe_3)]$ according to the following reaction (Eq. 30):

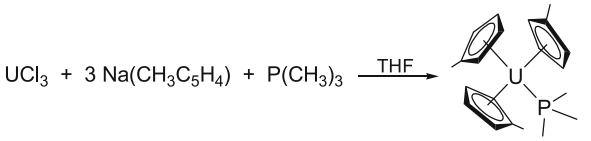

(30)

The complex $[(Cp^{\neq})_3U(PMe_3)]$ is monomolecular in the crystalline state [114] and consists of an U atom coordinated to the three methylcyclopentadienyl groups in a pentahapto bonding mode and to the P atom of the trimethylphosphine molecule in a distorted tetrahedral arrangement. While comparing the structure of this complex with analog U(III) alkylphosphine structures, the U(III)–P distance of 2.972(6) Å was found to be significantly shorter than the U–P distances of 3.211 Å and 3.092 Å in $\{(CH_3C)_5\}_2UH\{(CH_3)_2PCH_2CH_2P(CH_3)_2\}$ [137], 3.057 and 3.139 Å in $U(BH_4)_3\{(CH_3)_2PCH_2CH_2P(CH_3)_2\}_2$ [138], and 3.085 and 3.174 Å in $U(CH_3BH_3)_3\{(CH_3)_2PCH_2CH_2P(CH_3)_2\}_2$ [139].

On the other hand, the thiophene ligand SC_4H_8 reacted with $(Cp^{\neq})_3U(THF)$ in toluene to form a mononuclear complex $(Cp^{\neq})_3U(SC_4H_8)$ in solid state [112]. Like $(Cp^{\neq})_3UPMe_3$, here also the uranium atom is coordinated to Cp groups and to the sulfur atom of the tetrathiophene ligand in a distorted tetrahedral array. The structures of $[(C_5H_4Me)_3U(SC_4H_8)]$ and $(C_5H_4Me)_3U(THF)$ [111] are similar, but the U–S and U–O distances are found to be 2.986 and 2.55 Å respectively.

Another almost similar type of complex $[(Cp^{\neq})_3U\{4\text{-}(Me_2N)C_5H_4N\}]$ was synthesized from the U(III)·THF adduct [113]. The complex was characterized structurally, and like other U(III) molecules it also has the tetrahedral arrangement around the uranium atom with three cyclopentadienyl centroids and a pyridine. The average Cp–U–Cp angle in $[(Cp^{\neq})_3UL]$ (where L = $4\text{-}(Me_2N)C_5H_4N$) is 117° which is almost the same as the values of 118° for L = SC_4H_8 [112], 118° for $OPPh_3$ [130], and 118° in $CpU(OC_4H_8)$ [111] but different form angles 106, 109 and 119° found in $[(MeC_5H_4)_3UP(Me_3)]$, which can be explained with the help of the more crowding PMe_3 molecule.

Arliguie et al. [140] reported the synthesis of few uranium(III) thiolato complexes of the type $Na[Cp^*_2U(SR)_2]$ (where $Cp^* = \eta^5\text{-}C_5Me_5$; R = Ph, Me, *i*-Pr) by the reductive reaction of their corresponding uranium(IV) bis thiolate complexes with sodium amalgam. It is worth mentioning here that

a similar type of reductive product could not be obtained for R = *t*-Bu, rather it gave U(IV) sulfide $Na[Cp^*_2U(SBu\text{-}t)(S)]$. Compound $Na[Cp^*_2U(SPh)_2]$ was thermodynamically stable but, in contrast, the complexes with R = Me and *i*-Pr were not so stable. In solution they slowly decompose to their analog sulfide derivatives $Na[Cp^*_2U(SR)(S)]$ (R = Me and *i*-Pr). These facts suggested that compounds $Na[Cp^*_2U(SR)_2]$ (R = *t*-Bu, Me and *i*-Pr) undergo facile homolytic C–S bond cleavage of the SR ligand. From NMR studies, the C–S bond rupture was found to follow the order *t*-Bu > *i*-Pr > Me ≫ Ph. The complex $Na[Cp^*_2U(SBu\text{-}t)(S)]$ was also alternatively synthesized by treating the U(III) chloride $[Na(THF)_{1.5}][Cp^*_2UCl_2]$ [110] with NaSBu-*t* in THF. By using a bigger counter-cation like 18-crown-6-ether, the complex $[Na(18\text{-crown-}6)][Cp^*_2U(SBu\text{-}t)S]$ [141] could have been recrystallized (Fig. 11). As usual, the uranium coordination geometry was pseudotetrahedral, which is typical of the $Cp^*_2MX_2$ fragment. The U–S bond distances of 2.791(1) and 2.777(1) Å are 0.1 Å longer than in $Cp^*_2U(SMe)_2$, 2.640(5) Å, [142] in agreement with the difference of ionic radii between the U(III) and U(IV) centers.

In organometallic chemistry, the metal–ligand bond strength and the ligand displacement studies are fundamental problems. Brennan et al. [143] studied the relative affinity of Lewis bases towards $(Me_3C_5H_4)_3U$ on the basis of the equilibrium constant and reported a ligand displacement series as PMe_3 > $P(OMe)_3$ > pyridine > tetrahydrothiophene ∼ tetrahydrofuran ∼ $N(CH_2CH_2)_3CH$ > CO and towards $(Me_3SiC_5H_4)_3U$ the series is EtNC > EtCN [144]. The observation that phosphite and isocyanide molecules,

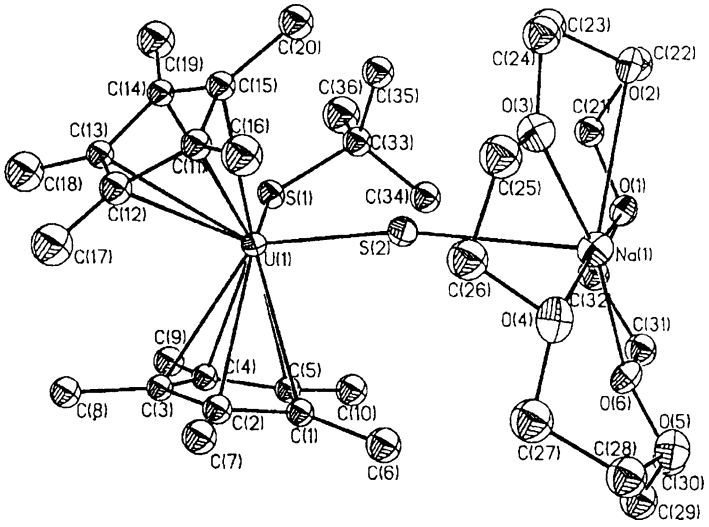

Fig. 11 Crystal structure of $[Na(18\text{-crown-}6)][Cp^*_2U(SBu\text{-}t)S]$. Reproduced with permission from the Royal Society of Chemistry

which are generally classified as π-acceptors, are good ligands toward the trivalent uranium metallocenes suggests that the uranium center can act as a π-donor. Again for the phosphine and amines, the ligand displacement towards $(RC_5H_4)_3U$ follows the order phosphine > amine [144]. To evaluate the U–P π-back bonding, complexes $(MeC_5H_4)_3U[N(CH_2CH_2)_3CH]$ and $(MeC_5H_4)_3U[P(OCH_2)_3CEt]$ were synthesized (Eq. 31) and characterized structurally. Table 3 shows a comparison of the M–L distance for the complexes of the type $(RC_5H_4)_3U(L)$:

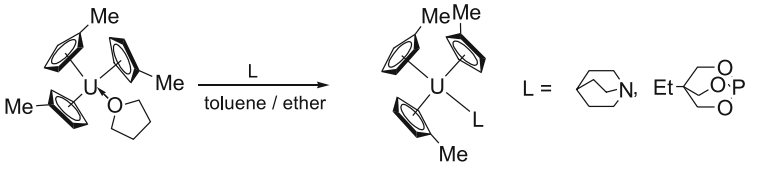

(31)

Ephritikhine and coworkers investigated the reactivity of U(III) metallocene towards various pyridine-based azine molecules and reported the Lewis base adducts $[(C_5H_4R)_3UL]$ (L = pyridine, 3-picoline, 3,5-lutidine, 3-chloropyridine, pyridazine, pyrimidine, pyrazine, 3,5-dimethylpyrazine and *s*-triazine). Except in the cases of L = 3-chloropyridine, pyridazine, pyrazine and *s*-triazine, the U(III) center was found to be oxidized (Scheme 10) [145].

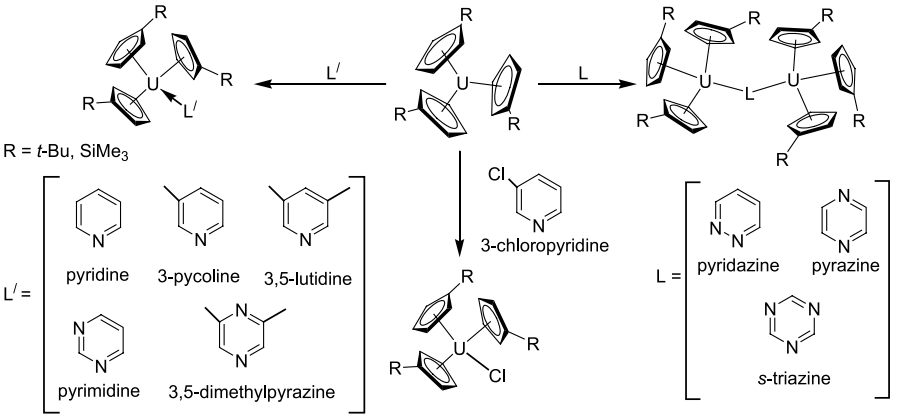

Scheme 10 Reactivity of tris(cyclopentadienyl)U molecule towards various azines [144]

The complexes $[(C_5H_4\text{-}t\text{-}Bu)_3UL]$ (L = pyridine, picoline) and $[(C_5H_4SiMe_3)_3UL]$ (L = pyridine, lutidine, pyrimidine, and dimethylpyrazine) have been characterized by single crystal X-ray crystallography (Table 4). All the mononuclear complexes were found in the familiar pseudotetrahedral arrangement of the three η^5-cyclopentadienyl ligands and the coordinated Lewis base.

Table 3 Some important bond length and angles of few of the cyclopentadienyl U(III) Lewis base complexes

Complexes	Bond distance		Bond angle			Refs.
	U–Cp_{av} (Å)	U–L (Å)	L–U–Cp_1 (°)	L–U–Cp_2 (°)	L–U–Cp_3 (°)	
$(MeC_5H_4)_3U[N(CH_2CH_2)_3CH]$	2.82±0.03	2.764(4)	100.9	101.3	101.4	[144]
$(MeC_5H_4)_3U[P(OCH_2)_3CEt]$	2.805	2.521	95.7	90.0	98.1	[144]
$(MeC_5H_4)_3U(PMe_3)$	2.789	2.972(6)	112.7	109.7	96.7	[114]
$(MeC_5H_4)_3U(O{=}PPh_3)$	2.82±0.04	2.389(6)	99.3	98.7	100.7	[130]

2.6 Metal Ligand Back Donation

In matrix isolation studies at cryogenic temperatures, it was observed that actinide carbonyl complexes, $U(CO)_6$, can exist below ca. 20 K. This led to studies on the synthesis of actinide carbonyl complexes, and in 1986 the first molecular actinide complex of carbon monoxide, $(Me_3SiC_5H_4)_3UCO$, was reported [146]. The coordination of CO to the metal center was found to be reversible. When a deep green solution of $(Me_3SiC_5H_4)_3U$ in either pentane or hexane was exposed to CO at 1 atm and 20 °C it turned to a burgundy colored complex $(Me_3SiC_5H_4)_3UCO$, which under vacuum or purging with argon gave back the original green colored complex. Examination of the IR spectrum of the burgundy solution using ^{12}CO showed ν_{CO} at 1976 cm^{-1}, with ^{13}CO ν_{CO} at 1935 cm^{-1}, and with ^{18}CO ν_{CO} at 1976 cm^{-1} [146]. The $(Me_3SiC_5H_4)_3U$ also reversibly absorbs ^{12}CO in the solid state. Exposure of $(Me_3SiC_5H_4)_3U$ in a KBr wafer to ^{12}CO at 1 atm results in the appearance of an absorption at 1969 cm^{-1}, which completely disappears when the sample is evacuated for 1.5 h. Using ^{13}CO (99%) causes the absorption to shift to 1922 cm^{-1}. To study the effect of substituents on the Cp ring, another few uranium carbonyl complexes with different substituted cyclopentadienyl ligands were synthesized [74, 147]. Both structural and spectroscopic studies indicate that in these complexes a strong degree of metal-to-ligand back donation occurs. The only complex which has been structurally characterized is $(\eta^5\text{-}C_5Me_4H)_3U(CO)$ (Fig. 12), which shows evidence of metal-to-ligand back donation with the presence of short $U–C_{CO}$ bond distances of 2.383(6) Å. Comparison of the υ_{CO} stretching frequencies for a series of compounds with different substituents on the ligand (Table 5) demonstrates that electron-donating groups on the ring increase the electron density at the metal center, increasing metal-to-ligand back donation. The ν_{CO} stretching lies in the order 1,3-$(Me_3Si)_2C_5H_3$ > $Me_3SiC_5H_4$ > $Me_3CC_5H_4$ > C_5Me_4H, which indicates $(C_5Me_4H)_3U$ is the best π-donor in this series of metallocenes.

Table 4 Comparative data for the trivalent uranium(III) complexes containing azine ligands

Complexes	Bond distance			Bond angle		Refs.
	U–N (Å)	U–C (Å)	U–Cp* (Å)	Cp–U–Cp (°)	Cp–U–N (°)	
$(C_5H_4$–*t*-Bu$)_3$U(pyridine)	2.665(6)	2.84(7)	2.570(3)	116.6–117.8	95.0–103.0	[145]
$(C_5H_4SiMe_3)_3$U(pyridine)	2.683(8)	2.82(4)	2.55(1)	114.5–118.9	96.4–100.9	[145]
$(C_5H_4$–*t*-Bu$)_3$U(picoline)	2.665(7)	2.83(7)	2.568(1)	116.2–117.8	95.6–102.9	[145]
$(C_5H_4SiMe_3)_3$U(lutidine)	2.646(4)	2.82(3)	2.55(2)	117.2–117.5	96.0–103.8	[145]
$(C_5H_4SiMe_3)_3$U(pyrimidine)	2.688(7)	2.81(3)	2.540(8)	115.6–119.0	94.9–102.9	[145]
$(C_5H_4SiMe_3)_3$U(dimethylpyrazine)	2.656(6)	2.81(3)	2.54(2)	117.4–117.6	96.2–13.2	[145]

* Centroid of the cyclopentadienyl ring

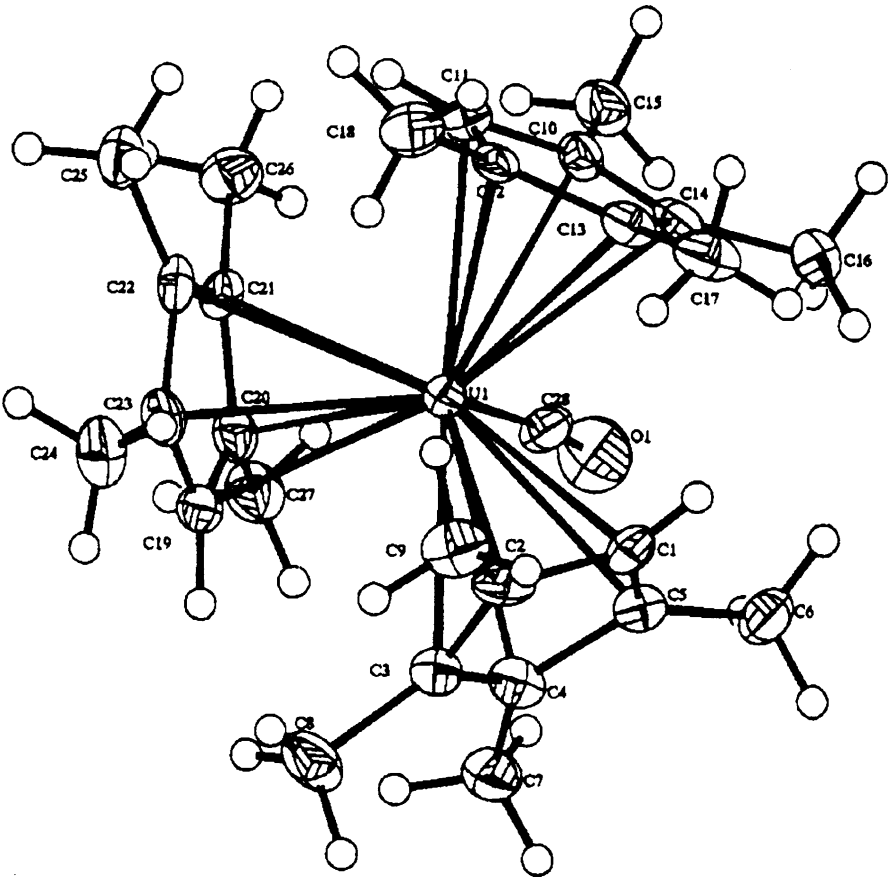

Fig. 12 Molecular structure of $(C_5Me_4H)_3U(CO)$ [147]. Reprinted with permission from [147]; © (1995) American Chemical Society

Table 5 υ(CO) frequencies of various U(III) complexes of the type $[U(\eta^5\text{-}C_5H_{5-n}R_n)_3CO]$

Complexes	State	$\nu_{CO}(cm^{-1})$	Refs.
$(\eta^5\text{-}C_5Me_4H)_3U(CO)$	Nujol	1880	[74]
$(\eta^5\text{-}Me_3CC_5H_4)_3U(CO)$	Hexane	1960	[74]
$(\eta^5\text{-}Me_3SiC_5H_4)_3U(CO)$	Hexane	1976	[74]
	KBr	1969	
$[\eta^5\text{-}(Me_3Si)_2C_5H_3]_3U(CO)$	Methylcyclohexane	1988	[74]

For the heavier actinides the situation is little bit different as the energy of the 6*d*-orbitals drops across the series and hence the metal–ligand interactions become weaker. This is consistent with the report that plutonium forms less robust adducts compared to its lower actinide analogs. The com-

plex $(\eta^5\text{-}C_5H_5)_3Pu(THF)$ could be isolated from solution, and the THF was removed by sublimation [53]; whereas in the analogous uranium compound, THF remains intact upon sublimation [55].

Different organic isocyanides adducts of uranium(III) metallocenes of the type $[(R'_nC_5H_{5-n})_3U(CNR)]$ have been isolated [74], where R′ = H, Me, Me_3Si, Me_3C and R = Et; R′ = $(1,3\text{-}(Me_3Si))_2$ and R = *t*-Bu; or R′ = Me_4 and R = 4-$(MeO)C_6H_4$, CH_3, *i*-Pr, *t*-Bu and 2,6-$Me_2C_6H_3$. All of the isocyanide complexes were made by the addition of an excess of CNR to the $[(R'_nC_5H_{5-n})_3U]$ complex in hexane, toluene or diethyl ether (Eq. 32):

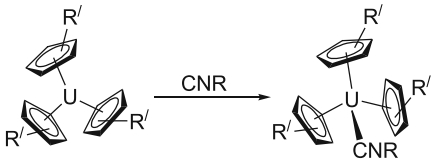

R' = H, Me, Me_3Si, Me_3C and R = Et;
R' = $\{1,3\text{-}(Me_3Si)\}_2$, Me_4 and R = *t*-Bu;
R' = Me_4 and R = Me, *i*-Pr, 4-$(MeO)C_6H_4$ and 2,6-$Me_2C_6H_3$;
R' = Me and R = 2,6-$Me_2C_6H_3$ (32)

All the isocyanides have 1 : 1 stoichiometry with the exception of MeC_5H_4 and R = 2,6-$Me_2C_6H_3$ for which both the 1 : 1 and 1 : 2 adducts were obtained. Table 6 lists the isocyanide complexes and the ν_{CNR} frequencies in the infrared spectrum. The IR spectra showed that ν_{CN} increased slightly for the alkyl isocyanide complexes and decreased slightly for the aryl isocyanide complexes relative to ν_{CN} for the free ligands. The substituents on the cyclo-

Table 6 IR data of different cyclopentadienyl U(III) isocyanide complexes [74]

Complex	ν_{CN} [a]
$(C_5H_5)_3U(CNEt)$	2170
$(MeC_5H_4)_3U(CNEt)$	2155
$(MeC_5H_4)_3U(CNXyl)$	2060
$(MeC_5H_4)_3U(CNXyl)_2$	2095
$(Me_3SiC_5H_4)_3U(CNEt)$	2178
$(Me_3CC_5H_4)_3U(CNEt)$	2180
$\{1,3\text{-}(Me_3Si)_2C_5H_3\}_3U(CNBu\text{-}t)$	2140
$(Me_4C_5H)_3U(CNMe)$	2165
$(Me_4C_5H)_3U(CNPr\text{-}i)$	2143
$(Me_4C_5H)_3U(CNBu\text{-}t)$	2127
$(Me_4C_5H)_3U(CNC_6H_4\text{–}p\text{–}OMe)$	2072
$(Me_4C_5H)_3U(CNXyl)$	2052

[a] In nujol mull, cm^{-1}

pentadienyl ligand also affect ν_{CN}, and for a given isocyanide the ν_{CN} values follow the order $Me_3C \approx Me_3Si \approx (Me_3Si)_2 > H > Me > Me_4$. To compare the ν_{CN} stretching frequencies between the 4*f* and 5*f* series it is worth mentioning here that for a given adduct, ν_{CN} for the uranium complex is always less than that of its cerium analog. This comparison clearly shows that uranium in the trivalent complexes is a better π-donor than its cerium analog.

2.7 Beyond the Tris-Cp Complexes

There exist relatively few examples of trivalent actinide complexes with two cyclopentadienyl rings. Compounds of the parent cyclopentadienyl ion are somewhat rare. Examples include the reported compounds $(\eta^5\text{-}C_5H_5)_2$ ThCl [52] and $(\eta^5\text{-}C_5H_5)_2$BkCl [59] that exist as dimers. The compounds $(\eta^5\text{-}C_5H_4Me)_2NpI(THF)_3$ and $(\eta^5\text{-}C_5H_4Me)NpI_2(THF)_3$ were prepared by reactions of $NpI_3(THF)_4$ with $Tl(C_5H_4Me)$ in tetrahydrofuran [148].

A cationic bis(pentamethylcyclopentadienyl)uranium(III) complex has been reported by Ephritikhine and coworkers [149]. The complex $[(\eta^5\text{-}C_5Me_5)_2U(THF)_2][BPh_4]$ is generated by the protonation of the complex $(\eta^5\text{-}C_5Me_5)_2U[N(SiMe_3)_2]$ with $[NH_4][BPh_4]$.

Cendrowski-Guillaume et al. reported the synthesis of a mixed cyclopentadienyl/cyclooctatetraenyl complex [U(COT)(Cp*)(HMPA)] (where COT = $\eta\text{-}C_8H_8$, HMPA = $OP(NMe_2)_3$) [150] by the treatment of $[U(COT)(HMPA)_3][BPh_4]$ with KCp*. The complex [U(COT)(Cp*)(HMPA)] was characterized crystallographically and was found to adopt trigonal configuration as shown

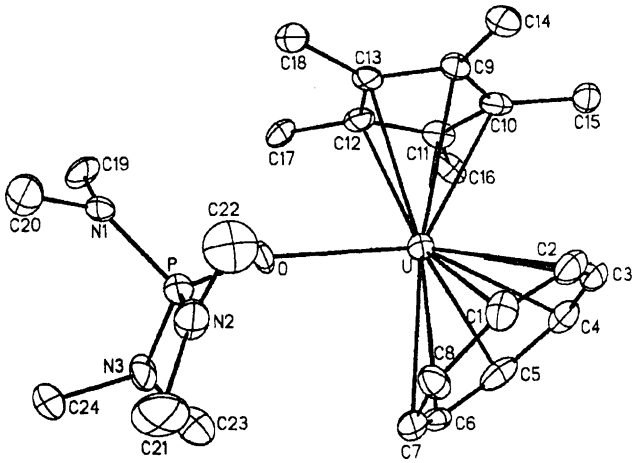

Fig. 13 Molecular structure of $[U(\eta\text{-}C_8H_8)(Cp^*)\{OP(NMe_2)_3\}]$ [150]. Reproduced with permission

in Fig. 13. The U–O, U–COT(centroid) and U–Cp*(centroid) bond distances were found to be 2.461(8), 2.01(1), and 2.50(1) Å, respectively.

Recently some mono- and bis(cyclopentadienyl) compounds $[(C_5H_4–t\text{-}Bu)UI_2]$ and $[(C_5H_4–t\text{-}Bu)UI]$ were synthesized by comproportionation reactions of $[U(C_5H_4–t\text{-}Bu)_3]$ and $[UI_3(L)_4]$ (where L = THF or py) in the molar ratio of 1 : 2 and 2 : 1, respectively. The treatment of $[UI_3(py)_4]$ with one or two molar equivalents of $LiC_5H_4–t\text{-}Bu$ in THF afforded the $[(C_5H_4–t\text{-}Bu)UI_2]$ and $[(C_5H_4–t\text{-}Bu)_2UI_2]$ compounds, respectively (Scheme 11) [151].

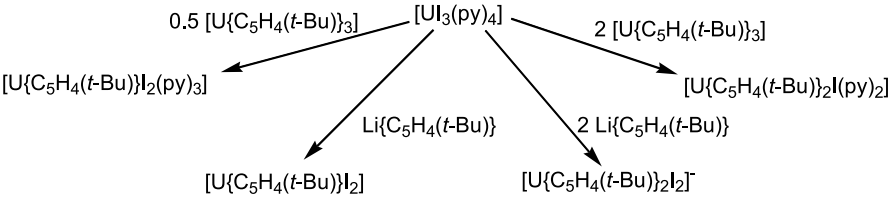

Scheme 11 Synthesis of various mono- and di-cyclopentadienyl complexes by comproportionation reaction [150]

The complex $[U(C_5H_4–t\text{-}Bu)I_2(py)_3]$ was characterized by X-ray crystallography and the average U–C, U–I and U–N bond distances were found to be 2.80(5), 3.17(2), and 2.66(5) Å, respectively. On investigating the affinity of cyclopentadienyl ligand, $(C_5H_4\text{-}t\text{-}Bu)$, towards Ln(III) (Ln = La, Ce, Nd) and U(III), it was reported that the U(III) center is relatively more prone to coordinate the cyclopentadienyl ligand [151].

Investigating the mix ligand complexes, Summerscales et al. discovered that the U(III) COT^R/Cp mixed sandwich complex $[U(\eta\text{-}C_8H_6\{Si\text{-}i\text{-}Pr_3\text{-}1,4\}_2)(Cp^*)(THF)]$ induces efficient cyclotrimerization of CO to give $[U(\eta\text{-}C_8H_6\{Si\text{-}i\text{-}Pr_3\text{-}1,4\}_2)(Cp^*)]_2(\mu\text{-}\eta^1\text{:}\eta^2\text{-}C_3O_3)$ [152].

Roger et al. reported [153] the synthesis of mixed cyclopentadienyl/dithiolene complexes and compared the structural parameters with the analog lanthanide complexes. The treatment of $[(Cp^*)_2UCl_2]$ with Na_2dddt in THF afforded the complex $[(Cp^*)_2UCl(dddt)Na(THF)_2]$, which upon treatment in toluene afforded the salt-free compound $[(Cp^*)_2U(dddt)]$ (dddt = 5,6-dihydro-1,4-dithiin-2,3-dithiolate). Reduction of $[(Cp^*)_2U(dddt)]$ with Na/Hg or addition of Na_2dddt to $[(Cp^*)_2UCl_2Na(THF)_x]$ in the presence of 18-crown-6 gave $[Na(18\text{-crown-}6)(THF)_2][(Cp^*)_2U(dddt)]$. The crystal structures of $[(Cp^*)_2U(dddt)]$, $[Na(18\text{-crown-}6)(THF)_2][(Cp^*)_2U(dddt)]\cdot THF$ were determined by X-ray diffraction analysis and a few selected parameters around the U center are given in Table 7.

To carry out a comparative study of structural features, magnetic properties, and reactivities of the lanthanides(III) and actinides(III), Mehdoui et al. [154] reported the synthesis of complexes of the type $[(Cp^*)_2MI(bipy)]$

Table 7 Selected crystal data, bond lengths (Å) and bond angles (°) in $[(Cp^*)_2U(dddt)]$ and $[Na(18\text{-crown-6})(THF)_2][(Cp^*)_2U(dddt)]\cdot THF$ [153]

	$[(Cp^*)_2U(dddt)]$	$[Na(18\text{-crown-6})(THF)_2][(Cp^*)_2U(dddt)]\cdot THF$
Crystal system	Orthorhombic	Triclinic
Space group	*P*nma	*P*I
U–S(1)	2.629(3)	2.7807(16)
U–S(2)	2.650(3)	2.7661(17)
U–Cp*(av)	2.73(2)	2.79(2)
Cp*–U–Cp*[a]	133.1	135.7
S(1)–U–S(2)	78.93(12)	76.24(5)

[a] Centroid

(where M = Ce, U; bipy = 2, 2′-bipyridine) by the treatment of $[(Cp^*)_2CeI]$ or $[(Cp^*)_2UI(py)]$ with one equivalent of bipy in THF. These complexes were found to be further transformed into $[(Cp^*)_2M(bipy)]$ (where M = Ce, U) by Na(Hg) reduction. On the other hand, the reaction of $[(Cp^*)_2CeI]$ or $[(Cp^*)_2UI(py)]$ with one equivalent of terpy (terpy = 2, 2′:6′, 2″-terpyridine) in THF afforded the ionic complex $[(Cp^*)_2M(terpy)]I$ (where M = Ce, U), which on reduction by Na(Hg) afforded the neutral complexes $[(Cp^*)_2M(terpy)]$ (where M = Ce, U) [154].

The uranium(III) complexes $[\eta^5\text{-}1,3\text{-}R_2C_5H_3]_3U$ react stoichiometrically with one equivalent of water to produce complexes of the type $\{[\eta^5\text{-}1,3\text{-}R_2C_5H_3]_2U(\mu\text{-}OH)\}_2$ (where R = Me_3Si or Me_3C) [155], which upon heating undergo an unusual "oxidative elimination" of hydrogen to yield the corresponding μ-oxo complexes. The kinetics of this process has been examined, and the reaction was found to be intramolecular, probably involving a stepwise α-elimination of hydrogen.

The triiodide complex $UI_3(THF)_4$ was found to be a valuable starting reagent in generating mono(cyclopentadienyl) uranium(III) complexes [156]. Reaction of one equivalent of $UI_3(THF)_4$ with $K(C_5Me_5)$ results in the formation of the complex $(\eta^5\text{-}C_5Me_5)UI_2(THF)_3$ (**9**). In the solid state this complex (**9**) exhibits a pseudo-octahedral *mer, trans*-geometry, with the cyclopentadienyl group occupying the axial position:

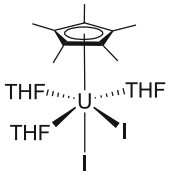

(**9**)

In the presence of excess pyridine, this complex can be converted to the analogous pyridine adduct, $(\eta^5\text{-}C_5Me_5)UI_2(py)_3$. The complex $(\eta^5\text{-}C_5Me_5)UI_2(THF)_3$ was found to be very reactive and generated the bis(ring) product $(\eta^5\text{-}C_5Me_5)_2UI(THF)$ by reaction with $K(C_5Me_5)$, or with two equivalents of $K[N(SiMe_3)_2]$ produced $(\eta^5\text{-}C_5Me_5)U[N(SiMe_3)_2]_2$. The solid state structure of the bis(trimethylsilyl) amide derivative reveals close contacts between the uranium center and two of the methyl carbons (2.80(2), 2.86(2) Å).

Oxidation of $(\eta^5\text{-}C_5Me_5)UI_2(THF)_3$ with CS_2 or ethylene sulfide produces a complex of the formula $[(\eta^5\text{-}C_5Me_5)UI_2(THF)_3]_2(S)$. This species undergoes slow decomposition in solution to yield a polynuclear complex (**10**) [157]:

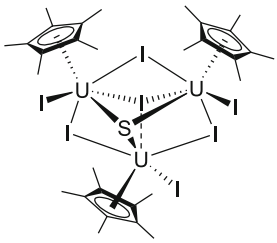

(**10**)

3 Tetravalent Chemistry

It is not surprising that the cyclopentadienyl ligands also dominate the tetravalent chemistry of the early actinide elements. Complexes of the type $(\eta^5\text{-}C_5H_5)_4An$ (where An = Th [158], Pa [159], U [42], and Np [160]) were the earliest actinide complexes with the tetrakis(cyclopentadienyl) ligand. Among these, the uranium and thorium compounds have been structurally characterized [161, 162]. Moreover, IR spectral and X-ray powder data confirm that all four complexes are isostructural. $(\eta^5\text{-}C_5H_5)_4U$ is found to be psuedotetrahedral, with a mean $U\text{–}C_{ring}$ bond distance of 2.81(2) Å. This is somewhat longer than average $U\text{–}C_{ring}$ distances for other U(IV) cyclopentadienyl complexes and reflects a degree of steric crowding. In 1986, Rebizant and coworker reported a related thorium complex containing the tetrakis(indenyl) ligand [163], in which the thorium atom is not bonded in η^5 fashion to the carbons of the five-membered ring portion of the indenyl ligand.

Once a complex has been synthesized, the next major challenge for the researcher is to find out the nature of bonding. Working on this, Burns et al. reported that in comparison to the lanthanides these complexes ex-

hibits more covalency in chemical bonding; unlike lanthanides they do not react with $FeCl_2$ to form ferrocene, but are still believed to be more ionic than the majority of *d*-transition metal cyclopentadienyl complexes [78]. The isolation of these tetrakis(cyclopentadienyl) complexes carved the path for the researchers to peep inside the chemistry of the actinide(IV) complexes. Reynolds and Wilkinson [2] were the pioneers reporting the preparation of $(\eta^5\text{-}C_5H_5)_3UCl$, the first complex of the type Cp_3AnX, by the reaction of uranium tetrachloride with sodium cyclopentadienide in tetrahydrofuran. Following this, the chemistry was extended to prepare other actinide complexes of this class [164, 165]. Later, alternative routes were also reported for the synthesis of the complex $(\eta^5\text{-}C_5H_5)_3UCl$ by the reaction of actinide halides with cyclopentadienyl thallium in DME (Eq. 33) [166]:

$$AnCl_4 + 3(C_5H_5)Tl \xrightarrow{DME} \eta^5\text{-}(C_5H_5)_3AnCl + 3TlCl \qquad (33)$$

Following this, to study the bonding and geometry of these kind of organoactinide complexes, a plethora of complexes of the type $[(R_nC_5H_{5-n})_3AnX]$ were synthesized and characterized structurally. Most of the tris(cyclopentadienyl)uranium halides were prepared by the reaction of uranium tetrachloride and a stoichiometric amount of either sodium or potassium salt of an appropriately substituted cyclopentadiene, generated in situ [2, 167–169]. The drawbacks of this procedure were the lack of careful control of stoichiometry and polymer formation resulting from the use of excess cyclopentadiene in the preparation of the alkali metal salt. To overcome these drawbacks, Anderson et al. [170] reported the synthesis of $(C_5H_5)_3UCl$ by the reaction of uranium tetrachloride and a stoichiometric amount of thallous cyclopentadienide in a suitable solvent. Later, a similar method was used to prepare $(C_5H_4CH_2C_6H_5)_3UCl$ [171]. In an attempt to obtain hydrocarbon-soluble complexes of thorium and uranium, bulky substituted tris(cyclopentadienyl)thorium(IV) or uranium(IV) halides were prepared by the ready transmetallation between MCl_4 (M = Th or U) and the appropriate lithium cyclopentadienyl [172]. On investigating the limiting factors of steric hindrance around the actinide metal center and sterically induced reduction chemistry, Evans et al. [173] could have synthesized Cp^*_3UCl, by the controlled reaction of Cp^*_3U with one equivalent of PhCl (Eq. 34):

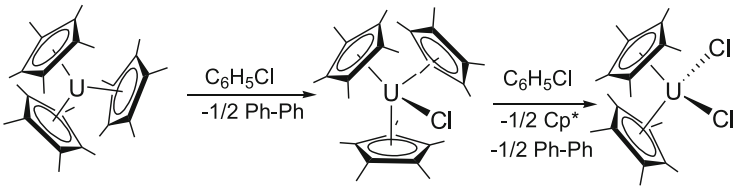

(34)

The molecule Cp^*_3UCl is considered to be a sterically highly crowded complex since the U^{4+} center is relatively small and is bonded to four ligands. Upon addition of another equivalent of PhCl, the complex Cp^*_3UCl subse-

quently forms $Cp^*_2UCl_2$ over several days (Eq. 34). Once the existence of the Cp^*_3UCl was established, several synthetic routes were developed [173, 174], as shown in Scheme 12. The fluorine analog of this complex was also isolated and readily synthesized by the reaction of Cp^*_3U with HgF_2. Although the bromide and iodide analog of this complex have been synthesized by the reaction of Cp^*_3U with PhX (X = Br, I) and analyzed spectroscopically, they have not yet been characterized crystallographically [173].

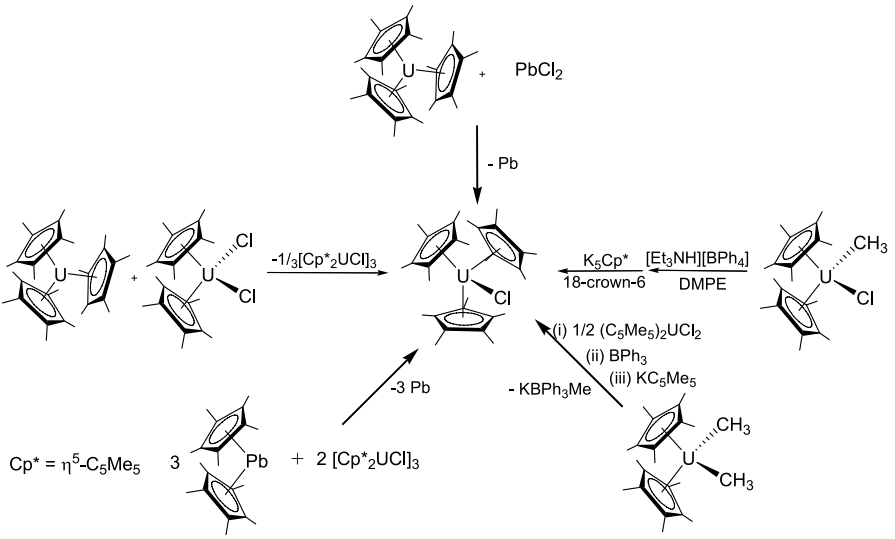

Scheme 12 Various synthetic routes towards Cp^*_3UCl [173, 174]

The existence and isolation of $(C_5Me_5)_3UCl$ (Fig. 14) clearly indicates that this class of complexes has not yet reached the limits of steric crowding. The structure of $(C_5Me_5)_3UCl$ was found to be rather similar to that of $(C_5Me_5)_3U$, as shown by the overlay of the two structures in Fig. 15 [94]. From Fig. 15 it is evident that in $(C_5Me_5)_3U$ [85] and $(C_5Me_5)_3UCl$ the ring centroids are coplanar, and that they also crystallize in the same space group $P6_3/m$. A molecular mirror plane bisects the three symmetry-equivalent C_5Me_5 rings, and the chloride ligand is disordered on either side. The U–C(C_5Me_5) bond distances fall within the range 2.780(6)–2.899(9) Å and average 2.833(9) Å. They are equivalent within experimental error to those of $(C_5Me_5)_3U$ (2.857(4) Å) and $(C_5Me_4H)_3UCl$ (2.791(12) Å) [175]. Thus, the chloride ligand does not appear to perturb the U–C(C_5Me_5) parameters, but the U–Cl bond of 2.90(1) Å is exceptionally longer than those in $(C_5Me_4H)_3UCl$ [175] (2.637 Å) and in $(C_4Me_4P)_3UCl$ (2.67(1) Å) [85, 176] (Table 8).

Apart from the cyclopentadienyl ligand, complexes with other ligands have also been reported. The tris(indenyl)uranium and tris(indenyl)thorium

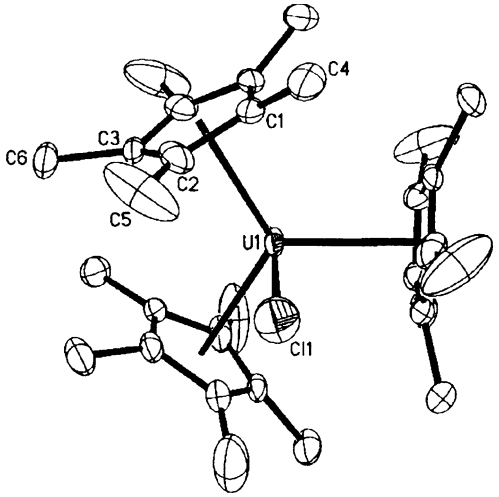

Fig. 14 Crystal structure of $(\eta^5\text{-}C_5Me_5)_3UCl$ [173]. Reprinted with permission from [173]; © (2000) American Chemical Society

complexes have been prepared by the metathesis reactions with $K(C_9H_7)$ in THF [167, 177–179], but in this review we have decided to restrict our discussion only to the cyclopentadienyl complexes.

The molecular structure of several tri(cyclopentadienyl)AnX complexes have been structurally determined. The structure of these complexes was found to possess pseudotetrahedral geometry, with the halide ligand on an approximate threefold axis of symmetry. To study the structural correlativity, the average M–C and M–X bond distances are tabulated (Table 8) for most of the common complexes of this class. The An–C and An–X bond lengths are consistent in most of the complexes for a particular metal center and in com-

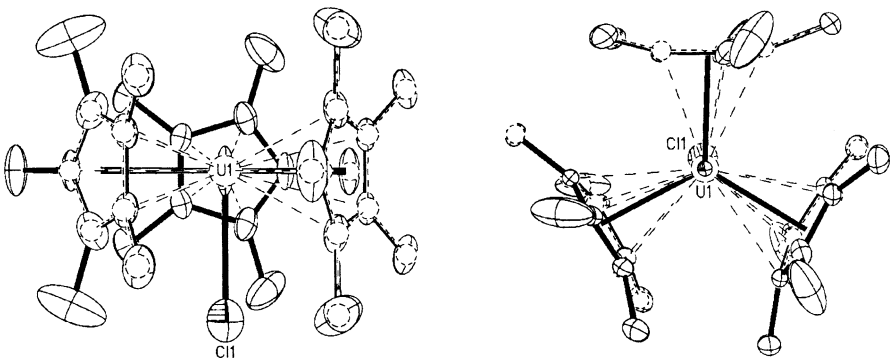

Fig. 15 Overlay drawing of $(C_5Me_5)_3U$ (- -) and $(C_5Me_5)_3UCl$(-) [94]. Reprinted with permission from [94]; © (2002) American Chemical Society

Table 8 Structural information for Cp_3AnX complexes

Complexes	Bond length		Bond angle			Refs.
	M–C_{Cp} (average) (Å)	M–X (Å)	Cp(2)–U–L (°)	Cp(1)–U–L (°)	Cp(3)–U–L (°)	
$(\eta^5\text{-}C_5H_5)_3UCl$	2.74	2.559(16)	101.28	101.42	99.30	[67]
$(\eta^5\text{-}C_5H_5)_3UBr$	2.72(1)	2.820(2)	101(1)	99.7(4)	101.0(8)	[168]
$(\eta^5\text{-}C_5H_5)_3UI$	2.73(3)	3.059(2)	101.3(6)	100.9(6)	100.0(6)	[169]
$(\eta^5\text{-}C_5H_4CH_2Ph)_3UCl$	2.733(1)	2.627(2)	101.2	99.9	98.8	[171]
$[\eta^5\text{-}(Me_3Si)_2C_5H_3]_3UCl$	2.77(1)	2.614(2)	116.6	118.0	116.4	[128]
$(\eta^5\text{-}C_5Me_4H)_3UCl$	2.79(1)	2.637	98.45	98.45	98.45	[175]
$(\eta^5\text{-}C_5Me_5)_3UF$	2.829(6)	2.43(2)	90.00	90.00	90.00	[173]
$(\eta^5\text{-}C_5Me_5)_3UCl$	2.833(9)	2.90(1)	90.00	90.00	90.00	[173]
$[\eta^5\text{-}(Me_3Si)_2C_5H_3]_3ThCl$	2.84(1)	2.651(2)	116.7	117.6	116.6	[172]
$[\eta^5\text{-}(Me_3Si)_2C_5H_3]_2(C_5Me_5)ThCl$	2.84(2)	2.657(5)	97.8	97.3	99.8	[172]
$[\eta^5\text{-}(SiMe_2\text{–}t\text{-}Bu)_2C_5H_3]_3ThCl$	2.85(1)	2.648(2)	99.4	99.7	100.9	[172]
$\{\eta^5\text{-}[(Me_3Si)_2CH]C_5H_4\}_3ThCl$	2.83(1)	2.664(2)	100.7	101.6	97.0	[172]

parison to U, Th–C and Th–X bond lengths are slightly longer, as expected from their large ionic radii. Among these, the smallest M–X bond length was found for the complex Cp^*_3UF, although it seems to be a sterically very crowded molecule. This difference may be due to the smaller size and higher electron affinity of the F atom.

Discovery of this interesting branch of uranium chemistry has given impetus to develop a similar type of chemistry for the Th(IV) system, as it may be also very interesting to the SIR (sterically induced reduction) processes. However, the synthesis of Cp^*_3ThX-type complexes was not so easy as the precursor Th(III) is much less accessible. Ultimately, the complex Cp^*_3ThH could have been synthesized (Eq. 35) and characterized crystallographically. The crystal structure reveals that it crystallized in the same space group ($P6_3/m$) as that of the complexes Cp^*_3UX (X = Cl, F). The Th–ring centoids distance lies almost in the same range as that of Cp^*_3UX and Cp^*_3U. The Th–H bond distance was found to be 2.00(13) Å, which is the shortest among all the other M–X (where M = U, Th; X = halides) bonds of the similar types of tris-cyclopentadienyl uranium or thorium halide complexes. Later, Berthet et al. reported the synthesis of thermally stable U(IV) hydride complexes, $[\{\eta^5\text{-}(Me_3Si)C_5H_4\}_3UH]$ and $[\{\eta^5\text{-}(Me_3C)C_5H_4\}_3UH]$ [180]:

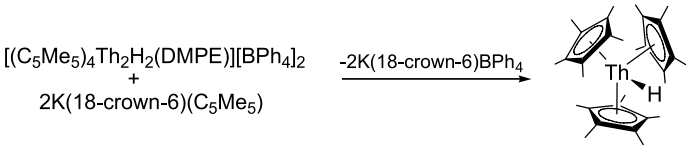

(35)

The existence of the crowded molecule Cp^*_3UX, catalyzed the researchers to find more facts of such type of complexes. A number of derivatives of the class Cp_3AnY (where An = U, Np, Pu; Y = CN, $CNBH_3$, NCS) have been generated either by prototype reactions, include protonation of $(\eta^5\text{-}C_5H_5)_4U$ or by metathesis reaction of $(\eta^5\text{-}C_5H_5)_3AnCl$ (Eqs. 36–37) [121, 181–187]:

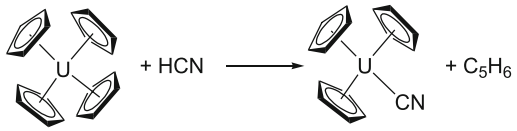

(36)

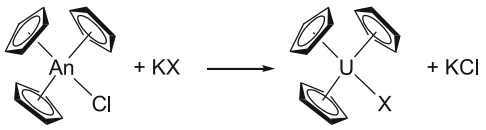

An = U, Np, Pu; X = CN^-, $CNBH_3$, NCS^-

(37)

In the case of the cyanide complexes, the metal–ligand bond is found to be very stable as the reaction of $(\eta^5\text{-}C_5H_5)_3UCl$ with KCN may be carried out in water [186]. The ionization of $(\eta^5\text{-}C_5H_5)_3UCl$ in water yielded the five-coordinate adduct $[(\eta^5\text{-}C_5H_5)_3U(H_2O)_2]^+$ [188]. The isolation of this complex opened the door for the researchers to investigate more about five-coordinated species like $[(\eta^5\text{-}C_5H_5)_3An(XY)]^-$. Bagnall et al. reported the successful synthesis of $[(\eta^5\text{-}C_5H_5)_3An(NCS)_2]^-$ (where An = U, Np, Pu) with a sufficiently large cation like [K(Crypt)] (Crypt = cryptofix-222), NMe_3, or $AsPh_4$ [186]. On the basis of spectrophotometric and other evidences a trigonal-bipyramidal coordination for the metal atoms has been proposed. This proposed structure was further supported by structural characterization of neutral base adducts such as $(\eta^5\text{-}C_5H_5)_3U(NCS)(NCMe)$ [189, 190] or $(\eta^5\text{-}C_5H_5)_3U(NCBH_3)(NCMe)$ [191]. The geometry of these complexes found to be trigonal-bipyramidal, in which the smaller ligands adopt the axial positions. While investigating this series of complexes, the cationic species $[(\eta^5\text{-}C_5H_5)_3U(NCR)_2]^+$ (where R = CH_3, C_2H_5, *n*-C_3H_7 or Ph) were able to isolate as a $[BPh_4]^-$ salt by the reaction of $(\eta^5\text{-}C_5H_5)_3UCl$ with $Na[BPh_4]$ in water/NCR mixtures [190]. Applying the protonolysis reaction to tris(cyclopentadienyl)diethylaminouranium, $[(Cp)_3U(NEt_2)]$, with $[NHEt_3][BPh_4]$ in THF yielded the cationic complex $[(Cp)_3U(THF)]BPh_4$ (Scheme 13) [192], which was easily transformed to its chloride derivative $[(Cp)_3UCl]$ by the addition of NBu_4Cl. Apart from these, a number of mono- and di-cationic species containing mono-, bis-cyclopentadienyl as well as mixed cyclopentadienyl and cyclotetraene complexes have been synthesized.

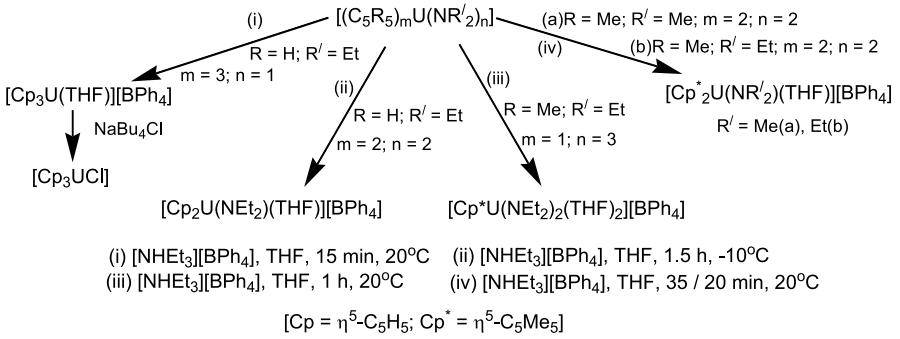

Scheme 13 Synthesis of various cationic uranium complexes [192]

The reaction of tris(cyclopendienyl)uranium chloride with potassium thiocyanate and potassium phenoxide in THF produced $[(\eta^5\text{-}C_5H_5)_3U(NCS)]$ [193] and $[(\eta^5\text{-}C_5H_5)_3U(C_6H_5O)]$ [194], respectively (Scheme 14). The complexes were characterized crystallographically and the bond distances between U–N and U–O were found to be 2.34(2)

and 2.119(7) Å, respectively. Although the complex $[(\eta^5\text{-}C_5H_5)_3U(C_6H_5O)]$ seems to be sterically more hindered, still the U–O bond distance is shorter. The placement of the phenyl ring in it divides the Cp rings into two classes. Two Cp rings are non-planar with the phenyl moiety, while the third one is almost planar (Fig. 16). Complexes $[(\eta^5\text{-}C_5H_5)_3UNCBH_3]$ and $[(\eta^5\text{-}C_5H_5)_3UNCB(C_6H_5)_3]$ were synthesized [184] by the reaction of $[(\eta^5\text{-}C_5H_5)_3UCl]$ with the corresponding anionic borates (Scheme 14). The complexes were characterized spectroscopically and found that they bind to the metal center through the N-donor site.

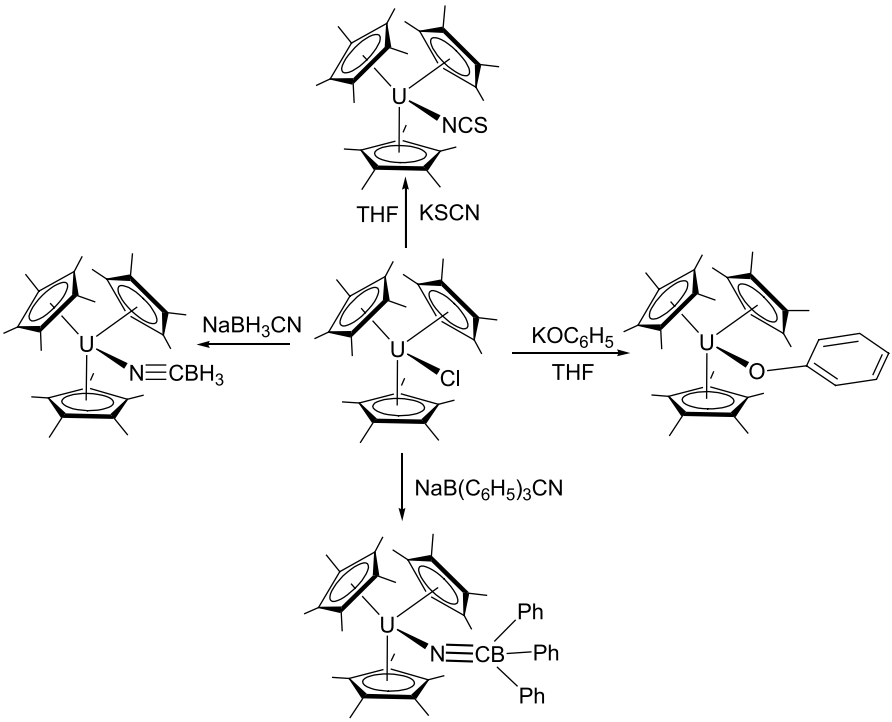

Scheme 14 Various derivatives of Cp_3UCl [184, 193, 194]

By using pyridinium triflate (pyHOTf) the protonolysis to U–C and U–N bonds in $[Cp_3UR]$ (where R = NEt_2, *n*-Bu) afforded triflate complexes $[(Cp)_3U(OTf)]$ and $[(Cp)_2U(OTf)_2(py)]$. Even with the precursor $[(Cp^*)_2UMe_2]$, $[(Cp^*)_2U(OTf)_2]$ (OTf = O_3SCF_3) was yielded [195–197]. The complex $[(Cp^*)_2U(OTf)_2]$ crystallized from THF-pentane solvent system as $[(Cp^*)_2U(OTf)_2(OH_2)]$ and was found to have the usual bent-sandwich configuration with an unsymmetrical arrangement of OTf and H_2O ligands in the equatorial position. In the presence of an excess of *t*-BuCN, the complex

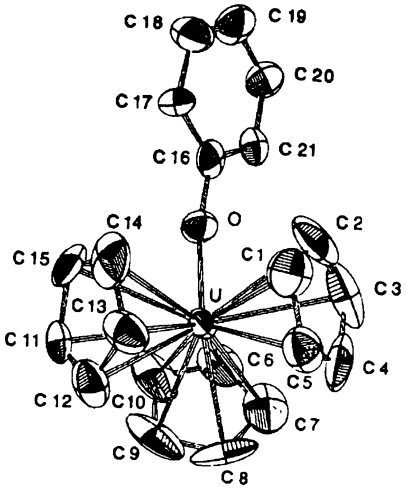

Fig. 16 Crystal structure of $[(\eta^5\text{-}C_5H_5)_3U(C_6H_5O)]$ [194]. Reprinted with permission from IUCr Journals, http://journals.iucr.org

$[(Cp)_3U(OTf)]$ was transformed into $[Cp_3U(OTf)(CNBu\text{-}t)]$. Interestingly, the triflate group was not displaced by the isocyanide molecule (Fig. 17).

It has been found that Cp_3AnX undergo metathesis and protonation reaction with various ligands like alkoxide (OR), amide (NR_2), phosphide (PR_2), and thiolate (SR) groups to generate the complexes of the type $Cp_3An(L)$ [142, 164, 198–201]. The alkyl thiolate complex $[(Cp^*)_3Th(SCH_2CH_2CH_3)_2]$ was synthesized by the reaction of $Cp^*_2ThMe_2$ with HS(*n*-Pr) in toluene. It crystallizes in the monoclinic space group *C*2/c with Th–C bond distance 2.718(3) Å [202]. The complexes of the type $Cp_3U^{(IV)}(SR)$ were prepared by two principal methods namely: (1) substitution of the chloride

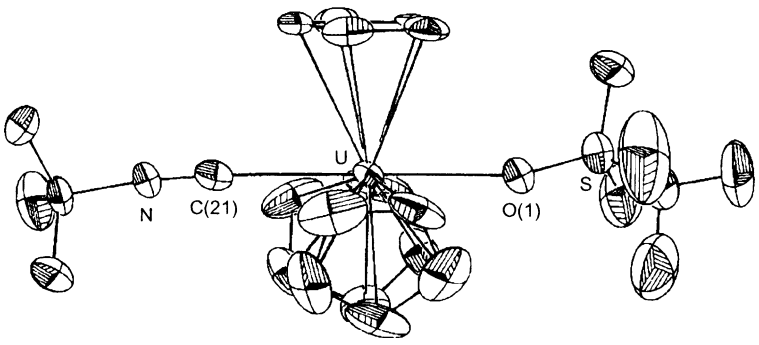

Fig. 17 Crystal structure of $[Cp_3U(O_3SCF_3)(CNBu\text{-}t)]$ [196]. Reproduced with permission from the Royal Society of Chemistry

group of $[(Cp)_3UCl]$ by SR^-, and (2) oxidation of the trivalent precursors $[(Cp)_3U(THF)]$. The method (1) was unsuccessful for the complexes containing the substituted cyclopentadienyl ligands ($C_5H_4SiMe_3$) and (C_5H_4Bu-*t*), hence they were treated with the disulfide RSSR (where R = Me, Et, *i*-Pr, *t*-Bu or Ph). Similarly, $[(Cp)_3U(SeMe)]$ and $[(C_5H_4SiMe_3)_3U(SeMe)]$ were afforded by the treatment of MeSeSeMe with the corresponding U(III) species [142]. Like most of the tris(cyclopentadienyl) complexes of the type Cp_3UX, the crystal structure of $[(Cp)_3U(SMe)]$ (Table 9) adopted pseudotetrahedral geometry. The U–S bond length (2.696(4) Å) and the U–S–C(1) angle, (107.2(5)°) were found to be almost similar to those in other uranium thiolate complexes [203–210]. While discussing the reactivity of $[(Cp)_3U(SPr\text{-}i)]$, it was found that the U–S bond was readily cleaved by various ligands, as shown in Scheme 15.

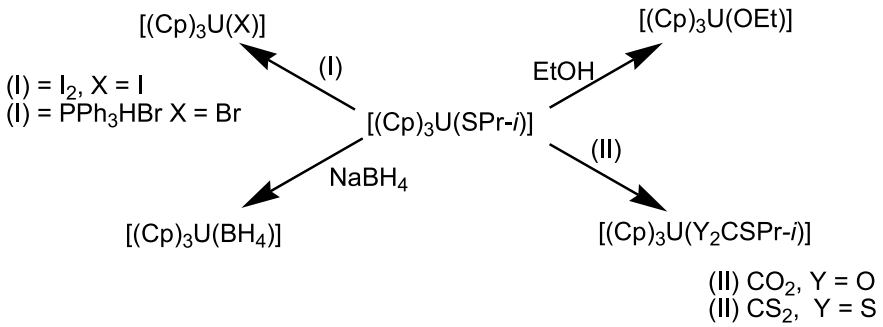

Scheme 15 Reactivity of $[(Cp)_3U(SPr\text{-}i)]$ [142]

Anderson et al. reported [73] the synthesis of the similar type of complexes $[(MeC_5H_4)_3U(SPr\text{-}i)]$ and $[(Me_3CC_5H_4)_3U(SPh)]$ by the reaction of $(MeC_5H_4)_3U(THF)$ with isopropyl thiol and $(Me_3CC_5H_4)_3U$ with HSPh, respectively.

By applying the Mössbauer spectroscopy technique the bonding nature of the Np(IV)–ligand bond was determined for a number of complexes of the type Cp_3NpOR, Cp_3NpR (R = alkyl), and Cp_3NpAr (Ar = aryl) [164]. Strong σ character for the Np–(*n*-Bu) and Np–($C_6H_4C_2H_5$) bonds were found, while in Np–OR it was less pronounced.

An interesting class of complexes, $(\eta^5\text{-}C_5H_5)_3AnR$ (An = Th, U, Np), where R is an alkyl or aryl group, were synthesized by the ligand substitution reaction of $(\eta^5\text{-}C_5H_5)_3AnX$ (X = halide) with Grignard or alkyllithium reagents. An extensive study was carried out by various research groups on the alkyl complexes [174, 211–218]. Many of the complexes have been characterized crystallographically and found to have pseudotetrahedral geometry (Table 10). The coordination environment of these

Table 9 Important bond distances in actinide complexes containing O- or N- or S-donor ligands

Complex	Bond distance (Å)				Refs.
	U–Cp(I) centroid	U–Cp(II) centroid	U–Cp(III) centroid	U–heteroatom	
$[(Cp)_3U(NCS)]$	2.45(4)	2.51(4)	2.47(4)	U–N 2.34(2)	[193]
$[(Cp)_3U(C_6H_5O)]$	2.45(2)	2.47(2)	2.48(2)	U–O 2.119(7)	[194]
$[(Cp)_3U(O_3SCF_3)(CNBu\text{-}t)]$	2.479	2.484	2.482	U–O 2.36(1) U–C 2.59(2)	[196]
$[(Cp)_2U(O_3SCF_3)_2(OH_2)]$	2.439	2.469	–	U–O 2.36(1) U–O 2.40(1) H–O_{H_2O} 2.57(2)	[196]
$[(\eta^5\text{-}C_5H_5)_3U(SMe)]$	2.468	2.477	2.477	U–S 2.696	[142]
$[(Cp)_2U(O_3SCF_3)_2(py)_2]$	2.454(5)	2.466(5)	–	U–O 2.395(4) U–O 2.385(4) U–N 2.685(5) U–N 2.614(5)	[197]

Table 10 Some bond lengths of uranium(IV) complexes containing U–C σ-bond

Complex	Bond distance (Å)		Refs.
	U–Cp average	U–Y	
$[(Cp)_2U\{\mu\text{-}CHP(Ph)_2(CH_2)\}]_2$	2.53 2.46 2.51 2.52	U_1–C_2 2.67(4) U_1–C_3 2.44(4) U_1–C_4 2.55(3) U_2–C_1 2.66(4) U_2–C_3 2.48(4) U_2–C_4 2.41(4)	[236]
$[(Cp)_3UCHP(CH_3)_2(Ph)]$	2.79(3)	U–C 2.29(3)	[238]
$[(Cp)_3U\{(CH_3)C(CH_2)_2\}]$	2.74(1)	U–C 2.48(3)	[219]
$(Cp)_3U(n\text{-}C_4H_9)$	2.728(12) 2.738(15) 2.747(14)	U–C 2.426(23)	[117]
$(Cp)_3U[CH_2(p\text{-}CH_3C_6H_4)]$	2.705(7) 2.742(5)	U–C 2.541(15)	[117]
$(Cp)_3U(CCH)$	2.73(5)	2.339	[217]
$(\eta^5\text{-}C_5Me_5)_3UMe$	2.418 *	2.66(2)	[174]
$(Cp)_4U$	2.81		[218]

* centroid

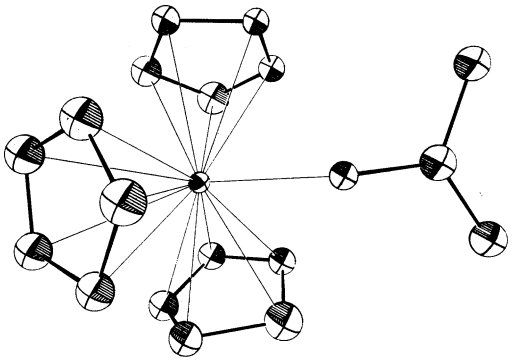

Fig. 18 Crystal structure of $(\eta^5\text{-}C_5H_5)_3U[CH_2C(CH_3)_2]$ [219]. Reprinted with permission from [219]; © (1975) American Chemical Society

complexes was found to be almost saturated as the allyl ligands can only be accommodated in a simple σ-bonded fashion [219], as shown in Fig. 18.

In this class of compounds, particularly with uranium, the metal–carbon bond possesses considerable ionic character. This is evident from the formation of Cp_3UOCH_3 by the reaction of methanol with Cp_3UR, which further confirms the existence of a metal–carbon σ-bond. Marks et al. [214] used NMR spectroscopy to study the nature of bonding in the class of complexes Cp_3UR (where R = CH_3, allyl, neopentyl, C_6F_5, *i*-C_3H_7, *n*-C_4H_9, *t*-C_4H_9, *cis*-2-butenyl, *trans*-2-butenyl, C_6H_5, vinyl). The allyl compound Cp_3U(allyl) was found to adopt the monohapto geometry in ground state at low temperature, but at room temperature it shows fluxional behaviors, presumably interconverting sites by means of π-bonding intermediates. Most of these complexes Cp_3UR (where R = CH_3, allyl, neopentyl, C_6F_5, *i*-C_3H_7, *n*-C_4H_9, *t*-C_4H_9, *cis*-2-butenyl, *trans*-2-butenyl, C_6H_5, vinyl) were found to have high thermal stability, which in turn depends on the nature of the R group. Based on kinetic studies in toluene solution, a general stability order was proposed as: primary > secondary > tertiary [214].

Another interesting σ-bonded organouranium complex containing acetylene or another organometallic moiety has been reported by Tsutsui et al. [215]. Complexes $(Cp)_3U(C\equiv CH)$, $(Cp)_3U(C_5H_4)Fe(C_5H_5)$, $(Cp)_3U(C_5H_4)Fe(C_5H_4)U(Cp)_3$ and $(Cp)_3U(p-C_6H_4)U(Cp)_3$ were synthesized by following the simple metathesis reactions shown in Eqs. 38–41:

$$(Cp)_3U\text{-}Cl + NaC\equiv CH \longrightarrow \begin{matrix} Cp \\ Cp-U-C\equiv CH \\ Cp \end{matrix} + NaCl \qquad (38)$$

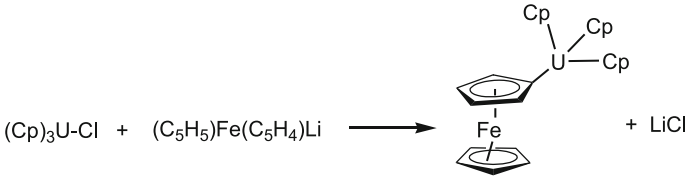

(39)

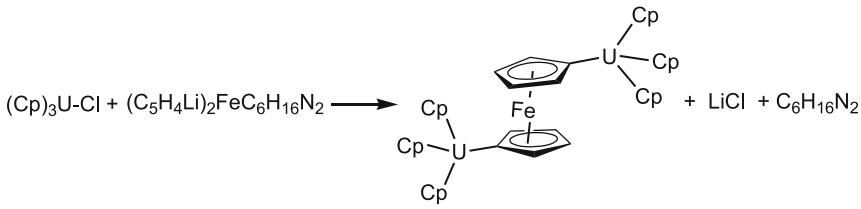

(40)

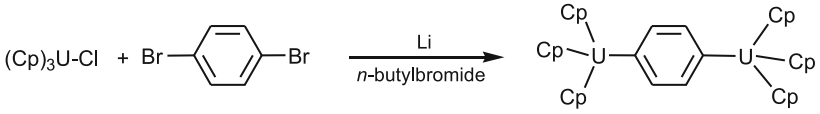

(41)

The complexes with ferrocene were found to be thermally stable in vacuo to at least 180 °C. The decomposed products were only ferrocene, cyclopentadiene, and uranium. This results further supports the mode of decomposition by the proton abstraction by R from a Cp group as suggested by Marks [214].

Complexes of the type $(\eta^5\text{-}C_5H_5)_3U(EPh_3)$ (where E = Si [220, 221], Ge [222]) were prepared by the reaction of $(\eta^5\text{-}C_5H_5)_3UCl$ with $Li(EPh_3)$. The stannyl analog $(\eta^5\text{-}C_5H_5)_3U(SnPh_3)$ was made from the protonolysis of $(\eta^5\text{-}C_5H_5)_3U(NEt_2)$ with $HSnPh_3$ or by the transmetallation reaction of $HSnPh_3$ with $(\eta^5\text{-}C_5H_5)_3U(EPh_3)$ (where E = Si, Ge) [221]. The silyl compound was found to be very reactive and can easily be converted into $(\eta^5\text{-}C_5H_5)_3U(OSiPh_3)$. The η^2-iminoacyl complexes $[(\eta^5\text{-}C_5H_5)_3U\{C(EPh_3) = N(xylyl)\}]$ (E = Si, Ge) were generated by the insertion of xylylisocyanide into the U–E bonds.

The study for the migratory insertion reaction of CO to a series of thorium hydrocarbyls complexes $[(\eta^5\text{-}C_5H_5)_3ThR]$ (where R = *i*-C_3H_7, *sec*-C_4H_9, *neo*-C_5H_{11}, *n*-C_4H_9, $CH_2Si(CH_3)_3$, CH_3, and $CH_2C_6H_5$) shows that η^2-acyl insertion products, $(C_5H_5)_3Th(\eta^2\text{-}COR)$, [223] can be obtained when R = *i*-C_3H_7, CH_3, *n*-C_4H_9, *sec*-C_4H_9 and *neo*-C_5H_{11} (Scheme 16). The structure of these complexes can best be described with the help of a "carbene like" resonance form **A** and **B** (Scheme 16). But when R = *i*-C_3H_7 or $CH_2Si(CH_3)_3$ enolate rearrangement products were isolated (Scheme 16). The relative rates of insertion for the ligands were found to follow the order *i*-Pr > *s*-Bu > *neo*-C_5H_{11} > *n*-Bu > $CH_2Si(CH_3)_3$ > Me > $CH_2C_6H_5$. The relative rates of CO insertion reflect both steric and electronic effects with significant correlation to the

Th-R bond disruption enthalpies. When this correlation was compared with the CO_2 insertion, to generate carbonate complexes, it showed that carboxylation is significantly slower than carbonylation, and exhibits different trends on the dependence of rate on the alkyl ligand [223].

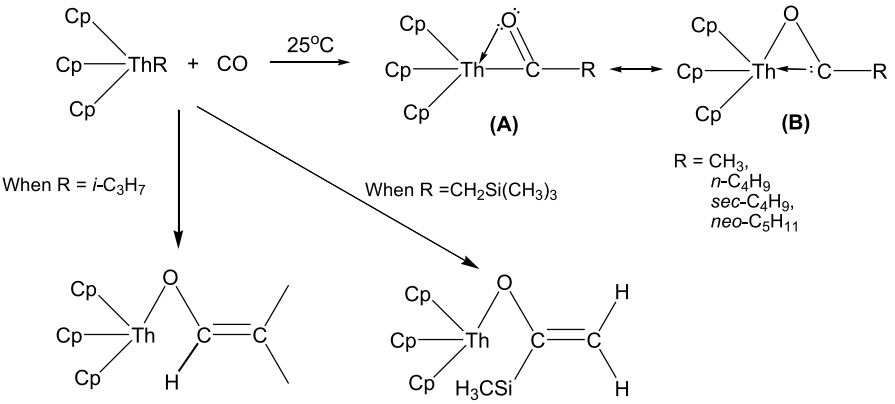

Scheme 16 CO insertion on thorium hydrocarbyls complexes [223]

In a similar manner, uranium complexes of the type $(\eta^5\text{-}C_5H_4R)_3UR'$ (where R′ = CH_3, C_2H_5, *i*-C_3H_7, *n*-C_4H_9, *t*-C_4H_9, $N(C_2H_5)_2$ and even $P(C_6H_5)_2$ and $NCBH_3$) [224, 225] also undergo CO insertion reactions. Mechanistic studies [225] showed that the insertion reaction appears first-order under the conditions of excess CO. The rate of insertion depends on the steric factors of the cyclopentadienyl ring and with different substituent follows the order H > Me > *i*-Pr > *t*-Bu. Interestingly the rate also depends on the identity of the alkyl ligand with an unusual order R′ = *n*-Bu > *t*-Bu > Me > *i*-Pr. The resulting η^2-acyl product was not stable and rearranged to yield alkylbenzenes C_6H_4RR', suggested to arise from ring enlargement of the cyclopentadienyl ligand by incorporation of the CR′ fragment.

Likewise, CO_2 reacts with $(Cp^{\phi})_3UH$ (where $Cp^{\phi} = \eta^5\text{-}C_5H_4SiMe_3$) [226] to afford the formate derivative $(Cp^{\phi})_3UOCHO$, which further reacted with the starting uranium hydride to give the dioxymethylene complex $(Cp^{\phi})_3UOCH_2OU(Cp^{\phi})_3$:

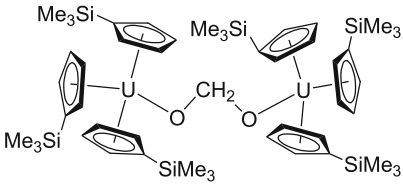

Isoelectronic isocyanide ligands also undergo insertion into uranium–carbon or uranium–nitrogen bonds [227, 228] to yield η^2-iminoalkyl (**11**) and η^2-iminocarbamoyl (**12**) adducts:

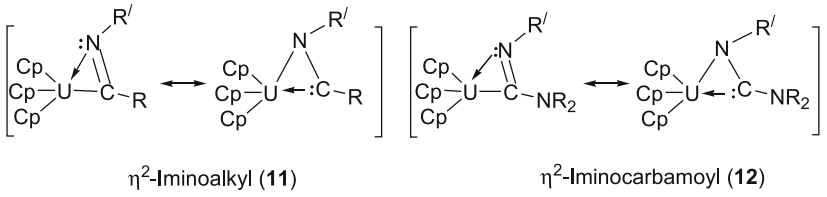

η^2-Iminoalkyl (**11**) η^2-Iminocarbamoyl (**12**)

Cramer et al. synthesized an unusual class of complexes of the type $(\eta^5\text{-}C_5H_5)_3UY$, which contains M–carbon/nitrogen multiple bond character [229–234]. They were also the pioneers in synthesizing the first actinide complexes containing phosphorus ligands (Scheme 17).

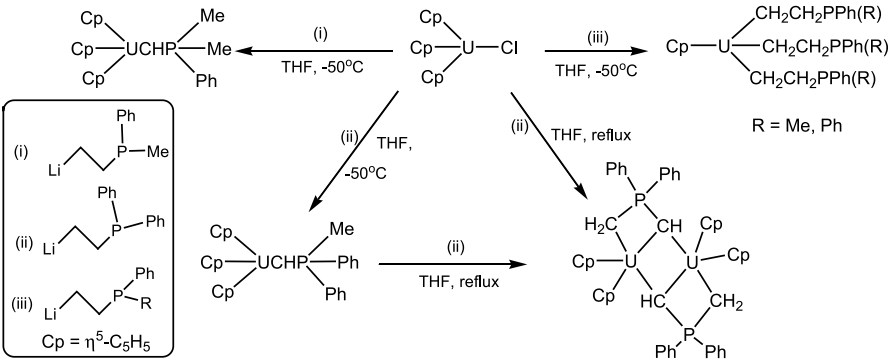

Scheme 17 Synthesis of various uranium phosphorus complexes [236, 238]

Among these, the complex $[\{\mu\text{-}(CH)(CH_2)P(C_6H_5)_2\}U(C_5H_5)_2]_2$ [235, 236] possesses an unusual coordination number for U(IV) and exhibits a unique mode of ylide bonding in which the ligand chelate as well as bridge between two metal centers (Fig. 19). The geometry about the each uranium atom is approximately tetrahedral with a U-U bond distance of 3.810(2) Å (Table 10), which is at the limit of van der Waals interactions (3.8 Å). The U–C bond lengths 2.46(1) and 2.53(2) Å in the U–C–U bridge were within the range of U–C σ-bonds found in several tris(cyclopentadienyl)uranium alkyl complexes like $Cp_3U(CH_2)_2CCH_3$ [219] (2.48 Å), $Cp_3UC_4H_9$ (2.426(23) Å), and $Cp_3UCH_2(p\text{-}CH_3C_6H_4)$ (2.541 Å) [117] (Table 10). Another interesting complex $[(\eta^5\text{-}C_5H_5)_2Th(\eta^5,\eta^1\text{-}C_5H_4)]_2$ was reported which contains an unusual μ-carbon bridge [237], where the cyclopentadienyl group was bonded in the pentahapto fashion towards one of the thorium atom, while to the other it is bonded through a σ-bond.

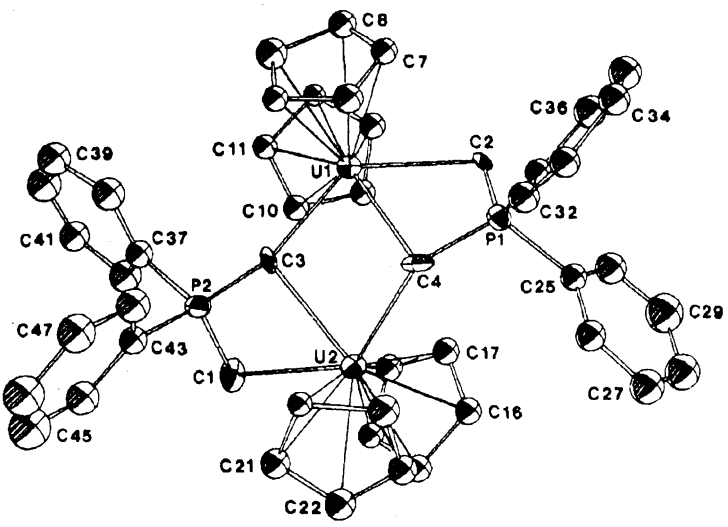

Fig. 19 Crystal structure of $[\{\mu\text{-}(CH)(CH_2)P(C_6H_5)_2\}U(C_5H_5)_2]_2$ [236]. Reprinted with permission from [236]; © (1980) American Chemical Society

Some other interesting uranium(IV) phosphoylide complexes, $Cp_3UCHPMe_2(Ph)$, $Cp_3UCHPMe(Ph)_2$, $CpU[(CH_2)_2P(Ph)_2]_3$, and $CpU[(CH_2)_2P(Me)(Ph)]_3$, were synthesized [238] by the metathesis reaction of Cp_3UCl with LiR (where R = $-CH_2CH_2P(Me)(Ph)$, $-CH_2CH_2P(Ph)_2$) (Scheme 17). The molecular structure of the complex $Cp_3UCHPMe_2(Ph)$ reveals that the uranium is bonded in tetrahedral fashion to three cyclopentadienyl ligands and fourth to the ligand "R" [229, 231]. The U–C bond was found to be the shortest in all these kinds of complexes (Table 10), which suggests multiple bond character. This was explained via the following two resonance forms (**C** and **D**) of the ligand:

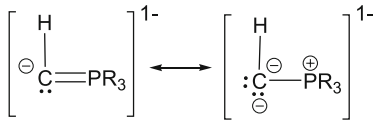

C **D**

In resonance form **D**, the carbon atom carried two pairs of electrons and has a double negative charge. Upon coordination to the metal center Cp_3U^+ the resonance structures **E–G** may be written:

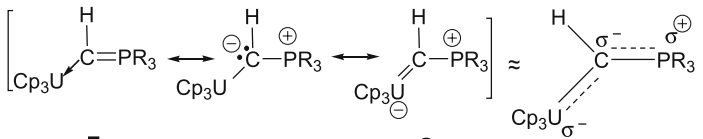

E **F** **G**

Working on this series of compounds, Cramer et al. reported [234] a complex which contains an uranium–nitrogen multiple bond, i.e., an (imido)uranium complex $(C_5H_5)_3UNC(CH_3)CHP(C_6H_5)_2CH_3$ (Eq. 42):

$$Cp_3U{=}CHP(Ph)_2Me + MeCN \xrightarrow[24\ h]{Toluene,\ 55^oC} Cp_3UNC(Me)CHP(Ph)_2Me \quad (42)$$

The U–N bond distance was found to be very short (2.06(1) Å), which suggests the existence of a multiple bond character. On the other hand, the bond angles around the C-atoms attach to the N or P are consistent with sp^2 hybridized state. Therefore, it was suggested that the molecule $(C_5H_5)_3UNC(CH_3)CHP(C_6H_5)_2CH_3$ might have the resonating structures as shown:

$$Cp_3U{\equiv}NC(Me){=}CHP(Ph)_2Me \longleftrightarrow Cp_3U{=}\ddot{N}C(Me){=}CHP(Ph)_2Me$$

$$\longleftrightarrow Cp_3U{=}N{=}C(Me)CH{=}P(Ph)_2Me$$

Their combination implies a highly delocalized π system and an uranium–nitrogen bond order between two and three.

Insertion reactions were extensively investigated in the complexes containing metal–ligand multiple bonds [49, 230, 233, 234, 239, 240]. The complexes $Cp_3U = CHP(CH_3)(C_6H_5)R_1$(**13**) are found to undergo CO insertions to give the complexes of the type $Cp_3U(\eta^2\text{-}OCCH)P(CH_3)(C_6H_5)R_1$(**14**), where R_1 is either CH_3(**14a**) or C_6H_5(**14b**), [230]. The complex $Cp_3U(\eta^2\text{-}OCCH)P(CH_3)(C_6H_5)_2$ was characterized by single crystal X-ray diffraction study and the U–C(1), U–O and U–Cp(av) distances were found to be 2.37, 2.27, and 2.81 Å, respectively. The insertion of Ph–N=C=O to complex **13** gives Cp_3U[(NPh)(O)CCHP(Me)(Ph)R] (**15a**, R = Me; **15b**, R = Ph) [49]. The complex **15a** was structurally characterized and found to have a four-membered chelate ring. The ligand Ph–N=C=O coordinated to the pyramidal Cp_3U^+ unit through its N- and O-coordination sites in such a way that minimized the steric interaction [49]. The U–O and U–N bond distances were found to be 2.34(1) and 2.45(1) Å, respectively, and are consistent with a single bond. The O–C and N–C bond lengths lie between the single and double bonds. In view of these, the bonding in **15** was best described with the help of the following resonating structures:

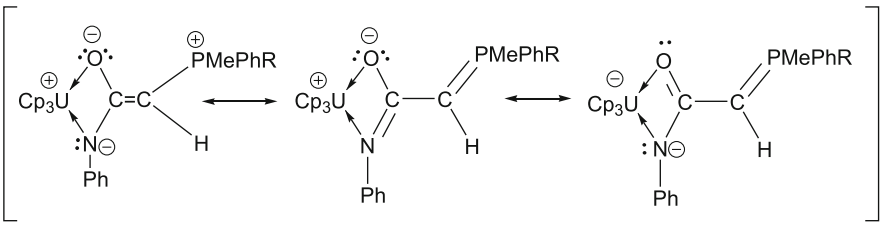

Bimetallic complexes of the type $Cp_n(OC)_mMC(OUCp_3)=CHPMePhR_1$ (M = Mn, n = 1, m = 2 (**16**); M = W, n = 0, m = 5 (**17**); M = Co, n = m = 1 (**18**): R = Me (**18a**), Ph (**18b**)) were synthesized by the insersion of terminal CO from the starting complexes like $CpMn(CO)_3$, $W(CO)_6$ and $CpCo(CO)_2$ to $Cp_3U=CHP(Ph)(R)Me$ respectively [233, 239, 241]. On the basis of the crystal data, the structure of the complex $Cp(CO)_2MnC(OUCp_3)=CHP(Ph)Me$ was best interpreted with the help of the following resonating structures:

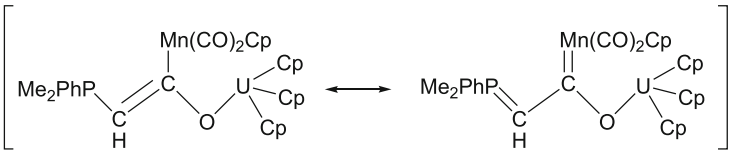

The complexes $(OC)_5WC(OUCp_3)=CHPMe(R)Ph$ undergo isomerization at 90 °C to form $Cp_3UOCH=CHPPh(R)CH_2W(CO)_6$ (**19**), R = Me (**19a**), Ph (**19b**) [239]. Some important bond lengths around the U metal center are given in Table 11.

The reaction between $Cp_3U=CHP(CH_3)(C_6H_5)_2$ and $HN(C_6H_5)_2$ produces $Cp_3UN(C_6H_5)_2$ in good yield [240]. The X-ray structure of $Cp_3UN(C_6H_5)_2$ shows the U–N bond distance of 2.29 (1) Å, which indicates that the U–N bond order is close to two.

The reaction of Cp_3AnCl with $LiNPPh_3$ produces $Cp_3AnNPPh_3$ (An = U or Th). The molecular structure of Cp_3UNPPh_3 was determined by single crystal X-ray crystallography [242] and the geometry around the U and P atoms was found to have the usual tetrahedron orientation. The average U–C(Cp) bond distance, 2.78(2) Å, is in the range reported for other Cp_3U–X type of complexes, but the U–N and U–P bond lengths are significantly shorter compared to the transition metal–phosphine imine complexes. Based on these structural parameters, the bonding in these phosphine imide complexes could only be described with the help of the following resonating structures:

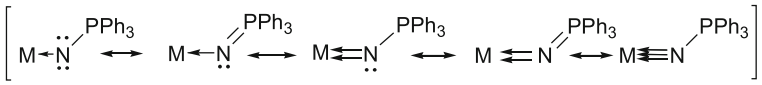

But, when electron delocalization does not occur within the R group of the N atom, the bonding consists of less resonating structures:

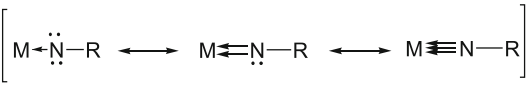

Table 11 Some selected bond lengths of bimetallic complexes of uranium(IV)

Complex	Bond length (Å)				Refs.
	U–Cp(I)	U–Cp(II)	U–Cp(III)	U–Y(1)	
$Cp(OC)_2MnC(OUCp_3)=CHPMe_2Ph$	2.504	2.513	2.495	U–O 2.13(2)	[233]
$(OC)_5WC(OUCp_3)=CHPMePh_2$	2.472	2.516	2.482	U–O 2.15(2)	[239]
$Cp_3UOCH=CHPPh_2CH_2W(CO)_6$	2.465	2.477	2.470	U–O 2.207(9)	[239]
$Cp(OC)CoC(OUCp_3)=CHPMe_2Ph$	2.498	2.496	2.489	U–O 2.08(2)	[241]

After the successful study of many An(IV) tris cyclopentedienyl complexes, chemists looked for some kind of organoactinide complexes that would have less steric hindrance. In view of this, synthesis of biscyclopentadienyl complexes of the type $(\eta^5\text{-}C_5H_5)_2AnX_2$ was explored, although these were difficult to synthesized due to ligand distribution to yield mono- and tris-cyclopentadienyl species [243]. Alternative approaches to generate complexes of this formula have generally involved introduction of the cyclopentadienyl ligands in the presence of other ligands that inhibit redistribution, as in Eqs. 43–45 [244–247]:

$$UCl_4 + 4LiN(C_2H_5)_2 \xrightarrow[-4LiCl]{THF} U(N(C_2H_5)_2)_4 \xrightarrow{2\ \text{C}_5\text{H}_5} (Cp)_2U\{N(C_2H_5)_2\}_2 + 2\ HN(Et)_2 \tag{43}$$

$$UCl_4 + NaBH_4 \xrightarrow[-2NaCl]{} (BH_4)_2UCl_2 \xrightarrow[-2TlCl]{2\ Tl(Cp)} (Cp)_2U(BH_4)_2 \tag{44}$$

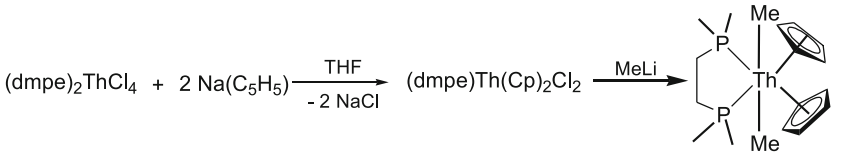

(45)

The complex $[Cp_2U\{N(C_2H_5)_2\}_2]$ reacts with ligands that have protons of more acidic nature than that of diethylamine [244], like toluene-3,4-dithiol, *o*-mercaptophenol, catechol, and 1,2-ethanediol (Eq. 46):

$$Cp_2U[N(C_2H_5)_2]_2 + 2\ H\text{-}X \longrightarrow (Cp)_2U(X)_2 + 2\ HN(C_2H_5)_2 \tag{46}$$

In 1978, Manriquez et al. reported [248] new bis(pentamethylcyc1opentadienyl) derivatives of thorium and uranium, which may be considered as the most chemically reactive and versatile organoactinides prepared up to that time. Following this, a number of communications came out with the

synthesis of successfully stabilizing bis(cyclopentadienyl) complexes involving the use of peralkylated derivatives (C_5Me_5 [249]; C_5Me_4Et [250]). The pentamethylcyclopentadienyl ligand is one of the most widely used ligands in organoactinide chemistry because the incorporation of this ligand substantially increases the stability, solubility, and crystallinity of the obtained compounds. Initial synthetic routes involved alkylation of the metal tetrahalides by Grignard or tin (Eqs. 47–49) reagents:

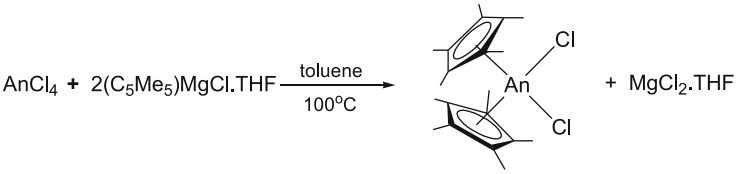

(47)

(48)

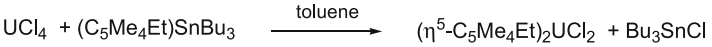

(49)

The molecular structure of many of these dihalide complexes, $(\eta^5\text{-}C_5Me_5)_2UCl_2$ [251], $(\eta^5\text{-}C_5Me_5)_2ThX_2$ (X = Cl, Br, I) [251–253] shows monomeric structures with a pseudotetrahedral, "bent metallocene" geometry having C_{2v} symmetry group.

The dichloride derivative can easily be alkylated with variety of alkyl- and aryllithium reagents to form dialkyl and diaryl complexes (Eq. 50) [249]:

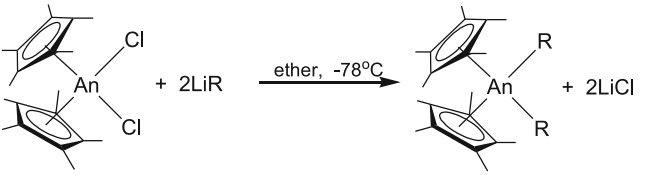

(50)

Recently, Barnea et al. reported the synthesis of $Cp^*_2UMe_2$ by the reaction of $Cp^*_2UCl_2$ with methyl lithium in presence of lithium bromide [254]. The crystal structure of $Cp^*_2UMe_2$ (Fig. 20) was also found to have a similar type of geometry to that of $Cp^*_2AnX_2$.

Apart from the per-substituted cyclopentadienyl ligand, other ligands like $[1,3\text{-}(Me_3Si)_2C_5H_3]$ and $[1,3\text{-}(Me_3C)_2C_5H_3]$ have also drawn attention to the field of organometallic chemistry. Metal complexes containing these ligands

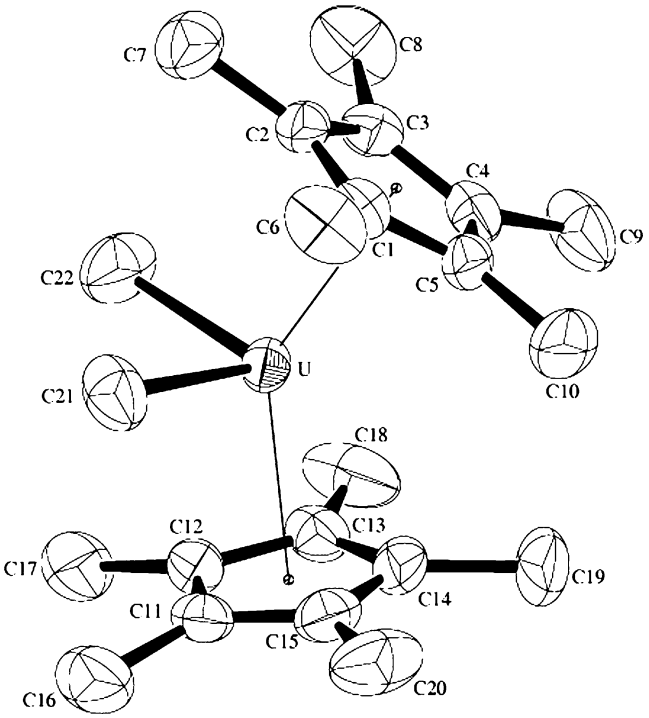

Fig. 20 Crystal structure of $\{[\eta^5\text{-}C_5Me_5]_2UMe_2\}$ [254]. Reprinted with permission from [254]; © (2004) American Chemical Society

have been prepared by reacting metal tetrahalides with the cyclopentadienyl lithium reagents (Eq. 51) [255]:

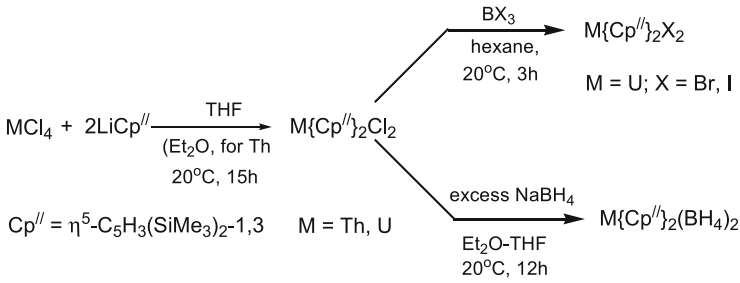

(51)

Luken et al. [122] reported successful synthesis of uranium metallocenes complexes by using magnesocenes as reagents (Scheme 18).

The molecular structures of the complexes $[L_2UX_2]$ (where L = η^5-1,3-$(R_2C_5H_3)_2UX_2$ and R = $SiMe_3$, X = F, Cl, Br; or R = *t*-Bu, X = F, Cl) characterized by single crystal X-ray crystallography and found isostructural with $[\eta^5\text{-}1,3\text{-}(Me_3Si)_2C_5H_3]_2ThCl_2$. Except for the dimeric fluoride complex,

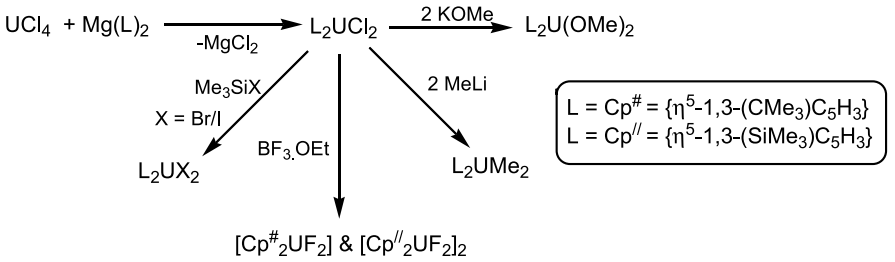

Scheme 18 Synthesis of various uranium metallocene complexes [122]

$\{[\eta^5\text{-}1,3\text{-}(Me_3Si)_2C_5H_3]_2UF(\mu\text{–}F)\}_2$ (Fig. 21), all the other complexes exists as monomers in solid state [122]. But in solution $\{[\eta^5\text{-}1,3\text{-}(Me_3Si)_2C_5H_3]_2UF(\mu\text{-}F)\}_2$ also presents in a monomer–dimer equilibrium form. The complexes Cp_2UX_2 have an idealized C_{2v} structure when X is F, Cl, or Br and a C_2 structure when X is I or Me; the conformations of the substituted Cp ligands are directly related to the radii of the X ligands. Some important bond lengths are given in Table 12.

Although in these complexes the bulky cyclopentadienyl ligands provide kinetic stability, in a limited number of cases base adduct complexes like $(\eta^5\text{-}C_5Me_5)_2UCl_2(pz)$ (pz = pyrazole) [256], $[\eta^5\text{-}1,3\text{-}(Me_3Si)_2C_5H_3]_2ThCl_2(dmpe)$ [19] have been generated. The complex $(\eta^5\text{-}C_5Me_5)_2U(OTf)_2(H_2O)$ (OTf = trifluoromethylsulfonate) was isolated in low yield from the reaction of $(\eta^5\text{-}C_5Me_5)_2UMe_2$ with triflic acid [196]. In compounds of the for-

Table 12 Some important bond lengths of bis(substituted cyclopentadinyl)actinide(IV) complexes of the type Cp_2AnX_2

Complex	Bond distance (Å) M–Cp average	M–X	Refs.
$(\eta^5\text{-}C_5Me_5)_2ThCl_2$	2.78(2)	2.600(5)	[126]
$(\eta^5\text{-}C_5Me_5)_2ThBr_2$	2.51 *	2.800(2)	[252]
$(1,3\text{-}(Me_3Si)_2C_5H_3)_2UCl_2$	2.72(1)	2.579(2)	[255]
$(1,3\text{-}(Me_3Si)_2C_5H_3)_2ThCl_2$	2.78(1)	2.632(7)	[255]
$(1,3\text{-}(Me_3Si)_2C_5H_3)_2UBr_2$	2.71(2)	2.734(1)	[255]
$(1,3\text{-}(Me_3Si)_2C_5H_3)_2UI_2$	2.70(3) and 2.72(3)	2.953(2) and 2.954(2)	[255]
$(1,3\text{-}(Me_3Si)_2C_5H_3)_2U(BH_4)_2$	2.72(2)	2.56(1)	[255]
$(1,3\text{-}(Me_3Si)_2C_5H_3)_2UCl_2$	2.49 *	2.573(1)	[123]
$(1,3\text{-}(Me_3C)_2C_5H_3)_2UCl_2$	2.49 *	2.577(4)	[123]
$(1,3\text{-}(Me_3C)_2C_5H_3)_2UF_2$	2.46 *	2.086(2)	[123]
$(1,3\text{-}(Me_3C)_2C_5H_3)_2UMe_2$	2.44 *	2.42(2)	[123]

* centroid of the Cp ring

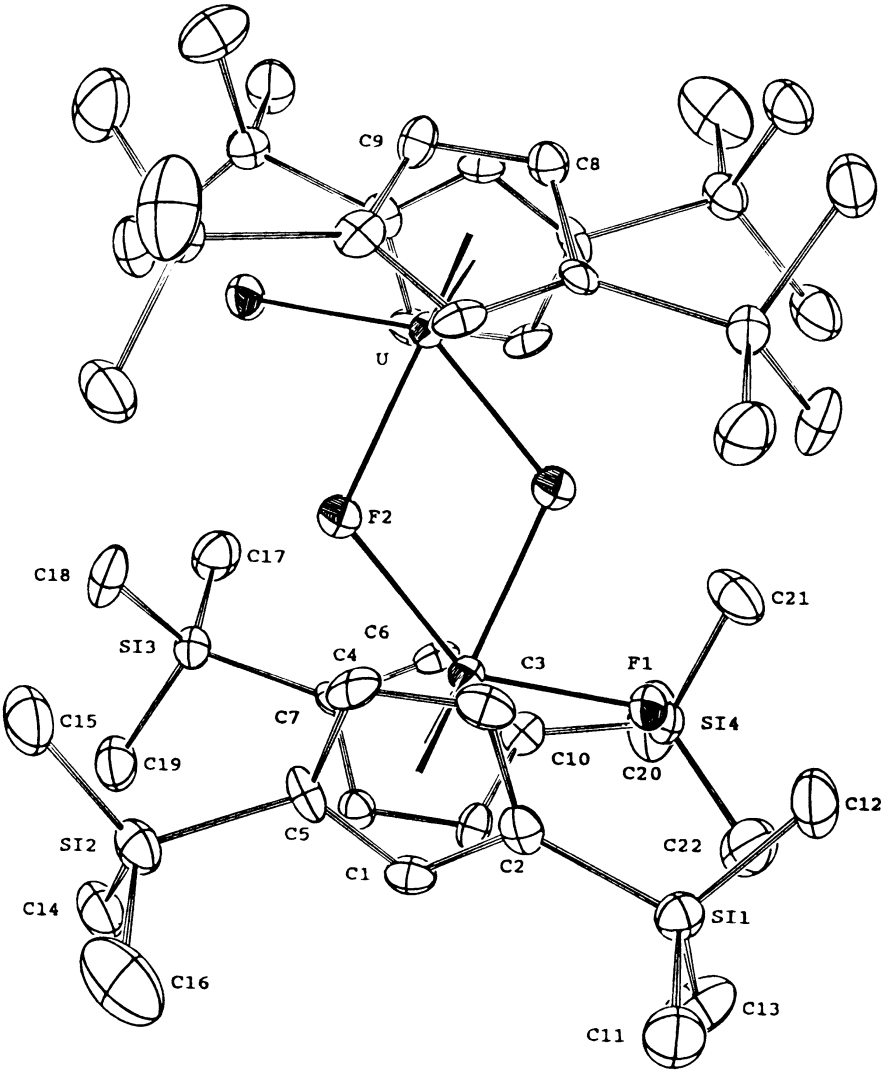

Fig. 21 Crystal structure of $\{[\eta^5\text{-}1,3\text{-}(Me_3Si)_2C_5H_3]_2UF(\mu\text{-}F)\}_2$ [122]. Reprinted with permission from [122]; © (1999) American Chemical Society

mula $(\eta^5\text{-}C_5Me_5)_2UX_2(L)$ (L = neutral ligand), the coordinated base generally occupies the central position in the equatorial wedge.

The introduction of the permethyl substituted cyclopentadienyl ligand into the coordination sphere of actinides afforded complexes with advantageous solubility, crystallizability, thermal stability, and resistance to ligand redistribution. However, abundant structural data indicate that despite these advantages the metal center suffers from a high steric congestion that may decrease

the reactivity relative to the known or hypothetical bis(cyclopentadieny1) analogs. In an effort to "open" the actinide coordination sphere while preserving the frontier orbitals and other advantages of Cp*, a totally new approach was made by linking two substituted cyclopentadienyl rings to afford a chelating bis-(permethylcyclopentadienyl) ligand $[Me_2Si(Me_4C_5)_2]^{2-}$, $[R_2Si(Me_4C_5)(C_5H_5)]^{2-}$ [257, 258] (Scheme 19).

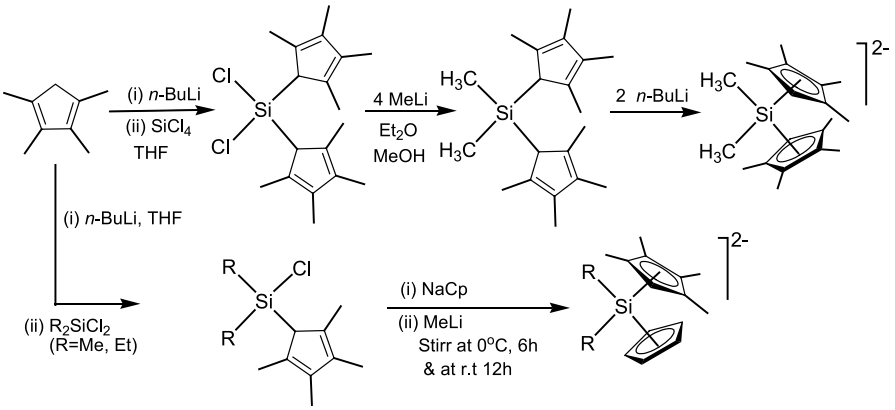

Scheme 19 Synthesis of chelating bis(cyclopentadienyl) ligand [257]

With these new sets of ligands a number of complexes have been reported of the type $Me_2SiCp'''_2AnCl_2 \cdot xLiCl \cdot y(sol)$ (where $Cp''' = (Me_4C_5)$; An = Th, U [257, 259, 260]). The complex of the type $[(Cp''')_2(\mu\text{-}SiMe_2)]\ U(\mu\text{–}Cl)_4\ [Li(tmeda)]_2$ was obtained when $(Cp''')_2(\mu\text{-}SiMe_2)UCl_2 \cdot 2LiCl_2 \cdot 4Et_2O$ was recrystallized from toluene and *N*,*N*,*N*′,*N*′-tetramethylethylenediamine-(tmeda). A typical bent structure was observed for the complex $[(Cp''')_2(\mu\text{–}SiMe_2)]\ U(\mu\text{-}Cl)_4[Li(tmeda)]_2$. The ring centroid–U–ring centroid angle (114.1°) is considerably smaller than that observed in nonchelated bis(cyclopentadienyl) uranium complexes (133–138°) and is comparable to the angle determined for the thorium dialkyl complex $[Me_2Si(C_5Me_4)_2]Th(CH_2Si(CH_3)_3)_2$ (118.4°) [257]. The contraction of the centroid–metal–centroid angle clearly indicates widening of the equatorial face of these types of complexes, which enhances room in its coordination sphere and thus further facilitates its reactivity. The uranium is coordinated to four bridging chloride ligands. Two of the uranium chloride bond distances U(1)–Cl(1) 2.885(3), U(1)–Cl(2) 2.853(3) Å are longer than the U(1)–Cl(3) 2.760(3) and U(1)–Cl(4) 2.746(3) Å. These complexes can easily be alkylated by lithium alkyl or Grignard reagents [257]. Wang et al. reported a similar type oxygen and chloride bridge complex $[\{[\eta^5\text{-}(C_5Me_4)_2SiMe_2]UCl\}_2(\mu\text{-}O)(\mu\text{-}Cl)\cdot Li\cdot 1/2DME]_2$ (Fig. 22), which was found to be very reactive and undergo facile alkylation to yield oxide-bridge dibutyl uranium complex $[\{[\eta^5\text{-}(C_5Me_4)_2SiMe_2]U(Bu)\}_2(\mu\text{-}O)]$ (Scheme 20) [260].

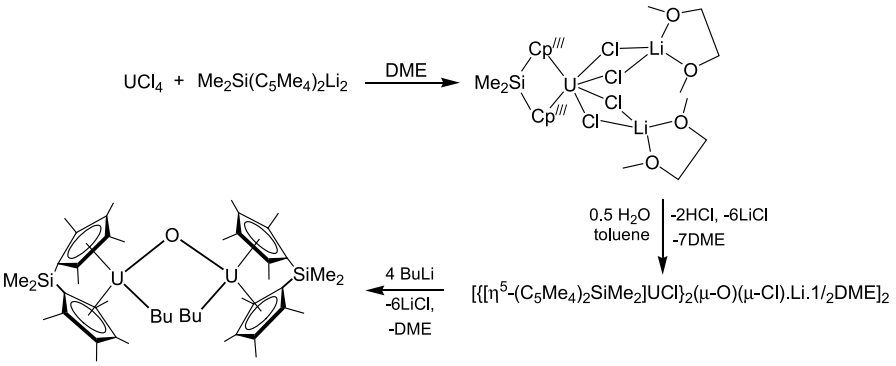

Scheme 20 Synthesis of O-bridged chelating bis(cyclopentadienyl) uranium complex [260]

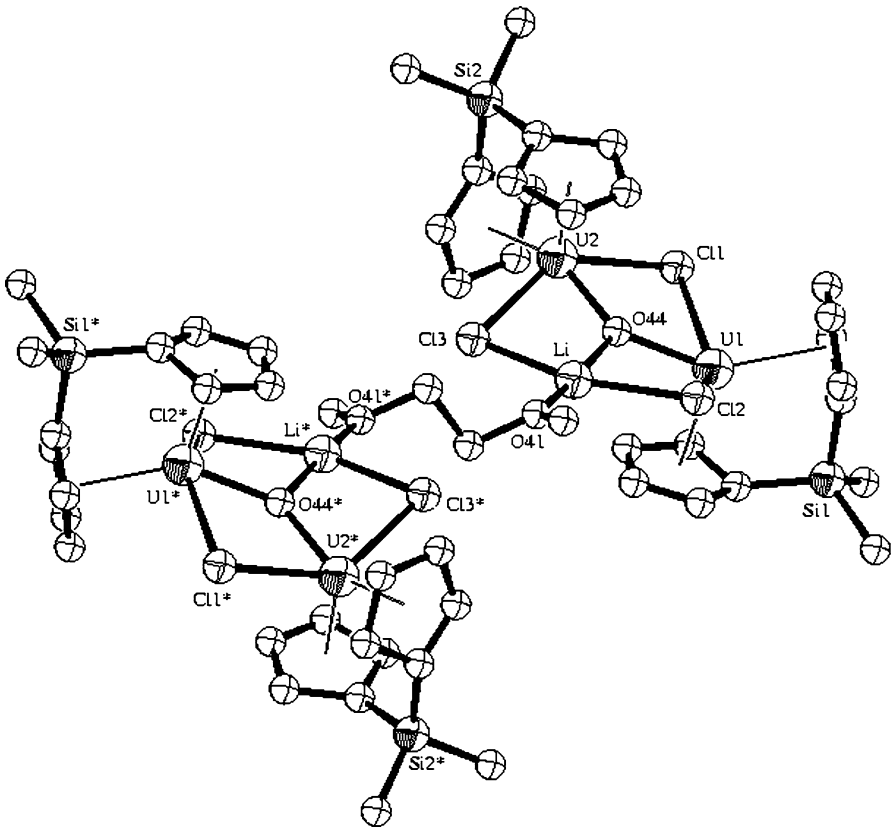

Fig. 22 Crystal Structure of $[\{[\eta^5\text{-}(C_5Me_4)_2SiMe_2]UCl\}_2(\mu\text{-}O)(\mu\text{-}Cl)\cdot Li\cdot 1/2DME]_2$ [260]. Reprinted with permission from [260]; © (2000) American Chemical Society

Following the establishment of this new series of complexes, their chemistry was well studied and a number of dialkyl derivatives, $[(\mu\text{-}SiMe_2)(\eta^5\text{-}C_5Me_4)_2]ThR_2$ (where R = CH_2SiMe_3, CH_2CMe_3, C_6H_5, *n*-C_4H_9, and $CH_2C_6H_5$) have also been reported [257, 261]. The dialkyl complexes undergo rapid hydrogenolysis under H_2 to yield a light-sensitive dihydride complex $\{[(\mu\text{-}SiMe_2)(\eta^5\text{-}C_5Me_4)_2]ThH_2\}_2$. IR spectroscopy and structural data (a short Th–Th distance of 3.632(2) Å) is in good agreement with the formulation of the compound having two bridging hydride ligands.

Looking at the aspect that the "tying" back of the Cp ligands provides many facilities to the metal center, other sets of ligands have been explored in which the two Cp rings were back-bonded with some bridging groups, like pyridine [262], ROR [263] etc. Paolucci et al. [262] reported a mononuclear bridged bipyridine Cp_2UCl_2 derivative, $\mu\text{-}\{2,6\text{-}CH_2C_5H_3NCH_2\}(\eta^5\text{-}C_5H_4)_2UCl_2$ according to Eq. 52:

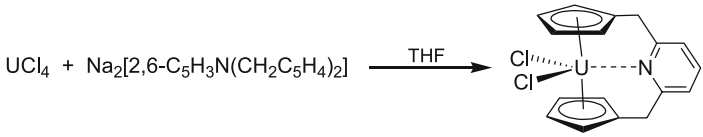

(52)

According to the single-crystal X-ray study of this complex, the $U\text{–}N_{av}$ bond distance was 2.62(1) Å, which clearly indicates a strong U–N interaction along with two Cl ligands (U–Cl 2.615(3) and 2.636(3) Å).

A plethora of bis(pentamethylcyclopentadienyl)uranium complexes have been synthesized and many of them were characterized crystallographically. Some of such complexes and their important $U\text{–}Cp_{av}$ and U–X bond distances are given in Table 13. In this respect, Th does not lag behind and was found to be the same in reactivity and to form almost similar types of derivatives [249, 264, 265]. These complexes were produced either by metathesis or by protonation reactions. A number of mixed alkyl–halide complexes were prepared, mainly by reaction of $(\eta^5\text{-}C_5Me_5)_2AnCl_2$ with one equivalent of alkylating agent, although the methyl–chloride complex is best prepared by redistribution from the dichloride complex $Cp^*_2AnCl_2$ and dimethyl complexes $Cp^*_2AnMe_2$. Straub et al. reported the synthesis of $Cp^*_2Th(Cl)(Me)$ by the reaction of an equimolar mixture of $Cp^*_2ThCl_2$ and $Cp^*_2ThMe_2$ in toluene [266]. The complex was characterized crystallographically (Fig. 23) and found to have normally disposed organoactinide metallocene with a ring centroid–metal–ring centroid angle of 135(2)°, metal to ring centroid distance of 2.56(9) Å, and Th–CH_3/Cl average distance of (∼ 2.67(8) Å).

Alkyl complexes of the type $(Cp^*)_2AnR_2$ are very reactive and undergo benzonitrile insertion reaction into the actinide–carbon bonds to afford bis(ketimide) complexes $(Cp^*)_2An[N{=}C(Ph)(R)]_2$ (where An = Th, U; R = CH_3, CH_2Ph, Ph) [267–270]. More recently, it has been reported that treatment of $(Cp^*)_2Th(CH_3)_2$ with excess 4-fluorobenzonitrile yielded

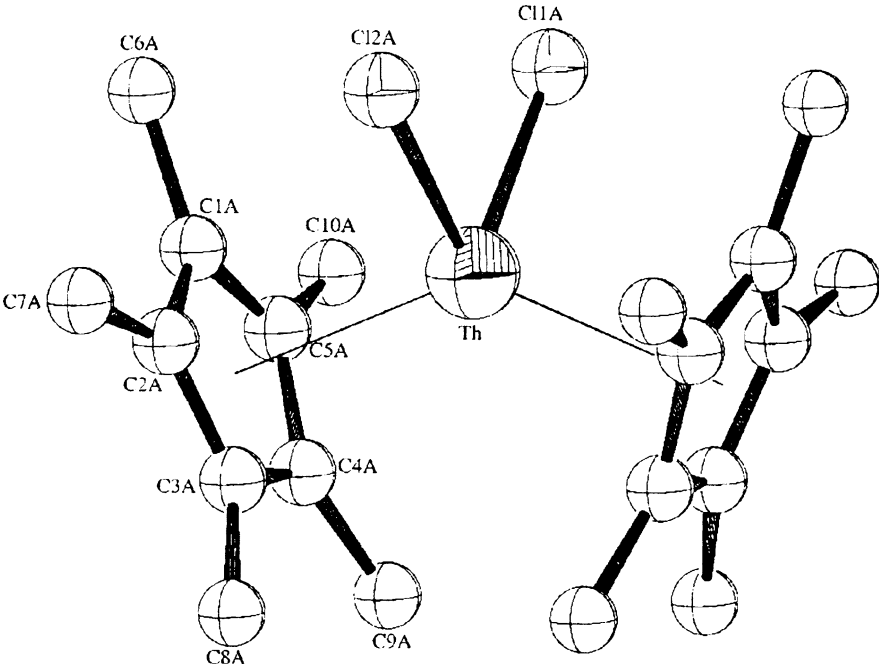

Fig. 23 Crystal structure of $Cp^*_2Th(Cl)(Me)$ [266]. Reprinted with permission from [266]; © (2001) American Chemical Society

bis(ketimide) complex $(Cp^*)_2Th[N{=}C(CH_3)(4\text{-}F\text{–}C_6H_4)]_2$ as the major product along with eight-membered thorium(IV) tetraazamacrocycle complex [271] as shown in Eq. 53:

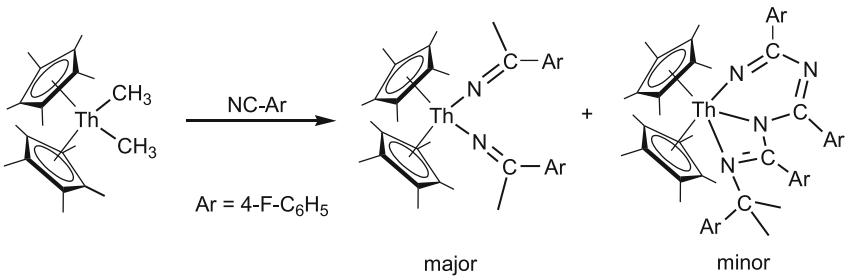

(53)

Reaction of $(\eta^5\text{-}C_5Me_5)_2ThCl_2$ with the bulkyl silyl salt $(THF)_3Li[Si(SiMe_3)_3]$ yields an unstable complex $(\eta^5\text{-}C_5Me_5)_2Th(Cl)[Si(SiMe_3)_3]$ that could be trapped by the reaction with two equivalents of carbon monoxide to produce a ketene complex $(\eta^5\text{-}C_5Me_5)_2Th(Cl)[O\text{–}C(=C=O)Si(SiMe_3)_3]$. In contrast, $(\eta^5\text{-}C_5Me_5)_2ThCl\{Si\text{–}(t\text{-}Bu)Ph_2\}$ could be isolated and its reaction with CO gave a similar silylthoroxyketene compound, and in this case the

Table 13 Some important bond lengths of various U(IV) complexes containing η^5-C_5Me_5 ligand

Complex	Bond distance (Å) U–Cp average	U–X	Refs.
$[Cp^*_2U]_2[\eta^2\text{-}CO(NMe_2)]_2$	2.78(2)	2.370(5) O	[273]
	2.342(7) O		
	2.405(8) C		
	2.402(9) C		
$[Cp^*_2U(OMe)]_2PH$	2.74(3)	2.046(14) O	[281]
	2.743(1) P		
$Cp^*_2UCl_2(HNPPh_3)$	2.77(2)	2.730(4) Cl	[313]
	2.658(4) Cl		
	2.43(1) N		
$Cp^*_2UCl[(CH_2)(CH_2)P(Ph)(Me)]$	2.78(3)	2.658(2) Cl	[316]
	2.62(1) C		
	2.58(1) C		
$Cp^*_2UCl[(CH_2)(CH_2)P(Ph)_2]$	2.80(3)	2.680(8) Cl	[316]
	2.62(3) C		
	2.54(3) C		
$(\eta^5\text{-}C_5Me_5)_2UCl_2$	2.72(2)	2.583(6)	[251]
$Cp^*_2U(BH_4)_2$	2.74(2)	2.58(3) B	[248]
$Cp^*_2U(N\text{–}2,4,6\text{-}t\text{-}Bu_3C_6H_2)$	2.790(12)	1.952(12) N	[278]
	2.951(15) C		
$Cp^*_2U_3(\mu_3\text{-}I)(\mu_3\text{-}S)(\mu_2\text{-}I_3)I_3$	2.71(6)	3.240(5) I	[157]
	3.094(5) I		
	3.115(5) I		
	2.943(5) I		
	2.779(15) S		
$[Li(tmed)][Cp^*_2U(NC_6H_5)Cl]$	2.77(2)	2.690(5) Cl	[278]
	2.051(14) N		
	3.19(4) Li		
$Cp^*_2UCl_2(HNSPh_2)$	2.77(6)	2.693 Cl	[314]
	2.646 Cl		
	2.438 N		
$Cp^*_2U(NH(C_6H_3Me_2\text{-}2,6))_2$	2.78(3)	2.267(6)	[307]
$[Cp^*_2U(P\text{–}2,4,6\text{-}t\text{-}Bu_3C_6H_2)](OPMe)$	2.79(2)	2.2562(3) P	[280]
	2.370(5) O		
$Cp^*_2U(NMe_2)(CN\text{–}t\text{-}Bu)_2[BPh_4]$	2.77(2)	2.22(1) N	[312]
	2.60(1) C		
	2.58(1) C		
$Cp^*_2U(SMe)_2$	2.73(2)	2.639(3) S	[284]
$[Na\text{-}(18\text{-crown-}6)(THF)_2][Cp^*_2U(SBu\text{-}t)(S)]$	2.79(3)	2.744(2) S	[141]
	2.477(2) S		
$Cp^*_2U(S\text{–}t\text{-}Bu)(S_2CBu\text{-}t)$	2.75(3)	2.643(4) S1	[284]
	2.885(4) S2		
	2.812(5) S3		

Table 13 (continued)

Complex	Bond distance (Å) U–Cp average	U–X	Refs.
$Cp^*_2UCl(\eta^2\text{-}t\text{-BuNSPh})$	2.76(2)	2.628(7) Cl	[310]
	2.20(2) N		
	2.825(8) S		
$Cp^*_2UBr(\eta^2\text{-}t\text{-BuNSPh})$	2.80(2)	2.794(12) Br	[310]
	2.309(6) N		
	2.840(4) S		
$[Na\text{-}(18\text{-crown-}6)(THF)_2][Cp^*_2U(SMe)(SCH_2)]$	2.79(2)	2.613(3) S	[140]
	1.85(1) S		
	2.44(1) C		
$[Na\text{-}(18\text{-crown-}6)(THF)_2][Cp^*_2U(SPr\text{-}i)_2]$	2.81	2.791(1) S	[140]
	2.777(1) S		
$Cp^*_2U(N{=}CPh_2)_2$	2.77(3)	2.179(6) N1	[267]
	2.185(5) N2		
$Cp^*_2UMe_2$	2.73(2)	2.409(5)	[254]
$Cp^*_2U(O)[C(NMeCMe)_2]$	2.80(5)	1.917(6) O	[107]
	2.637(9) C		
$[Cp^*_2U]_2(\mu\text{-O})$	2.74	2.094(14) O	[315]
	2.125(13) O		
$Cp^*_2UCl(OH)(HNSPh_2)$	2.78(2)	2.117(9) O	[315]
	2.47(2) N		
	2.746(4) Cl		
$Cp^*_2UMe(THF)[MeBPh_3]$	2.71(2)	2.419(8) O	[174]
	2.393(12) C		
$Cp^*_2U(dddt)^a$	2.73(2)[b]	2.629(3) S1	[153]
	2.650(3) S2		
$Cp^*_2U(C_4Ph_4)$	2.75(2)	2.395(2) C	[104]
$[Cp^*_2U(\mu\text{-N})U(\mu\text{-N}_3)Cp^*_2]_4$	2.78(4)	2.055(8)–	[308]
	2.090(8) N[c]		
	2.467(8)–		
	2.494(7) N[d]		
$Cp^*_2UI_2(NCPh)$	2.74(5)	2.53(1) N	[309]
	2.942(3) I		
	3.092(2) I		
$Cp^*_2U(CH_2Ph)[\eta^2\text{-(O, C)-}ONC_5H_4]$	2.77(2)	2.361(9) O	[311]
	2.561(13) C		
	2.505(14) C		
$Cp^*_2U[N{=}C(CH_2C_6H_5)(tpy)]_2$	2.77	2.205 N	[306]
	2.205 N		
$Cp^*_2U[N{=}C(CH_2C_6H_5)(tpy)]_2YbCp^*_2$	2.77(8)	2.054(8) N	[306]
	2.135(8) N		

Table 13 (continued)

Complex	Bond distance (Å) U–Cp average	U–X	Ref.
$[Cp^*_2U(NCMe)_5][BPh_4]$	2.80(1)	2.537 N 2.570 N 2.529 N 2.576 N 2.521 N	[317]
$[Cp^*_2U(NCMe)_5]I_2$	2.80(1)	2.556 N 2.547 N 2.548 N 2.535 N 2.551 N	[317]

[a] 5,6-Dihydro-1,4-dithiin-2,3-dithiolate
[b] Centrid
[c] Nitride
[d] Azide

transient η^2-acyl complex $(\eta^5\text{-}C_5Me_5)_2ThCl[\eta^2\text{-}CO\{Si\text{–}(t\text{-}Bu)Ph_2\}]$ could be detected [272].

Metathesis and protonation reactions are found to be very important reaction as they produce a variety of derivatives of various bis-substituted pentadienyl complexes [249, 256, 273]; even many metallocene phosphide complexes have been generated by this route [274, 275]. Polysulfides are also a very interesting class of chelating ligands. The complex $Cp^*_2ThCl_2$ undergoes metathesis reaction with Li_2S_5 to form $Cp^*_2ThS_5$ [276]. In a similar manner, the complex $(C_5Me_4Et)_2ThS_5$ was also synthesized and characterized by NMR spectroscopy. It has been proposed that the complexes $(C_5Me_4Et)_2ThS_5$ consists a fluxional twist-boat ThS_5 ring conformation [276] and the energy barrier to the interconverting isomers was ca. 57.4 kJ mol^{-1}:

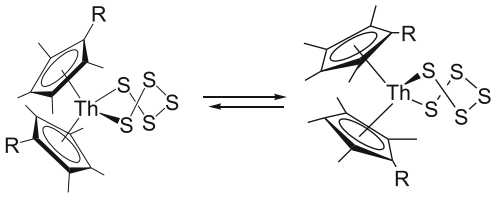

A series of bis(pentamethylcyclopentadienyl)uranium and thorium complexes containing bis(trimethylsilyl)phosphide ligand, $Cp^*_2An(X)[P(SiMe_3)_2]$, have been synthesized, where X = C1 (An = U, Th) or CH_3 (An = U,

Th). Thermal decomposition of the complexes $(Cp^*_2)_2AnMe[P(SiMe_3)_2]$ results in the formation of the P–C bridging complexes $(Cp^*_2)_2AnMe$ $[\eta^2\text{-}P(SiMe_3)SiCH_3CH_2]$ (Eq. 54):

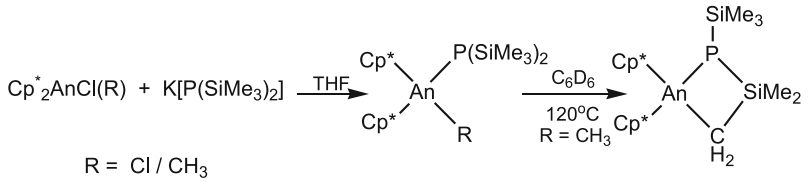

(54)

It has been observed that the trivalent organouranium complexes undergo one- or two-electron transformations into organic molecules. To extend this concept to the actinide(IV) complexes, Brennan et al. synthesized complexes of the type $[(RC_5H_4)_3U][\mu\text{-}\eta^1,\eta^2\text{-}CS_2]$ [72], where R is Me or $SiMe_3$, with the aim that these may also act as a tight-ion-pair complex of CS_2^{2-}. Similar type of bridging complexes $(MeC_5H_4)_4U_2(\mu\text{-}NR)_2$ [130, 277] were also synthesized and structurally characterized. The crystal structures of $(MeC_5H_4)_4U_2(\mu\text{-}NR)_2$ (where R = Ph and $SiMe_3$) revealed that the NPh group asymmetrically bridges the two uranium fragments, whereas the $NSiMe_3$ group symmetrically bridges the two uranium fragments. The bridging U–N distances are 2.156(8) and 2.315(8)Å in the NPh complex (Fig. 24) and 2.217(4) and 2.230(4) Å, in the $NSiMe_3$ complex.

Organoimido ligands have proven to be of great interest to synthetic chemists, but they are still dominating the *d*-element complexes. Burns and coworkers tried to explore the chemistry of this potential ligand towards

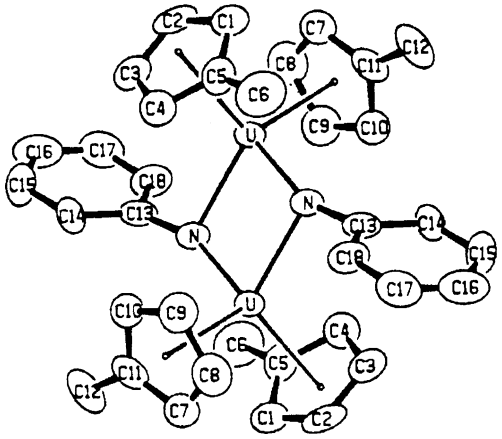

Fig. 24 Crystal structure of $(MeC_5H_4)_4U_2(\mu\text{-}NPh)_2$ [277]. Reprinted with permission from [277]; © (1988) American Chemical Society

f-elements by synthesizing metallocene complexes $(\eta^5\text{-}C_5R_5)_2An(=NR')$ [278]. They reported the synthesis of a number of monoimido derivatives of U(IV) by both metathesis and direct protonation routes [278]. The base free neutral monoimido complex $(\eta^5\text{-}C_5Me_5)_2U(=N\text{–}2,4,6\text{-}(t\text{-}Bu_3)C_6H_2)$ could have been prepared by α-elimination reactions as shown in Scheme 21.

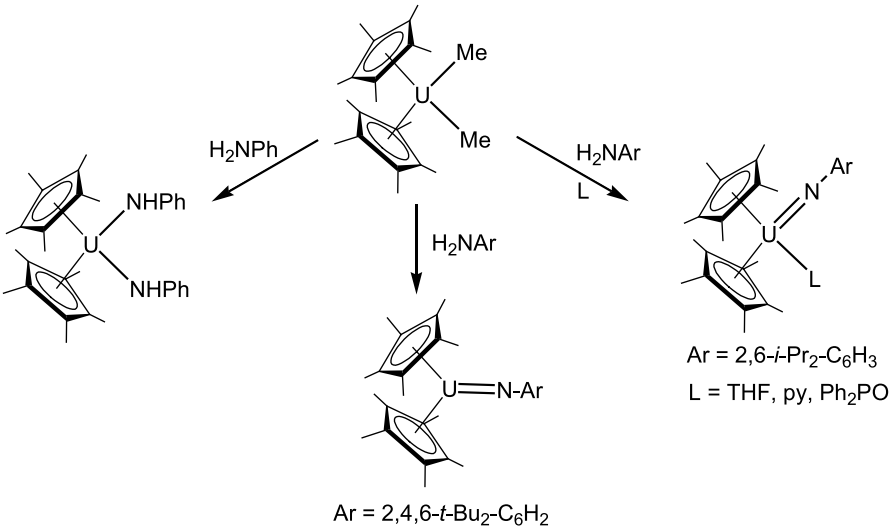

Scheme 21 Synthesis of various U(IV) organoimido complexes from $(Cp^*)_2UMe_2$ [278]

The molecular structure of the complex $(\eta^5\text{-}C_5Me_5)_2U\{=N\text{–}2,4,6\text{-}(t\text{-}Bu_3)C_6H_2\}$ displays considerable asymmetry in the conformation of the two *ortho tert*-butyl groups with respect to their orientation toward the uranium metal center. As expected from the steric point of view, one of the *tert*-butyl groups oriented in space in such a way that its methyl molecules can stay as far as away from the uranium atom. In contrast, one of the methyl molecules of the other *tert*-butyl group pointed direct1y toward the uranium metal center at a distance of 2.951(15) Å and with an C–U–N angle of 66.2(5)°. The extremely short U–N bond length (1.952(12) Å) suggests a relatively high formal bond order where one or both nitrogen lone pairs are involved in bonding to the uranium atom. The steric bulk of the aryl group is important in stabilizing a base free organoimido complex; the smaller $(\eta^5\text{-}C_5Me_5)_2U\{=N\text{–}2,6\text{-}(i\text{-}Pr)_2C_6H_3\}$ is best isolated as the THF adduct [278], and the parent phenylimido has only been isolated as a uranate salt, $[Li(tmeda)][(\eta^5\text{-}C_5Me_5)_2U(=NC_6H_5)Cl]$ [278]. The significantly short U–N bond distance of 2.51(14) Å and the U–N–C bond angle of 159.8(13)° (Table 13) indicate the polarization of the lone pair of electrons on the nitrogen towards the uranium center. The complex $(\eta^5\text{-}C_5Me_5)_2U(=N\text{–}2,6\text{-}Me_2C_6H_3)$ has also been reported. The organoimido

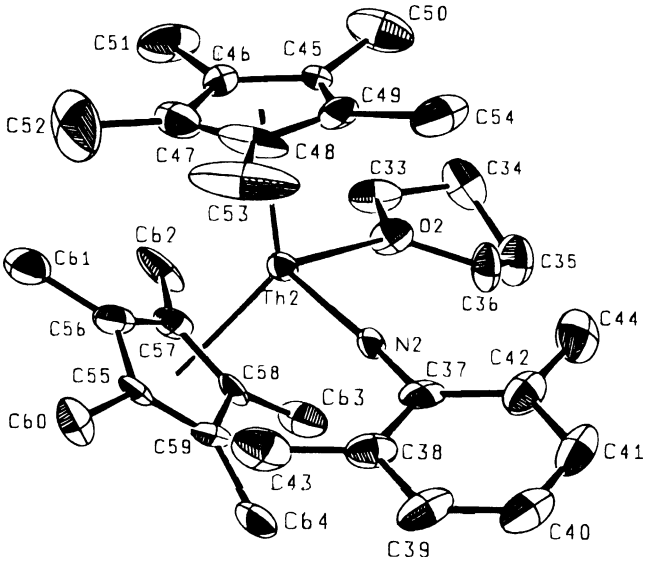

Fig. 25 Crystal structure of $(Cp^*)_2Th(=N\text{-}2,6\text{-}Me_2C_6H_3)$ [279]. Reprinted with permission from [279]; © (1996) American Chemical Society

complexes of the type $Cp^*_2An(=NR)$, (where An = U and Th) have been found as a reactive species in the catalytic cycle of hydroamination of terminal alkynes [266, 279]. The monoimido thorium complex $(Cp^*)_2Th(=N\text{–}2,6\text{-}Me_2C_6H_3)$ has been synthesized by the reaction of $(Cp^*)_2ThMe_2$ with 2,6-dimethylaniline in THF and was structurally characterized as a mono-THF adduct (Fig. 25) [279].

By applying almost the same synthetic method, the phosphinidine analog of uranium has been synthesized (Eq. 55) [280]:

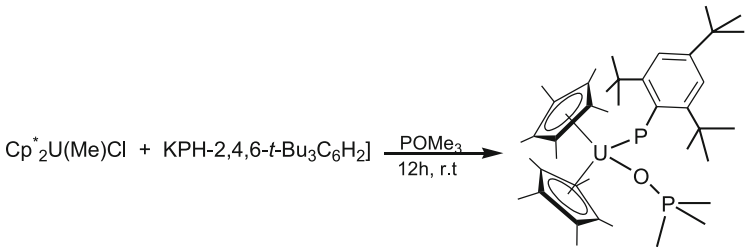

(55)

In the complex $(Cp^*)_2U\{P\text{–}2,4,6\text{-}(t\text{-}Bu)_3C_6H_2\}(OPMe_3)$, the uranium atom lies at the center of a tetrahedral with the U–O and U–P bond distance of 2.370(5) and 2.562(3) Å, respectively (Table 13). Interestingly, when the bis-cyclopentadienyl ligand was replaced by bridging *ansa*-ligand $\{(R_4C_5)_2(\mu\text{-}SiMe_3)\}$ (where R = CH_3 or H) the reaction of $\{(R_4C_5)_2(\mu\text{-}SiMe_3)\}UMe_2$ with $H_2\text{–}P\text{–}2,4,6\text{-}(t\text{-}Bu)_3C_6H_2$ produced the dimeric complexes $\{(R_4C_5)_2$

$(\mu\text{-SiMe}_2)\text{U}(\mu\text{-P–2,4,6-}t\text{-Bu}_3\text{C}_6\text{H}_2)\}_2$, (where R = Me or H) (Eq. 56):

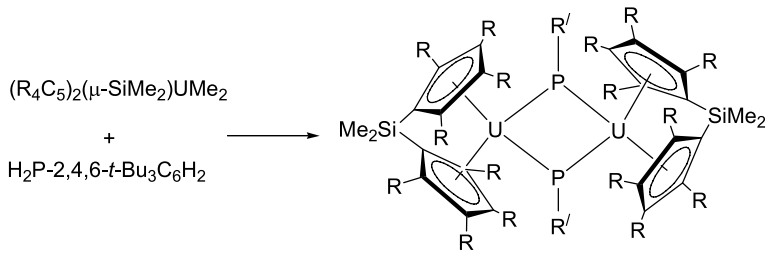

(56)

The hydride bridge actinide complex, $[(\eta^5\text{-}C_5Me_5)_2UH_2]_2$, reacts with $P(OMe)_3$ to generate a bridging phosphinide complex $[(\eta^5\text{-}C_5Me_5)_2U(OMe)]_2(\mu\text{-PH})$ by P–O cleavage with sacrificial formation of $(\eta^5\text{-}C_5Me_5)_2U(OMe)_2$ [281]. The molecular structure of $[(\eta^5\text{-}C_5Me_5)_2U(OMe)]_2(\mu\text{-PH})$ has a C_2 symmetry, with the $\mu\text{-PH}^{2-}$ ligand lying on a crystallographic twofold axis. The coordination geometry about each uranium ion is of the typical pseudotetrahedral.

With the help of the metathesis reaction of $Cp^*_2ThCl_2$ with $LiPR_2$, the first diorganophosphido actinide complexes $Cp^*_2Th(PR_2)$ (where R = Ph, Cy, Et) were prepared [274]. The molecule $Cp^*_2Th(Ph_2)$ exhibits a pseudotetrahedral geometry about the thorium atom with the pentamethylcyclopentadienyl ligands and two diphenylphosphido groups occupying the four coordination sites. The angles about the phosphorus atoms are far from the tetrahedral, and there is no evidence for significant Th–P multiple bonding (Th–P_{av} 2.87 (2) Å).

The cothermolysis of the butadiene complex $(\eta^5\text{-}1,3\text{-}t\text{-}Bu_2C_5H_3)_2Th(\eta^4\text{-}C_4H_6)$ with P_4 or As_4 gives the binuclear Th complex $[(\eta^5\text{-}1,3\text{-}t\text{-}Bu_2C_5H_3)_2Th]_2(\mu,\eta^3,\eta^3\text{-}E_6)$ (where E = P, As) [282, 283]. When the reaction of P_4 was carried out in presence of $MgCl_2$ only the complex $[(\eta^5\text{-}1,3\text{-}t\text{-}Bu_2C_5H_3)_2Th](\mu,\eta^3\text{-}P_3)[Th(Cl)(\eta^5\text{-}1,3\text{-}t\text{-}Bu_2C_5H_3)_2]$ was formed (Scheme 22).

Although the monomeric complexes of actinides with N, P or O donor ligands are stable and could be synthesized without much problem, mono- and dithiol complexes are very difficult to synthesized because they tend to support a monomer–dimer equilibrium [244]. Only lately have a few complexes of bis(pentamethylcyclopentadienyl) metallocene dithiolates, $(\eta^5\text{-}C_5Me_5)_2Th(SPr)_2$ [202] and $(\eta^5\text{-}C_5Me_5)_2U(SR)_2$ (where R = Me, *i*-Pr, *t*-Bu, Ph) [284] appeared.

The C–S bond cleavage in the complexes $[(Cp^*)_2U(SR)_2]$ (where R = *i*-Pr, and *t*-Bu) has been studied and it was found that the complex $(\eta^5\text{-}C_5Me_5)_2U(SBu\text{-}t)_2$ undergoes reduction by Na–Hg with cleavage of a C–S bond [141]. The product was isolated with an 18-crown-6-ether and proved to be a complex with a terminal sulfido ligand bound to the sodium coun-

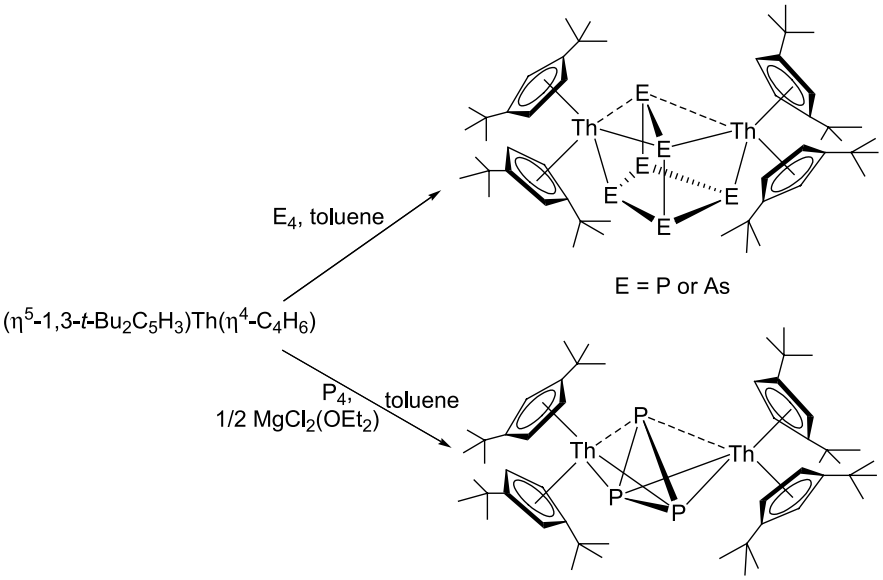

Scheme 22 Reactivity of P_4 and As_4 towards thorium butadiene complex [282, 283]

terion. The complex [Na(18-crown-6-ether)][$(\eta^5$-$C_5Me_5)_2$U(SBu-*t*)(S)] possesses a significantly shorter U–S bond distance of 2.462(2) Å than the typical U–SR bond ca. 2.64 Å).

Recently, the diene compounds have emerged into the field of organometallic chemistry as a successful ligand. However, the existence of diene complexes of 5*f*-elements was in a big shadow. Marks and coworkers [264] took the challenge to synthesize the actinide *cis*-2-butene-1,4-diyl complexes $Cp^*_2U(\eta^4$-$C_4H_6)$, $Cp^*_2Th(\eta^4$-$C_4H_6)$, and $Cp^*_2Th(\eta^4$-$CH_2CMeCMeCH_2)$ from their corresponding halides $Cp^*_2MCl_2$ (where M = U, Th) and the appropriate $(THF)_2Mg(CH_2CRCRCH_2)$ reagent. The molecular structure of $Cp^*_2Th(\eta^4$-$C_4H_6)$ has been determined by single-crystal X-ray diffraction and was found to consist of a "bent sandwich" $(Cp^*)_2$Th fragment coordinated to an *s-cis*-η^4-butadiene ligand (Fig. 26).

The crystal structure supports the η^4-hapticity of the butadiene ligand. The average Th–C distance to the terminal carbon atoms of the butadiene ligand (2.57(3) Å) is only slightly smaller than that to the internal carbon atoms (2.74(2) Å), and are comparable to those found in other thorium alkyl complexes. The C(1)–C(2) and C(3)–C(4) average distances (average of four independent molecules in the unit cell) is 1.46(5) Å, which is compared to the average C(2)–C(3) distance of 1.44(3) Å.

The actinide butadiene complexes undergo inversion of the metallacyclopentene ring, which is rapid on the NMR time scale at higher temperatures (Scheme 23). The measured energy barrier $\Delta G^{\star}$ (T_c, K) is 17.0 ± 0.3

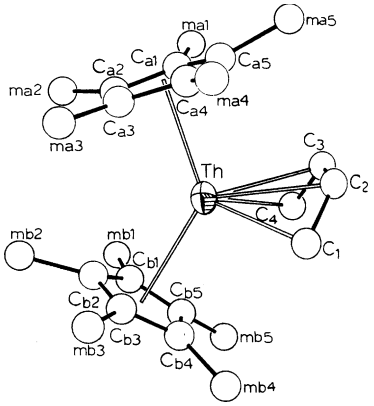

Fig. 26 Crystal Structure of $(\eta^5\text{-}C_5Me_5)_2Th(\eta^4\text{-}C_4H_6)$ [264]. Reprinted with permission from [264]; © (1986) American Chemical Society

(394), 15.0 ± 0.3 (299), and 10.5 ± 0.3 (208) kcal mol^{-1} for the complexes $Cp^*_2U(\eta^4\text{-}C_4H_6)$, $Cp^*_2Th(\eta^4\text{-}C_4H_6)$, and $Cp^*_2Th(\eta^4\text{-}CH_2CMeCMeCH_2)$, respectively [264].

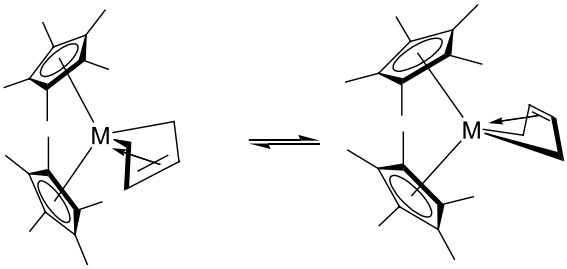

Scheme 23 Rapid ring inversion in actinide diene complexes [264]

The uranium contingent of this butadiene molecule was characterized by NMR spectroscopy. At room temperature, the NMR data is consistent with a folded metallacyclopentene structure having magnetically nonequivalent Cp* ligands and α-methylene protons [264] as shown in the structure below:

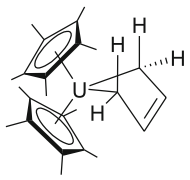

The actinide–carbon bonds in these complexes appear to be reasonably polar; hence they undergo facile hydrogenolysis and protonolysis, but do not undergo the activation of C–H bonds on the exogenous hydrocarbon molecules. Hydrogenolysis with one atmosphere of dihydrogen yielded the dihydride complexes [264] (Eq. 57):

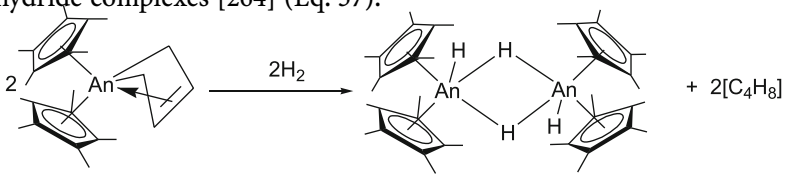

An = U, Th (57)

The dimeric formulation of the dihydride complexes is well supported by both cryoscopic molecular weight determinations and a single crystal neutron diffraction structure of the thorium compound [285]. A rapid exchange between the bridge and terminal hydrides was observed over the NMR time scale in solution at $-85\,^{\circ}C$. In the case of uranium, the ring methyl protons appear to interchange rapidly with the hydrides, resulting in isotopic scrambling. The thorium complex is thermally stable whereas, in contrast, the uranium complex loses dihydrogen at room temperature in vacuo over a period of 3 h to generate a U(III) hydride.

Thermochemical investigations have been carried out to find out the bond disruption enthalpies for a number of metallocene alkyl halide and dialkyl complexes [286, 287]. The Th–R bond enthalpies are uniformly larger than those for U–R. The bond dissociation enthalpy for Th–H in $\{(\eta^5\text{-}C_5Me_5)_2Th(\mu\text{-}H)H\}_2$ was observed to be $407.9 \pm 2.9\,kJ\,mol^{-1}$, which is somewhat larger than for the typical Th–C values, $300–380\,kJ\,mol^{-1}$, but not larger enough to produce a strong driving force for the formation of hydrides. Therefore, unlike mid- to late-transition metal compounds, reactions such as β-hydride elimination will not be strongly favored and hence expected to affect C–C bond forming reactions, like olefin polymerization.

Similar to the tris(cyclopentadienyl)actinides, bis(cyclopentadienyl)actinide complexes also undergo insertion reaction of various unsaturated substrates such as CO, CNR, CO_2, and CS_2 into U–C, U–Si, U–N, and U–S bonds [221, 249, 265, 273, 284] and commonly have η^2-C(R) = E types of bonding and might exists with a "carbene-like" structure [288]:

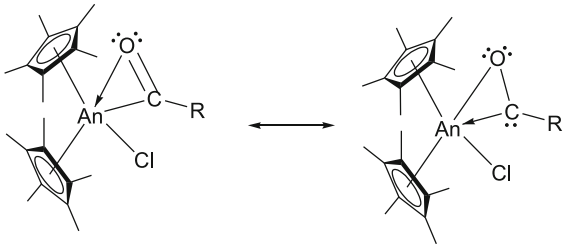

The syntheses, structures, and cyclometallation reactions of a series of bis(pentamethylcyclopentadieny1)thorium dialkyl complexes of the type $Cp^*_2Th(CH_2EMe_2R)_2$ (where E = C, R = Me, Et; E = Si, R = Me, Ph) yielded the thoracyclobutane $Cp^*_2Th(\eta^2\text{-}CH_2EMeRCH_2)$ (Scheme 24) [289]. The complex $Cp^*_2Th(\eta^2\text{-}CH_2SiMePhCH_2)$ undergoes further thermolysis to form $Cp^*_2Th(\eta^2\text{-}CH_2SiMe_2\text{–}o\text{-}C_6H_4)$. An interesting results was observed when thermolysis was carried out with $Cp^*_2Th(CH_2CMe_3)(CH_2SiMe_3)$, which leads to the formation of $Cp^*_2Th(\eta^2\text{-}CH_2SiMe_2CH_2)$ by an intramolecular elimination reaction.

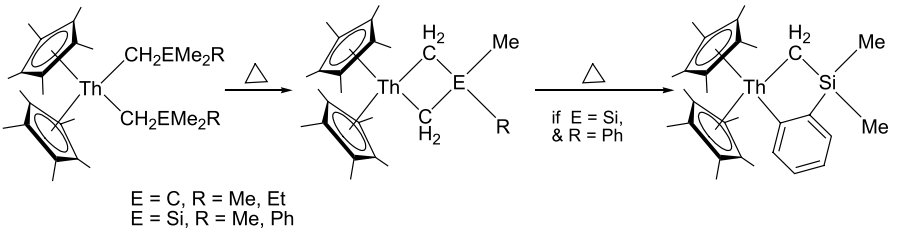

Scheme 24 Thermometallation of bis(cyclopentadienyl)thorium dialkyl complexes [289]

The mechanism for cyclometallation was proposed to involve a concerted heterolytic process with hydrogen atom abstraction and metallacycle formation occurring in a four-center transition state. Kinetic and labeling studies in the cyclometallation reactions indicate that intramolecular γ-C–H activation is the rate-limiting step [290].

The high reactivity of bis-arylactinide complexes can be observed by the benzene elimination that takes place to form actinide benzyne-type complexes, which further undergo reverse reaction of benzene to form *o*-diphenylene (Scheme 25) [249].

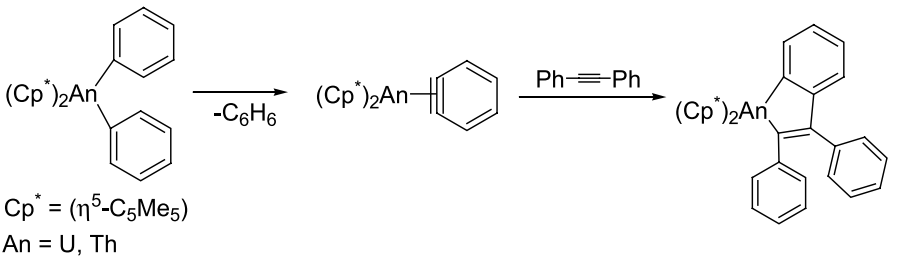

Scheme 25 Elimination of benzene from diaryl complexes [249]

The benzyne intermediate for the uranium is unstable and, hence, the uranium complexes undergo a much faster *ortho*-activation process than the corresponding thorium complexes.

More recently it has been observed that $Cp^*_2UI_2$ reacts with KCN and NR_4CN to give the familiar bent sandwich complex $[Cp^*_2U(CN)_3][NR_4]$ and the pentacyanide complex $[Cp^*_2U(CN)_5][NR_4]_3$ (where R = Et, *n*-Bu) (Eq. 58) [291]:

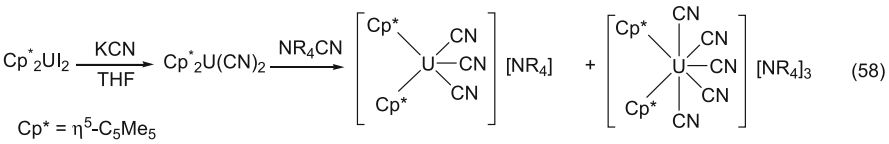

(58)

The complex $[Cp^*_2U(CN)_3][N–Bu_4\text{-}n]$ was characterized crystallographically and found to posses a bent sandwich-like structure. The average U–Cp and U–(CN) distances 2.727(15) and 2.520(16) Å, respectively, is 0.1 Å smaller than its U(III) analog is in good agreement with the variation in the radii of U^{4+} to U^{3+} ions.

Recently, another class of ligand, N-heterocyclic carbene, has jumped into the race for σ-donor ligands. Among these, imidazole carbene has received more emphasis because of its tunable stability with the help of substituents in the ring as well as on the nitrogen atom. Addition of one molar equivalent of the heterocyclic carbene, $C_3Me_4N_2$ (tetramethylimidazolylidine), to $Cp^*_2UI(py)$ in toluene led to the immediate substitution of the pyridine ligand to give the carbene complex $Cp^*_2UI(C_3Me_4N_2)$ [292]. The metal coordination geometry was found to adopt the pseudotetrahedral arrangement as (Fig. 27) found in the series of complexes Cp^*_2AnXY.

Apart from these *bis* or *tris*-cyclopentadienyl complexes, there was an early report of mono-Cp complex $(Cp)UCl_3(DME)$ (DME = 1,2-dimethoxy-

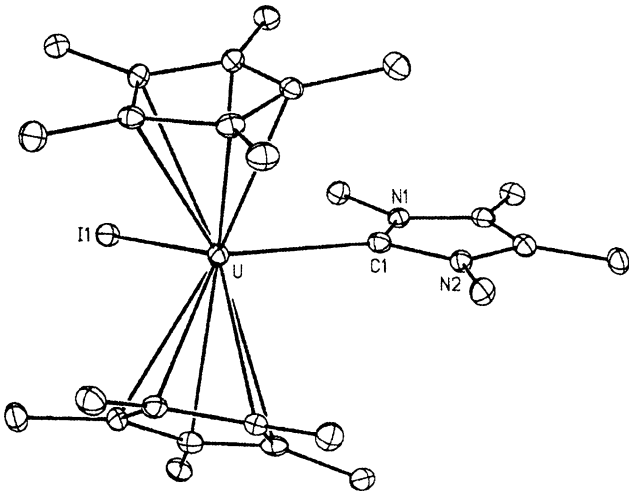

Fig. 27 Crystal structure of $Cp^*_2UI(C_3Me_4N_2)$ [292]. Reproduced with permission from the Royal Society of Chemistry

ethane) [293]. The coordination chemistry of mono-Cp actinide complexes has not yet been elaborated much and there are few reports of such compounds as they are highly reactive. The complex $(Cp)UCl_3(DME)$ was initially prepared by reaction of UCl_4 with $Tl(C_5H_5)$ in DME. After that, a number of other base adducts of the uranium mono-ring compound have been prepared using both mono- [294, 295] and bi-dentate bases [296]. Similarly, the complex $U(BH_4)_4$ reacts with $Tl(C_5H_5)$ to yield $(Cp)U(BH_4)_3$ [297], which in presence of Lewis bases redistributed to $CpU(BH_4)_3L_2$ (where L = THF, DME, HMPA). On the basis of solution NMR investigation, the structure of the complex $(Cp)U(BH_4)_3(THF)_2$ was proposed to be *mer*-octahedral with *cis*-THF ligands and a pentahapto cyclopentadienyl ring. This structure was confirmed for the complex $(Cp)UCl_2(THF)_2$, but a rigorous NMR study [298] showed that there is an equilibrium between two isomers in solution for a variety of base adducts of $(Cp)UCl_3$. Analogous compounds of the formula $(Cp)AnX_3L_2$ (X = halide, NCS^-) have been produced for thorium [294], neptunium [51, 299], and plutonium [300].

Working with the tri-substituted cyclopentadienyl ligand, 1,2,4-trimethylsilylcyclopentadienyl, Edelman and coworker [301] reported the first mono *tris*-substituted actinide complex $[U\{\eta^5\text{-}C_5H_2(SiMe_3)_3\text{-}1,2,4\}Cl_2(THF)(\mu\text{-}Cl)_2Li(THF)_2]$ and found to have an approximately octahedral environment around the U center, with four equatorial Cl^- ligands, *trans*-axial sub-

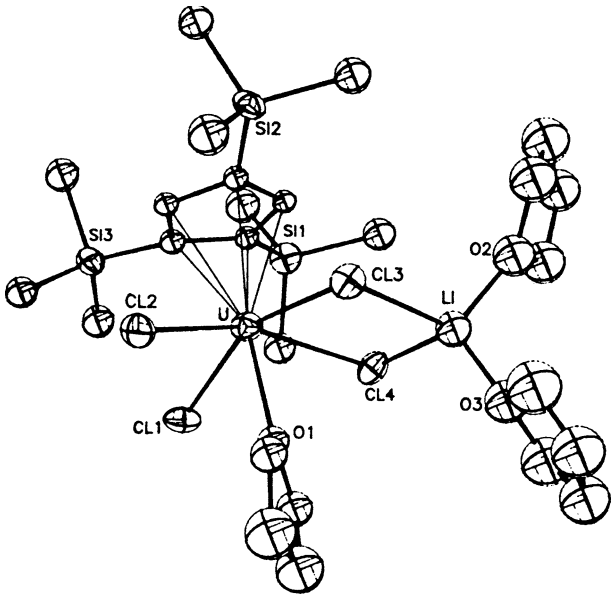

Fig. 28 Crystal structure of $[U\{\eta^5\text{-}C_5H_2(SiMe_3)_3\text{-}1,2,4\}Cl_2(THF)(\mu\text{-}Cl)_2Li(THF)_2]$ [301]. Reprinted with permission from Elsevier

stituted Cp and THF ligands (Fig. 28). In a similar reaction, the $ThCl_4$ reacts with $Na\{\eta^5\text{-}C_5H_2(SiMe_3)_3\text{-}1,2,4\}$ and $Na\{\eta^5\text{-}C_5H_2(SiMe_3)_3\text{-}1,2,4\}$(pmdeta) to produce $[\{\{Th(\eta^5\text{-}C_5H_2(SiMe_3)_3\text{-}1,2,4)Cl_3\}_2NaCl(OEt_2)\}_2]$ and $[\{Th(\eta^5\text{-}C_5H_2(SiMe_3)_3\text{-}1,2,4)Cl_3\}(pmdeta)]$, (pmdeta = $MeN(CH_2CH_2NMe_2)_2$), respectively [19]. The molecular structure of $[\{\{Th(\eta^5\text{-}C_5H_2(SiMe_3)_3\text{-}1,2,4)Cl_3\}_2 NaCl(OEt_2)\}_2]$ is quite interesting as: (i) it is tetranuclear, (ii) it contains two types of bridging chlorides, eight μ_2- and two μ_3-chlorine atoms. Each thorium center occupies a distorted octahedral environment and is bonded η^5- to an axial substituted-Cp ligand with a triply bridging chloride in the *trans*-axial position as shown below:

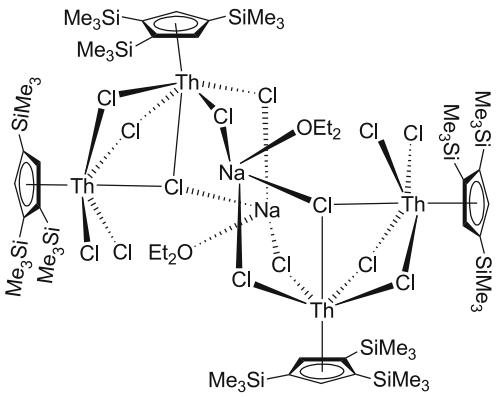

Grignard reagents were also found to be suitable for the formation of mono-ring pentamethylcyclopentadienylthorium and pentamethylcyclopentadienyluranium complexes by the reaction with their tetrahalides [302, 303]. Spectroscopic data indicate a meridional disposition of the chloride ligands in a pseudo-octahedral geometry. In addition, the trihalide base adduct also undergoes a similar type of reaction (Eq. 59) [302, 304, 305]:

$$Cp^*AnX_3(THF)_2 + RLi / RMgX \longrightarrow Cp^*AnR_3$$

An = Th; R = alkyl, $CH_2C_6H_5$, CH_2CMe_3, *o*-$C_6H_4NMe_2$

An = U; R = alkyl, 2-methylalkyl, $CH_2C_6H_5$ (59)

By this metathesis process the mono(pentamethylcyclopentadienyl) complex $Cp^*ThBr_3(THF)_3$ was synthesized [303] and its reactivity extensively studied (Scheme 26).

Complexes $Cp^*ThBr_3(THF)$, $Cp^*Th(OAr)(CH_2SiMe_3)_2$ and $Cp^*Th[\eta^2\text{-}OC_6H_3\text{–}(t\text{-}Bu)CMe_2CH_2](OAr)(O{=}PPh_3)$ were characterized by single crystal X-ray diffraction studies. $Cp^*ThBr(OAr)_2$ exhibits somewhat a distorted three-legged piano-stool geometry with Th–Cp* centroid, Th–O,

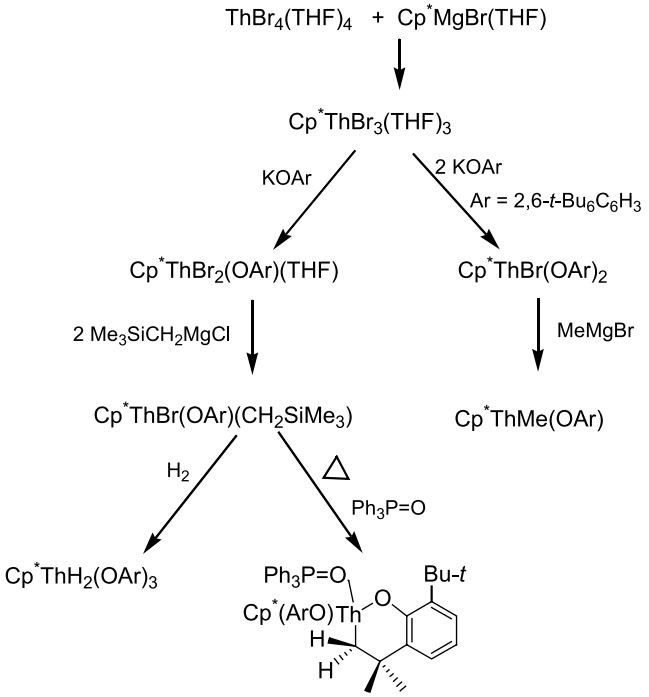

Scheme 26 Synthesis and reactivity of mono cylopentadienyl thorium complex [303]

and Th–Br distances of 2.57(1), 2.16(1) (av), and 2.821(2) Å, respectively. $Cp^*Th(OAr)(CH_2SiMe_3)_2$ also displays a three-legged piano-stool geometry with Th–C distances to the alkyl groups of 2.460(9) and 2.488(12) Å. Th–Cp* centroid and Th–O distances are very similar to those found in $Cp^*ThBr(OAr)_2$, at 2.53(1) and 2.186(6) Å, respectively. $Cp^*Th[\eta^2\text{-}OC_6H_3\text{–}(t\text{-}Bu)CMe_2CH_2](OAr)(O{=}PPh_3)$ features a distorted trigonal bipyramidal geometry about the metal center, with the Cp* ligand and the oxygen atom of the cyclometallated aryloxide ligand occupying axial sites (Cp* centroid–Th–O of 168.3(3)°). The Th–C distance to the *tert*-butyl methylene group is 2.521(12) Å, while Th–O distances to the aryloxide and triphenylphosphine oxide ligands are 2.199(7) (average) and 2.445(7) Å, respectively.

4 Conclusion and Perspectives

In this review we have shown the unique properties of the actinide complexes and some of the many novel features such as multielectron oxidation–reduction, catalytic activities towards various organic conversions etc. The catalytic chemistry of the organoactinide complexes is new, demanding, and

sophisticated. The ability to tailor a catalytic precursor of actinide complexes with controlled electronic and steric features is challenging and opens a new field in this branch of chemistry. The authors believe that in the next few years we will see a higher implementation of these complexes and new ones in demanding chemical transformations.

Acknowledgements This research was supported by the Israel Science Foundation Administered by the Israel Academy of Science and Humanities under Contract 83/01-1. M.S. thanks the Lady Davis Trust for a postdoctoral Fellowship.

References

1. Kealy TJ, Pauson PL (1951) Nature 168:1039
2. Reynolds LT, Wilkinson G (1956) J Inorg Nucl Chem 2:246
3. Cotton FA, Wilkinson G, Murillo CA, Bochmann M (1999) Advanced inorganic chemistry, 6th edn. Wiley, New York
4. Allen FH (2002) Acta Cryst, Struct Sci B 58:380
5. Gilman H (1968) Adv Organomet Chem 7:1
6. Li X-F, Guo A-L (1987) Inorg Chim Acta 134:143
7. Li X, Feng X, Xu Y, Wang H, Shi J, Liu L, Sun P (1986) Inorg Chim Acta 116:85
8. Li X-F, Xu Y-T, Feng X-Z, Sun P-N (1986) Inorg Chim Acta 116:75
9. Marcalo J, Pires de Matos A (1989) Polyhedron 8:2431
10. Leal JP, Simoes JAM (1994) J Chem Soc Dalton Trans, p 2687
11. Leal JP, Marques N, Pires de Matos A, Calhorda MJ, Galvao AM, Simoes JAM (1992) Organometallics 11:1632
12. Leal JP, Marques N, Takats J (2001) J Organomet Chem 632:209
13. Marks TJ, Gagne MR, Nolan SP, Schock LE, Seyam AM, Stern D (1989) Pure Appl Chem 61:1665
14. Jemine X, Goffart J, Ephritikhine M, Fuger J (1993) J Organomet Chem 448:95
15. Jemine X, Goffart J, Berthet JC, Ephritikhine M (1992) J Chem Soc Dalton Trans, p 2439
16. King WA, Marks TJ, Anderson DM, Duncalf DJ, Cloke FGN (1992) J Am Chem Soc 114:9221
17. King WA, Marks TJ (1995) Inorg Chim Acta 229:343
18. Marks TJ, Fragala IL (eds) (1985) Fundamental and technological aspects of organo-*f*-element chemistry. Proceedings NATO Advanced Study Institute, Acquafredda di Maratea, Italy, 10–21 September 1984. NATO ASI Series C, vol 155
19. Edelman MA, Hitchcock PB, Hu J, Lappert MF (1995) New J Chem 19:481
20. Edelmann FT, Lorenz V (2000) Coord Chem Rev 209:99
21. Edelmann FT (1995) Scandium, yttrium and the 4*f* and 5*f* elements, excluding their zero oxidation state complexes. In: Abel EW, Stone FGA, Wilkinson G (eds) Comprehensive organometallic chemistry II, vol 4. Elsevier, Oxford, p 12
22. Edelmann FT (2006) Coord Chem Rev 250:2511
23. Edelmann FT, Gun'ko YK (1997) Coord Chem Rev 165:163
24. Ephritikhine M (1997) Chem Rev 97:2193
25. Burns CJ, Eisen MS (2006) Organoactinide chemistry. In: Morss LR, Edelstein NM, Fuger J, Katz JJ (eds) The chemistry of actinide and transactinide elements, 3rd edn. Springer, Berlin Heidelberg New York, pp 2799–3012

26. Gottfriedsen J, Edelmann FT (2007) Coord Chem Rev 251:142
27. Gottfriedsen J, Edelmann FT (2006) Coord Chem Rev 250:2347
28. Gottfriedsen J, Edelmann FT (2005) Coord Chem Rev 249:919
29. Hyeon J-Y, Gottfriedsen J, Edelmann FT (2005) Coord Chem Rev 249:2787
30. Hyeon J-Y, Edelmann FT (2003) Coord Chem Rev 247:21
31. Hyeon J-Y, Edelmann FT (2003) Coord Chem Rev 241:249
32. Apostolidis C, Edelmann FT, Kanellakopulos B, Reissmann U (1999) Z Naturforsch B 54:960
33. Gun'ko Y, Edelmann FT (1996) Coord Chem Rev 156:1
34. Richter J, Edelmann FT (1996) Coord Chem Rev 147:373
35. Kilimann U, Edelmann FT (1995) Coord Chem Rev 141:1
36. Wedler M, Gilje JW, Noltemeyer M, Edelmann FT (1991) J Organomet Chem 411:271
37. Wedler M, Knoesel F, Noltemeyer M, Edelmann FT, Behrens U (1990) J Organomet Chem 388:21
38. Recknagel A, Witt M, Edelmann FT (1989) J Organomet Chem 371:C40
39. Wedler M, Noltemeyer M, Edelmann FT (1992) Angew Chem 104:64
40. Knoesel F, Noltemeyer M, Edelmann FT (1989) Z Naturforsch B 44:1171
41. Barnea E, Eisen MS (2006) Coord Chem Rev 250:855
42. Fischer EO, Hristidu Y (1962) Z Naturforsch 173:275
43. Bursten BE, Strittmatter RJ (1991) Angew Chem 103:1085
44. Strittmatter RJ, Bursten BE (1991) J Am Chem Soc 113:552
45. Bursten BE, Rhodes LF, Strittmatter RJ (1989) J Less-Common Met 149:207
46. Bursten BE, Fang A (1985) Inorg Chim Acta 110:153
47. Bursten BE, Casarin M, DiBella S, Fang A, Fragala IL (1985) Inorg Chem 24:2169
48. Bursten BE, Fang A (1983) J Am Chem Soc 105:6495
49. Cramer RE, Jeong JH, Gilje JW (1987) Organometallics 6:2010
50. Kanellakopulos B, Fischer EO, Dornberger E, Baumgartner F (1970) J Organomet Chem 24:507
51. Karraker DG, Stone JA (1972) Inorg Chem 11:1742
52. Kanellakopulos B, Dornberger E, Baumgaertner F (1974) Inorg Nucl Chem Lett 10:155
53. Crisler LR, Eggerman WG (1974) J Inorg Nucl Chem 36:1424
54. Moody DC, Odom JD (1979) J Inorg Nucl Chem 41:533
55. Wasserman HJ, Zozulin AJ, Moody DC, Ryan RR, Salazar KV (1983) J Organomet Chem 254:305
56. Baumgartner F, Fischer EO, Billich H, Dornberger E, Kanellakopulos B, Roth W, Stieglitz L (1970) J Organomet Chem 22:C17
57. Baumgaertner F, Fischer EO, Kanellakopulos B, Laubereau P (1965) Angew Chem Int Edit Engl 4:878
58. Baumgaertner F, Fischer EO, Kanellakopulos B, Laubereau P (1966) Angew Chem Int Edit Engl 5:134
59. Laubereau PG (1970) J Inorg Nucl Chem Lett 6:611
60. Laubereau PG, Burns JH (1970) J Inorg Nucl Chem Lett 6:59
61. Laubereau PG, Burns JH (1970) Inorg Chem 9:1091
62. Fischer EO, Fischer H (1966) J Organomet Chem 6:141
63. Kalina DG, Marks TJ, Wachter WA (1977) J Am Chem Soc 99:3877
64. Bruno JW, Kalina DG, Mintz EA, Marks TJ (1982) J Am Chem Soc 104:1860
65. Zanella P, Rossetto G, De Paoli G, Traverso O (1980) Inorg Chim Acta 44:L155
66. Chang CC, Sung-Yu NK, Hseu CS, Chang CT (1979) Inorg Chem 18:885
67. Wong C-H, Yen T-M, Lee T-Y (1965) Acta Cryst 18:340

68. Le Marechal JF, Villiers C, Charpin P, Lance M, Nierlich M, Vigner J, Ephritikhine M (1989) J Chem Soc Chem Commun, p 308
69. Klosin J, Kruper WJ Jr, Nickias PN, Patton JT, Wilson DR (1998) Patent application WO1998/006727. Dow Chemical Company, USA
70. Zwick BD, Sattelberger AP, Avens LR (1992) Transuranium organometallic elements: the next generation. In: Morss LR, Fuger J (eds) Transuranium elements: a half century. American Chemical Society, Washington, DC, p 239
71. Brennan JG, Andersen RA (1985) J Am Chem Soc 107:514
72. Brennan JG, Andersen RA, Zalkin A (1986) Inorg Chem 25:1756
73. Stults SD, Andersen RA, Zalkin A (1990) Organometallics 9:1623
74. Del Mar Conejo M, Parry JS, Carmona E, Schultz M, Brennann JG, Beshouri SM, Andersen RA, Rogers RD, Coles S, Hursthouse M (1999) Chem Eur J 5:3000
75. Stults SD, Andersen RA, Zalkin A (1990) Organometallics 9:115
76. Blake PC, Lappert MF, Atwood JL, Zhang H (1986) J Chem Soc Chem Commun, p 1148
77. Blake PC, Edelstein NM, Hitchcock PB, Kot WK, Lappert MF, Shalimoff GV, Tian S (2001) J Organomet Chem 636:124
78. Burns CJ, Bursten BE (1989) Comments Inorg Chem 9:61
79. Pappalardo R, Carnall WT, Fields PR (1969) J Chem Phys 51:842
80. Nugent LJ, Laubereau PG, Werner GK, Vander Sluis KL (1971) J Organomet Chem 27:365
81. Kot WK, Shalimoff GV, Edelstein NM, Edelman MA, Lappert MF (1988) J Am Chem Soc 110:986
82. Tolman CA (1972) Chem Soc Rev 1:337
83. White D, Taverner BC, Leach PGL, Coville NJ (1993) J Comput Chem 14:1042
84. Stahl L, Ernst RD (1987) J Am Chem Soc 109:5673
85. Evans WJ, Forrestal KJ, Ziller JW (1997) Angew Chem Int Edit Engl 36:774
86. Evans WJ, Nyce GW, Forrestal KJ, Ziller JW (2002) Organometallics 21:1050
87. Evans WJ, Nyce GW, Clark RD, Doedens RJ, Ziller JW (1999) Angew Chem Int Edit Eng 38:1801
88. Evans WJ (2000) Coord Chem Rev 206/207:263
89. Evans WJ, Nyce GW, Ziller JW (2000) Angew Chem Int Edit Eng 39:240
90. Gordon JC, Giesbrecht GR, Brady JT, Clark DL, Keogh DW, Scott BL, Watkin JG (2002) Organometallics 21:127
91. Raymond KN, Eigenbrot CW Jr (1980) Acc Chem Res 13:276
92. Evans WJ, Foster SE (1992) J Organomet Chem 433:79
93. Edelmann FT, Freckmann DMM, Schumann H (2002) Chem Rev 102:1851
94. Evans WJ, Davis BL (2002) Chem Rev 102:2119
95. Evans William J, Kozimor Stosh A, Nyce Gregory W, Ziller Joseph W (2003) J Am Chem Soc 125:13831
96. Evans William J, Kozimor Stosh A, Ziller Joseph W (2003) J Am Chem Soc 125:14264
97. Evans WJ, Ulibarri TA, Ziller JW (1988) J Am Chem Soc 110:6877
98. Campazzi E, Solari E, Floriani C, Scopelliti R (1998) Chem Commun, p 2603
99. Roussel P, Scott P (1998) J Am Chem Soc 120:1070
100. Odom AL, Arnold PL, Cummins CC (1998) J Am Chem Soc 120:5836
101. Ganesan M, Gambarotta S, Yap GPA (2001) Angew Chem Int Edit Eng 40:766
102. Cloke FGN, Hitchcock PB (2002) J Am Chem Soc 124:9352
103. Evans WJ, Zucchi G, Ziller JW (2003) J Am Chem Soc 125:10
104. Evans WJ, Kozimor SA, Ziller JW (2005) Chem Commun, p 4681
105. Arney DSJ, Burns CJ, Smith DC (1992) J Am Chem Soc 114:10068

106. Evans WJ, Kozimor SA, Ziller JW, Kaltsoyannis N (2004) J Am Chem Soc 126:14533
107. Evans WJ, Kozimor SA, Ziller JW (2004) Polyhedron 23:2689
108. Villiers C, Ephritikhine M (1990) J Organomet Chem 393:339
109. Manriquez JM, Fagan PJ, Marks TJ, Vollmer SH, Day CS, Day VW (1979) J Am Chem Soc 101:5075
110. Fagan PJ, Manriquez JM, Marks TJ, Day CS, Vollmer SH, Day VW (1982) Organometallics 1:170
111. Wasserman HJ, Zozulin AJ, Moody DC, Ryan RR, Salazar KV (1983) J Organomet Chem 254:305
112. Zalkin A, Brennan JG (1985) Acta Cryst C 41:1295
113. Zalkin A, Brennan JG (1987) Acta Cryst C 43:1919
114. Brennan JG, Zalkin A (1985) Acta Cryst C 41:1038
115. Zalkin A, Brennan JG, Andersen RA (1987) Acta Cryst C 43:1706
116. Stults SD, Andersen RA, Zalkin A (1989) J Am Chem Soc 111:4507
117. Perego G, Cesari M, Farina F, Lugli G (1976) Acta Cryst B 32:3034
118. Arnaudet L, Charpin P, Folcher G, Lance M, Nierlich M, Vigner D (1986) Organometallics 5:270
119. Blake PC, Lappert MF, Taylor RG, Atwood JL, Hunter WE, Zhang H (1986) J Chem Soc Chem Commun, p 1394
120. Zalkin A, Brennan JG, Andersen RA (1988) Acta Cryst C 44:2104
121. Spirlet M-R, Rebizant J, Apostolidis C, Dornberger E, Kanellakopulos B, Powietzka B (1996) Polyhedron 15:1503
122. Lukens WW Jr, Beshouri SM, Blosch LL, Stuart AL, Andersen RA (1999) Organometallics 18:1235
123. Lukens WW Jr, Beshouri SM, Stuart AL, Andersen RA (1999) Organometallics 18:1247
124. Lukens WW Jr, Allen PG, Bucher JJ, Edelstein NM, Hudson EA, Shuh DK, Reich T, Andersen RA (1999) Organometallics 18:1253
125. Blake PC, Lappert MF, Taylor RG, Atwood JL, Zhang H (1987) Inorg Chim Acta 139:13
126. Beshouri SM, Zalkin A (1989) Acta Cryst C 45:1221
127. Zalkin A, Beshouri SM (1989) Acta Cryst C 45:1219
128. Blake PC, Lappert MF, Atwood JL, Zhang H (1988) J Chem Soc Chem Commun, p 1436
129. Blake PC, Hey E, Lappert MF, Atwood JL, Zhang H (1988) J Organomet Chem 353:307
130. Brennan JG, Andersen RA, Zalkin A (1986) Inorg Chem 25:1761
131. Baird MC, Wilkinson G (1966) J Chem Soc Chem Commun, p 514
132. Baird MC, Wilkinson G (1967) J Chem Soc A 1967:865
133. Berthet JC, Le Marechal JF, Nierlich M, Lance M, Vigner J, Ephritikhine M (1991) J Organomet Chem 408:335
134. Berthet JC, Ephritikhine M (1993) J Chem Soc Chem Commun, p 1566
135. Berthet J-C, Ephritikhine M, Lance M, Nierlich M, Vigner J (1993) J Organomet Chem 460:47
136. Mehdoui T, Berthet J-C, Thuery P, Ephritikhine M (2004) Eur J Inorg Chem:1996
137. Duttera MR, Fagan PJ, Marks TJ, Day VW (1982) J Am Chem Soc 104:865
138. Wasserman HJ, Moody DC, Ryan RR (1984) J Chem Soc Chem Commun, p 532
139. Brennan J, Shinomoto R, Zalkin A, Edelstein N (1984) Inorg Chem 23:4143
140. Arliguie T, Lescop C, Ventelon L, Leverd PC, Thuery P, Nierlich M, Ephritikhine M (2001) Organometallics 20:3698

141. Ventelon L, Lescop C, Arliguie T, Ephritikhine M, Leverd PC, Lance M, Nierlich M (1999) Chem Commun, p 659
142. Leverd PC, Ephritikhine M, Lance M, Vigner J, Nierlich M (1996) J Organomet Chem 507:229
143. Brennan JG, Stults SD, Andersen RA, Zalkin A (1987) Inorg Chim Acta 139:201
144. Brennan JG, Stults SD, Andersen RA, Zalkin A (1988) Organometallics 7:1329
145. Mehdoui T, Berthet J-C, Thuery P, Ephritikhine M (2004) Dalton Trans, p 579
146. Brennan JG, Andersen RA, Robbins JL (1986) J Am Chem Soc 108:335
147. Parry J, Carmona E, Coles S, Hursthouse M (1995) J Am Chem Soc 117:2649
148. Karraker DG (1987) Inorg Chim Acta 139:189
149. Boisson C, Berthet JC, Ephritikhine M, Lance M, Nierlich M (1997) J Organomet Chem 533:7
150. Cendrowski-Guillaume SM, Le Gland G, Nierlich M, Ephritikhine M (2003) Eur J Inorg Chem:1388
151. Mehdoui T, Berthet J-C, Thuery P, Ephritikhine M (2005) Dalton Trans, p 1263
152. Summerscales OT, Cloke FGN, Hitchcock PB, Green JC, Hazari N (2006) Science 311:829
153. Roger M, Belkhiri L, Thuery P, Arliguie T, Fourmigue M, Boucekkine A, Ephritikhine M (2005) Organometallics 24:4940
154. Mehdoui T, Berthet J-C, Thuery P, Salmon L, Riviere E, Ephritikhine M (2005) Chem Eur J 11:6994
155. Lukens WW Jr, Beshouri SM, Blosch LL, Andersen RA (1996) J Am Chem Soc 118:901
156. Avens LR, Burns CJ, Butcher RJ, Clark DL, Gordon JC, Schake AR, Scott BL, Watkin JG, Zwick BD (2000) Organometallics 19:451
157. Clark DL, Gordon JC, Huffman JC, Watkin JG, Zwick BD (1995) New J Chem 19:495
158. Fischer EO, Treiber A (1962) Z Naturforsch 173:276
159. Baumgaertner F, Fischer EO, Kanellakopulos B, Laubereau PG (1969) Angew Chem Int Edit Engl 8:202
160. Baumgaertner F, Fischer EO, Kanellakopulos B, Laubereau P (1968) Angew Chem Int Edit Engl 7:634
161. Burns JH (1974) J Organomet Chem 69:225
162. Maier R, Kanellakopulos B, Apostolidis C, Meyer D, Rebizant J (1993) J Alloys Compd 190:269
163. Rebizant J, Spirlet MR, Kanellakopulos B, Dornberger E (1986) J Less-Common Met 122:211
164. Karraker DG, Stone JA (1979) Inorg Chem 18:2205
165. Fischer EO, Laubereau P, Baumgaertner F, Kanellakopulos B (1966) J Organomet Chem 5:583
166. Marks TJ, Seyam AM, Wachter WA (1976) Inorg Synth 16:147
167. Laubereau PG, Ganguly L, Burns JH, Benjamin BM, Atwood JL, Selbin J (1971) Inorg Chem 10:2274
168. Spirlet MR, Rebizant J, Apostolidis C, Andreetti GD, Kanellakopulos B (1989) Acta Cryst C 45:739
169. Rebizant J, Spirlet MR, Apostolidis C, Kanellakopulos B (1991) Acta Cryst C 47:854
170. Anderson ML, Crisler LR (1969) J Organomet Chem 17:345
171. Leong J, Hodgson KO, Raymond KN (1973) Inorg Chem 12:1329
172. Blake PC, Edelman MA, Hitchcock PB, Hu J, Lappert MF, Tian S, Muller G, Atwood JL, Zhang H (1998) J Organomet Chem 551:261
173. Evans WJ, Nyce GW, Johnston MA, Ziller JW (2000) J Am Chem Soc 122:12019

174. Evans WJ, Kozimor SA, Ziller JW (2005) Organometallics 24:3407
175. Cloke FGN, Hawkes SA, Hitchcock PB, Scott P (1994) Organometallics 13:2895
176. Gradoz P, Boisson C, Baudry D, Lance M, Nierlich M, Vigner J, Ephritikhine M (1992) J Chem Soc Chem Commun, p 1720
177. Burns JH, Laubereau PG (1971) Inorg Chem 10:2789
178. Goffart J, Duyckaerts G (1978) Inorg Nucl Chem Lett 14:15
179. Goffart J, Desreux JF, Gilbert BP, Delsa JL, Renkin JM, Duyckaerts G (1981) J Organomet Chem 209:281
180. Berthet JC, Le Marechal JF, Lance M, Nierlich M, Vigner J, Ephritikhine M (1992) J Chem Soc Dalton Trans, p 1573
181. Fischer RD, Sienel GR (1976) Z Anorg Allg Chem 419:126
182. Fischer RD, Sienel GR (1978) J Organomet Chem 156:383
183. Kanellakopulos B, Dornberger E, Billich H (1974) J Organomet Chem 76:C42
184. Marks TJ, Kolb JR (1975) J Am Chem Soc 97:27
185. Bagnall KW, Plews MJ, Brown D (1982) J Organomet Chem 224:263
186. Bagnall KW, Plews MJ, Brown D, Fischer RD, Klaehne E, Landgraf GW, Sienel GR (1982) J Chem Soc Dalton Trans, p 1999
187. Von Ammon R, Kanellakopulos B, Fischer RD, Laubereau P (1969) Inorg Nucl Chem Lett 5:219
188. Fischer RD, Klaehne E, Sienel GR (1982) J Organomet Chem 238:99
189. Fischer RD, Klaehne E, Kopf J (1978) Z Naturforsch 33B:1393
190. Aslan H, Yunlu K, Fischer RD, Bombieri G, Benetollo F (1988) J Organomet Chem 354:63
191. Adam M, Yunlu K, Fischer RD (1990) J Organomet Chem 387:C13
192. Berthet J-C, Boisson C, Lance M, Vigner J, Nierlich M, Ephritikhine M (1995) J Chem Soc Dalton Trans, p 3027
193. Spirlet MR, Rebizant J, Apostolidis C, Kanellakopulos B (1993) Acta Cryst C 49:929
194. Spirlet MR, Rebizant J, Apostolidis C, Van den Bossche G, Kanellakopulos B (1990) Acta Cryst C 46:2318
195. Berthet J-C, Nierlich M, Ephritikhine M (2002) Compt Rend Chimie 5:81
196. Berthet JC, Ephritikhine M, Berthet JC, Lance M, Nierlich M (1998) Chem Commun, p 1373
197. Berthet JC, Nierlich M, Ephritikhine M (2002) Eur J Inorg Chem:850
198. Jamerson JD, Masino AP, Takats J (1974) J Organomet Chem 65:C33
199. Goffart J, Gilbert B, Duyckaerts G (1977) Inorg Nucl Chem Lett 13:189
200. Paolucci G, Rossetto G, Zanella P, Fischer RD (1985) J Organomet Chem 284:213
201. Arduini AL, Edelstein NM, Jamerson JD, Reynolds JG, Schmid K, Takats J (1981) Inorg Chem 20:2470
202. Lin Z, Brock CP, Marks TJ (1988) Inorg Chim Acta 141:145
203. Leverd PC, Arliguie T, Ephritikhine M, Nierlich M, Lance M, Vigner J (1993) New J Chem 17:769
204. Tatsumi K, Matsubara I, Inoue Y, Nakamura A, Cramer RE, Tagoshi GJ, Golen JA, Gilje JW (1990) Inorg Chem 29:4928
205. Leverd PC, Arliguie T, Lance M, Nierlich M, Vigner J, Ephritikhine M (1994) Dalton Trans, p 501
206. Domingos A, Pires de Matos A, Santos I (1992) Polyhedron 11:1601
207. Domingos A, Marcalo J, Pires De Matos A (1992) Polyhedron 11:909
208. Leverd PC, Lance M, Nierlich M, Vigner J, Ephritikhine M (1993) Dalton Trans, p 2251
209. Leverd PC, Lance M, Nierlich M, Vigner J, Ephritikhine M (1994) J Chem Soc Dalton Trans, p 3563

210. Leverd PC, Lance M, Vigner J, Nierlich M, Ephritikhine M (1995) J Chem Soc Dalton Trans, p 237
211. Brandi G, Brunelli M, Lugli G, Mazzei A (1973) Inorg Chim Acta 7:319
212. Calderazzo F (1973) Pure Appl Chem 33:453
213. Gebala AE, Tsutsui M (1973) J Am Chem Soc 95:91
214. Marks TJ, Seyam AM, Kolb JR (1973) J Am Chem Soc 95:5529
215. Tsutsui M, Ely N, Gebala A (1975) Inorg Chem 14:78
216. Marks TJ (1979) Prog Inorg Chem 25:223
217. Atwood JL, Tsutsui M, Ely N, Gebala AE (1976) J Coord Chem 5:209
218. Burns JH (1973) J Am Chem Soc 95:3815
219. Halstead GW, Baker EC, Raymond KN (1975) J Am Chem Soc 97:3049
220. Porchia M, Casellato U, Ossola F, Rossetto G, Zanella P, Graziani R (1986) J Chem Soc Chem Commun, p 1034
221. Porchia M, Brianese N, Casellato U, Ossola F, Rossetto G, Zanella P, Graziani R (1989) J Chem Soc Dalton Trans, p 677
222. Porchia M, Ossola F, Rossetto G, Zanella P, Brianese N (1987) J Chem Soc Chem Commun, p 550
223. Sonnenberger DC, Mintz EA, Marks TJ (1984) J Am Chem Soc 106:3484
224. Paolucci G, Rossetto G, Zanella P, Yunlu K, Fischer RD (1984) J Organomet Chem 272:363
225. Villiers C, Ephritikhine M (1994) J Chem Soc Dalton Trans, p 3397
226. Berthet JC, Ephritikhine M (1992) New J Chem 16:767
227. Dormond A, Elbouadili AA, Moise C (1984) J Chem Soc Chem Commun, p 749
228. Zanella P, Brianese N, Casellato U, Ossola F, Porchia M, Rossetto G, Graziani R (1987) J Chem Soc Dalton Trans, p 2039
229. Cramer RE, Maynard RB, Paw JC, Gilje JW (1981) J Am Chem Soc 103:3589
230. Cramer RE, Maynard RB, Paw JC, Gilje JW (1982) Organometallics 1:869
231. Cramer RE, Maynard RB, Paw JC, Gilje JW (1983) Organometallics 2:1336
232. Cramer RE, Mori AL, Maynard RB, Gilje JW, Tatsumi K, Nakamura A (1984) J Am Chem Soc 106:5920
233. Cramer RE, Higa KT, Gilje JW (1984) J Am Chem Soc 106:7245
234. Cramer RE, Panchanatheswaran K, Gilje JW (1984) J Am Chem Soc 106:1853
235. Cramer RE, Maynard RB, Gilje JW (1978) J Am Chem Soc 100:5562
236. Cramer RE, Maynard RB, Gilje JW (1980) Inorg Chem 19:2564
237. Baker EC, Raymond KN, Marks TJ, Wachter WA (1974) J Am Chem Soc 96:7586
238. Cramer RE, Maynard RB, Gilje JW (1981) Inorg Chem 20:2466
239. Cramer RE, Jeong JH, Gilje JW (1986) Organometallics 5:2555
240. Cramer RE, Engelhardt U, Higa KT, Gilje JW (1987) Organometallics 6:41
241. Cramer RE, Jeong JH, Richmann PN, Gilje JW (1990) Organometallics 9:1141
242. Cramer RE, Edelmann F, Mori AL, Roth S, Gilje JW, Tatsumi K, Nakamura A (1988) Organometallics 7:841
243. Kanellakopulos B, Aderhold C, Dornberger E (1974) J Organomet Chem 66:447
244. Jamerson JD, Takats J (1974) J Organomet Chem 78:C23
245. Zanella P, De Paoli G, Bombieri G, Zanotti G, Rossi R (1977) J Organomet Chem 142:C21
246. Zalkin A, Brennan JG, Andersen RA (1987) Acta Cryst C 43:418
247. Gradoz P, Baudry D, Ephritikhine M, Lance M, Nierlich M, Vigner J (1994) J Organomet Chem 466:107
248. Manriquez JM, Fagan PJ, Marks TJ (1978) J Am Chem Soc 100:3939

249. Fagan PJ, Manriquez JM, Maatta EA, Seyam AM, Marks TJ (1981) J Am Chem Soc 103:6650
250. Green JC, Watts O (1978) J Organomet Chem 153:C40
251. Spirlet MR, Rebizant J, Apostolidis C, Kanellakopulos B (1992) Acta Cryst C 48:2135
252. Rabinovich D, Schimek GL, Pennington WT, Nielsen JB, Abney KD (1997) Acta Cryst C 53:1794
253. Rabinovich D, Bott SG, Nielsen JB, Abney KD (1998) Inorg Chim Acta 274:232
254. Barnea E, Andrea T, Kapon M, Berthet J-C, Ephritikhine M, Eisen MS (2004) J Am Chem Soc 126:10860
255. Blake PC, Lappert MF, Taylor RG, Atwood JL, Hunter WE, Zhang H (1995) J Chem Soc Dalton Trans, p 3335
256. Eigenbrot CW Jr, Raymond KN (1982) Inorg Chem 21:2653
257. Fendrick CM, Schertz LD, Day VW, Marks TJ (1988) Organometallics 7:1828
258. Stern D, Sabat M, Marks TJ (1990) J Am Chem Soc 112:9558
259. Schnabel RC, Scott BL, Smith WH, Burns CJ (1999) J Organomet Chem 591:14
260. Wang J, Gurevich Y, Botoshansky M, Eisen MS (2006) J Am Chem Soc 128:9350
261. Dash AK, Gourevich I, Wang JQ, Wang J, Kapon M, Eisen MS (2001) Organometallics 20:5084
262. Paolucci G, Fischer RD, Benetollo F, Seraglia R, Bombieri G (1991) J Organomet Chem 412:327
263. Deng DL, Zhang XF, Qian CT, Sun J, Zheng PJ, Chen J (1996) Chin Chem Lett 7:1143
264. Smith GM, Suzuki H, Sonnenberger DC, Day VW, Marks TJ (1986) Organometallics 5:549
265. Erker G, Muehlenbernd T, Benn R, Rufinska A (1986) Organometallics 5:402
266. Straub T, Haskel A, Neyroud TG, Kapon M, Botoshansky M, Eisen MS (2001) Organometallics 20:5017
267. Kiplinger JL, Morris DE, Scott BL, Burns CJ (2002) Organometallics 21:3073
268. Morris DE, Re RED, Jantunen KC, Castro-Rodriguez I, Kiplinger JL (2004) Organometallics 23:5142
269. Jantunen KC, Burns CJ, Castro-Rodriguez I, Da Re RE, Golden JT, Morris DE, Scott BL, Taw FL, Kiplinger JL (2004) Organometallics 23:4682
270. Da Re RE, Jantunen KC, Golden JT, Kiplinger JL, Morris DE (2005) J Am Chem Soc 127:682
271. Schelter EJ, Morris DE, Scott BL, Kiplinger JL (2007) Chem Commun, p 1029
272. Radu NS, Engeler MP, Gerlach CP, Tilley TD, Rheingold AL (1995) J Am Chem Soc 117:3621
273. Fagan PJ, Manriquez JM, Vollmer SH, Day CS, Day VW, Marks TJ (1981) J Am Chem Soc 103:2206
274. Wrobleski DA, Ryan RR, Wasserman HJ, Salazar KV, Paine RT, Moody DC (1986) Organometallics 5:90
275. Hall SW, Huffman JC, Miller MM, Avens LR, Burns CJ, Sattelberger AP, Arney DSJ, England AF (1993) Organometallics 12:752
276. Wrobleski DA, Cromer DT, Ortiz JV, Rauchfuss TB, Ryan RR, Sattelberger AP (1986) J Am Chem Soc 108:174
277. Brennan JG, Andersen RA, Zalkin A (1988) J Am Chem Soc 110:4554
278. Arney DSJ, Burns CJ (1995) J Am Chem Soc 117:9448
279. Haskel A, Straub T, Eisen MS (1996) Organometallics 15:3773
280. Arney DSJ, Schnabel RC, Scott BC, Burns CJ (1996) J Am Chem Soc 118:6780
281. Duttera MR, Day VW, Marks TJ (1984) J Am Chem Soc 106:2907

282. Scherer OJ, Werner B, Heckmann G, Wolmershaeuser G (1991) Angew Chem Int Edit Eng 103:562
283. Scherer OJ, Schulze J, Wolmershaeuser G (1994) J Organomet Chem 484:C5
284. Lescop C, Arliguie T, Lance M, Nierlich M, Ephritikhine M (1999) J Organomet Chem 580:137
285. Broach RW, Schultz AJ, Williams JM, Brown GM, Manriquez JM, Fagan PJ, Marks TJ (1979) Science 203:172
286. Bruno JW, Marks TJ, Morss LR (1983) J Am Chem Soc 105:6824
287. Bruno JW, Stecher HA, Morss LR, Sonnenberger DC, Marks TJ (1986) J Am Chem Soc 108:7275
288. Tatsumi K, Nakamura A, Hofmann P, Stauffert P, Hoffmann R (1985) J Am Chem Soc 107:4440
289. Bruno JW, Smith GM, Marks TJ (1986) J Am Chem Soc 108:40
290. Fendrick CM, Marks TJ (1986) J Am Chem Soc 108:425
291. Maynadie J, Berthet J-C, Thuery P, Ephritikhine M (2007) Organometallics 26:4585
292. Mehdoui T, Berthet J-C, Thuery P, Ephritikhine M (2005) Chem Commun, p 2860
293. Doretti L, Zanella P, Faraglia G, Faleschini S (1972) J Organomet Chem 43:339
294. Bagnall KW, Edwards J (1974) J Organomet Chem 80:C14
295. Bagnall KW, Edwards J, Tempest AC (1978) J Chem Soc Dalton Trans, p 295
296. Ernst RD, Kennelly WJ, Day CS, Day VW, Marks TJ (1979) J Am Chem Soc 101:2656
297. Baudry D, Dorion P, Ephritikhine M (1988) J Organomet Chem 356:165
298. Le Marechal JF, Ephritikhine M, Folcher G (1986) J Organomet Chem 299:85
299. Bagnall KW, Payne GF, Alcock NW, Flanders DJ, Brown D (1986) J Chem Soc Dalton Trans, p 783
300. Bagnall KW, Payne GF, Brown D (1985) J Less-Common Met 113:325
301. Edelman MA, Lappert MF, Atwood JL, Zhang H (1987) Inorg Chim Acta 139:185
302. Mintz EA, Moloy KG, Marks TJ, Day VW (1982) J Am Chem Soc 104:4692
303. Butcher RJ, Clark DL, Grumbine SK, Scott BL, Watkin JG (1996) Organometallics 15:1488
304. Cymbaluk TH, Ernst RD, Day VW (1983) Organometallics 2:963
305. Marks TJ, Day VW (1985) NATO ASI Ser, Ser C 155:115
306. Schelter EJ, Veauthier JM, Thompson JD, Scott BL, John KD, Morris DE, Kiplinger JL (2006) J Am Chem Soc 128:2198
307. Straub T, Frank W, Reiss GJ, Eisen MS (1996) J Chem Soc Dalton Trans, p 2541
308. Evans WJ, Kozimor SA, Ziller JW (2005) Science 309:1835
309. Enriquez AE, Scott BL, Neu MP (2005) Inorg Chem 44:7403
310. Danopoulos AA, Hankin DM, Cafferkey SM, Hursthouse MB (2000) Dalton Trans, p 1613
311. Pool JA, Scott BL, Kiplinger JL (2005) J Am Chem Soc 127:1338
312. Boisson C, Berthet JC, Lance M, Nierlich M, Ephritikhine M (1997) J Organomet Chem 548:9
313. Cramer RE, Roth S, Gilje JW (1989) Organometallics 8:2327
314. Cramer RE, Ariyaratne KANS, Gilje JW (1995) Z Anorg Allg Chem 621:1856
315. Ariyaratne KANS, Cramer RE, Jameson GB, Gilje JW (2004) J Organomet Chem 689:2029
316. Cramer RE, Roth S, Edelmann F, Bruck MA, Cohn KC, Gilje JW (1989) Organometallics 8:1192
317. Maynadie J, Berthet J-C, Thuery P, Ephritikhine M (2006) J Am Chem Soc 128:1082

Struct Bond (2008) 127: 87–117
DOI 10.1007/430_2007_078

Published online: 24 January 2008

Activation of Small Molecules by U(III) Cyclooctatetraene and Pentalene Complexes

Owen T. Summerscales · F. Geoffrey N. Cloke (✉)

Department of Chemistry, School of Life Sciences, University of Sussex, Brighton BN1 9Q, UK
f.g.cloke@sussex.ac.uk

Abstract The low-valent complexes of uranium (i.e. those containing U(III) centres) are characterised as reactive, highly reducing species that can effect novel, and potentially useful, transformations of small molecules. In this chapter we review one particular class of these compounds – those supported by cyclooctatetraene and pentalene ligands – whose reduction chemistry has recently demonstrated novel and unexpected results, including the cyclooligomerisation of CO. The syntheses and structures of these compounds are presented, and their reactivity towards a variety of small molecules is examined and reviewed. The reactivity towards carbon monoxide is discussed in reference to the historical development of obtaining oxocarbons from CO.

Keywords Activation · Cyclooctatetraene · Pentalene · Reduction chemistry · Small molecule · Uranium

Abbreviations

$COT^{\dagger}$	1,4-Bis(tri-isopropylsilyl)cyclooctatetraene
COT	Cyclooctatetraene
Cp*	Pentamethylcyclopentadienyl
Cp^{Me_4H}	Tetramethylcyclopentadienyl

Cp^{Me}	Monomethylcyclopentadienyl
Cp	Cyclopentadienyl
DFT	Density functional theory
HMPA	Hexamethylphosphoramide
Ln	Lanthanide
Me_2bipy	4,4′-Dimethyl-2,2′-bipyridine
Pent	Pentalene
SCE	Standard calomel electrode
tacn	Triazacyclononane
THF	Tetrahydrofuran
tmp	Tetramethylphospholyl
Tp*	3,5-Dimethyl tris(pyrazolyl)borate
TXP	Tetra-(3,5-dimethylphenyl)porphyrinato

1 Introduction

The controlled activation of small, relatively inert molecules has been a constant theme in organometallic chemistry since the 1950s [1]. It is concerned with new transformations of chemical feedstocks that are cheap and readily available, and challenges chemists to develop a new chemistry of simple molecules whose formulations have been known for centuries, where the old chemistries may appear apparently "exhausted". Current research is particularly focused on developing "green" chemistry – such as the utilisation of the planet's alkane resources more effectively via C – H activation [2], the development of new methods to store and/or usefully transform the greenhouse gas CO_2 [3], efficient methods of removing polluting CFCs with C – F activation [4], conversion of N_2 into nitrogen-containing organic products [5, 6], and the use of renewable sources of CH_4 and CO as C1 building blocks for pharmaceuticals, materials or fuels [7].

Many of the reported successful activation processes are powered by electron-rich metal complexes; recently, uranium(III) compounds have displayed high, and in some cases, previously unknown types of reactivity in this context [8, 9]. These exciting discoveries made over the last 10 years or so by a number of workers represent a renewed effort at understanding and exploring the often unpredictable nature of U(III) reactivity [10–13]. This chemistry ultimately attempts to combine the control afforded by an organometallic reaction with the sheer reductive power of an alkali metal, in order to achieve useful transformations of small molecules. Furthermore, at a time when escalating energy needs are putting nuclear power in greater demand, it is of clear importance to find industrial uses for depleted uranium, a major side-product of the nuclear industry.

Somewhat overlooked by "mainstream" organometallic chemistry (there are practical difficulties associated with handling the highly oxygen- and

moisture-sensitive complexes of the low-valent *f*-elements) organoactinide, and closely related lanthanide, chemistry has been developed at a much slower rate than the corresponding chemistry of the *d*-block [14, 15]. Pioneering work by the Evans and Andersen groups has previously shown that ring-substituted cyclopentadienyl ligands can be extremely effective for harnessing the reduction chemistry of low-valent *f*-element centres. In particular, a wealth of remarkable chemistry demonstrating many new small molecule transformations has been shown for $Sm(Cp^*)_2(THF)_x$ ($x = 0$, 2; Cp^* = pentamethylcyclopentadienyl) and $U(Cp^R)_3(THF)_x$ (R = alkyl, trialkylsilyl; $x = 1$, 0). This work has been comprehensively reviewed elsewhere [9, 14].

In *f*-element reduction chemistry, it is usual for two equivalents of a reducing species "M(L)" to react with a substrate "S" to give a sandwiched product of the type $[M(L)]_2{}^{n+}(\mu\text{-}S)^{2n-}$, in which each metal donates one electron (or sometimes more, vide infra) to give a doubly reduced substrate, which is held between the two monoxidised fragments. The simple electronic reduction to give $(S)^{2n-}$ is appropriate for some cases but reductive homologation of substrates to units of $(S)_x{}^{2n-}$ and transformations to totally new substrates are also well documented. Most of these reductions derive from either a pair of one-electron Ln(II)/Ln(III) or U(III)/U(IV) processes; however, two-electron U(III)/U(V) processes are also known and demonstrate a further interest in uranium reduction chemistry. Uranium(III) centres possess accessible higher oxidation states, and thus may in theory participate in one-, two-, or three-electron reductions whilst the divalent lanthanides are limited to one-electron processes. Having said this, the U(IV) state is a relatively stable configuration for "soft" ligands under anaerobic conditions, and therefore most of these reductions simply involve a one-electron U(III)/U(IV) process.

Maintaining the approach of using "soft", sterically hindered carbocyclic ligands to engender high reactivity, the chemistry of U(III) has been investigated using the substituted, eight-membered carbocycles cyclooctatetraene (COT) and pentalene (a bicyclic analogue of COT), in conjunction with a cyclopentadienyl co-ligand, to give a variety of mixed-sandwich $COT^{R'}/Cp^R$ and $Pent^{R'}/Cp^R$ U(III) complexes. Their reactivity towards small molecules has produced some unique and exciting results, which are the subject of this chapter.

2 Synthesis of Mixed Sandwich U(III) Cyclooctatetraene and Pentalene Complexes

In order to reflect the order in which the research was carried out, chemistry of the $Pent^{R'}/Cp^R$ uranium systems will be discussed first. Pentalene is an eight-membered bicyclic carbocycle; the planar dianion is a 10π Hückel

aromatic, analogous to COT^{2-}. As a ligand in organometallic chemistry, it may be commonly considered to act as two fused Cp rings; however, it is also extremely versatile with bonding modes varying from a bent, fully coordinated η^8-mode to simply η^1-bound [16]. The analogy with Cp is more structural than electronic – pentalene has fewer "aromatised" electrons than two Cp rings (10 vs. 12) – but crucially, can engage in δ-type bonding with the f-elements when fully coordinated, allowing more electron density to be donated overall. This was demonstrated originally for COT in the "classic" sandwich compound uranocene $U(\eta\text{-}COT)_2$. The bonding in uranocene is found to consist of strong δ-type donation into vacant d- and f-orbitals, which are of similar energy in the $5f$ metal uranium [17].

Synthesis of the uranocene analogue, bis(pentalene) U(IV), was achieved in 1997 using the dipotassium salt of the 1,4-bis(tri-isopropylsilyl) derivative $C_8H_4{}^{\dagger}[K]_2$ {† = 1,4-bis(tri-isopropylsilyl)} and UCl_4 to give $U(\eta - C_8H_4{}^{\dagger})_2$ [18]. Potassium salts are commonly used in preference to lithium salts for salt metathesis reactions with f-element halides to avoid the formation of aggregated "-ate" complexes; the bulky silyl groups impart solubility and crystallinity to the resulting organometallic compounds, aiding both manipulation and characterisation, and can sterically protect reactive metal centres. The same benefits can of course be achieved by the use of alkyl substituents, with the added benefit of enhanced electronic activation (electron-withdrawing silyl vs. electron-donating alkyl). However, preparing multiply alkylated pentalene or COT ligands is difficult; it has only been very recently achieved by O'Hare et al. with hexamethylpentalene [19]. Although routes are known to 1,4-dialkyl and 1,3,5,7-tetraalkyl COT species, the syntheses are multi-step, low-yielding reactions [20, 21]. In comparison, the 1,4-disilylated derivatives may be easily prepared in good yield by addition of the appropriate silyl electrophile to either the COT or pentalene dianion, followed by double deprotonation with KNH_2 (Fig. 1) [22]. The origin of the asymmetry of substitution in the $COT^{\dagger}$ dianion is the stable arrangement of C = C double bonds in the triene precursor.

DFT analysis on the unsubstituted compound $U(\eta - C_8H_6)_2$ showed that the primary interaction between the ligand and the metal is of δ-symmetry, in a manner similar to that found in uranocene [23]. Comparison of photoelectron spectra gave evidence that the electron "richness" at the tetravalent centre of the uranium compounds varies in the order $U(C_8H_4{}^{\dagger})_2 > U(COT)_2 > U(Cp)_4$, implying a similar trend in the electron-donating properties of the ligands.

The dianionic ligands COT and pentalene act as stronger electron donors for uranium than the anionic Cp ligands, due to the additional δ-interactions, and the U(IV) compounds $U(COT)_2$ and $U(C_8H_4{}^{\dagger})_2$ are extremely stable under anaerobic conditions. Use of the ligands with the lower oxidation state, U(III), would be expected to make these compounds even more electron-rich than the $U(Cp^R)_3(THF)_x$ systems (i.e. more reducing) and, at least partly

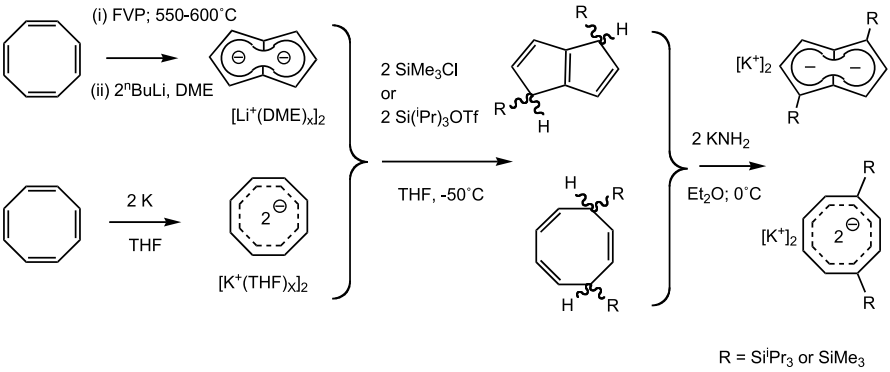

Fig. 1 Synthetic routes to silylated eight-membered carbocycles

for this reason, has consequently allowed us to observe new types of small molecule activation.

The synthesis of $UI_3(THF)_4$ in 1989 has undoubtedly opened up the field of low-valent organouranium chemistry, as it provides a readily prepared, reasonably soluble starting material for the synthesis of U(III) complexes [24]. However, the THF solvent molecules are irreversibly bound to the metal centre, which has created difficulties in synthesising "base-free" uranium compounds, i.e. those without coordinated Lewis bases (such as THF) that can otherwise bind strongly to the uranium centre and block the active site that is required for small molecule activation. For example, only the base-free versions of the compounds $Sm(Cp^*)_2$ and $U(Cp^{Me_4H})_3$ have shown any reactivity with N_2 and CO (respectively); the THF adducts are unreactive [25, 26]. Both these oxophilic compounds were obtained by desolvation of the corresponding THF adducts, therefore initial attempts at the synthesis of a $Pent^{R'}/Cp^R$ mixed-sandwich U(III) complex involved synthesis of the THF adduct and subsequent desolvation.

Addition of one equivalent of $C_8H_4^{\dagger}[K]_2$ to $UI_3(THF)_4$ gave the U(IV) compound $U(C_8H_4^{\dagger})_2$ exclusively, the product of a disproportionation. The high stability of the bis(pentalene) sandwich compound means that it is often found to be a thermodynamic sink for many of these reactions. The compound $U(Cp^*)I_2(THF)_3$ is known [27], and addition of one equivalent of $C_8H_4^{\dagger}[K]_2$ to the latter in THF gave the desired U(III) compound $U(C_8H_4^{\dagger})(Cp^*)(THF)$ (**1.THF**; see Appendix for list of structures) in good yield (Cloke FGN, unpublished results). However, this compound proved resistant to thermal desolvation in vacuo, and decomposed (at > 130 °C) before losing any bound THF. Therefore, the synthesis of a base-free starting material was clearly desirable.

Base-free UI_3 may be obtained in almost quantitative yield by using a modification of a method described by Corbett for the synthesis of base-free lanthanide triiodides [28]: a mixture of oxide-free uranium turnings and

two equivalents of HgI_2 are heated in a thick-walled tube, sealed in vacuo, at 320 °C for 3 days. Use of excess HgI_2 is acceptable as the tetravalent compound UI_4 is unstable with respect to disproportionation to I_2 plus UI_3 [29]. The base-free material UI_3 is a purple-black solid, insoluble in all common solvents; it may be readily converted to the semi-soluble $UI_3(THF)_4$ by addition of THF. The lack of solubility of UI_3 is not problematic as it is typically solubilised by reaction with potassium salts in solvents such as diethyl ether and toluene.

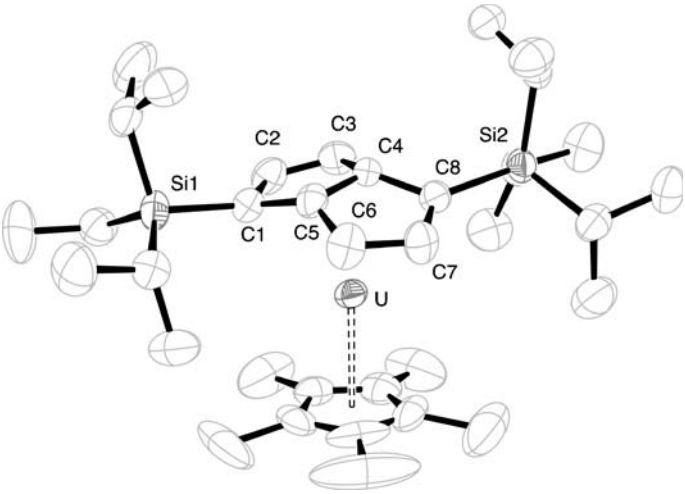

Structure 1

The synthesis of base-free $U(C_8H_4^{\dagger})(Cp^*)$ (**1**) was achieved by the reaction of UI_3 and KCp^* in Et_2O, giving a green intermediate that was rigorously dried under vacuum, and subsequent addition of $C_8H_4^{\dagger}[K]_2$ in toluene [30]. The U(III) compound, obtained in 40% yield after work-up, was found to be extremely air- and moisture-sensitive and could only be handled with the use of very high purity argon and freshly degassed, dry solvents. Structural determinations showed a slightly bent mixed-sandwich arrangement of fully coordinated ligands, requiring the pentalene ligand to adopt the bent η^8-mode.

Although in the original paper describing this synthesis, the green intermediate material was assumed to be $\{UCp^*I_2\}_n$ or an etherate thereof, more recent work has shown that the compound is in fact a mixed-valence U(III)/U(IV) trimer $[U(Cp^*)(\mu\text{-}I)_2]_3(\mu^3\text{-}O)$ [31]. The oxo unit has been scavenged from the solvent, giving a cluster structurally very similar to the U(IV) sulfide $[U(Cp^*)I(\mu\text{-}I)]_3(\mu^3\text{-}I)(\mu^3\text{-}S)$ (derived from $U(Cp^*)I_2(THF)_3$ and CS_2 [32]). This illustrates the enhanced reducing power of the THF-free U(III) centres as $U(Cp^*)I_2(THF)_3$ will not activate Et_2O.

It was envisaged that subtle variations in the steric and/or electronic properties of the $Pent^{R'}/Cp^{R}$ U(III) reducing agent might significantly affect the activation of small molecules, as observed in other systems. For example, Schrock has reported that slight variations in the substitution of terphenyl rings attached to a triamidoamine ligand significantly affect the outcome of dinitrogen activation in molybdenum systems [33, 34]. Thus, the synthesis of the less sterically hindered tetramethyl-Cp derivative was attempted, but resulted in the formation of the U(IV) dimer $[U(C_8H_4{}^{\dagger})(Cp^{Me_4H})(\mu\text{-I})]_2$ (**2**) [35]. Presumably this tetravalent compound is generated from a disproportionation reaction of the type already described for the synthesis of the U(IV) tris-amide $U(I)[N(^{t}Bu)(1,3\text{-}C_6H_3Me_2)]_3$ from $UI_3(THF)_4$ [36]. This result implies that there is a level of steric unsaturation above which these mixed-sandwich molecules become unstable as trivalent compounds.

In order to further investigate these mixed-sandwich systems, the synthesis of the COT analogue, viz. $U(COT^{\dagger})(Cp^{*})$, of the pentalene compound was explored. Unlike pentalene, COT is a commonly used ligand in organometallic chemistry, and has been much more thoroughly researched as such. The unsubstituted complex U(COT)(Cp*)(THF) (**3.THF**) was first reported by Sattelberger et al. in 1993 [37]; crystallographic characterisation remains elusive; however, adducts of the type U(COT)(Cp*)(L) (**3.L**) have been structurally characterised for L = Me_2bipy and HMPA, and show typical η^8- and η^5- coordination of the rings [37, 38]. A tetramethylphospholyl (PC_4Me_4; tmp) derivative, $U(COT)(tmp)(HMPA)_2$ [38], is also known and would be of interest in this context as tmp is closely related to Cp^{Me_4H} (C_5Me_4H), as borne out by the isostructural nature of the U(IV) compounds $U(tmp)_3Cl$ and $U(Cp^{Me_4H})_3Cl$ [39, 40].

Attempts at repeating the synthetic route for base-free **1** from UI_3, using $COT^{\dagger}[K]_2$ in the place of the pentalene salt, failed for reasons unknown. Therefore, the adduct $U(COT^{\dagger})(Cp^{*})(THF)$ (**4.THF**) was prepared in THF with the intention of removing the bound solvent molecule in vacuo. A one-pot reaction of UI_3 with KCp* in THF, and $COT^{\dagger}[K]_2$, furnished **4.THF** as a THF adduct in moderate yield [41]. Further variants were synthesised with

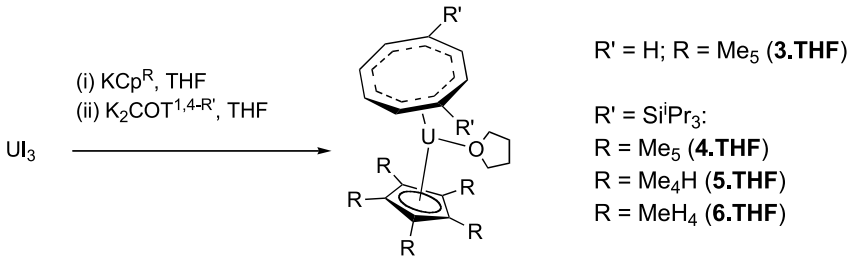

Fig. 2 Synthesis of mixed-sandwich compounds **3.THF–6.THF** from UI_3

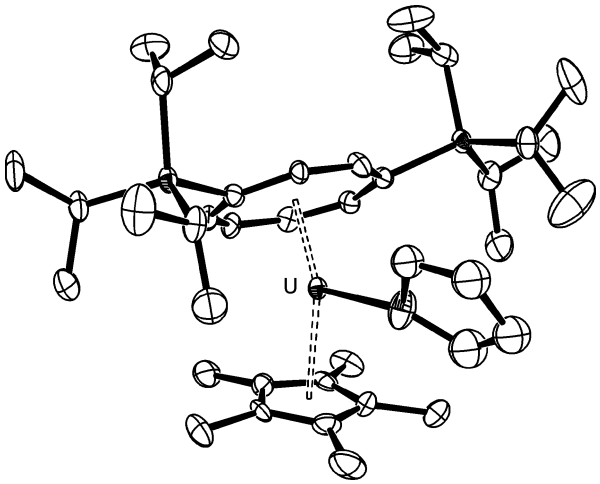

Structure 2

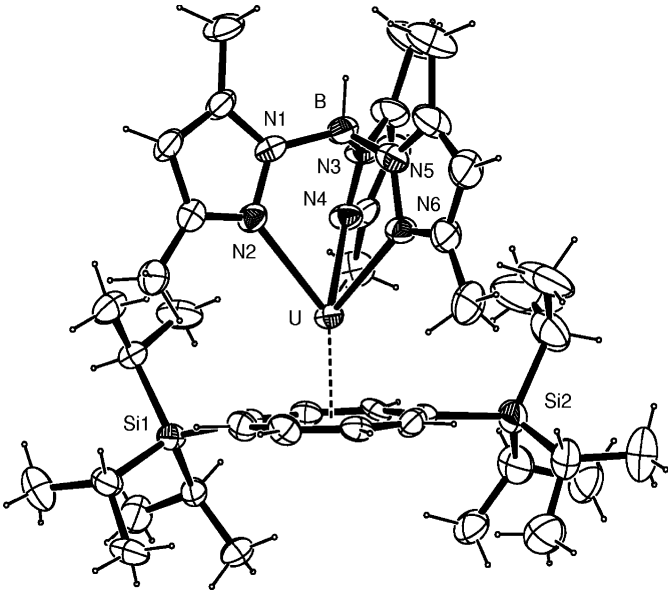

Structure 3

the tetra- and monomethylated Cp rings, giving U(COT†)(Cp^{Me_4H})(THF) (**5.THF**) and U(COT†)(Cp^{Me})(THF) (**6.THF**), respectively (Fig. 2) [35, 42]. Use of the Cp analogue tris(3,5-dimethylpyrazolyl)borate (Tp*) gave the base-free uranium complex U(COT†)(Tp*) (**7**) despite the use of THF, presumably due to the extra steric crowding exerted by the Tp* ligand (Farnaby J, Hitchcock PB, Cloke FGN, unpublished results). The structure of **7** shows full η^8- and η^3-

coordination of the ligands, with a non-linear centroid($COT^{\dagger}$)–U–B angle, i.e. a slightly bent arrangement between the $COT^{\dagger}$ and Tp* ligands.

No uranocene impurities were detected in the isolated samples, although it was detected in the mother-liquor; its formation appears to limit the yield of these reactions. This novel uranocene $U(COT^{\dagger})_2$, which may be obtained directly from UCl_4, is found to be too soluble to crystallise from pentane, unlike the trimethylsilyl analogue $U(COT^{1,4\text{-}SiMe_3})_2$, which has been found to crystallise readily from hydrocarbon solvents and contaminates samples of the less sterically hindered $U(COT^{1,4\text{-}SiMe_3})(Cp^*)(THF)$ (**8.THF**), limiting the utility of the bis-trimethylsilyl derivative in reduction chemistry [43].

X-ray analyses of **4.THF–6.THF** revealed a typical bent, fully coordinated η^8- and η^5-arrangement of the rings in the $COT^{\dagger}/Cp^R$ complexes, and also some very long U–O(THF) distances (average 2.710(4) Å), larger than any others in the literature for a U(III) species. These values reflect a very weak bond, and it was consequently discovered that they could all be desolvated without decomposition at 100–110 °C and 10^{-6} mbar to give $U(COT^{\dagger})(Cp^*)$ (**4**), $U(COT^{\dagger})(Cp^{Me_4H})$ (**5**) and $U(COT^{\dagger})(Cp^{Me})$ (**6**) [35]. The base-free compounds were all found to be extremely soluble (and very reactive) and could not be crystallised, therefore structural data are currently lacking; however, they have been characterised by ^1H NMR spectroscopy and mass spectrometry. Attempted desolvation of the less sterically hindered **3.THF** resulted in thermal decomposition (at > 130 °C).

2.1 Electronic Spectroscopy

Electronic spectra for the *f*-elements often contain many weak, sharp peaks in the visible to near-infrared region; these originate from Laporte-forbidden *f*–*f* transitions, and are observed in the late-visible/near-infrared (700–1200 nm) for solutions of these U(III) complexes [29]. The ground state of trivalent uranium is $5f^3$; however, the $5f^26d$ state is sufficiently low-lying for $5f^3 \rightarrow 5f^26d$ transitions to occur in the early-visible region, often in the range 15 000–30 000 cm^{-1} (ca. 350–650 nm). These transitions are parity-allowed, often observed as broad, intense absorption peaks, and give U(III) compounds the dark, strong colorations that are distinctive of the oxidation state. These are noted as two main peaks for **4.THF**, **5.THF** and **6.THF** at similar wavelengths; in **4.THF** these occur at 497 and 584 nm (Summerscales OT, Hitchcock PB, Cloke FGN, unpublished results). These parameters are important as they allow a simple method of testing the oxidation state of the compounds. The higher U(IV) and U(V) oxidation states have more stabilised *f*-orbitals with respect to the *d*-orbitals, therefore the energy gap (i.e. $5f^2 \rightarrow 5f6d$ for tetravalent centres) is larger and hence the transitions occur in the UV part of the spectrum. Thus, U(IV) and U(V) are observed to be less darkly colored and more translucent in solution than the U(III) complexes.

3
Activation of Small Molecules

3.1
Dinitrogen

Dinitrogen activation at *any* metal centre is very challenging; the N≡N triple bond is strong (945 kJ mol^{-1}) and apolar, restricting both bond-breaking and coordination mechanisms [5, 44]. These difficulties are compounded for the *f*-elements by the high nodality and poor radial extension of the *f*-orbitals, which are ill-suited for π back-bonding [15]. Nonetheless, a small number of *f*-element N_2 complexes have been reported, most of which demonstrate the side-on activation mode. This is a noteworthy feature, given that this bonding mode has been recently demonstrated to be highly active towards further functionalisation (e.g. hydrogenation with H_2 to give NH_3) using other metals such as zirconium [44–46]. Intriguingly, uranium metal was used as a catalyst in the original Haber–Bosch reaction chambers [47].

Exposure of $U(C_8H_4{}^{\dagger})(Cp^*)$ to atmospheric pressures of dinitrogen generated a new species, the U(IV) dimer $[U(C_8H_4{}^{\dagger})(Cp^*)]_2(\mu\text{-}\eta^2\text{:}\eta^2\text{-}N_2)$ (**9**), in which crystallographic studies revealed a side-on bound N_2 unit bridging two opposing uranium fragments [30]. The binding of N_2 is reversible and does not go to 100% completion. The dimer is in equilibrium with the U(III) monomer (Fig. 3), and even under 50 psi of dinitrogen, the reaction only goes to ca. 75% completion. The N_2 is bound loosely, and is easily lost under vacuum in both solid and solution states. Both structural and theoretical data are consistent with a doubly reduced $(N_2)^{2-}$ moiety. The N – N distance in the crystal structure was found to be in agreement with a double bond at 1.232(10) Å. DFT studies performed on the unsubstituted compound (in order to reduce computational time) were consistent with $5f^2$ centres, i.e. a U(IV) configuration, with two electrons in a molecular orbital derived from the N_2 π_g orbitals and the uranium 5*f* and 6*d* orbitals [48]. This implies a sig-

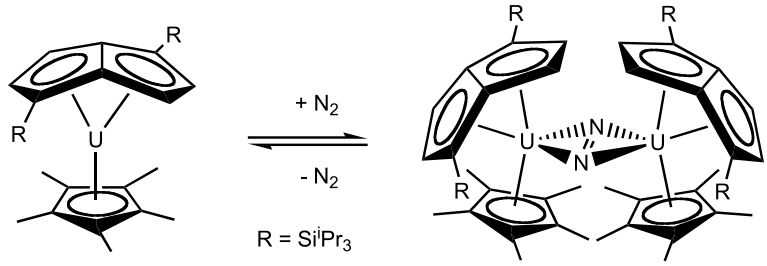

Fig. 3 Reversible binding and reduction of N_2 by **1**

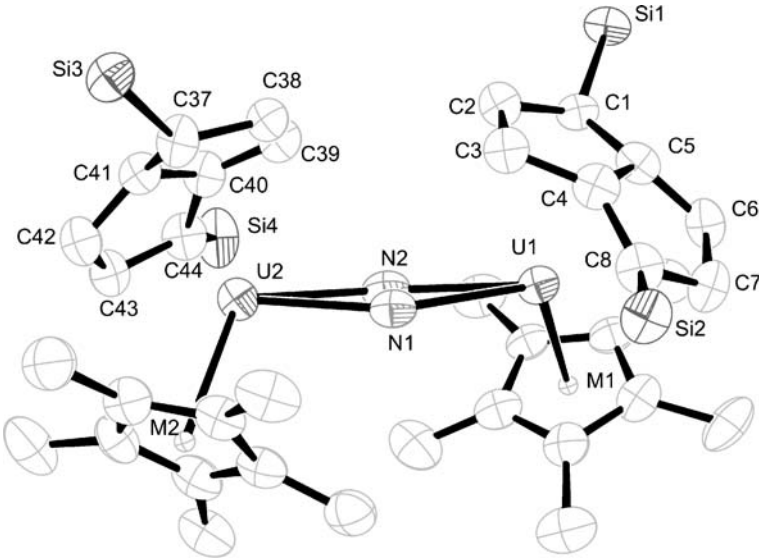

Structure 4

nificant π back-donation from the U(IV) 5*f* and 6*d* orbitals to give a formal dianionic unit of $(N_2)^{2-}$.

The case is not so clear for the first uranium N_2 compound, synthesised by Scott and co-workers in 1998, the triamidoamine complex $[\{NN_3\}U]_2(\mu\text{-}\eta^2\text{:}\eta^2\text{-}N_2)$ (NN_3 = $N(CH_2CH_2NSi^tBuMe_2)_3$) [49]. The N – N distance (1.109(7) Å) is similar to that found in dinitrogen gas (1.0975 Å), and the UV/vis. spectrum is very close to those to that of the U(III) parent $[\{NN'_3\}U]$. Therefore it was concluded that no reduction of N_2 has occurred; however, the uranium centres would have to act as an extremely strong Lewis acid to maintain this dimeric structure, which is formed in quantitative yield (as opposed to being part of an equilibrium state, vide supra). The compound loses N_2 under vacuum. Computational studies, conversely, indicate that the most stable structure of the dimer contains a reduced N_2 moiety with U(IV) $5f \rightarrow \pi_g$ back-donation, similar to the pentalene compound above [50]. The first lanthanide N_2 compound, $[Sm(Cp^*)_2]_2(\mu\text{-}\eta^2\text{:}\eta^2\text{-}N_2)$, shares features of both these uranium compounds. The N_2 is bound weakly, in equilibrium with its monomer, as with **9**; however, although crystallographic data show no lengthening of the N – N bond in the solid state, ^{1}H NMR evidence indicates two Sm(III) centres in solution [25]. It should be noted that the X-ray crystallographic data for this, and the triamidoamine uranium compound may be inaccurate, especially considering that the difference between N≡N and N = N is so small. Raman spectroscopy could be used to help clear up these discrepancies; however, spectra have not as yet been reported.

These studies are of both academic and practical interest. A vital step for a catalyst for converting N_2 into useful products is the electronic reduction of the bound molecule, and therefore it is important to gauge how actively the *f*-elements are capable transferring electrons to N_2, if any such homogeneous catalysts are to be synthesised. Homometallic *f*-element systems generally do not demonstrate activation beyond $(N=N)^{2-}$. However, heterometallic systems incorporating alkali metals have shown higher activation to give $(N-N)^{4-}$ and even complete cleavage to form nitrides [51–54]. End-on binding, fundamental to the Chatt cycle and the catalytic molybdenum(III) system reported by Schrock et al. [33], would be expected to be less preferable for uranium, due to the contracted *f*-orbitals. Nevertheless, one example has been recently shown of an end-on bound U(III) complex. $U(Cp^*)_3(\eta^1\text{-}N_2)$ was prepared by Evans et al. using an 80 psi overpressure of N_2 [55]. The N_2 bond length is basically unchanged, therefore it is concluded that no formal reduction has occurred. However, data from Raman spectroscopy show the ν_{N_2} stretching frequency at 2207 cm^{-1} (versus the 2331 cm^{-1} reported for free N_2), therefore indicating that electron density has been transferred to the ligand. The compound readily loses N_2.

None of the base-free uranium $COT^{\dagger}/Cp^R$ compounds **4**, **5** or **6** gave any changes in the ^1H NMR or UV/vis. spectra when reacted with 1–2 bar N_2, compared with those obtained under argon. The tris-aryloxide-tacn (tacn = triazacyclononane) U(III) systems described by Meyer et al., although highly reactive to many types of small molecule, similarly do not show any reactivity with N_2, even with 80 psi overpressure [56].

The difference between the pentalene complex **1** and the COT complexes **4–6** may be explained by both the higher levels of steric congestion in the latter, and the increased flexibility of the η^8-pentalene ligand in the former, which folds at a decreased angle in order to create space for the dinitrogen moiety. Such folding has not been observed with η^8-COT bound to a single metal centre, and fully coordinated COT ligands have only been observed to bend in metal–metal bonded dimers, e.g. $[M(L)]_2(\mu{:}\eta^5{:}\eta^5\text{-COT})$ (L = Cp, M = V, Cr; L = COT, M = Ti, Cr, Mo, W) [57–60].

3.2 Carbon Monoxide

Although a stronger σ-donor than isolectronic dinitrogen, carbon monoxide is also a better π-acceptor, a factor which similarly limits its capabilities as a ligand in *f*-element chemistry [15]. Its triple bond is likewise very difficult to cleave and kinetically inert (formally the strongest bond in nature at 1076 kJ mol^{-1}). Its polarity and susceptibility to oxidation, however, allow a wealth of chemistry not easily observed with N_2, including the facile formation of transition metal carbonyl compounds, in which strong bonds result from σ-donation and π back-bonding [1]. Conversely, the factors that pro-

mote transition metal-based reactivity generally limit lanthanide or actinide-based activation, as this polarity – reflected in the concentration of electron density found at the carbon atom – renders the molecule a soft σ-donor, and it thus binds poorly with the hard acceptor *f*-elements.

Actinide carbonyl complexes were historically of interest for isotope separation under the Manhatten Project during the Second World War, because $M(CO)_x$ complexes of the transition metals are volatile [17]. These investigations failed to produce any stable carbonyl compounds, although $U(CO)_6$ has since been characterised at liquid helium temperatures (it decomposes upon warming above 20 K) [61, 62]. Only one class of stable *f*-element carbonyl complex has been characterised in over 60 years of research, $U(Cp^R)_3(\eta^1\text{-CO})$ (R = $SiMe_3$, CMe_3, Me_4H, Me_5), first prepared by Andersen et al. by exposing base-free $U(Cp^{SiMe_3})_3$ to CO [26, 63–65]. The reduced values of ν_{CO} in the IR spectrum give evidence for U – CO back-bonding, and therefore noticeable 5*f* participation. The CO is weakly bound and lost upon exposure to vacuum, although two of this series (R = Me_5 and Me_4H) have proved stable enough to be crystallographically characterised, and show a typical terminal M – CO moiety [26, 65].

Reduction of CO is thermodynamically challenging and is known for just three examples from the *f*-block. $Sm(\eta\text{-}Cp^*)_2(THF)_2$ reacts under 90 psi overpressure CO to give a dianionic ketene carboxylate unit, $(O_2C - C = C = O)^{2-}$, the product of a $2e^-$ reduction [66]. The mechanism for the formation of this unit is unclear, and the chemistry is unique. Very recently it has been shown that $[La(\eta\text{-}Cp^*)_2]_2(\mu\text{-}N_2)$ will reduce CO to give an identical ketene carboxylate unit, with loss of N_2 [67].

The tris-aryloxide-tacn complex $\{(^{t\text{Bu}}ArO)_3tacn\}U$ has been shown to react under room temperature and pressure with CO to produce $[\{(^{t\text{Bu}}ArO)_3tacn\}U]_2(\mu{:}\eta^1{:}\eta^1\text{-CO})$, bridged by a mono-anionic $(CO)^-$ unit – an unusual dimerisation in that only one of the two uranium centres has been oxidised [68]. The bridging unit resulting from one-electron reduction of CO gave the first evidence that U(III) was capable of reducing carbon monoxide.

Reaction of the pentalene compound **1** with 1 bar CO in pentane gave a translucent red solution, indicative of oxidation to U(IV). Mass spectral analysis of the product showed strong peaks at $m/z = 1818$ and 1846, corresponding to $[\mathbf{1}]_2(CO)_3^+$ and $[\mathbf{1}]_2(CO)_4^+$, but in the absence of structural data the identity of the product(s) remains unclear (Cloke FGN, unpublished results).

3.2.1 Deltate Formation

Although no reaction was observed between $U(COT^\dagger)(Cp^*)$ and N_2, CO showed remarkable reactivity under mild conditions. Exposure of the darkly colored solutions of either base-free **4** or **4.THF** to ambient pressures of CO ir-

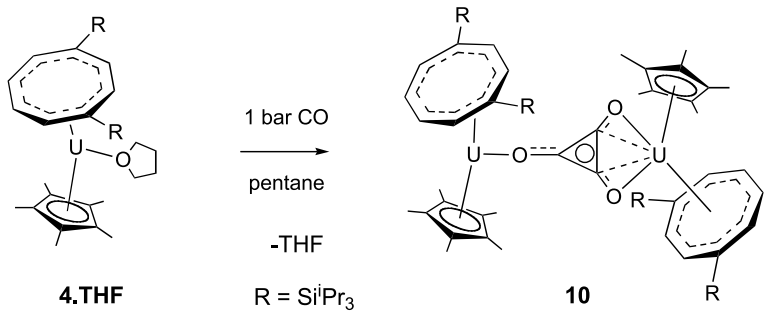

Fig. 4 Reductive cyclotrimerisation of CO by **4.THF** to give the deltate dianion in **10**

reversibly formed the dark red crystalline U(IV) dimer $[U(COT^{\dagger})(Cp^*)]_2(\mu$:$\eta^1$:$\eta^2$-$C_3O_3)$ (**10**) in 40% isolated yield (Fig. 4) [41]. The structure showed the two uranium centres to be bridged by a planar, carbocyclic (C_3O_3) unit. DFT studies and electronic spectroscopy gave strong evidence that the metal centres were tetravalent and therefore this unit, derived from a two-electron reductive cyclooligomerisation of CO, is formally a dianion. The deltate dianion is the first member of the aromatic oxocarbons, described in detail below. This reaction provided the first selective synthesis of the deltate dianion from CO, and the first crystallographic study of a deltate salt.

Thorough investigation demonstrated that this reaction proceeds in both non-coordinating solvents (pentane, toluene) and coordinating (THF) solvents (with or without prior cooling) to give **10** [35]. Atmospheric pressures of CO were used, but sub-atmospheric, and even stoichiometric quantities of CO will react to form **10**. It was shown that the adduct **4.THF** reacts

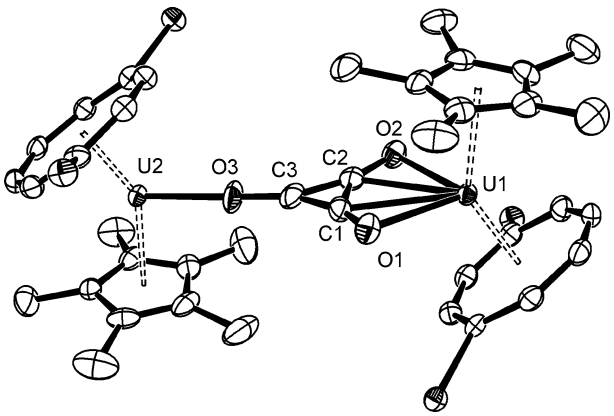

Structure 5

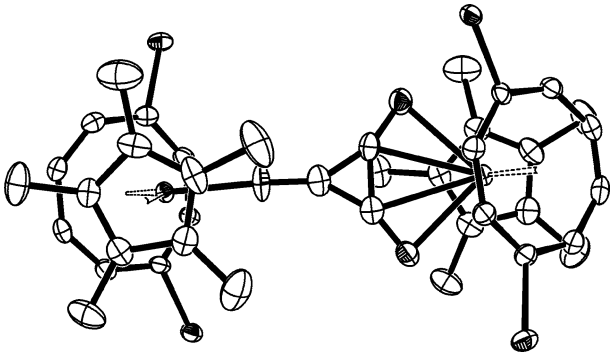

Structure 6 (top view)

in an identical manner to **4**, albeit with facile loss of THF, and in similar yield. Although the use of a base-free compound would be thought to be a pre-requisite for carbonyl formation, this reduction and indeed all of the reductions reviewed in the rest of this article proceed as readily whether the U(III) centres are solvated or not. In fact, the reactions proceed when using THF as solvent.

The structure of **10** contains a novel C – C agostic bond, resulting from σ-donation from one C – C bond in the deltate ring (on the η^2-bound portion of the oxocarbon) into an empty 5*f* orbital on the uranium. This has been shown in a DFT study, and observed experimentally by a lengthening of the corresponding C – C bond distance, and concomitant lengthening of the adjacent C – O distances [41]. This is the first example of this type of bonding for an *f*-element, but it is known in other areas of the periodic table, e.g. in NbClTp*(c-C_3H_5)(MeCCMe) [69], LiOC(Me)(c-C_3H_5)$_2$ [70] and [Rh(P^iPr_3)($C_{14}H_{16}$)][BAr_4^F] [71]. Three-membered rings seem especially susceptible to this type of bonding, as the tight C – C – C bond angles in the triangular skeleton lead to non-optimal overlap of the hybridised orbitals, so destabilising the C – C σ-orbitals [72]. The relative instability of these orbitals is manifested in the corresponding difficulty in synthesis of three-membered carbocycles such as deltate. The agostic interaction in **10** may be in part responsible for stabilising the deltate dianion, enabling this facile synthesis from CO. Due to the quantity of unoccupied, highly-nodal *f*-orbitals, these compounds may be especially well-suited for effecting this reduction of CO under mild conditions. It is unlikely that the less radially diffuse 4f orbitals would be capable of supporting this type of agostic bond. Evans has commented that the ketene carboxylate obtained by Ln(II) reduction of CO (vide supra) may be a ring-opened derivative of the deltate [67]; however, it should be noted that no evidence for this pathway has yet been given.

3.2.2
Oxocarbons from CO

The oxocarbon series $(CO)_n^{2-}$ were first formally recognised during the 1960s by West and co-workers, following the discovery of squaric acid (the conjugate acid of the squarate dianion) in 1959 (Fig. 5) [73, 74]. They are all dianionic, comprising a carbocyclic skeleton with oxygen attached by bonds of intermediate bond order, and have been shown to be planar, and hence highly aromatic; the level of delocalisation decreases as the ring size increases.

Despite their relatively recent recognition as members of a homologous aromatic series, salts of croconate and rhodizonate ($n = 5$ and 6) were first isolated in 1825 by Gmelin, in a solid state reaction of carbon with KOH at high temperatures [75].

The oxocarbons are reduced oligomers of carbon monoxide, and work by Liebig in 1834 first demonstrated that these carbocyclic compounds can be synthesised directly from CO; this was achieved by heating potassium metal in the presence of CO at 180 °C [76]. Again, as Gmelin found, mixtures of croconate and rhodizonate were isolated. In 1837 Heller deduced that the rhodizonate was in fact a precursor to the smaller croconate [77]. This was definitively proved in 1887, with the discovery that oxidative ring-contraction of $(C_6O_6)^{2-}$ gives $(C_5O_5)^{2-}$, a reaction that proceeds quantitatively using either O_2 in alkaline aqueous solution, or MnO_2 [78]. This is a very effective method of preparing croconate, and to date, no other synthesis is known [74].

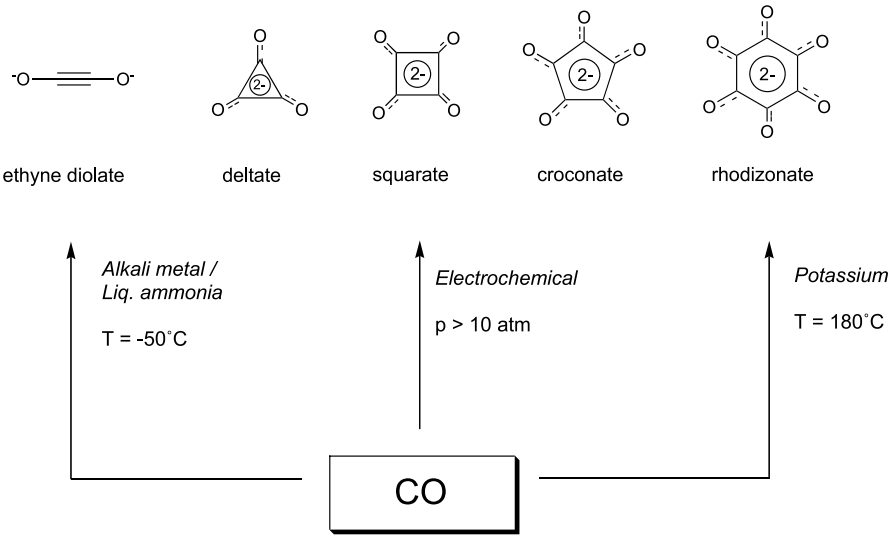

Fig. 5 Known routes to the oxocarbons via reductive cyclooligomerisation of CO (uranium reactions discussed in this chapter not included)

Low temperature studies of the reaction of the alkali metals with CO in liquid ammonia (at −50 °C) were shown to give salts of the reactive ethyne diolate dianion $(OC{\equiv}CO)^{2-}$, which are found to be explosive when dry [79–81]. Upon heating, these salts trimerise to give the hexaanion $(C_6O_6)^{6-}$, which oxidises rapidly in air to give the rhodizonate dianion $(C_6O_6)^{2-}$ (still the largest oxocarbon known) [82]. Although the mechanism for Liebig's preparation of rhodizonate has not been proven (vide supra), these results strongly suggest that the formation proceeds via the reactive ethyne diolate dianion, formed from initial $2e^-$ reduction of CO.

High pressure electrochemical methods developed in the 1970s have yielded salts of squarate, in approx. 35% yield at 400 bar in polar solvents such as THF and DMF [83, 84]. Further work in the late 1990s showed the reaction may proceed in similar yields under 10 bar pressure, but no products were obtained below this pressure [85]. In separate work using similar high-pressure systems, a concerted mechanism has been proposed for these cyclisations involving simultaneous electron transfer and bond formation between four molecules of surface-bound CO [86]. Similar investigations of the reaction of alkali metals with CO under high pressures did not yield any squarate salts.

Further electrochemical experiments involving CO, conducted in liquid ammonia at −50 °C, gave the ethyne diolate [87], cf. the reactions with alkali metals in liquid ammonia. This reduction occurred at around −2.3 V vs. SCE, whereas the high pressure routes described above were reportedly in the range −2.2 to −2.6 V vs. SCE. These are very high reduction potentials, approaching those of sodium and potassium metals (−2.7 V and −2.9 V, respectively).

Deltate is the most difficult oxocarbon to access, due to its highly strained three-membered ring, and to date there are only two reported "organic" preparations: a low-yield photolytic route from a di-silylated squarate, which undergoes ring contraction to give the di-silylated deltate [88], and the carbene insertion of CCl_2 into di-*tert*-butoxyacetylene, which gives deltic acid after acidic work-up [89]. There is ^{13}C NMR evidence for the formation of trace amounts of deltate in a complex mixture of products from the reaction of CO with Na–K alloy in THF [90]; however, the U(III) synthesis described above is the first selective synthesis of this oxocarbon from CO [41].

Surface catalysis routes using alkaline earth oxides have yielded mixtures of various $(CO)_n^{2-}$ ($n = 2–6$) species from CO [91]. These routes are of mechanistic interest, but are of no synthetic value as only trace amounts of product are detected. Recent work has been reported that shows the formation of the rhodizonate mono-anion from the reaction of CO with molybdenum suboxide cluster anions $Mo_xO_y^-$ ($y < 3x$), which are generated using pulsed laser ablation/molecular beam methods [92]. The results suggest that a series of reactions occur involving the oxidation of CO until the oxygen content of the clusters is depleted, followed by metal carbonyl formation and, ultimately, free $C_6O_6^-$ formation.

No mechanism for the formation of oxocarbons from various reductions of CO has been definitively proved. The most widely accepted notion is that $2e^-$ reduction of two molecules of CO initially forms the ethyne diolate $(OC{\equiv}CO)^{2-}$ moiety, via combination of $(CO^{\cdot})^-$ radicals, and consequent addition of neutral CO molecules forms progressively larger oxocarbons $(CO)_n{}^{2-}$, the final product obtained depending on specific reaction conditions. However, it appears that the route Liebig pioneered using molten potassium at 180 °C may proceed via cyclotrimerisation of ethyne diolate, and subsequent oxidation to give croconate and rhodizonate. Also there is the intriguing possibility of a concerted reduction pathway, whereby the oxocarbon is formed directly, e.g. a $2e^-$ reduction of four molecules of CO to give squarate without intermediates.

3.2.3
Squarate Formation

On the basis of decreasing ring strain from $n = 3$ to $n = 5$ in the oxocarbon series $(CO)_2{}^{2-}$, it was proposed that higher homologues of deltate ($n > 3$) could be accessed with these U(III) systems by simply allowing a larger activation "pocket" for CO oligomerisation to occur following $2e^-$ reduction. Indeed, tetramethylated **5.THF** reacts with CO gave the squarate compond $[U(COT^{\dagger})(Cp^{Me4H})]_2(\mu{:}\eta^2{:}\eta^2\text{-}C_4O_4)$ (**11**) in isolated yields of up to 66% (Fig. 6) [42]. This is the first chemical synthesis of squarate from CO, and proceeds under mild conditions, unlike the pressurised electrochemical routes. Remarkably, the addition or removal of just one methyl group between the starting U(III) mixed-sandwich complexes **4**↔**5** allows selective access to either deltate or squarate, respectively, directly from CO.

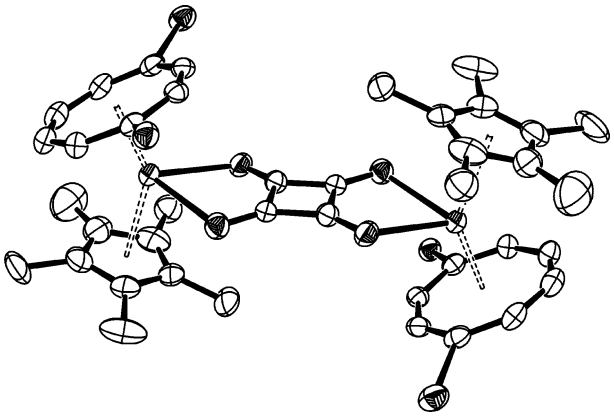

Structure 7

The effect of such a slight change in ligand environment has been previously noted for Cp* vs. Cp^{Me4H}, e.g. strikingly in zirconocene–dinitrogen

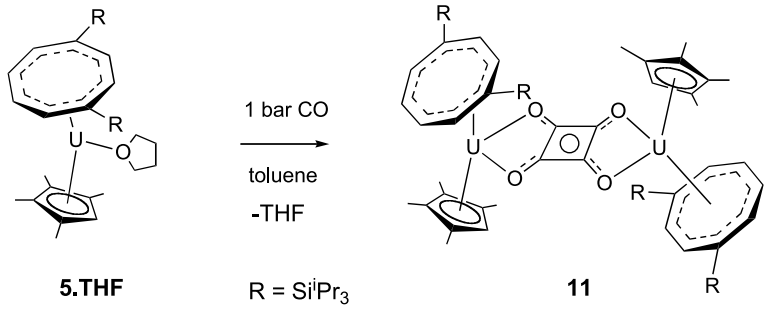

Fig. 6 Formation of squarate from CO by **5.THF**

systems, where the Cp^{Me_4H} ligand allows side-on binding and consequent hydrogenation of N_2 to occur, whereas the use of Cp* prevents side-on binding and renders the $(N_2)^{2-}$ units inert to functionalisation [46, 93–95].

The squarate unit in **11**, unlike the agostically bound deltate in **10**, contains no geometrical distortions in the carbocyclic skeleton; DFT studies confirm the lack of the agostic bond in **11**. This is presumably due to the lower ring strain in the four-membered ring.

Gas phase SCF energies of the U(IV)-bound oxocarbon series $[U(COT)(Cp)]_2(CO)_n$ ($n = 3–6$) have been calculated, and are illustrated in Fig. 7. Energies of η^2:η^2-bound croconate and rhodizonate complexes were found to be

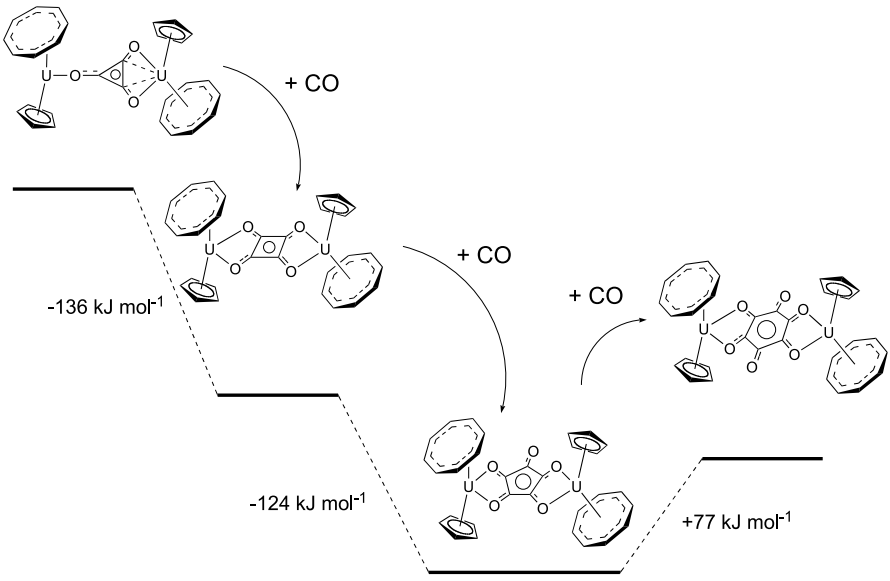

Fig. 7 Relative gas phase SCF energies of the U(IV) oxocarbons $[U(\eta-COT)(\eta-Cp)]_2(CO)_n$; $n = 3–6$

lower in energy than any combination of η^1-bound modes [35] (Hazari N, Green JC, unpublished results).

These calculations imply that the croconate should also be accessible in these systems by using an even less sterically hindered system. Unfortunately, the product(s) from the reaction of monomethylated **6.THF** with CO could not be successfully crystallised (although readily soluble in all hydrocarbon solvents) and remain unidentified [35]. Reaction of the unsilylated compound **3.THF** with CO gave a colour change to cherry red, distinctive of oxidation of the U(III) centres. However, the products were extremely insoluble and could not be purified. Thus the choice to use silyl groups for solubility factors has been shown to be a valid one.

3.2.4
Functionalisation and Extraction of U(IV)-Bound Oxocarbons

The reductions described above may be considered the first syntheses of oxocarbons from CO under mild conditions (room temperature and pressure), and therefore give encouragement for the development of a useful (i.e. catalytic) process to generate these type of carbocycles from CO (a cheap and renewable feedstock) using a uranium catalyst. This type of reduction – a cyclooligomerisation of CO to give an oxocarbon product – is thermodynamically challenging and has only been previously demonstrated for the alkali metals. These metals suffer from a lack of solubility and selectivity, factors which have only been overcome up to now by using unattractive reaction conditions (high temperatures/pressures or liquid ammonia).

The low-valent *f*-element complexes are characterised by a combination of solubilising ligands and high redox potentials, approaching those of the alkali metals. This is very clearly demonstrated by the U(III) complex **4**, whose reactivity towards CO has only been otherwise observed using Na–K alloy as the reductant. Electrochemical evidence suggests that CO reduction requires highly reducing potentials in the range –2.2 to –3.0 V, so it is unsurprising that very few metal compounds have been shown to effect these reductions. The stabilising agostic interaction seen in **10** may be further responsible for enabling these reductions under mild conditions, and thus further limit this type of reactivity to metals that are suited to this interaction.

The Fischer–Tropsch process utilises CO as a carbon source, with H_2 as the reductant, for the production of hydrocarbons and oxygenates, especially in times of limited crude oil supply (CO may be derived from methane or coal). Fischer–Tropsch systems do not, however, give carbocyclic products, nor homologate CO under mild conditions (pressures typically used are >300 bar and temperatures >500 °C, in conjunction with either homogeneous or heterogeneous catalysts [96]). Carbocycles often form the backbone of many pharmaceutical drugs, therefore a catalytic process that could synthesise them from a non-crude oil source (e.g. CO) under mild or even

moderate conditions could be of considerable commercial and industrial importance [7].

Work by Wayland et al. has shown that the low-valent rhodium compounds such as $[(TXP)Rh]_2$ (TXP = tetra-(3,5-dimethylphenyl)porphyrinato), can reduce CO to form ethane dionyl compounds of the type [(TXP)Rh-C(O)-C(O)-Rh(TXP)] [97–100]. The late transition metals prefer to bind to carbon, and therefore this is formed in preference to an ethyne diolate product. Although carbocyclic products are not observed, the reactions demonstrate that reductive homologation of CO is feasible with transition metals under mild conditions. Related are the reactions of hydrosilanes with CO using rhodium and cobalt carbonyl catalysts, which give straight-chain products containing up to two or three coupled CO units (however, at elevated pressures and temperatures) [101, 102].

Clearly an important initial step towards designing and/or demonstrating the feasibility of a future catalytic process is to cleave the newly generated substrate from the metal centres.

The labelled squarate compound **11-^{13}CO** (generated from ^{13}CO) reacted cleanly with two equivalents of $SiMe_3Cl$ to give the new compounds $U(COT^{\dagger})(Cp^{Me_4H})Cl$ (**12**) and $^{13}C_4O_4(SiMe_3)_2$ in quantitative yield (Fig. 8) (Summerscales OT and Cloke FGN, unpublished results). The free squarate in this case contained a fully labelled ^{13}C ring, and demonstrates a straightforward method of obtaining these rare organic compounds. Squaric acid itself may be obtained from $C_4O_4(SiMe_3)_2$ by use of *n*-butanol [88]. Simple derivatives of squaric acid and the squarate dianion have many uses and are currently utilised in medicinal and biological chemistry, bioconjugate chemistry, materials science (using squarate to form conjugated polymers with low HOMO-LUMO gaps), dyes, photochemistry and organic synthesis (for ring expansions and in total synthesis) [103–112].

The deltate **10-^{13}CO** also reacted with $SiMe_3Cl$ to give $U(COT^{\dagger})(Cp^*)Cl$ (**13**) [35]. However, the expected bis(trimethylsilyl) deltate derivative was not

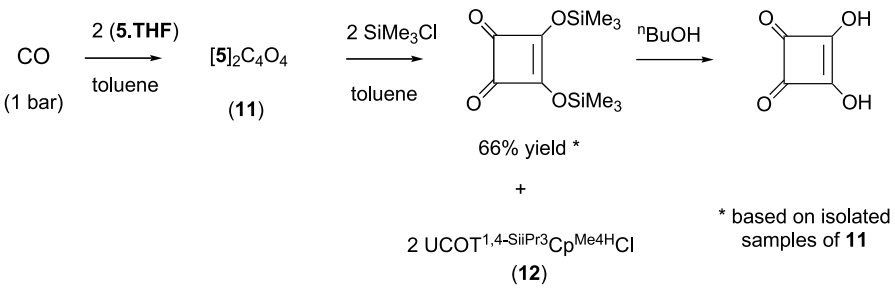

Fig. 8 Synthesis of bis(trimethylsilyl)squarate from CO and $SiMe_3Cl$, with the uranium complex providing electrons for reductive oligomerisation and steric control; conversion to squaric acid previously reported

detected and it is possible that it underwent an electrophilic ring-opening and was still bound to an, as yet, unidentified uranium species.

Routes for "completing the cycle" back to the U(III) compounds, and other catalytic routes, are currently under investigation in our laboratory.

3.3 Carbon Dioxide

Carbon dioxide is more easily reduced than CO, and reductive activation may be chemical [113, 114], enzymatic [115], electrochemical or photochemical [116, 117], proceeding by one-, two-, four-, six- or even eight-electron steps. Two-electron processes are the most common and are known to produce salts of formate, oxo, carbonate, and oxalate dianions, and carbon monoxide [118].

Reaction of **4.THF** with $^{13}CO_2$ gave ^{13}CO and an unidentified U(IV) or U(V) product. No ^{13}C peaks attributable to a uranium species were observed in the ^{13}C spectrum, and therefore it is most likely that the product is oxo $(O)^{2-}$ plus CO – an already reported reactivity pattern for the U(III) complexes $U(Cp^{SiMe3})_3(THF)$ [119] and $\{(^{tBu}ArO)_3tacn\}U$ [68].

However, exposure of **5.THF** to excess CO_2 (1 bar) gave the structurally characterised U(IV) carbonate product $[U(COT^{\dagger})(Cp^{Me_4H})]_2(\mu\text{-}\eta^1\text{:}\eta^2\text{-}CO_3)$ (**14**) and free CO (Summerscales OT, Hitchcock PB, Cloke FGN, unpublished results). This is a new CO_2 reduction product for an actinide compound, but the formation of carbonate by this route is known for the transition metals and lanthanides [120, 121]. The transformation is a reductive disproportionation, involving a $2e^-$ reduction of two molecules of CO_2 to CO_3^{2-} with concomitant formation of CO (Eq. 1):

$$2CO_2 + 2e^- \rightarrow CO_3^{2-} + CO\,. \qquad (1)$$

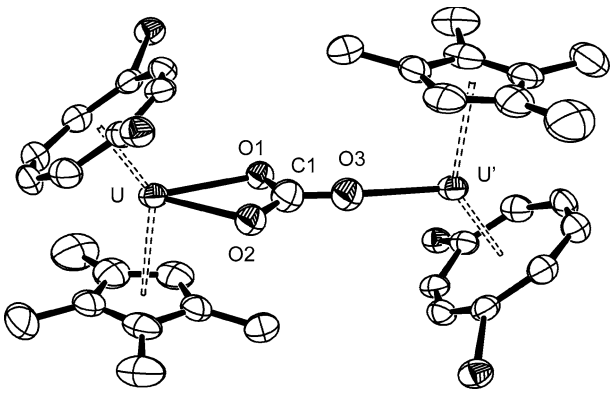

Structure 8

Given that **5.THF** has been shown to cyclotetramerise CO (vide supra) it is clear that it must react much faster with the excess of CO_2 than the CO produced by the reductive disproportionation. However, if the correct stoichiometry of reactants is employed (5:4 **5.THF**:CO_2, as shown in Scheme 1), the evolved CO can also be reduced, so that the overall result is the formation of **14** and the squarate product **11** (Fig. 9).

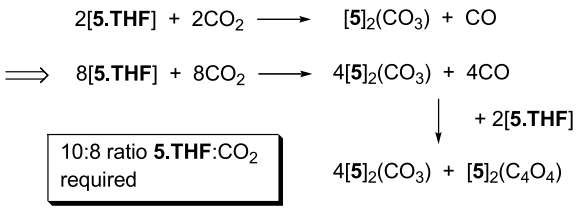

Scheme 1 Worked justification for the 5:4 ratio of U(III):CO_2 used to obtain highest yields of squarate

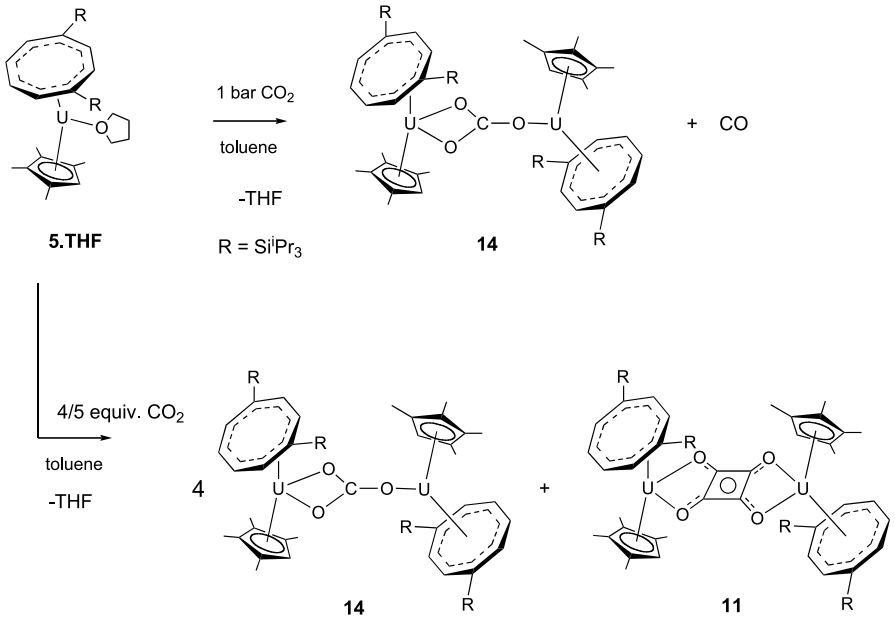

Fig. 9 Reductions of CO_2 using U(III) cyclooctatetraene complex **5.THF**

This is the first synthesis of an oxocarbon from a CO_2 carbon source and its synthesis may be considered as the product of successive $2e^-$ reductions of CO_2. The first reduction gives carbonate plus CO, the second then reduces this liberated CO to the squarate dianion (Eq. 2). However, it must be noted that

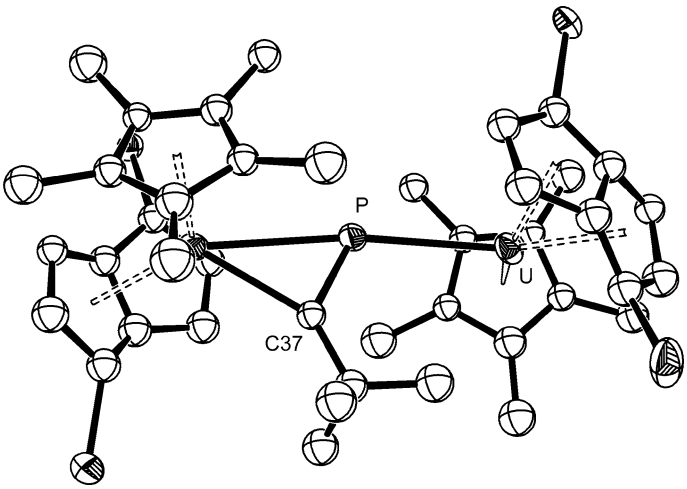

Structure 9

the maximum yield of the squarate by this method is clearly never going to be higher than 20%:

$$8CO_2 \xrightarrow{8e^-} 4CO_3^{2-} + 4CO \xrightarrow{2e^-} 4CO_3^{2-} + C_4O_4^{2-} . \quad (2)$$

3.4
Phosphorous Species

The reaction of **1** with phosphaalkyne P≡C^{t}Bu gave [U(C$_8$H$_4$†)(Cp*)]$_2$(μ-η^1:η^2-PC^{t}Bu) (**15**), in which a bent PC^{t}Bu moiety bridges the two uranium centres via the phosphorous atom (Summerscales OT, Hitchcock PB, Cloke FGN, unpublished results).

The P – C – C angle is consistent with an sp^2 hybridised centre, the product of a two-electron reduction of the phosphaalkyne. This is the first isolation of a phosphaalkyne dianion, although the electron-acceptor properties of PC^{t}Bu previously studied by electron transmission spectroscopy have indicated its accessibility [122]. One-electron reductions of phosphaalkynes are known, and give homologated and cyclised compounds [123–126]. The analogous reactions using the COT compounds **4** or **5**, however, did not lead to isolable products.

White phosphrous (P$_4$) is reduced by **4.THF** and **5.THF** to give [U(COT†)(Cp*)]$_2$(μ-η^2:η^2-P$_4$) (**16**) and [U(COT†)(Cp^{Me4H})]$_2$(μ-η^2:η^2-P$_4$) (**17**), respectively (Frey ASP, Hitchcock PB, Cloke FGN, unpublished results). Two P – P bonds have been cleaved, resulting in a planar dianionic moiety that bridges the two centres. This cyclo-P$_4$ form has been observed previously in the products of photochemical and thermal reactions of white phosphorous with

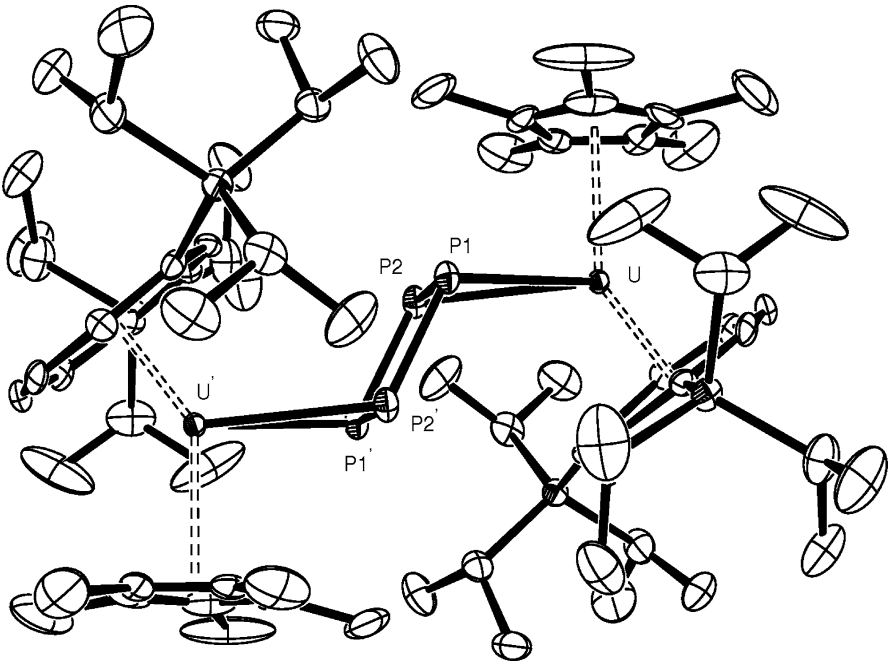

Structure 10

transition metal carbonyl compounds [127–129]; the U(III) reactions give this product under ambient conditions.

3.5 Other Small Molecules

Initial estimates of the reductive power of U(COT)(Cp*)(THF) were underwhelming; the redox potential was reported at $E^{\circ}\{U(IV)/U(III)\} = -0.69$ V vs. SCE [37]. The reaction with dimethylbipyridine seemed to confirm this view, as a U(III) adduct **3.Me$_2$bipy** was formed without reduction of the substrate, in spite of the relatively low-lying π^* acceptor orbitals of bipy [37]. Later work, however, showed that **3.THF** could reduce neutral COT to give the U(IV) complex [U(COT)(Cp*)](μ-η^3:η^3-COT) (**18**) [130], in spite of the lower electron affinity of COT vs. bipy [131]. Clearly it is misleading to use these reduction potentials as a strict guide for measuring the reactivity of these compounds. It has been shown that the silylated derivatives **4** and **5** display reactivities with CO only previously observed with alkali metals ($E^{\circ}\{Na(I)/Na(0)\} = -2.7$ V vs. SCE) [41, 42]. There is also mention in the literature of the reduction of CS_2 to give [U(COT)(Cp*)]$_2$(μ:η^1:η^2-CS_2) (**19**), however, this has not been substantiated by any characterising data [32].

None of the complexes **1**, **4**, **5** or **6** react with H_2 under mild conditions [35], consistent with the observation that hydride ligands can be good reducing agents for U(IV) compounds [132–135]. Indeed, reaction of U($COT^{1,4\text{-}SiMe_3}$)(Cp*)(Me) (**20**) with H_2 gave U($COT^{1,4\text{-}SiMe_3}$)(Cp*) (**8**) plus methane [43]; we presume a transient U(IV) hydride complex [U($COT^{1,4\text{-}SiMe_3}$)(Cp*)(H)]$_x$ disproportionates to hydrogen and the observed U(III) compound.

Reaction of **5.THF** with MeCN gave no reduction products. A simple U(III) nitrile adduct U($COT^{\dagger}$)(Cp^{Me_4H})(η^1-NCMe) (**5.MeCN**) was formed instead, with loss of THF. Similar adduct formation is known for the tris-cyclopentadienyl systems; however, upon heating the latter, the ligand is reduced to give U(IV) cyanide and methyl products [136]. Thermolysis of **5.MeCN** has yet to be investigated.

4.THF reacted with one equivalent of ^{i}PrNCO to give free isocyanide ^{i}PrNC and an unidentified oxidised uranium product – presumably an oxo species [35]. Reduction of isocyanates is known for one other U(III) system: U(η-Cp^{Me})$_3$(THF) reacts with PhNCO to give the reduced bridged species [U(η-Cp^{Me})$_3$]$_2$(μ:η^1:η^2-PhNCO) [137]. The $2e^-$ reduction of RNCO to RCN plus $(O)^{2-}$ appears to be unprecedented, although it is, perhaps, an unsurprising reaction for a low-valent *f*-element complex, given the noted oxophilicity of the latter.

4 Summary

This article has reviewed the synthesis and reactivity towards small molecules of a range of U(III) cyclooctatetraene and pentalene complexes. It is evident that in many cases the uranium centre is capable of π back-bonding through the 5*f* orbitals; additionally, a C – C agostic interaction between a bound substrate and a U(IV) centre has been observed. Clearly uranium is capable of bonding with a degree of "covalency", and this is perhaps why the reduction chemistry of U(III) is so rich and diverse, and not simply an iteration of low-valent lanthanide chemistry.

A U(III) pentalene complex has been shown to be capable of binding and reducing N_2, in a similar manner to the divalent lanthanide complexes reported by Evans. However, the reactivity of the COT complexes towards CO is completely novel for organometallic compounds of *any* type, and shows considerable promise for the future design of a system capable of producing oxocarbon products from CO or CO_2 catalytically.

Appendix

Compound	Number	Refs.
$U(C_8H_4^{\dagger})(Cp^*)$	(**1**)	[30]
$U(C_8H_4^{\dagger})(Cp^*)(THF)$	(**1.THF**)	(Cloke FGN unpublished results)
$[U(C_8H_4^{\dagger})(Cp^{Me_4H})(\mu-I)]_2$	(**2**)	[35]
$U(COT)(Cp^*)(THF)$	(**3.THF**)	[37]
$U(COT)(Cp^*)(Me_2bipy)$	(**3.Me$_2$bipy**)	[37]
$U(COT)(Cp^*)(HMPA)$	(**3.HMPA**)	[38]
$U(COT^{\dagger})(Cp^*)$	(**4**)	[35]
$U(COT^{\dagger})(Cp^*)(THF)$	(**4.THF**)	[41]
$U(COT^{\dagger})(Cp^{Me_4H})$	(**5**)	[35]
$U(COT^{\dagger})(Cp^{Me_4H})(THF)$	(**5.THF**)	[42]
$U(COT^{\dagger})(Cp^{Me_4H})(\eta^1-NCMe)$	(**5.MeCN**)	(Farnaby J, Hitchcock PB, Cloke FGN, unpublished results)
$U(COT^{\dagger})(Cp^{Me})$	(**6**)	[35]
$U(COT^{\dagger})(Cp^{Me})(THF)$	(**6.THF**)	[35]
$U(COT^{\dagger})(Tp^*)$	(**7**)	(Farnaby J, Hitchcock PB, Cloke FGN, unpublished results)
$U(COT^{1,4\text{-}SiMe_3})(Cp^*)$	(**8**)	[43]
$U(COT^{1,4\text{-}SiMe_3})(Cp^*)(THF)$	(**8.THF**)	[43]
$[U(C_8H_4^{\dagger})(Cp^*)]_2(\mu\text{-}\eta^2\text{:}\eta^2\text{-}N_2)$	(**9**)	[30]
$[U(COT^{\dagger})(Cp^*)]_2(\mu\text{:}\eta^1\text{:}\eta^2\text{-}C_3O_3)$	(**10**)	[41]
$[U(COT^{\dagger})(Cp^{Me_4H})]_2(\mu\text{:}\eta^2\text{:}\eta^2\text{-}C_4O_4)$	(**11**)	[42]
$U(COT^{\dagger})(Cp^{Me_4H})Cl$	(**12**)	(Summerscales OT and Cloke FGN, unpublished results)
$U(COT^{\dagger})(Cp^*)Cl$	(**13**)	(Summerscales OT and Cloke FGN, unpublished results)
$[U(COT^{\dagger})(Cp^{Me_4H})]_2(\mu\text{-}\eta^1\text{:}\eta^2\text{-}CO_3)$	(**14**)	(Summerscales OT, Hitchcock PB and Cloke FGN, unpublished results
$[U(C_8H_4^{\dagger})(Cp^*)]_2(\mu\text{-}\eta^1\text{:}\eta^2\text{-}PC^tBu)$	(**15**)	(Summerscales OT, Hitchcock PB, Cloke FGN, unpublished results)
$[U(COT^{\dagger})(Cp^*)]_2(\mu\text{-}\eta^2\text{:}\eta^2\text{-}P_4)$	(**16**)	(Frey ASP, Hitchcock PB, Cloke FGN, unpublished results)
$[U(COT^{\dagger})(Cp^{Me_4H})]_2(\mu\text{-}\eta^2\text{:}\eta^2\text{-}P_4)$	(**17**)	(Frey ASP, Hitchcock PB, Cloke FGN, unpublished results)
$[U(COT)(Cp^*)](\mu\text{-}\eta^3\text{:}\eta^3\text{-}COT)$	(**18**)	[130]
$[U(COT)(Cp^*)]_2(\mu\text{:}\eta^1\text{:}\eta^2\text{-}CS_2)$	(**19**)	[32]
$U(COT^{1,4\text{-}SiMe_3})(Cp^*)(Me)$	(**20**)	[43]

† = 1,4-bis(tri-isopropylsilyl)

References

1. Wilkinson G, Stone FGA, Abel EW (1982) Comprehensive organometallic chemistry, vol 1. Pergamon, Oxford
2. Labinger JA, Bercaw JE (2002) Nature 417:507
3. Marks TJ et al. (2001) Chem Rev 101:953
4. Burdeniuc J, Jedlicka B, Crabtree RH (1997) Chem Ber Recueil 130:145
5. MacKay BA, Fryzuk MD (2004) Chem Rev 104:385
6. Leigh GJ (1992) Acc Chem Res 25:177
7. Wayland B, Fu X (2006) Science 311:790
8. Ephritikhine M (2006) Dalton Trans 13:2501
9. Evans WJ, Kozimor SA (2006) Coord Chem Rev 250:911
10. Castro-Rodriguez I, Nakai H, Zakharov LN, Rheingold AL, Meyer K (2004) Science 305:1757
11. Evans WJ, Kozimor SA, Ziller JW (2005) Science 309:1835
12. Hayton TW, Boncella JM, Scott BL, Palmer PD, Batista ER, Hay PJ (2005) Science 310:1941
13. Cummins CC, Diaconescu PL, Arnold PL, Baker TA, Mindiola DJ (2000) J Am Chem Soc 122:6108
14. Evans WJ (2000) Coord Chem Rev 206:263
15. Kaltsoyannis N, Scott P (1999) The f elements. Oxford University Press, Oxford
16. Summerscales OT, Cloke FGN (2006) Coord Chem Rev 250:1122
17. Seyferth D (2004) Organometallics 23:3562
18. Cloke FGN, Hitchcock PB (1997) J Am Chem Soc 119:7899
19. Ashley AE, Cowley AR, O'Hare D (2007) Chem Commun, p 1512
20. Miller MJ, Lyttle MH, Streitweiser A (1981) J Org Chem 46:1977
21. Boussie TR, Streitweiser A (1993) J Org Chem 58:2377
22. Cloke FGN, Kuchta MC, Harker RM, Hitchcock PB, Parry JS (2000) Organometallics 19:5795
23. Cloke FGN, Green JC, Jardine CN (1999) Organometallics 18:1080
24. Clark DL, Sattelberger AP, Bott SG, Vrtis RN (1989) Inorg Chem 28:2496
25. Evans WJ, Ulibarri TA, Ziller JW (1988) J Am Chem Soc 110:6877
26. Parry J, Carmona E, Coles S, Hursthouse M (1995) J Am Chem Soc 117:2649
27. Avens LR, Burns CJ, Butcher RJ, Clark DL, Gordon JC, Schake AR, Scott BL, Watkin JG, Zwick BD (2000) Organometallics 19:451
28. Corbett JD (1983) Inorg Synth 22:31
29. Katz J, Seaborg GT, Morss LR (1986) The chemistry of the actinide elements. Chapman and Hall, London
30. Cloke FGN, Hitchcock PB (2002) J Am Chem Soc 124:9352
31. Larch C, Cloke FGN, Hitchcock PB (2008) Chem Commun, p 82. doi:10.1039/b714211k
32. Clark DL, Gordon JC, Huffman JC, Watkin JG, Zwick BD (1995) New J Chem 19:495
33. Yandulov DV, Schrock RR (2003) Science 301:5629
34. Weare WW, Dai X, Byrnes MJ, Chin JM, Schrock RR, Muller P (2006) Proc Natl Acad Sci USA 103:17099
35. Summerscales OT (2007) DPhil thesis, University of Sussex
36. Odom AL, Arnold PL, Cummins CC (1998) J Am Chem Soc 120:5836
37. Schake AR, Avens LR, Burns CJ, Clark DL, Sattelberger AP, Smith WH (1993) Organometallics 12:1497
38. Cendrowski SM, Le Gland G, Nierlich M, Ephritikhine M (2003) Eur J Inorg Chem 1388

39. Gradoz P, Boisson C, Baudry D, Lance M, Nierlich M, Vigner J, Ephritikhine M (1992) J Chem Soc, Chem Commun 1720
40. Cloke FGN, Hawkes SA, Hitchcock PB, Scott P (1994) Organometallics 13:2895
41. Summerscales OT, Cloke FGN, Hitchcock PB, Green JC, Hazari N (2006) Science 311:829
42. Summerscales OT, Cloke FGN, Hitchcock PB, Green JC, Hazari N (2006) J Am Chem Soc 128:9602
43. O'Sullivan JA (1997) DPhil Thesis, University of Sussex
44. MacLachlan EA, Fryzuk MD (2006) Organometallics 25:1530
45. Fryzuk MD, Love JB, Rettig SJ, Young VG (1997) Science 275:1445
46. Pool JA, Lobkovsky E, Chirik PJ (2004) Nature 427:527
47. Mittasch A (1950) Adv Catal 2:81
48. Cloke FGN, Green JC, Kaltsoyannis N (2004) Organometallics 23:832
49. Scott P, Roussel P (1998) J Am Chem Soc 120:1070
50. Scott P, Kaltsoyannis N (1998) Chem Commun,p 1665
51. Korobkov I, Gambarotta S, Yap GPA (2002) Angew Chem Int Ed 41:3433
52. Dube T, Conoci S, Gambarotta SJ, Yap GPA, Vasapollo G (1999) Angew Chem Int Ed Engl 38:3657
53. Berube CD, Yazdanbakhsh M, Gambarotta SJ, Yap GPA (2003) Organometallics 22:3742
54. Ganesan M, Lalonde MP, Gambarotta SJ, Yap GPA (2001) Organometallics 20:2443
55. Evans WJ, Kozimor SA, Ziller JW (2003) J Am Chem Soc 125:14264
56. Castro-Rodriguez I, Meyer K (2006) Chem Commun, p 1353
57. Brauer DJ, Kruger C (1976) Inorg Chem 15:2511
58. Cotton FA, Koch SA, Schultz AJ, Williams JM (1978) Inorg Chem 17:2093
59. Elschenbroich C, Heck J, Massa W, Nun E, Schmidt R (1983) J Am Chem Soc 105:2905
60. Elschenbroich C, Heck J, Massa W, Schmidt R (1983) Angew Chem Int Ed Engl 22:330
61. Slater JL, Sheline RK, Lin KC, Welter WJ (1971) J Chem Phys 55:5129
62. Sheline RK, Slater JL (1975) Angew Chem Int Ed Engl 14:309
63. Andersen RA, Brennan JG, Robbins JL (1986) J Am Chem Soc 108:335
64. del Mar Conejo M, Parry JS, Carmona E, Schultz M, Brennan JG, Beshouri SM, Andersen RA, Rogers RD, Coles S, Hursthouse M (1999) Chem Eur J 5:3000
65. Evans WJ, Kozimor SA, Nyce WJ, Ziller JW (2003) J Am Chem Soc 125:13831
66. Evans WJ, Grate JW, Hughes LA, Zhang H, Atwood JL (1985) J Am Chem Soc 107:3728
67. Evans WJ, Lee DS, Ziller JW, Kaltsoyannis N (2006) J Am Chem Soc 128:14176
68. Castro-Rodriguez I, Meyer K (2005) J Am Chem Soc 127:11242
69. Jaffart J, Etienne M, Reinhold M, McGrady JE, Maseras F (2003) Chem Commun, p 876
70. Goldfuss B, von Rague Schleyer P, Hampel F (1996) J Am Chem Soc 118:12183
71. Brayshaw SK, Green JC, Kociok-Kohn G, Sceats EL, Weller AS (2006) Angew Chem Int Ed 45:452
72. Wiberg KB (1996) Acc Chem Res 29:229
73. West R (1980) Oxocarbons. Academic, New York
74. Seitz G, Imming P (1992) Chem Rev 92:1227
75. Gmelin L (1825) Ann Phys 2 4:1 (Leipzig)
76. Liebig J (1834) Ann Chem 11:182
77. Heller JF (1837) Justus Liebig's Ann Chem 24:1

78. Nietzki R (1887) Ber Dtsch Chem Ges 20:2114
79. Weiss VE, Buchner W (1964) Z Allorg Allg Chem 330:251
80. Buchner W, Weiss E (1964) Helv Chim Acta 47:1415
81. Buchner W (1965) Helv Chim Acta 48:1229
82. Sager WF, Fatiadi A, Parks PC, White DG, Perros TP (1963) J Inorg Nucl Chem 25:187
83. Silvestri G, Gambino S, Filardo G, Guainazzi M, Ercoli R (1972) Gazz Chim Ital 102:818
84. Silvestri G, Gambino S, Filardo G, Spadaro G, Palmisano L (1978) Electrochim Acta 23:413
85. Shibata M, Omori D, Furuya N (1999) Electrochemistry 67:355
86. Bockmair G, Fritz HPZ (1975) Z Naturforsch B 30:330
87. Uribe FA, Sharp PR, Bard AJ (1983) J Electroanal Chem 152:173
88. Eggerding D, West R (1976) J Am Chem Soc 98:3641
89. Pericas MA, Serratosa F (1977) Tet Lett 50:4437
90. Lednor PW, Versloot PC (1983) J Chem Soc, Chem Commun, p 284
91. Morris RM, Klabunde KJ (1983) J Am Chem Soc 105:2633
92. Wyrwas RB, Jarrold CC (2006) J Am Chem Soc 128:13688
93. Pool JA, Bernskoetter WH, Chirik PJ (2004) J Am Chem Soc 126:14326
94. Manriquez JM, Bercaw JE (1974) J Am Chem Soc 96:6229
95. Manriquez JM, Sanner RD, Marsh RE, Bercaw JE (1976) J Am Chem Soc 98:3042
96. Rofer-DePorter CK (1981) Chem Rev 81:447
97. Wayland BB, Sherry AE, Coffin VL (1989) J Chem Soc, Chem Commun, p 662
98. Coffin VL, Brennen W, Wayland BB (1988) J Am Chem Soc 110:6063
99. Zhang XX (1997) J Am Chem Soc 119:7938
100. Wayland BB, Woods BA, Coffin VL (1986) Organometallics 5:1059
101. Chatani N, Shinohara M, Ikeda S, Murai S (1997) J Am Chem Soc 119:4303
102. Sisak A, Marko L, Angyalossy Z, Ungvary F (1994) Inorg Chim Acta 222:131
103. Liebeskind LS (1989) Tetrahedron 45:3053
104. Law KY (1993) Chem Rev 93:449
105. Huffman MA, Liebeskind LS (1993) J Am Chem Soc 115:4895
106. Detty MR, Henne B (1993) Heterocycles 35:1149
107. Paquette LA, Sturino CF, Doussot P (1996) J Am Chem Soc 118:9456
108. Tomooka CS, Liu H, Moore HW (1996) J Org Chem 61:6009
109. Aime S, Botta M, Crich SG, Giovenzana G, Palnisana G, Sisti M (1999) Bioconjugate Chem 10:192
110. Terao H, Sugawara T, Kita Y, Sata N, Kaho E, Takeda S (2001) J Am Chem Soc 123:10468
111. Ajayaghosch A, Eldo J (2001) Org Lett 3:2595
112. Xie J, Comeau AB, Seto CT (2004) Org Lett 6:83
113. Halmann MM (1993) Chemical fixation of carbon dioxide: methods for recycling CO_2 into useful products. CRC, London
114. Eisenberg R, Hendriksen DE (1979) Adv Catal 28:79
115. Mauser H, King WA, Gready JE, Andrews TJ (2001) J Am Chem Soc 123:10821
116. Raebiger JW, Turner JW, Noll BC, Curtis CJ, Miedaner A, Cox B, DuBois DL (2006) Organometallics 25:3345
117. Fujita E (1999) Coord Chem Rev 185–186:373
118. Darensbourg DJ, Kudaroski RA (1983) Adv Organomet Chem 22:129
119. Berthet JC, Le Marechal M, Nierlich M, Lance M, Vigner J, Ephritikhine M (1991) J Organomet Chem 408:335

120. Lee GR, Maher JM, Cooper NJ (1987) J Am Chem Soc 109:2956
121. Davies NW, Frey ASP, Gardiner MG, Wang J (2006) Chem Commun, p 4853
122. Nixon JF, Modelli A, Clentsmith GKB (2002) Chem Phys Lett 366:122
123. Recknagel A, Stalke D, Roesky HW, Edelmann FT (1989) Angew Chem Int Ed 28:445
124. Clentsmith GKB, Cloke FGN, Green JC, Hanks J, Hitchcock PB, Nixon JF (2003) Angew Chem Int Ed Engl 42:1038
125. Bartsch R, Nixon JF (1989) Polyhedron 8:2407
126. Arnold PL, Cloke FGN, Hitchcock PB, Nixon JF (1996) J Am Chem Soc 118:7630
127. Barr ME, Smith SK, Spencer B, Dahl LF (1991) Organometallics 10:3983
128. Scheer M, Herrmann E, Sieler J, Oehme M (1991) Angew Chem Int Ed 8:969
129. Scherer OJ (1999) Acc Chem Res 32:751
130. Evans WJ, Nyce GW, Ziller JW (2000) Angew Chem Int Ed 39:240
131. Bohr ED (1964) Adv Organomet Chem 2:115
132. Fagan PJ, Manriquez JM, Maatta EA, Seyam AM, Marks TJ (1981) J Am Chem Soc 103:6650
133. Duttera MR, Fagan PJ, Marks TJ (1982) J Am Chem Soc 104:865
134. Le Marechal M, Villiers C, Charpin P, Lance M, Nierlich M, Vigner J, Ephritikhine M (1989) J Chem Soc, Chem Commun, p 308
135. Zanella P, Rossetto G, De Paoli G (1980) Inorg Chim Acta 44:L155
136. Adam R, Villiers C, Ephritikhine M, Lance M, Nierlich M, Vigner J (1993) J Organomet Chem 445(1–2):99
137. Andersen RA, Brennan JG (1984) J Am Chem Soc 107:514

Struct Bond (2008) 127: 119–176
DOI 10.1007/430_2007_081

Published online: 26 February 2008

Highlights in Uranium Coordination Chemistry

Suzanne C. Bart · Karsten Meyer (✉)

Department of Chemistry and Pharmacy, Inorganic Chemistry,
Friedrich-Alexander University of Erlangen-Nürnberg, Egerlandstraße 1,
91058 Erlangen, Germany
kmeyer@chemie.uni-erlangen.de

Abstract The coordination chemistry of uranium has become an increasingly popular topic in the last 15 years. Much of the reason for this interest has come from the development of easy to synthesize, stable starting materials. These materials allowed an entry point for the exploration of uranium with any ligand imaginable. This chapter covers the most significant developments in the coordination chemistry of non-cyclopentadienyl uranium complexes and their reactivity with small molecules.

Keywords Coordination chemistry · Molecular and electronic structure · Small molecule activation · Uranium

Abbreviations

Ac	Acetyl
bipy	2,2′-Bipyridine
Bu	Butyl
COT	Cyclooctatetraene

Cp^*	1,2,3,4,5-Pentamethylcyclopentadiene
Cp^{Me4}	1,2,3,4-Tetramethylcyclopentadiene
dme	1,2-Dimethoxyethane
DMF	*N*,*N*′-Dimethylformamide
DMSO	Dimethyl sulfoxide
fc	Ferrocene
OTf	Triflate
phen	1,10-Phenanthroline
py	Pyridine
tacn	1,4,7-Triazacyclononane
terpy	Terpyridine
THF	Tetrahydrofuran
tppo	Triphenylphosphine oxide
ttcn	1,4,7-Trithiaazacyclononane

1 Introduction

The coordination chemistry of uranium has undergone substantial growth in the last 10–15 years [1–8]. One impetus for this forward movement was the lack of knowledge about the bonding in *f* elements. Exploring uranium chemistry began to give new insights into the coordination behavior and bonding interactions of 5*f* elements, and allowed the exploration of ionic and covalent metal–ligand interactions. Studying topics such as these offers the potential for new complexes and catalytic applications. This chapter encompasses recent significant work on the structure and bonding of uranium coordination chemistry over the last 10–12 years. The complexes discussed have all types of molecular architectures with a wide array of donor ligands. Uranium complexes supported by cyclopentadienyl ligands have been reviewed elsewhere [1]. Exceptional examples have been included. A review has also appeared on uranium complexes with multidentate N-donor ligands [2]. Some of these complexes will be repeated as applications to other types of chemistry.

2 Entry into Uranium Coordination Chemistry: The First Convenient Uranium Starting Materials

The generation of mid-valent uranium starting complexes has played a key role in the recent growth of uranium coordination chemistry. The synthesis of $[UI_3(THF)_4]$, originally reported by Clark and Sattelberger in 1994 [9–11], was a spark that ignited interest in the chemistry of low-valent U(III) because it is operationally simple to make on a large scale with high yields. Cleaned and amalgamated uranium turnings are oxidized with elemental iod-

ine in the presence of THF to produce a dark blue solid easily isolated by filtration. Recently, a procedure for solvent-free UI_3 was reported, allowing this starting material to be used in solvent-sensitive reactions as well [12]. The more difficult synthesis of UCl_3 involves using elemental uranium metal and hydrogen chloride gas at elevated temperatures of 250–300 °C [13]. The trivalent uranium triflate analogue, $[U(OTf)_3]$, is synthesized by treating UH_3 with an excess of triflic acid, HOTf, at 20 °C to produce a fine green powder accompanied by liberation of hydrogen gas [14]. The next generation complex, $[U(N(SiMe_3)_2)_3]$, was initially reported by Andersen and synthesized by addition of three equivalents of the sodium amide to $[UI_3(THF)_4]$ (Fig. 1) [15, 16].

Ligand exchange has been studied with $[UI_3(THF)_4]$ by dissolution of this complex in other donating solvents. For instance, green crystals of the nine-

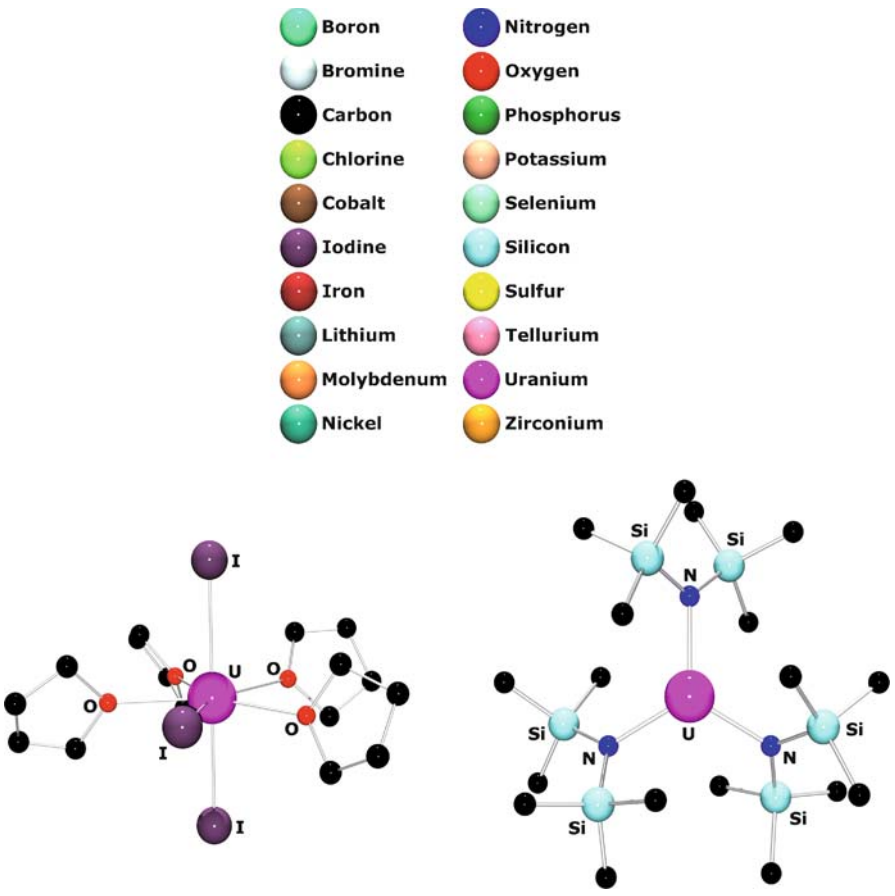

Fig. 1 Molecular structure of seminal uranium(III) complexes, $[UI_3(THF)_4]$ (*right*) and $[U(N(SiMe_3)_2)_3]$ (*left*). Hydrogen atoms omitted for clarity

coordinate uranium(III) acetonitrile salt, $[UI_3(MeCN)_9]$ were obtained by addition of acetonitrile to $[UI_3(THF)_4]$ [17]. Significantly, this work demonstrates the ability to easily displace iodine from the coordination sphere through addition of N-donor ligands. Addition of two equivalents of 2,2′-bipyridine to $[UI_3(py)_4]$ furnished $[UI_3(bipy)_2(py)]$ [18]. The coordination polymer $[U(OTf)_3(MeCN)_3]_n$ was formed via salt metathesis of $[UI_3(THF)_4]$ with potassium triflate in acetonitrile [19].

Uranium(IV) halide complexes have also been synthesized recently. Elemental uranium is used for the synthesis of UBr_4 and is treated with elemental bromine, while UCl_4 is conveniently made from UO_3 and hexachloropropene [20]. The synthesis of the solvent-free uranium(IV) analogue, UI_4, is accomplished by heating a mixture of uranium metal and iodine to 530 °C [21]. Once synthesized, UI_4 can also be isolated as various solvates, including $[UI_4(MeCN)_4]$ and $[UI_4(py)_3]$ [22]. The reaction of oxide-free uranium metal turnings with 1.3 equivalents of elemental iodine in benzonitrile provides $[UI_4(NCPh)]$, a versatile U(IV) synthon which is soluble in organic solvents and has been fully characterized [23]. A volatile uranium derivative, $[U(BH_4)_4]$, is made by addition of $Al(BH_4)_3$ to UF_4 [24]. The uranium(IV) triflate compound, $[U(OTf)_4]$, was synthesized by heating UH_3 and an excess of triflic acid to 180 °C or by treating UCl_4 with triflic acid at 120 °C [14]. This compound has been used to make many different types of derivatives [25].

Uranium oxo derivatives of varying oxidation states have been widely used as starting materials. For instance, the synthesis of uranium(IV) oxide involves hydrogenation of U_3O_8 to produce UO_2 and H_2O. Uranyl starting complexes of the form $[UO_2][X_2]$ are very important as an entry into U(VI) chemistry. These starting complexes include $[UO_2Cl_2]$, $[UO_2(OTf)_2]$, and $[UO_2(NO_3)_2]$. Exposure of UCl_4 to oxygen at 350 °C produces uranyl dichloride, while uranium(VI) triflate can be made by addition of oxygen to U_3O_8. The latter is also formed by treating UO_3 with triflic acid TfOH at 110 °C or with boiling triflic anhydride, TfOTf, affording $[UO_2(OTf)_2]$ in high yields [26]. Synthesis is also possible by addition of UO_3 to TfOH in water, or by dehydration of $[UO_2(OTf)_2(H_2O)_n]$ in boiling TfOTf. Uranyl nitrate, $[UO_2(NO_3)_2]$, is commercially available and is synthesized by the addition of N_2O_5 to UO_3.

3 Synthesis of Highly Reactive Uranium Precursors with Monomeric, Chelating, and Macrocyclic Ligands

From these initial uranium starting materials, low- and mid-valent coordination complexes have been made with many molecular architectures, and vary depending on the type of ligands used. Because it is well documented that subtle changes in ligand sterics produce drastic changes in reactivity, choice

of the proper ligand initially is very important [27–29]. The uranium centers in the complexes discussed here are either coordinatively unsaturated or have a labile neutral ligand, allowing these molecules to participate in further chemistry, including small molecule activation.

Uranium(III) systems have been developed using a tris(anilide) framework [30]. The uranium(III) species $[(N[^tBu]Ar)_3U(THF)]$ (Ar=$C_6H_3Me_2$-3,5) was isolated as a black solid (Fig. 2). ^{1}H NMR data at 25 °C indicate a single ligand environment. Crystallographic characterization showed the U(III) complex has average U–N bond lengths of 2.320 Å. The *ipso* carbons of the adjacent phenyl rings are also closely associated with the uranium center, with U–C bond lengths of ~2.9 Å. This is consistent with U(III)–arene π complexation [31]. The molecular structure also shows an interesting feature: the THF ligand is located in the arene "bowl" above the uranium center, rather than in the "pocket" formed by the *tert*-butyl groups underneath the uranium [32].

A uranium derivative of the constrained geometry ligand has been synthesized, $[(CGC)U(NMe_2)]$ (CGC=$Me_2Si(\eta^5$–$Me_4C_5)(^tBuN)$), containing a dimethylamide to complete the coordination sphere [33]. Crystallographic analysis of brown microcrystals revealed an η^5 coordination mode of the cyclopentadienyl ring and a U–N(L)(^{t}Bu) bond length of 2.207(4) Å (Fig. 3). The U–N(dimethylamide) distance is similar at 2.21(1) Å. This compound has been demonstrated to perform intermolecular hydroamination/cyclization of amine substrates with unsaturated C–C tethers.

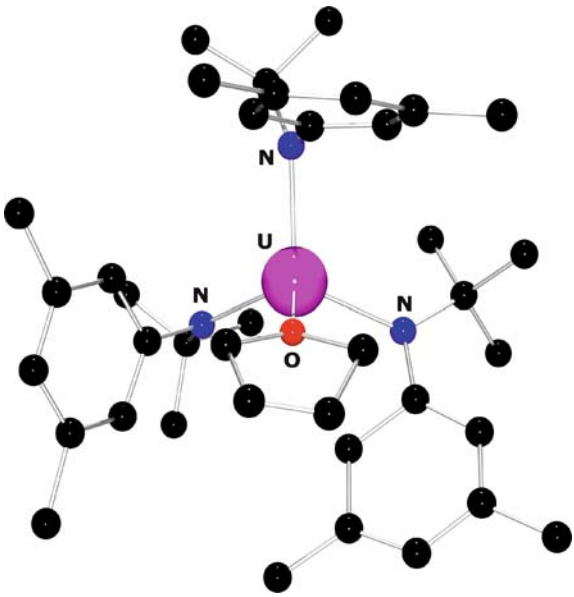

Fig. 2 Molecular structure of $[(N[^tBu]Ar)_3U(THF)]$. Hydrogen atoms omitted for clarity

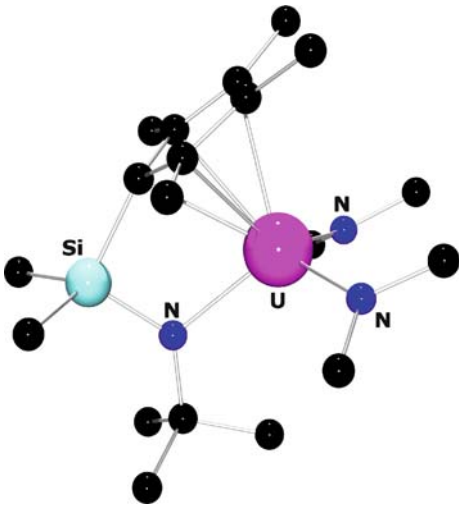

Fig. 3 Molecular structure of $[Me_2Si(\eta^5\text{–}Me_4C_5)(^tBuN)U(NMe_2)_2]$. Hydrogen atoms omitted for clarity

Similar to the famous uranocene complex, $[(C_8H_8)_2U]$ [34, 35], a bispentalene uranium complex, $[(\eta^8\text{–}C_8H_4(1,4\text{–}Si^iPr_3)_2)_2U]$, was prepared via the reaction of UCl_4 with two equivalents of $[K_2(C_8H_4\{1,4\text{–}Si^iPr_3\}_2)]$ [36]. The binding of the pentalene ligand in an η^8 mode is examined by density functional calculations and photoelectron spectroscopy. The uranium complex is modeled as D_{2d} symmetric and has a ground triplet state. The HOMO of the pentalene dianion is an orbital of δ symmetry with respect to an η^8-coordinated metal. In this bispentalene complex, actinides provide both 5*f* and 6*d* orbitals that can overlap with the symmetry adapted linear combinations of these pentalene HOMOs and form covalent bonds. The HOMO-1 of the pentalene dianion is also able to form bonds with metal *d* and *f* orbitals, but with a smaller contribution from the metal. Overall, the 6*d* orbitals make a larger contribution to bonding than the 5*f*. The conformation of the ligand arrangement is dictated mostly by steric effects [36].

The twelve-coordinate, icosahedral U(III) complex, $[(HB(3\text{-}(2\text{-pyridyl})\text{-}pz)_3)_2U]$, was reported in 1995 (Fig. 4). This complex features the typical tris(pyrazol-1-yl)hydroborate ligand substituted with a 2-pyridine group in the 3-position. Synthesis was achieved by salt metathesis, by addition of the potassium salt of the ligand to $[UI_3(THF)_4]$ [37]. This complex is the first example of an actinide species with N_{12} coordination, as both the pyrazolyl and pyridyl substituents are coordinated to the uranium center through their nitrogen atoms. The uranium–pyridyl bond lengths average 2.95 Å, and are longer than the corresponding metal–pyrazolyl average distance of 2.66 Å. The two ligands fit comfortably around the large metal center, as indicated by

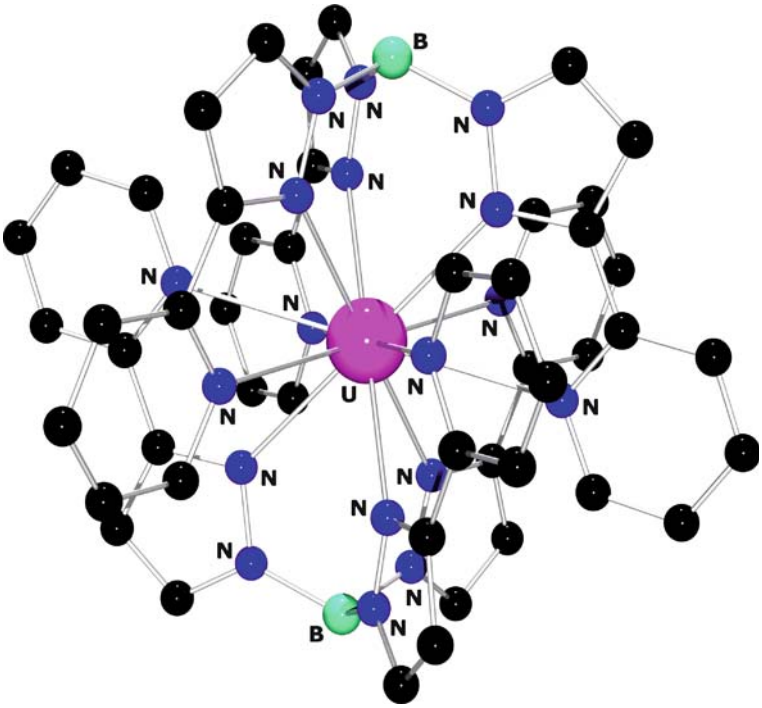

Fig. 4 Molecular structure of $[(HB(3\text{-}(2\text{-pyridyl})\text{-}pz)_3)_2U]$. Hydrogen atoms omitted for clarity

the unstrained N–B–N bond angle of ~109–110°. The bite angles of the *N*,*N* chelating fragments are between 57 and 59° [37].

Another variation on the typical tris(pyrazol-1-yl)hydroborate ligand has been synthesized in which two pyrazolyl units are substituted by two sulfur-based 2-mercapto-1-methylimidazolyl rings [38]. The cationic complexes $[(\kappa^3\text{-}H(R)B(tim^{Me})_2)_2U(THF)_3][BPh_4]$ (R=H, Ph; tim^{Me} = (2-mercapto-1-methylimidazolyl)borate) that were isolated and fully characterized are unprecedented cationic U(III) complexes anchored by poly(thioimidazolyl)borate ligands. Each ligand is bound in a tridentate fashion through two thione sulfurs and an agostic hydrogen interaction. The coordination mode is similar to that of the analogous nitrogen-based ligand $[H(R)B(pz^*)_2]^-$ (R=H, Ph; pz* = pz, 3,5-Me_2-pz, 3-^{t}Bu-5-Me-pz) [39–41]. The phenyl derivative was crystallographically characterized (Fig. 5) and showed U–B distances of 3.547(13) and 3.616(3) Å. Crystallography confirmed agostic U–H bonds of length 2.61 and 2.71 Å were calculated by positioning the H(B) atoms at their idealized location. The average U–S bond distance is 2.928(11) Å. The C–S bond distances ranging from 1.668(12) to 1.726(12) Å (avg. = 1.71(3) Å) are intermediate of single and double bonds, indicating partial reduction of the π character of the C–S bond. The labile THF allows accessibility to the metal

center, thus opening the way to a new class of uranium compounds via ligand substitution reactions.

The ^{1}H NMR spectra of this class of molecules display a single set of three resonances for the four thioimidazolyl groups in the ratio 12(Me) : 4(H_a) : 4(H_b). The resonances attributed to the tetraphenylborate counterion appear as three signals near the diamagnetic region, integrating in a ratio of 8(H_c) : 8(H_d) : 4(H_e). For the phenyl derivative, the aromatic rings appear also as two triplets and one doublet. The ^{1}H NMR spectrum is consistent with a fluxional molecule on the NMR timescale at room temperature.

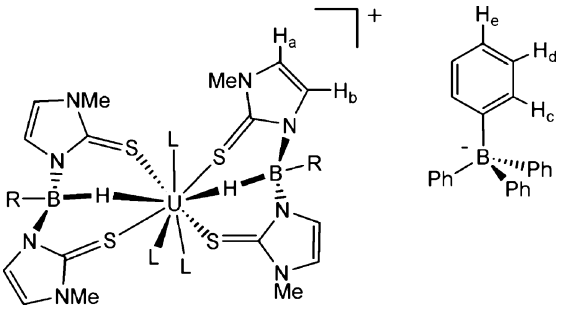

(1)

Uranium chemistry has also been explored with functionalized triazacyclononane frameworks. Several generations of uranium compounds have been developed using a triazacyclononane substituted with aryloxide groups containing bulky alkyl substituents [42]. The first generation system has ligands substituted with *tert*-butyl groups in the *ortho* position of the aryloxide ring, to afford the monomeric uranium complex [(($^{t\mathrm{Bu}}$ArO)$_3$tacn)U] (($^{t\mathrm{Bu}}$ArO)$_3$tacn^{3-} = trianion of 1,4,7-tris(3-*tert*-butyl-5-*tert*-butyl-2-hydroxybenzyl)-1,4,7-triazacyclononane) [43, 44].

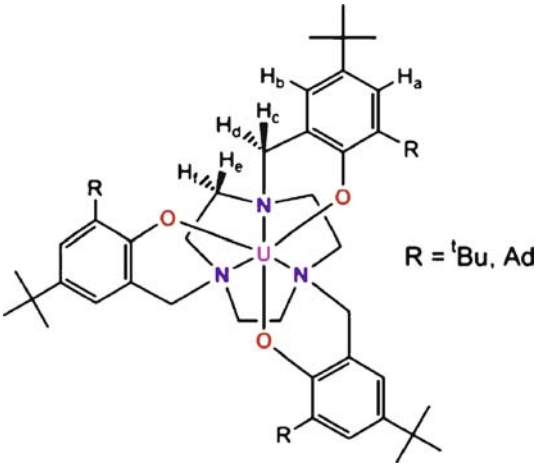

(2)

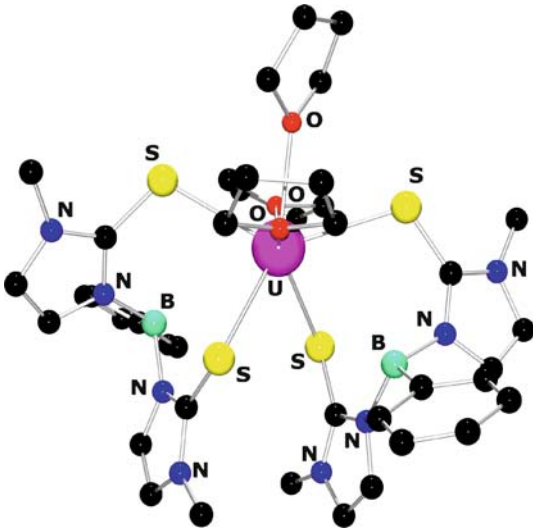

Fig. 5 Molecular structure of $[(\kappa^3\text{-H(R)B(tim}^{Me})_2)_2U(THF)_3][BPh_4]$. Hydrogen atoms omitted for clarity

The ^{1}H NMR spectrum (benzene-d_6) at 20 °C displays resonances between –22 and +13 ppm. Two sharp and intense signals at 4.15 and 2.63 ppm are assigned to the *tert*-butyl groups on the aryloxide pendant arms. The other protons on the frame of the ligand (H_a–H_f) are diastereotopic. Due to their similar integration values, assignments could not be made. The magnetic moment of solid samples is temperature dependent, varying from 1.77 μB at 5 K to 2.92 μB at 300 K. The low-temperature magnetic moment agrees well with the low-temperature EPR signal, which is a metal-centered isotropic signal with $g = 2.005$ in an X-band experiment. This complex is highly reactive and crystallization attempts in the presence of methylcyclohexane vapor in the glove box atmosphere produced single crystals of an unprecedented alkane complex $[((^{tBu}ArO)_3tacn)U(^{Me}Cy\text{–}C_6)]$, where a C–H bond of methylcyclohexane is bound in an η^2 fashion to the electron-rich uranium center [44]. The U–C and U–H distances were found to be 3.864 and 3.192 Å, respectively. This molecule is significant as it is the first fully documented example of stable, crystallographically well-defined metal–alkane coordination. This alkane coordination is a general transformation, as complexes containing cyclohexane, methylcyclopentane, and neohexane were also synthesized and crystallographically characterized. The respective U–O and U–N average distances are 2.244(3) and 2.676(4) Å. The uranium is situated 0.66 Å below the aryloxide oxygen atoms, which is slightly less than the value of 0.75 Å obtained for six-coordinate $[((^{tBu}ArO)_3tacn)U]$. The difference can be attributed to uranium–ligand bonding interactions, where the alkane has the ability to "pull" the uranium center closer to the plane of the aryloxide oxygen atoms. A simi-

lar seven-coordinate acetonitrile complex, [(($^{t\mathrm{Bu}}$ArO)$_3$tacn)U(CH$_3$CN)], has a uranium center with an even lower value of 0.45 Å, indicating that interaction with π-type ligands causes the uranium center to become even closer to the plane of the oxygen atoms.

A second generation of ligands was developed using larger adamantyl groups to prevent undesired reactions, such as bimolecular decomposition and dimer formation. Van der Waals interactions among the adamantyl groups place the reactive U(III) center deep inside the sterically encumbering ligand, resulting in the uranium being displaced 0.88 Å below the plane defined by the three aryloxide oxygen atoms. This compound, [(($^{\mathrm{Ad}}$ArO)$_3$tacn)U] (($^{\mathrm{Ad}}$ArO)$_3$tacn^{3-} = trianion of 1,4,7-tris(3-adamantyl-5-*tert*-butyl-2-hydroxybenzyl)-1,4,7-triazacyclononane), has a protected uranium center with a narrow cylindrical cavity formed by the adamantyl substituents with access to small molecules (Fig. 6) [45]. The ^{1}H NMR spectrum exhibits the expected 14 paramagnetically shifted and broadened resonances between –22 and 14 ppm. X-ray quality crystals were analyzed and reveal a distorted trigonal prismatic uranium center that is well protected by the bulky adamantyl substituents from the top and the weakly coordinated triazacyclononane ligand from the bottom. The average ligand distances are 2.22(1) Å for U–O and 2.64(3) Å for U–N. Variable temperature magnetic data were in the range from 1.74 at 5 K to 2.83 μB at 300 K. The EPR spectrum acquired as a frozen benzene solution at 14 K displayed an isotropic signal at $g = 2.005$.

Replacing the aryloxide functionality with pendant amide arms has been accomplished to make the 1,4,7-tris(dimethylsilylaniline)-1,4,7-triazacyclononane ligand [46]. The synthesis of the brownish-green uranium complex, [((SiMe$_2$NPh)$_3$tacn)U], was accomplished by stirring the sodium salt of the ligand with [UI$_3$(THF)$_4$]. Crystallographic analysis revealed a six-coordinate uranium center in a distorted trigonal prismatic conformation, with the two

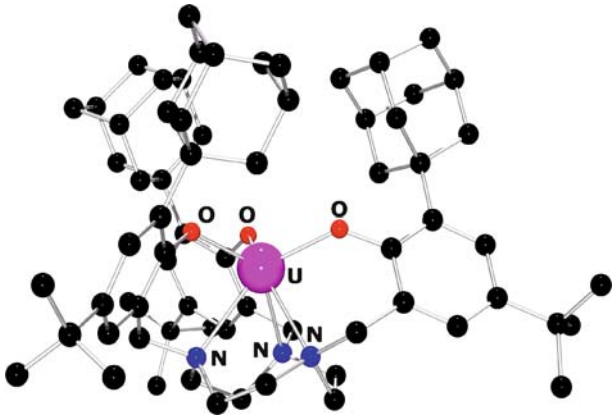

Fig. 6 Molecular structure of [(($^{\mathrm{Ad}}$ArO)$_3$tacn)U$^{\mathrm{III}}$]. Hydrogen atoms omitted for clarity

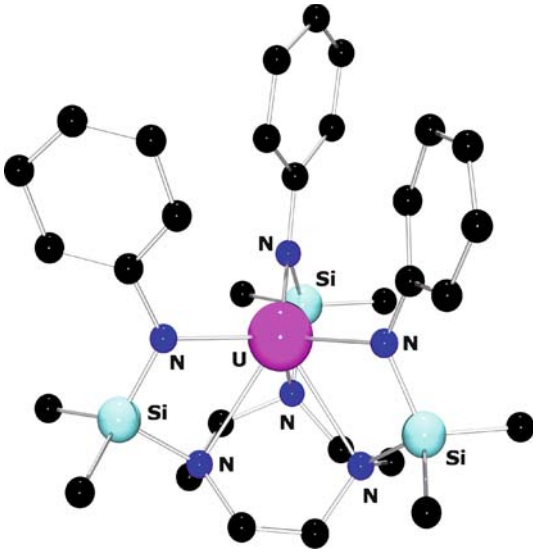

Fig. 7 Molecular structure of [((SiMe$_2$NPh)$_3$tacn)U]. Hydrogen atoms omitted for clarity

trigonal planes defined by each set of nitrogen atoms (Fig. 7). The average U–N(amido) distance of 2.35(2) Å is similar to that of 2.320(4) observed in the uranium(III) complex [U(N(SiMe$_3$)$_2$)$_3$] [39]. The U–N(tacn) distance of 2.66(2) Å is similar to that observed for the previously mentioned aryloxide derivatives, [((^{R}ArO)$_3$tacn)U] (R=^{t}Bu, Ad) [42]. The paramagnetically broadened and shifted ^{1}H NMR spectrum revealed a single resonance for the 18 protons of the SiMe$_2$ linkers, two resonances for the six H$_o$ and H$_m$, and three resonances for H$_p$ protons of the anilide. Three resonances with the integration value of six protons each were also observed (H$_a$). Cooling the sample in the NMR probe caused the resonances assigned to the SiMe$_2$ groups and to the methylenic protons to shift, broaden, and collapse. At –60 °C the spectrum sharpened, and four broad resonances in a 1 : 1 : 1 : 1 intensity ratio were visible and assigned to the CH$_2$ groups. The SiMe$_2$ groups also decoalesced at this temperature, and appeared as two peaks in a 9 : 9 intensity ratio, consistent with C_3 symmetric structures. The resonances of the aromatic protons of the amido groups did not collapse, indicating fast rotation of the phenyl groups on the NMR timescale at –80 °C.

(3)

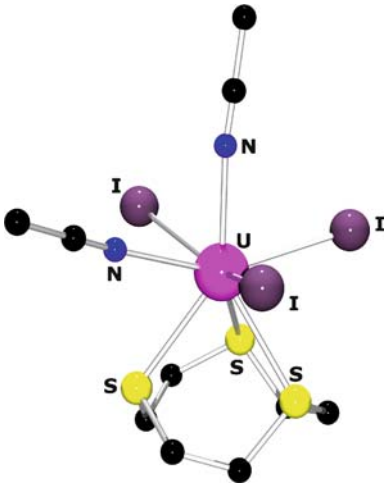

Fig. 8 Molecular structure of $[(ttcn)UI_3(MeCN)_2]$. Hydrogen atoms omitted for clarity

Substitution of nitrogen for sulfur in the tacn ring allowed isolation of a 1,4,7-trithiacyclononane derivative [47]. Green crystals of the acetonitrile adduct, $[(ttcn)UI_3(MeCN)_2]$ (ttcn = 1,4,7-trithiaazacyclononane) suitable for X-ray analysis were obtained (Fig. 8). The uranium center is eight-coordinate by three sulfurs of the trithiacrown and can be described as a distorted square antiprism. The U–S bond distances of 3.0456(9), 3.0146(9), and 3.0779(9) Å could indicate a covalent contribution to the U–S bonding. Characterization of this complex by ^{1}H NMR in acetonitrile solution revealed two resonances integrating to six protons each at 12.67 and 13.65 ppm, presumably due to the ttcn ring.

4
High-Valent Uranium Complexes with Multiply Bonded Ligands

4.1
Complexes Containing the $[O=U=O]^{2+/+}$ Subunit

The most commonly recognized molecular unit in uranium chemistry is no doubt the uranyl ion, $[UO^{2+}]$, which has undergone intense study for the past 150 years. The bonding in this linear $[UO_2{}^{2+}]$ unit is quite distinctive, and is made up of a combination of *d*–*p* and *f*–*p* π interactions. This unit is convenient to work with, because it is stable to moisture and oxygen, and has a convenient handle for infrared spectroscopy, the O=U=O unit. Typically, this band appears from 920 to 980 cm^{-1} for the asymmetric O–U–O stretch. A band for the symmetric stretch can be viewed by Raman spectroscopy, and

appears at 860 cm^{-1}. This measure is important, as the frequency of the symmetric ($\nu 1$) and asymmetric ($\nu 3$) UO_2 stretch is inversely proportional to the donor strength of the equatorial ligands which lie orthogonal to the [UO_2^{2+}] moiety [48, 49]. Electronic absorption spectroscopy typically shows an absorption around 450 nm for the O=U=O unit and is identified by vibrational fine structure typically associated with it [17].

The substitution chemistry of the more common starting materials [$UO_2(OTf)_2$] and [UO_2Cl_2] has been studied. Derivatives of these complexes have been explored by dissolving each in strongly donating solvents or by addition of neutral donor ligands. Exposure to pyridine forms the pyridine adducts [$UO_2(OTf)_2(py)_3$] and [$UO_2Cl_2(py)_3$]. An X-ray crystallographic analysis performed on the triflate complex shows a neutral monomer in the solid state with monodentate triflate ligands [26]. The analogous complexes, [$UO_2(OTf)_2(THF)_3$] and [$UO_2(OTf)_2(dme)$], were formed by dissolution in the respective solvents. Addition of two equivalents of 2,2′-bipyridine, three equivalents of phenanthroline, one or two equivalents of terpyridine, or four equivalents of triphenylphosphine oxide (tppo) to [$UO_2(OTf)_2(py)_3$] afforded the respective ligand substitution products [$UO_2(OTf)_2(bipy)_2$], [$UO_2(phen)_3$][$OTf]_2$, [$UO_2(OTf)_2(terpy)$], [$UO_2(terpy)_2$][$OTf]_2$, and [$UO_2(tppo)_4$][$OTf]_2$ [50]. The uranyl derivatives obtained using 2,2′-bipyridine and 1,10-phenanthroline show unprecedented rhombohedral coordination geometries around the uranium center [51]. This coordination geometry was also observed for the hydroxide derivative of terpyridine, [{$UO_2(OH)(terpy)$}$_2$][$OTf]_2$ [51, 52].

The triphenylphosphine oxide derivative, [$UO_2(tppo)_4$][$OTf]_2$, is well studied. In attempts to crystallize this uranium(VI) complex, serendipitous crystals of the uranium(V) compound, [$UO_2(tppo)_4$][OTf], were obtained along with the uranyl compound [50]. Both were characterized by X-ray crystallography and exhibit a square pyramidal geometry around the uranium center (Fig. 9). The uranium(VI) derivative featured a linear {UO_2} fragment perpendicular to the equatorial plane defined by the uranium center and the four oxygen atoms of the tppo ligands. The mean U=O bond length of 1.76(1) Å and the average equatorial U–O bond length of 2.29(1) Å are typical [53]. The U(V) complex has slightly longer U=O bond lengths of 1.817(6) and 1.821(6) Å as expected. The U–O($OPPh_3$) bond lengths in the pentavalent complex range from 2.427(5) to 2.455(6) Å (average 2.44(2) Å), again longer than in the uranyl derivative, indicating that equatorial bond elongation is favored over elongation of the axial U=O unit.

The similar phosphine oxide derivatives [$UO_2(tppo)_4$][$BF_4]_2$ and [$UO_2(dppmo)_2(OPPh_3)$][X]$_2$ (dppmo = $Ph_2P(O)CH_2P(O)Ph_2$) were also prepared from the corresponding uranyl(VI) chloride precursor and two equivalents each of AgX and phosphine oxide [54]. A mixed metal triphenylphosphine oxide derivative, [$UO_2(ReO_4)_2(tppo)_3$], was prepared as a monomeric uranyl complex as well. Interestingly, photolytic generation

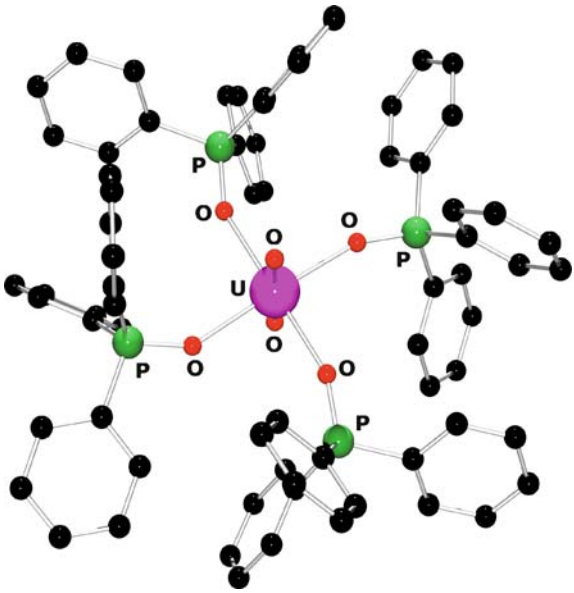

Fig. 9 Molecular structure of dication of $[UO_2(tppo)_4][OTf]_2$. Hydrogen atoms omitted for clarity

of peroxide in EtOH solutions of this compound forms trace quantities of $[((UO_2)(tppo)_3)_2\{\mu_2\text{–}O_2\}][ReO_4]_2$, where the coordinated $[ReO_4]$ groups were displaced by a bridging O_2 ligand derived from atmospheric dioxygen [55, 56].

The substitution of the uranyl ion in the presence of biologically relevant neutral donors has produced a class of interesting molecules. For instance, treating $[UO_2(NO_3)_2]$ with citric, D-(–)-citramalic, or tricarballylic (1,2,3-propanetricarboxylic) acids produces two- and three-dimensional frameworks [57–59]. Imidazole coordination has also been explored with the first definitive high-resolution single-crystal X-ray structure for the coordination of 1-methylimidazole (^{Me}imid) to $[UO_2(Ac)_2]$ (Ac=CH_3CO_2) (Fig. 10). The

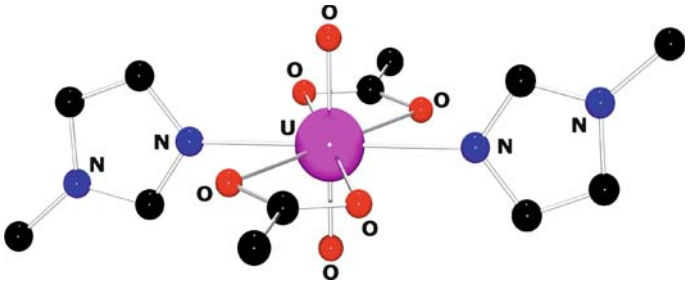

Fig. 10 Molecular structure of $[UO_2(Ac)_2(^{Me}imid)_2]$. Hydrogen atoms omitted for clarity

resulting complex, $[UO_2(Ac)_2(^{Me}imid)_2]$ [60], features a hexagonal bipyramidal uranium center, with the hexagonal plane occupied by four oxygen and two nitrogen atoms. Further characterization by Raman spectroscopy reveals a stretch at 840 cm^{-1} for the O=U=O unit. The IR spectrum shows an intense band at 916 cm^{-1} for the asymmetric uranyl stretch. Infrared spectroscopy also confirms the bidentate coordination mode of the acetate ligands, which have respective symmetric ν_s(COO) and antisymmetric ν_a(COO) carboxylate stretching modes at 1468 and 1538 cm^{-1}. Methylimidazolium uranyl salts have also been reported [61]. Addition of 4,6-*O*-ethylidene-α-D-glucopyranosylamine with *trans*-$[UO_2^{2+}]$ species produced the corresponding pentagonal bipyramidal product (4) [62].

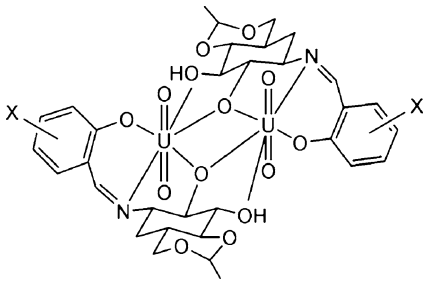

(4)

The substitution chemistry of $[UO_2Cl_2(L)_n]_n$ via salt metathesis has produced aryloxide and iminophosphorane derivatives. The di-*tert*-butyl phenoxy derivative was synthesized via salt metathesis in THF, producing the dark red $[UO_2(O-2,6-tert\text{–}Bu_2C_6H_3)_2(THF)_2]\cdot THF$, featuring *cis*-aryloxides and THF molecules [63]. However, when the *tert*-butyl groups are replaced by phenyl groups, the geometry changes to accommodate *trans*-aryloxide groups. Using sterically less bulky chlorine or methyl substituents produces the dimeric products $[UO_2(O\text{–}2,6\text{–}Cl_2C_6H_3)_2(THF)_2]_2$ (one terminal phenoxide, two bridging) and $[UO_2Cl(O\text{–}2,6\text{–}Me_2C_6H_3)(THF)_2]_2$ (one terminal chloride, two bridging phenoxides). The bis-iminophosphorane complexes $[UO_2Cl\{\eta^3\text{–}CH(Ph_2PNSiMe_3)_2\}(THF)]$ and $[UO_2Cl\{\eta^3\text{–}N(Ph_2PNSiMe_3)_2\}(THF)]$ were synthesized from the reaction of $[UO_2Cl_2(THF)_3]$ with $Na[CH(Ph_2PNSiMe_3)_2]$ and $Na[N(Ph_2PNSiMe_3)_2]$, respectively [64]. Both are dinuclear complexes in the absence of a coordinating solvent. The crystal structures of both have been determined (Fig. 11), and each display distorted pentagonal bipyramidal geometries with the bis-iminophosphorane ligands coordinating in a tridentate chelating manner. The former complex contains a U–C bond that is out of the equatorial plane by 0.842(3) Å in contrast to the latter complex, where the U–N bond is close to the equatorial plane (0.154(3) Å).

The first structurally characterized isocyanate actinide derivative, $[(UO_2)_2(NCO)_5O]_2[(Et_4N)_6]\cdot 2MeCN\cdot H_2O$ and isocyanato uranate $(Et_4N)_6[(UO_2)_2(NCO)_5O]_2\cdot 2MeCN\cdot H_2O$ were reported (Fig. 12) [65].Structural

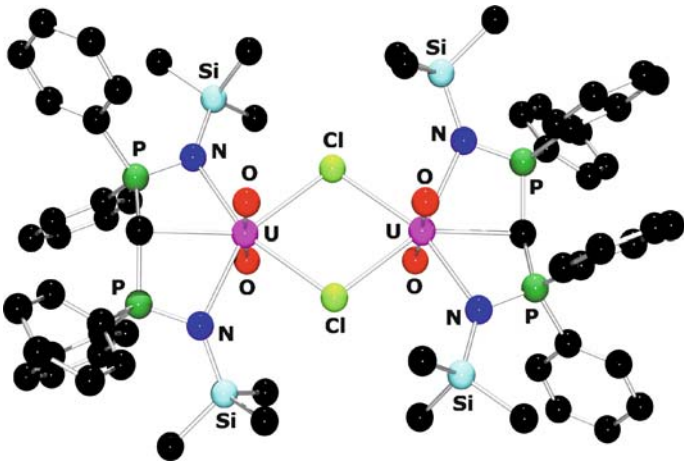

Fig. 11 Molecular structure of $[UO_2Cl\{\eta^3\text{-}CH(Ph_2PNSiMe_3)_2\}(THF)]$. THF and hydrogen atoms omitted for clarity

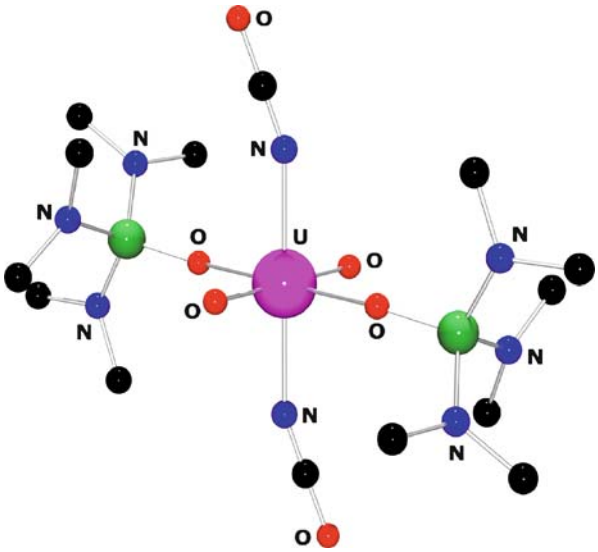

Fig. 12 Molecular structure of $[UO_2(NCO)_2(OP(NMe_2)_3)_2]$. Hydrogen atoms omitted for clarity

characterization revealed that both complexes contain N-bound isocyanate units, similar to [*trans*-$UF_4(NCO)_2$] [66]. In $[UO_2(NCO)_2(OP(NMe_2)_3)_2]$, the *d*(U–N) bond lengths of 2.336(5) Å are significantly shorter than those in the corresponding isothiocyanate derivative $[UO_2(NCS)_2(OPPh_3)_2]$ which are 2.44(2) Å [67]. The U=O bond lengths of 1.765(4) Å are comparable

with those of other uranyl derivatives. Characterization by infrared spectroscopy reveals a band at 2172 cm^{-1} assigned to the NCO group as well as one at 911 cm^{-1} for the O=U=O unit. The isocyanato uranate complex has uranyl bond lengths of 1.786(6) and 1.795(7) Å. The terminal U–NCO (d(U–N) = 2.45(1) Å) and bridging (d(U–N) = 2.58(1) Å) bond lengths are significantly longer than the those for the isocyanate compound.

Chelating sulfur ligands have been explored with the uranyl unit. For instance, Denning reports the synthesis and characterization of $[Ph_4P][UOCl_4(NSPh_2)]$ from $[Ph_4P][UOCl_5]$ and the sulfimine ligand, $[Ph_2S{=}NSiMe_3]$ (Fig. 13) [68]. In this analogue, one of the *trans*-uranyl oxygen atoms has been replaced by the sulfimine. The infrared spectrum of this complex shows a stretch at 845 cm^{-1}, assignable to the antisymmetric O=U=X vibrational mode, which is shifted from that of $[UO_2Cl_4]^{2-}$ which appears at 922 cm^{-1}. There is also a band at 1008 cm^{-1} for the antisymmetric stretch of the U–N–S linkage. The molecular structure of the anion determined by X-ray crystallography shows a pseudooctahedral geometry around the uranium center. The U–O (1.786(3) Å) and U–Cl (2.6161(8)–2.6270(8) Å) distances are typical for a uranyl anion, while the U–N distance of 1.920(3) Å is normal for a U(VI) imido species. The corresponding phosphoriminato was also synthesized and characterized and the U–O and U–N bond is very similar to the sulfur analogue. Infrared data collected on this compound reveal a symmetric stretch for the O–U–N unit at 863 cm^{-1}.

Bifunctional carbamoyl methyl sulfoxide ligands were treated with $[UO_2(NO_3)_2]$ to make the corresponding uranyl complexes. The structure of one derivative, $[UO_2(NO_3)_2(PhSOCH_2CON^iBu_2)]$, was determined by a single crystal X-ray diffraction method (Fig. 14) [69]. The uranium atom is

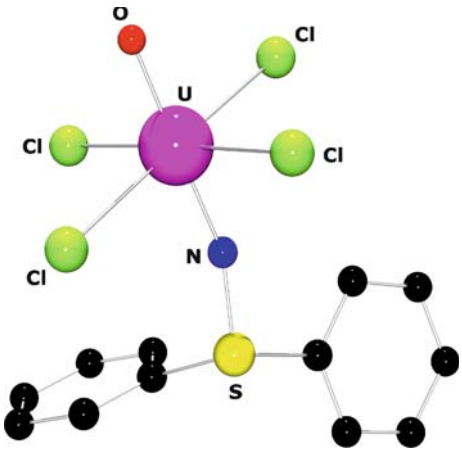

Fig. 13 Molecular structure of the cation of $[Ph_4P][UOCl_4(NSPh_2)]$. Hydrogen atoms omitted for clarity

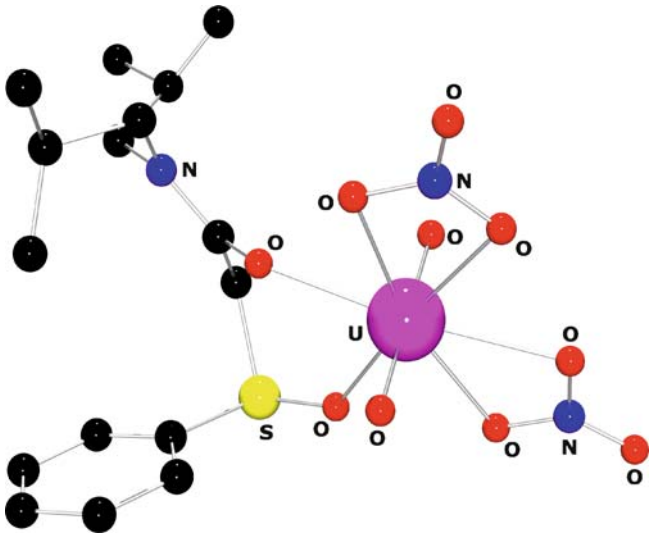

Fig. 14 Molecular structure of $[UO_2(NO_3)_2(PhSOCH_2CON^iBu_2)]$. Hydrogen atoms omitted for clarity

in a hexagonal bipyramidal geometry ligated by eight oxygen atoms. The bidentate chelating ligand is coordinated through both the sulfoxo and amido oxygen atoms to the uranyl group. The observed bond distance for U–O(sulfoxide) is 2.442(9) Å, and the U–O(amide) distance is 2.408(9) Å.

Although the coordination of carbenes to uranium has been previously explored to uranium(III) [45], the first examples of uranyl–carbon bonds have recently been reported. Treatment of $[UO_2Cl_2(THF)_3]$ with two equivalents of either 1,3-dimesitylimidazole-2-ylidene (IMes) or 1,3-dimesityl-4,5-dichloroimidazole-2-ylidene ($IMesCl_2$) produced monomeric uranyl N-heterocyclic carbene complexes [70]. Both complexes were studied by X-ray crystallography, which revealed a near-perfect octahedral uranium center (Fig. 15). The respective U=O bond lengths of 1.761(4) and 1.739(3) Å are in the range of those previously observed for $[UO_2Cl_2L_2]$ complexes [71–73]. The U=O bond length for the chloride substituted carbene ligand is significantly shorter, due to the fact that this ligand is a poorer σ donor. The U–C bond lengths are 2.626(7) and 2.609(4) Å, respectively. The carbene ligands are oriented so that they avoid steric interaction with the chloride ligands. The U–Cl bond lengths are in the expected range. Analysis of these complexes by infrared spectroscopy showed respective stretches at 938 and 942 cm^{-1}. These are high in comparison to other derivatives, and thus indicate weak electron donation from the NHC ligands. Soon after this report, the first uranium–methine bond was demonstrated in the centrosymmetric chloro-bridged dimer $[UO_2Cl\{CH(Ph_2PNSiMe_3)_2\}]$, which consists of two distorted pentagonal bipyramidal units [74]. In the Raman spectrum the

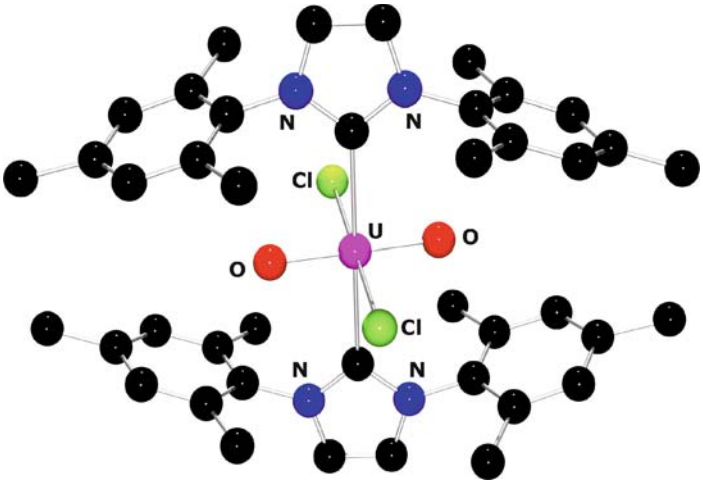

Fig. 15 Molecular structure of $[UO_2Cl_2(IMes)_2]$. Hydrogen atoms omitted for clarity

symmetric O=U=O stretch is observed at 838 cm^{-1} while the asymmetric stretch is visible in the IR spectrum at 924 cm^{-1}. The coupling constants calculated from NMR spectroscopy $^1J_{CX}$ (X=H, P) give insight into the percentage of *s* character in the C–X bond, in that the larger the value, the more the *s* character. The coupling constant measured for this complex is $^1J_{CH}$ = 136.5 Hz, CD_2Cl_2, and is intermediate of the neutral ligand $CH_2(Ph_2PNSiMe_3)_2$ ($^1J_{CH}$ = 123.7 Hz) containing an sp^3 carbon and of the ligand precursor $[Na\{CH(Ph_2PNSiMe_3)_2\}]$ ($^1J_{CH}$ = 144.2) with an sp^2 carbon. This is consistent with an interaction between uranyl and the methine carbon atom. The $^1J_{CP}$ value is less reliable. Electronic absorption data collected on this complex show two strong absorption bands at 515 and 434 nm in CH_2Cl_2. Examination of this compound by X-ray crystallography reveals two distorted pentagonal bipyramidal uranyl units each bridged by two chlorine atoms in a centrosymmetric dimer. Interestingly, the methine unit in this compound is displaced significantly (0.8877(96) Å) from the uranyl plane. The author suggests this is due to the filled *p* orbital, which points toward the uranium center to form an *s*–*p* type bond. The U=O bond lengths are 1.777(8) and 1.789(8) Å. The uranium–carbon distance in the methine unit is 2.691(8) Å, suggesting a U(VI)–C bond, since the sum of the van der Waals radii is 3.56 Å. This is only slightly longer than the U–N bonds of 2.514(7) and 2.458(7) Å. Functionalization of an N-heterocyclic carbene with a pendant amine arm afforded a uranyl amido-NHC derivative, $[UO_2L_2]$ (L=1-ethylene-*tert*-butylamino-2-R-imidazol-2-ylidene, R=^{t}Bu) [75]. This molecule features distortion of the U–C bond from the expected trigonal planar hybridization. The carbene–uranium distance is 2.64 Å and the bent geometry of the carbene ligand indicates that this interaction is electrostatic. Characterization by

FTIR showed a spectrum with a peak at 929 cm^{-1} assigned to the asymmetric stretch for the O=U=O unit. Similar work has been performed with an alkoxide functionality [76].

The chemistry of uranyl units with nitrogen-containing ligands, such as Schiff bases and salen ligands (L), has been explored. *trans*-Dioxouranium dinuclear complexes of OH-containing ligands with N-, O-coordination sites were synthesized and characterized [77]. Seven of these were also structurally characterized by single crystal X-ray diffraction (Fig. 16). All of these complexes exhibit symmetric $[U_2O_2]$ core structures with a seven-coordinate uranium center. Ligands with more than one CH_2OH group only had one involved in chelation and in bridging. Despite the similarity of their molecular structures, their lattice arrangements display novel types of structures such as channel, herringbone, and corrugated sheets from extended weak interactions. Characterization of the 11 reported complexes by infrared spectroscopy revealed a band in the range 897–912 cm^{-1} assignable to asymmetric stretching of the *trans*-dioxouranyl ion. The $\nu_{(CN)}$ vibrations in the region 1610–1629 cm^{-1} are shifted by at least 10–20 cm^{-1} to lower frequency as compared to those of the corresponding "free" ligands, indicating that the nitrogen of azomethine is coordinated to the metal center. In several cases this band for the Schiff base ligand disappears due to the reduction of the imine by the metal center; hydroxyl groups are observed in the expected region. Another example explores solvated derivatives of the type $[UO_2(salophen)L]$ (salophen = *N*,*N*′-disalicylidene-*o*-phenylenediaminate, L = DMF, DMSO),

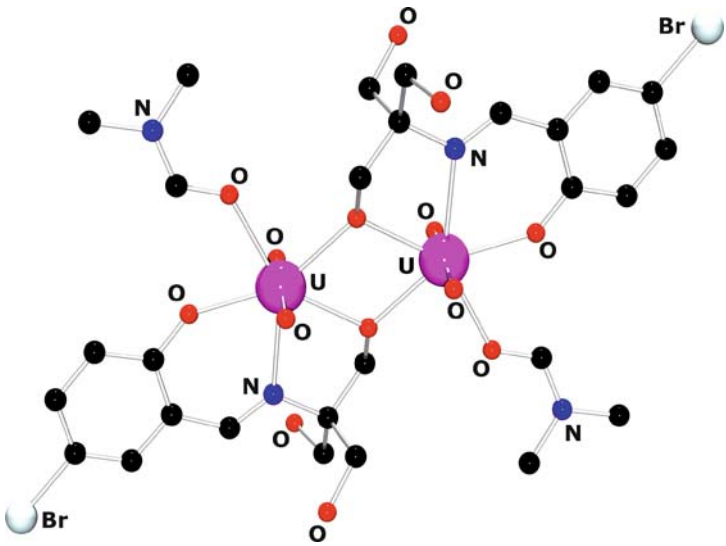

Fig. 16 Molecular structure of $[UO_2(5\text{–Br–}H_2L(DMF)]$. Dimethylformamide molecules and hydrogen atoms omitted for clarity

as well as the unsolvated version [78]. The unsolvated version is a racemic dimeric complex, $[UO_2(salophen)]_2$, which undergoes equilibrium with the solvated complex.

Another study reports the first example of UO_2^+–UO_2^+ interaction and unambiguous evidence of the presence of the resulting tetrameric cation–cation complex in pyridine solution [79]. Reaction of coordination polymer $[(UO_2(py)_5)(KI_2(py)_2)]_n$ with two equivalents of Kdbm (dbm^- = dibenzoylmethanate) in pyridine allows the isolation, after diffusion of diisopropyl ether, of blue crystals of the tetrameric pentavalent uranium complex $[UO_2(dbm)_2]_4[K_6py_{10}] \cdot I_2 \cdot 2py$ in which four $[UO_2(dbm)_2]$ complexes are assembled by cation–cation interactions between the $[UO_2^+]$ units (Fig. 17). Analysis of the crystals by X-ray crystallography revealed a centrosymmetric tetramer of $[UO_2^+]$ units coordinated to each other in a monodentate fashion to form a square plane with two crystallographically inequivalent uranium units. Each $[UO_2^+]$ coordinates two adjacent groups and is involved in two T-shaped cation–cation interactions (two linear $[UO_2^+]$ groups arranged perpendicular to each other). Each $[UO_2^+]$ is also involved in a cation–cation interaction with a potassium ion. The $[UO_2^+]$ groups have U–O distances of 1.923(10) and 1.934(8) Å, and are much shorter than those observed for the dbm oxygens (2.44(2) Å). However, the uranium distance is very similar to

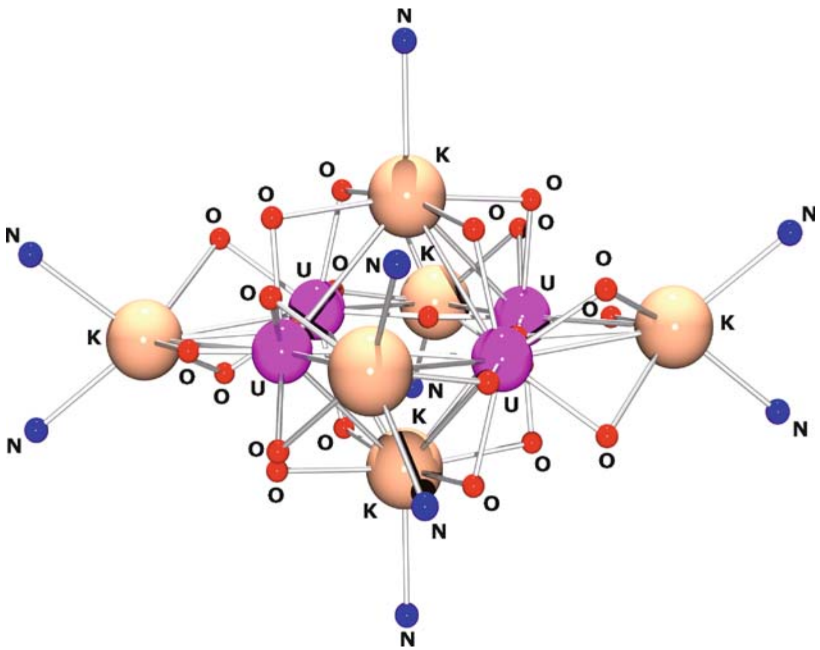

Fig. 17 Molecular structure of $[UO_2(dbm)_2]_4[K_6py_{10}] \cdot I_2 \cdot 2py$. Hydrogen, carbon, and iodine atoms omitted for clarity

that of the starting material, indicating that the uranium(V) oxidation state is preserved. The asymmetric stretch for the O=U=O units by infrared spectroscopy is found at 782 cm^{-1}. These results are significant as they expand the possibilities for the preparation of polymetallic assemblies involving *f* elements [80]. In addition, they offer the possibility for reaction of the pentavalent O=U=O fragment with other metals, including 3*d* transition and other actinide metals.

4.2 High-Valent Uranium Complexes with Nitrogen Donor Ligands

Some studies have examined the formation of high-valent uranium complexes which do not contain a uranyl unit. Hexakisamido uranium complexes have recently been explored by using the sterically bulky amine precursor Hdbabh (Hdbabh = 2,3 : 5,6-dibenzo-7-azabicyclo[2.2.1]hepta-2,5-diene) [81]. Addition of seven equivalents of the corresponding lithium salt to $[UI_3(THF)_4]$ produced an orange solid assigned as $[Li(THF)_x][U(dbabh)_6]$. EPR in frozen acetonitrile/toluene solution displayed a single isotropic resonance at $g = 1.12$, similar to other uranium(V) complexes. The magnetic moment of the $^nBu_4N^+$ salt is 1.16 μB between 5 and 35 K and increases to 3.7 μB at room temperature, supporting the U(V) formulation. Electrochemical studies confirmed an oxidation wave at –1.10 V. X-ray crystallography showed a near perfect octahedral complex, with U–N distances ranging from 2.230(11) to 2.267(13) Å. DFT calculations indicate that the unpaired electron resides in an *f*(*xyz*) orbital. Oxidation by air or silver nitrate produces the neutral U(VI) complex, $[U(dbabh)_6]$ (Fig. 18). Crystallographic analyses of both uranium complexes revealed near perfect octahedral coordination, with typical U–N bond distances ranging from 2.230(11) to 2.267(13) Å for the U(V) compound and 2.178(6) to 2.208(5) Å for U(VI). The electronic absorption spectrum of the uranium(VI) derivative has two distinct bands at 353 nm ($\varepsilon = 2200\ M^{-1}\ cm^{-1}$) and 501 nm ($\varepsilon = 1200\ M^{-1}\ cm^{-1}$). DFT confirms that the neutral molecule features amido to uranium π bonding. The HOMOs are mostly nitrogen 2*p* in character, with contributions from U 5*f* and 6*d*. This chemistry is unique because both the U(V) and U(VI) analogues can be studied with minimal structural change.

Cummins has described the synthesis of bimetallic μ-cyanoimide complexes made from an [NCN] transfer reagent, the cyanoimide based on Hdbabh [82]. Treating $[(Ar[R]N)_3U(THF)]$ with 0.5 equivalents of NCdbabh produced the corresponding μ-cyanoimide complex $[((Ar[R]N)_3U)_2\{\mu_2, \eta^1, \eta^1\text{-NCN}\}]$ (Ar=$C_6H_3Me_2$-3,5; R=^{t}Bu). X-ray crystallography revealed a bent geometry at the cyanoimide nitrogens, with a U–N–C angle of 162.6(5)° (Fig. 19). The bent geometry of the cyanoimide nitrogens in (μ-NCN) and the similarity of the $U–N_{amide}$ and $U–N_{cyanoimide}$ distances indicate that there is little π bonding in the uranium–cyanoimide interaction. The isotopomer

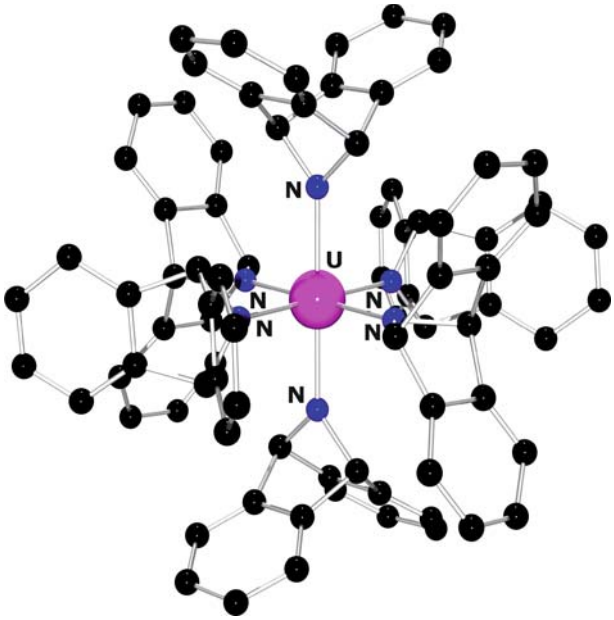

Fig. 18 Molecular structure of $[U(dbabh)_6]$. Hydrogen atoms omitted for clarity

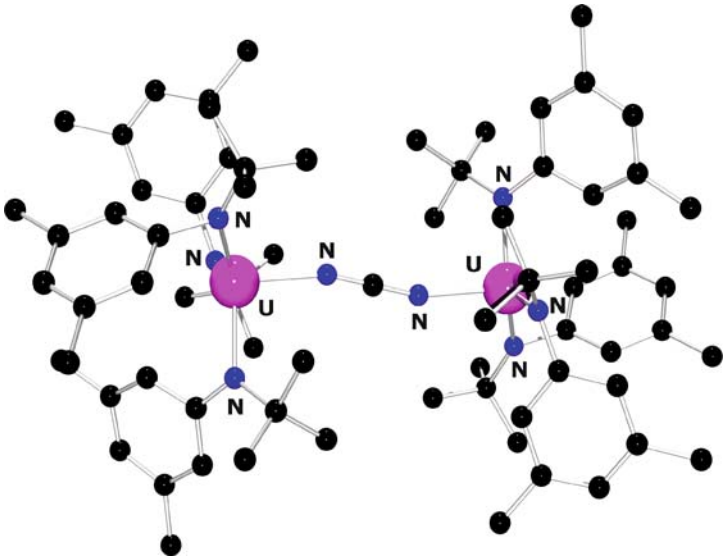

Fig. 19 Molecular structure of $[((Ar[R]N)_3U)_2\{\mu_2, \eta^1, \eta^1\text{-NCN}\}]$. Hydrogen atoms omitted for clarity

made by using the ^{13}C-labeled reagent N^{13}Cdbabh displays a broad ^{13}C NMR resonance at 133 ppm assigned to the central carbon in the μ-cyanoimide unit [82].

While uranium(V) imido species have previously been synthesized, these compounds are metallocene based [83–85]. Recently, non-cyclopentadienyl ancillary ligands have been shown to support uranium(V) imido complexes as well. For instance, the triamidoamine ligand scaffold [NN_3'] protects a trimethylsilyl uranium imido species [86]. Uranium(V) imido complexes based on the aryloxide substituted tacn system have also been explored. Addition of an equivalent of trimethylsilyl azide to either [(($^{t\mathrm{Bu}}$ArO)$_3$tacn)U] or [(($^{\mathrm{Ad}}$ArO)$_3$tacn)U] in benzene forms the high-valent uranium(V) imido compounds, [(($^{\mathrm{R}}$ArO)$_3$tacn)U$^{\mathrm{V}}$(NSiMe$_3$)] (R=*t*Bu, = Ad) [44, 87]. Variable temperature magnetic data collected for the *tert*-butyl derivative show a magnetic moment of μ_{eff} = 2.34 μB at 300 K that lowers to μ_{eff} = 1.46 μB at 5 K. The room temperature moment is smaller than the expected value of 2.54 μB calculated for the free ion in the L–S coupling scheme due to increased covalency in the bonding interactions. Electronic absorption spectroscopy shows an intense charge-transfer band at 400 nm (ε = 3800 M^{-1} cm^{-1}). High-valent uranium(V) and (VI) imido species typically exhibit short, formal U–N(imido) triple bonds with bond distances ranging from 1.85 to 2.01 Å and ∠(U–N–R) bond angles varying from slightly bent to linear (163.33–180.0°). Accordingly, the structural parameters of the *tert*-butyl derivative (*d*(U–N(imido)) = 1.989(5) Å and ∠(U–N–R) = 173.7(3)°) are similar. DFT calculations support the formulation of the U–N bond as a formal triple bond, containing two π-bonding and one σ-bonding interactions. The more sterically hindered adamantyl compound (Fig. 20) exhibits a U–N(imido) bond distance that is the longest ever reported for a metal imido complex, and deviates

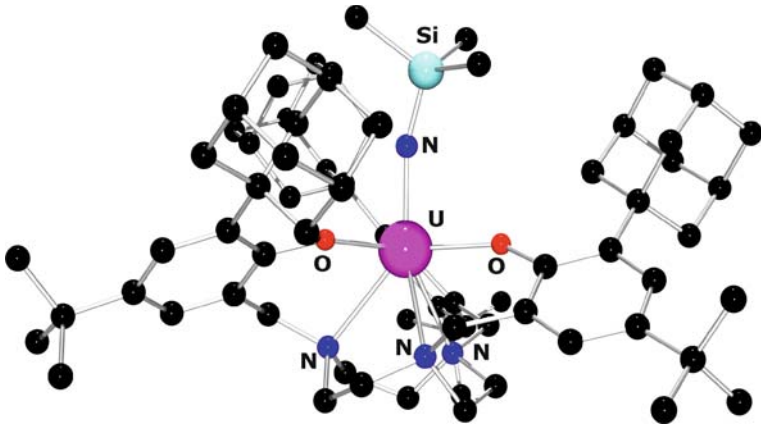

Fig. 20 Molecular structure of [(($^{\mathrm{Ad}}$ArO)$_3$tacn)U$^{\mathrm{V}}$(NSiMe$_3$)]. Hydrogen atoms omitted for clarity

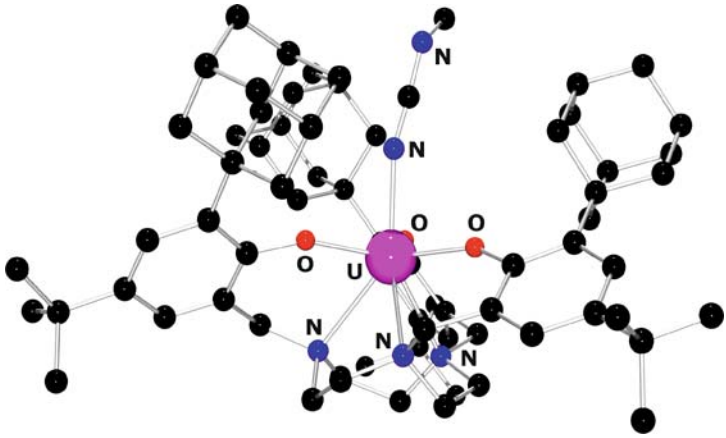

Fig. 21 Molecular structure of [((^{Ad}ArO)$_3$tacn)U(NCNMe)]. Hydrogen atoms omitted for clarity

from linearity (d(U–N(imido)) = 2.1219(18) Å and ∠(U–N–R) = 162.55(12)°). This conformation is most likely due to the steric pressure imparted by the adamantyl groups as they form a narrow cylindrical cavity and prevent the Me_3SiN^{2-} ligand from optimal binding. Accordingly, the imido nitrogen p orbitals cannot participate in efficient M–L π bonding, resulting in the long U–N bond and increased reactivity. Addition of π acids such as carbon monoxide or methyl isocyanide to [((^{Ad}ArO)$_3$tacn)U^{V}(NSiMe$_3$)] resulted in formation of the respective uranium(IV) isocyanate and carbodiimide complexes, [((^{Ad}ArO)$_3$tacn)U(η^1-NCO)] and [((^{Ad}ArO)$_3$tacn)U(η^1-NCNMe)], with loss of Me_6Si_2 (Fig. 21). The respective IR spectra show strong bands at 2185 and 2101 cm^{-1} assigned to the η^1-coordinate isocyanate and carbodiimide ligand. The U–N bond lengths and ∠U–N4–C70 angles were determined to be 2.389(6) Å and 171.2(6)8° for the isocyanate complex and 2.327(3) Å and 161.9(3)8° for the carbodiimide derivative. Magnetic and electronic absorption data are consistent with the uranium(IV) formulation. The UV/vis/NIR spectra of both colorless complexes are similar with various sharp, low-intensity bands (ε = 5–80 M^{-1} cm^{-1}), which are characteristic for spectra of U(IV), f^2 complexes with a $^3H_4$ ground state. This additional reactivity is due to the bend in the imido fragment, which imparts additional nucleophilic character. These transformations are believed to occur through multiple bond metathesis with π acids [27].

4.3 Unprecedented Uranium(IV) Coordination Complexes

The uranium(IV) complex [(C–N–C)UCl$_4$(THF)] with the "pincer" 2,6-bis(imidazolylidene)pyridine [88] ((C–N–C) = 2,6-bis(arylimidazol-2-ylid-

ene)pyridine, aryl = 2,6-$Pr^{i}_{2}C_6H_3$) has been synthesized, and is only the second U(IV) N-heterocyclic carbene complex (Fig. 22). The first is the metallocene-based compound, $[Cp^*_2U(O)(C(MeNCMe)_2)]$ [89]. The uranium in $[(C–N–C)UCl_4(THF)]$ has a distorted seven-coordinate geometry with an approximate C_2 axis passing through the pyridine N atom and the uranium. The U–Cl bond distances range from 2.587 to 2.673 Å. The U–C carbene bond lengths (2.573(5)–2.587(5) Å) are shorter than those observed previously for U(IV) (2.636(9) Å), U(III) (2.672(5)–2.789(14) Å) [45, 75], and U(VI) complexes (2.64 Å) [70]. However, they are *longer* than other known U–C $\sigma(sp^3)$-alkyl bonds (2.405–2.539 Å) [90–92].

The high-yield synthesis and spectroscopic and structural characterization of a dimeric uranium(IV) halide complex $[\{[^t BuNON]UCl_2\}_2]$ supported by the doubly deprotonated diamidosilyl ether ligand $[((CH_3)_3CNH(Si(CH_3)_2))_2O][^t BuNON]_2)$ are reported (Fig. 23) [93]. The $–C(CH_3)_3$ protons are assigned to the singlet at δ 68.9. Two broad upfield peaks at δ –17.7 and –23.8 correspond to the $–Si(CH_3)_2$ groups. The presence of two resonances for the $–Si(CH_3)_2$ substituents is consistent with the dimeric nature of the complex in toluene-d_8. A variable temperature NMR study between 293 and 353 K showed that the two resonances became broader as the temperature increased, coalescing at 353 K. Either the rapid interconversion of the bridging and terminal chlorides or a monomer–dimer equilibrium could yield equivalent ligand silyl methyl moieties. The solid-state structure of the dimer, with partial occupancy of Br for Cl, showed a U–O distance of 2.479(11) Å. The

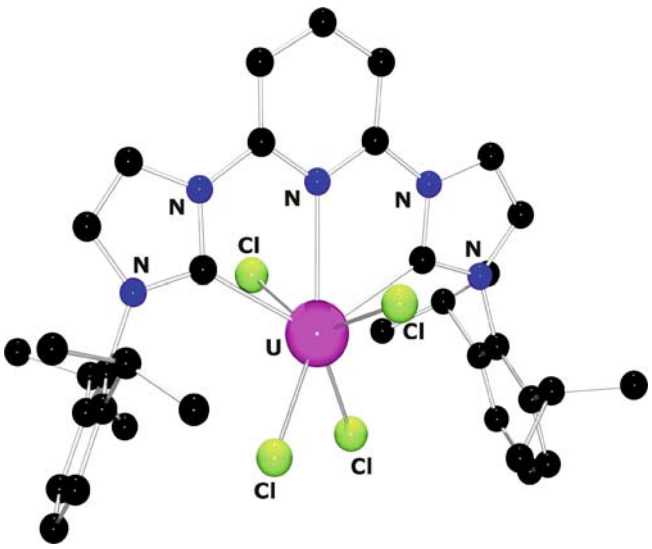

Fig. 22 Molecular structure of $[(C–N–C)UCl_4(THF)]$. Hydrogen atoms and THF omitted for clarity

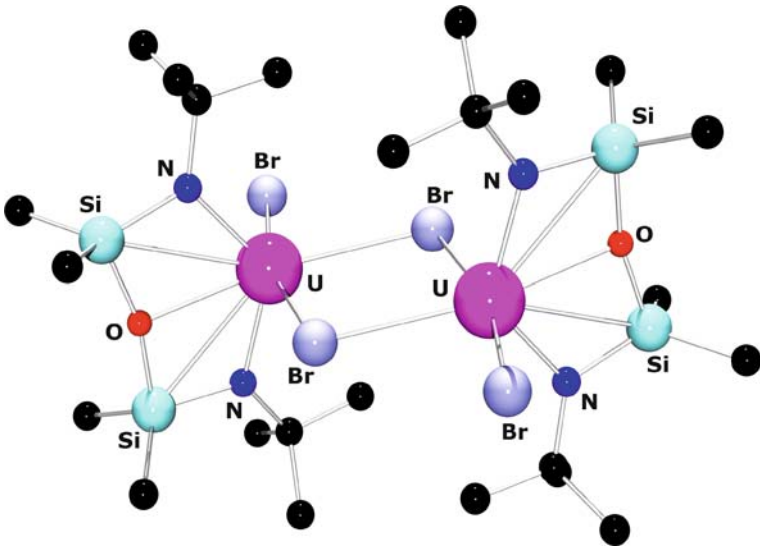

Fig. 23 Molecular structure of $[\{[^t\text{BuNON}]UCl_2\}_2]$. Hydrogen atoms omitted for clarity

U–Br has chloride/bromide disorder in the structure, precluding a meaningful discussion of structural parameters. Variable temperature magnetic data were recorded and produced a μ_{eff} value of 2.63 μB at 300 K which decreases to 0.81 μB at 2 K per uranium center. The author states that the change in μ_{eff} values at low T may be partially attributed to weak antiferromagnetic interactions between the two uranium(IV) centers, mediated by the chloride bridges. However, complexes of U(IV) with $^3H_4$ ground states typically show magnetic moments around 0.5–0.8 μB. Addition of alkylating agents to the halide precursor produced both the η^1-bis(allyl) and bis(alkyl) species. The η^1 coordination mode of the allyl species was confirmed by both the ^{1}H NMR spectrum (294 K), showing broad resonances of δ 29.7 and 11.4 for $CH(CH_2)_2$, as well as the the IR spectrum, which has a stretch at 1617 cm^{-1} typically absent in the η^3-coordinated species. For the bis(alkyl) compound, $[\{^{t\text{Bu}}\text{NON}\}U(CH_2Si(CH_3)_3)_2]$, the ^{1}H NMR spectrum displays sharp resonances which are paramagnetically shifted. The protons on the α carbon are shifted significantly upfield to δ –148.9 due to their proximity to the uranium center.

The first non-metallocene uranium silyl compound, $[(Ar[^t\text{Bu}]N)_3USi(SiMe_3)_3]$ (Ar = 3,5-$C_6H_3Me_2$), has been synthesized using the tris(*N-tert*-butylanilide) ligand scaffold (Fig. 24) [94]. Addition of $(THF)_3LiSi(SiMe_3)_3$ to $[(N[^t\text{Bu}]Ar)_3UI]$ (Ar=3, 5–$C_6H_3Me_2$) (diethyl ether, –100 to 25 °C, 10.5 h) afforded a red solid in ca. 80% yield after filtration, concentration, and recrystallization. Crystallographic and computational studies were performed to elucidate the bonding. This unique uranium silyl compound has a U–Si

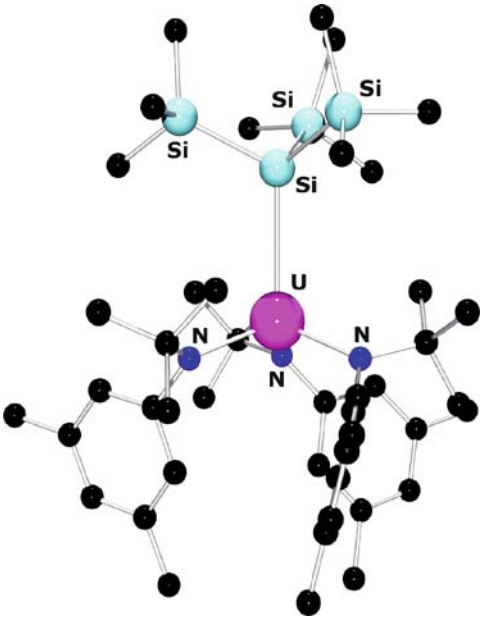

Fig. 24 Molecular structure of $[(Ar[^tBu]N)_3USi(SiMe_3)_3]$. Hydrogen atoms omitted for clarity

bond distance of 3.091(3) Å; however, no other molecular U–Si distances have been reported in the literature for comparison. Geometry optimizations were carried out for the model systems $H_3EU(NH_2)_3$ (E=C, Si, Ge, Sn) with a set of reasonable constraints; calculated U–E distances and bond energies are in accord with experimental data obtained for both $[(Ar[^tBu]N)_3USi(SiMe_3)_3]$ and $[(Ar[^tBu]N)_3UMe]$. There is a slight disparity of the calculated and experimental bond distances for U–Si, which may signify a stressed U–Si contact due to the bending of the $SiMe_3$ groups away from the bulky anilide ligand. The U–N distances (2.210(5) Å) are typical for a uranium(IV) derivative supported by the *N-tert*-butylanilide ligand [30, 95] and compare well with the 2.230 Å calculated value.

Ephritikhine reports the first oxalamidino compound of a 5*f* element. Addition of $\{Li(THF)\}_2(m\text{-}C_2N_4R_4)$ (R=Cy) to UCl_4 produced $[Li(py)_4]_2[(UCl_4(py))_2\{\mu\text{-}C_2N_4R_4\}]$ (R=Cy) [96]. The crystal structure of the dark green pyridine adduct was determined, and revealed a binary axis containing the two uranium atoms, the two central carbon atoms of the diamidinate ligand, and the nitrogen atoms of the coordinated pyridine molecules (Fig. 25). The two $(CyN)_2C$ fragments of the bridging tetradentate ligand are nearly perpendicular to one another, the dihedral angles between the two UN_2C mean planes being 89.9(4) and 88.2(4)° in the two anions, respectively, to minimize the interactions between the cyclohexyl groups. The uranium

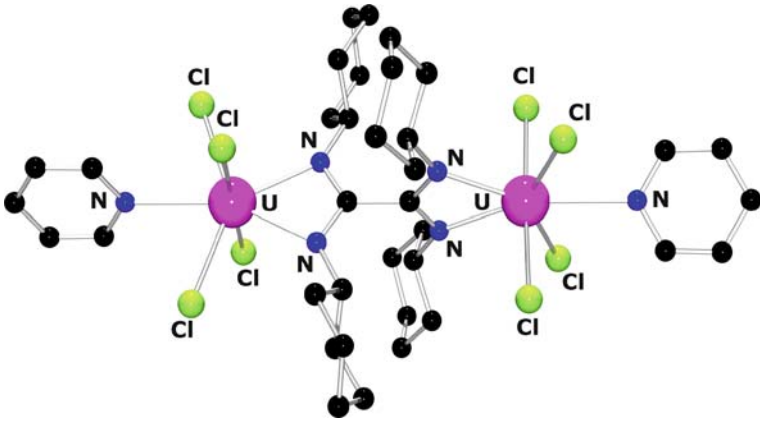

Fig. 25 Molecular structure of $[Li(py)_4]_2[(UCl_4(py))_2\{\mu\text{-}C_2N_4R_4\}]$. Lithium cation and hydrogen atoms omitted for clarity

atoms are seven coordinate in a distorted pentagonal bipyramidal configuration, in which two chlorine atoms and the three nitrogen atoms define the basal plane and the other two chlorine atoms are in apical positions. The U–N(py) and U–Cl bond lengths, which average 2.68(3) and 2.66(2) Å, respectively, are unexceptional for U(IV) complexes and may be compared with those of 2.702(1) and 2.638(4) Å in $[UCl_4(py)_4]$. The mean U–N(oxalamidino) bond length is 2.417(7) Å.

The complex $[U\{N(SiMe_3)_2\}_2\{N(SiMe_3)(SiMe_2CH_2B(C_6F_5)_3)\}]$ is formed by hydrogen evolution in the reaction between the hydride complex $[U(N(SiMe_3)_2)_3(H)]$ and $B(C_6F_5)_3$. The X-ray and neutron structures have been determined and show an electron-deficient uranium center capable of forming multicenter bonds between U and three $Si–CH_2$ units of the amido ligands. The similar complex $[U(C(Ph)(NSiMe_3)_2)_2\{\mu_3\text{-}BH_4\}_2]$ was analyzed as well, and the X-ray structure proves unequivocally the η^3 coordination of the BH_4 moieties. In both single-crystal structure determinations, all hydrogen and deuterium atoms could be located and isotropically refined, including those which are directly coordinated to the uranium (Fig. 26). The ability to locate the hydrogen and deuterium positions in these uranium compounds by single-crystal X-ray diffraction is due to good crystal quality, the measurement of data at low temperature, and the use of image plate technology for data collection [97].

The first organometallic dication of an *f* element was recently reported. Treating $[(COT)U(BH_4)(HMPA)_3][BPh_4]$ with NEt_3HBPh_4 gave $[(COT)U(HMPA)_3][BPh_4]_2$ (HMPA = hexamethylphosphoramide). The crystal structure of the pyridine solvate shows that the dications adopt a three-legged piano-stool configuration in which the O–U–O angles have a mean value of 87(3)°, and the COT–U–O angles centroid of the C_8H_8 ring range between

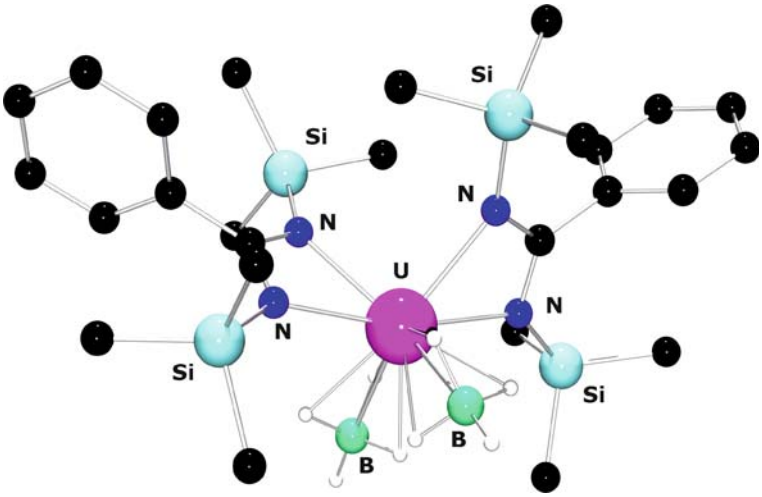

Fig. 26 Molecular structure of $[U(C(Ph)(NSiMe_3)_2)_2\{\mu_3\text{-}BH_4\}_2]$. Hydrogen atoms omitted for clarity

127.2 and 128.7°, averaging 127(1)°. The uranium atom is 1.92(2) Å from the planar cyclooctatetraene ring (within 0.01 Å), and the mean U–C bond distance is 2.65(3) Å (Fig. 27).

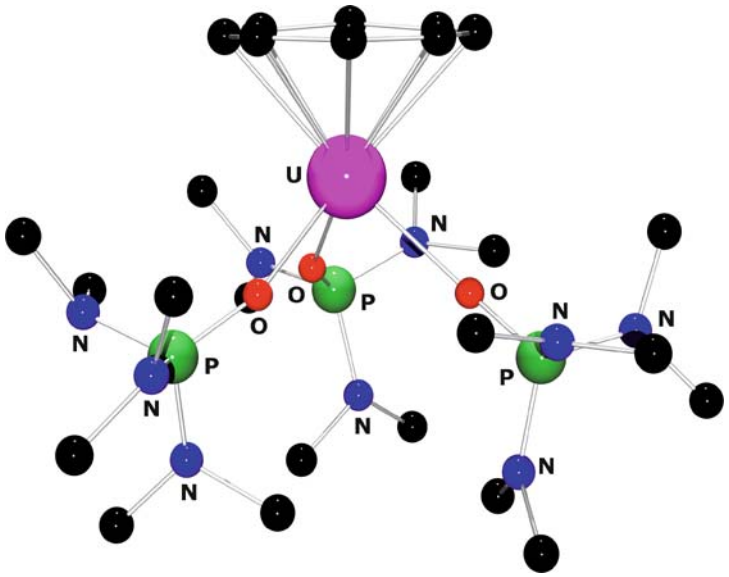

Fig. 27 Molecular structure of the cation of $[(COT)U(HMPA)_3][BPh_4]_2$. Anion and hydrogen atoms omitted for clarity

5
Uranium Coordination Complexes with Chalcogen-Containing Ligands

Although there have been extensive studies of the coordination chemistry of uranium with nitrogen-based ligands, far less work has been done using softer chalcogenide-based ones. Uranium is an ideal choice for reactivity with these elements because of its extreme oxophilicity and high reduction potential. Industrially, these complexes are attractive due to their potential use as nuclear fuels [98]. In addition, sulfur-based ligands are used in nuclear waste management for lanthanide(III)/actinide(III) differentiation [99]. The complexes described here show the variety of oxidation states and coordination environments accessible to these elements.

The first uranium(IV) dithiolene complex, $[Na(18\text{-crown-}6)]_2[(COT)U(dddt)_2]$, was synthesized by treating $[(COT)UX_2(THF)_n]$ (X=BH_4 and n = 0; X = I and n = 2) with $[Na_2(dddt)]$ (dddt = 5,6-dihydro-1,4-dithiin-2,3-dithiolate) (Fig. 28). Analysis of the red crystals revealed an average U–S bond length of 2.7782(6) Å and an *exo–exo* conformation of the two dithiolate ligands. Oxidation with Ag^+ gave the black uranium(V) complex $[Na(18\text{-crown-}6)(THF)][(COT)U(dddt)_2]$, whose crystal structure revealed an *exo–endo* conformation of the dddt ligands and a mean U–S distance of 2.693(5) Å (Fig. 28) [100, 101]. The uranium center has a distorted square pyramidal geometry and lies 1.286(1) Å above the basal plane formed by the four S atoms. The C–S (average 1.75(1) Å) and C=C (1.357(9) and 1.363(9) Å) distances indicate that there is little electron delocalization on the dithiolene ligands. The unsolvated derivative, $[Na(18\text{-crown-}6)][(COT)U(dddt)_2]$, was also prepared, and assigned as uranium(V) based on its characteristic dark purple color.

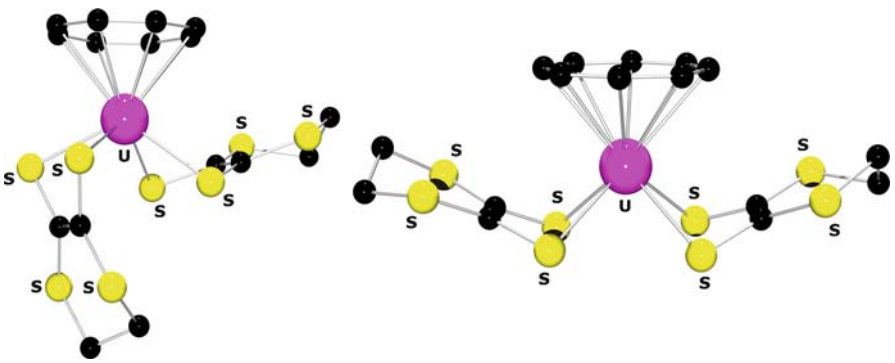

Fig. 28 Molecular structures of the anions of $[Na(18\text{-crown-}6)(THF)][(COT)U^{V}(dddt)_2]$ (*left*) and $[Na(18\text{-crown-}6)]_2[(COT)U^{IV}(dddt)_2]$ (*right*). Cations and hydrogen atoms omitted for clarity

The difference in the ligand conformation between the U(V) and the U(IV) ddt derivatives was explored extensively by DFT, which confirmed that the oxidation state was responsible for the difference in the conformation of the ligand [101]. The calculations also confirm a significant U–(C=C) interaction between the metal center and the C=C bond of the *endo* dithiolene ligand in the uranium(V) complex, which does not exist in the dianionic uranium(IV) species. A metal *f* ligand back-donation occurs in both complexes from the partially occupied uranium 5*f* orbitals toward the vacant π^*(C=C) antibonding MO of the dithiolene ligand, which becomes partially occupied after interaction.

Subsequent to this initial report, the neutral derivative of [Na(18-crown-6)]$_2$[(COT)U(dddt)$_2$] was synthesized by reaction of dddtCO with the same starting material to produce the green [(COT)U(dddt)$_2$] dimer. A similar black derivative, [(COT)U(dmio)]$_2$ (dmio = 1,3-dithiole-2-one-4,5-dithiolate), was also synthesized and decarboxylated by $BH_3{}^*Me_2S$ to produce the neutral [(COT)U(mdt)]$_2$ (mdt = 1,3-dithiole-4,5-dithiolate). This complex (Fig. 29) as well as its pyridine derivative (Fig. 30) were crystallographically characterized [102]. The parent complex, [(COT)U(mdt)]$_2$, exists as an unsymmetric dimer, where the U–S bond lengths of 2.810(2) and 2.816(2) Å are 0.13 Å shorter than those on the other side of the dimer. Also, the $S_2C_2S_2$ core of the mdt ligand is outside the bisecting plane of U–U and forms a dihedral angle of 60°. This deviation corresponds to a folding of the US_2C_2 ring by 81.9(2)° along the S–S axis, bringing the C–C atoms in proximity to the uranium atom, and causes the deviation of the $U_2S_4C_4$ core from D_{2h} symmetry. The U–C bond lengths are 2.950(8) and 2.948(8) Å, but the C=C fragment shows no

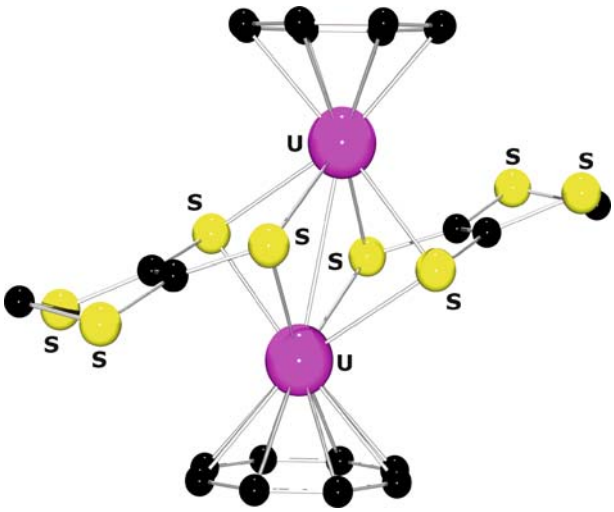

Fig. 29 Molecular structure of [(COT)U(mdt)]$_2$. Hydrogen atoms omitted for clarity

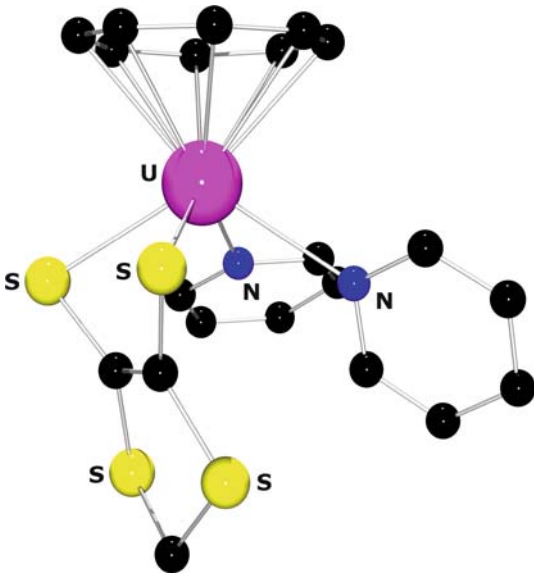

Fig. 30 Molecular structure of [(COT)U(mdt)(py)$_2$]. Hydrogen atoms omitted for clarity

elongation from reduction with the uranium center. The molecular structure of the pyridine derivative, [(COT)U(mdt)(py)$_2$], displayed a monomer with an η^4 coordination mode of the mdt ligand. The U–S distances of 2.720(3) and 2.751(3) Å are ca. 0.08 Å shorter than in the parent dimer. The interaction of the C=C bond and the uranium center is observed in the pyridine adduct as well. The U–C distances are 2.89(1) and 2.97(1) Å. The folding dihedral angle of the mdt group (75.6(3)°) is also similar to the parent, but in this case the dithiolene ligand has an *endo* conformation. The solvated derivative shows fluxional behavior by ^{1}H NMR spectroscopy.

The first tris- and tetrakis(dithiolene) complexes have also been synthesized and characterized [103]. Treating UCl_4 with 3 or 4 mol equiv of Na_2dddt (dddt = 5,6-dihydro-1,4-dithiin-2,3-dithiolate) in THF afforded the first example of a homoleptic tetrakis(dithiolene) metal compound, [Na_4(THF)$_8$U(dddt)$_4$] (Fig. 31). The complex was characterized by a singlet at δ 5.98 (pyridine-d_6) in the ^{1}H NMR spectrum, consistent with magnetically equivalent dddt ligands due to rapid exchange of the dithiolene ligands and sodium ions on the NMR timescale. Red crystals of [Na_4(THF)$_8$U(dddt)$_4$] were grown in THF, and X-ray diffraction analysis revealed that the crystals are composed of infinite chains in which each U(dddt)$_4$ unit is surrounded by four Na atoms, two of those being involved in bridging Na_2(μ-THF)$_3$ fragments; the uranium atom is eight coordinate and has a dodecahedral geometry. The U–S distances vary from 2.7900(19) to 2.8654(18) Å, with an average value of 2.83(3) Å. Treatment of UCl_4 with 3 mol equiv of

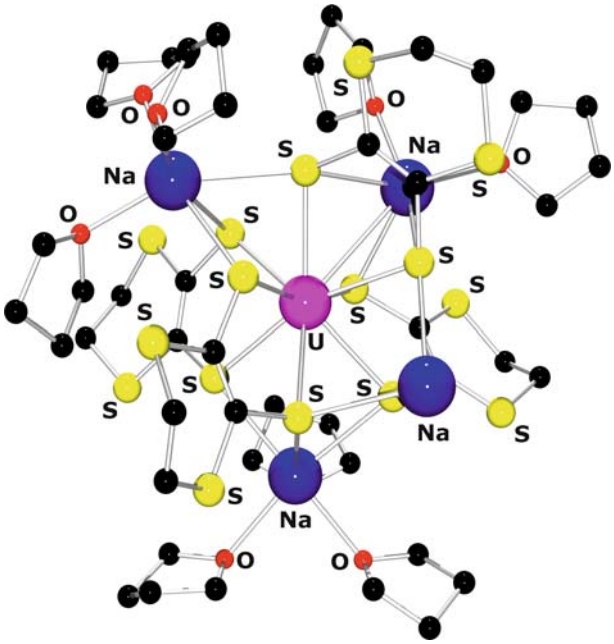

Fig. 31 Molecular structure of $[Na_4(THF)_8U(dddt)_4]$. Hydrogen atoms omitted for clarity

Na_2dddt in pyridine gave a mixture of tris- and tetrakis(dithiolene) compounds. Analysis by ^{1}H NMR spectroscopy of a pyridine solution showed the tris(dithiolene) compound, $[Na_2(py)_xU(dddt)_3]$, as a resonance at δ –2.84. After addition of 18-crown-6, only the tris(dithiolene) complex was obtained as orange crystals of $[Na(18\text{-crown-6})(py)_2]_2[U(dddt)_3] \cdot 2py$, in which the isolated $[U(dddt)_3]^{2-}$ anion adopts a slightly distorted trigonal prismatic configuration. A few red crystals of the trinuclear anionic compound $[Na(18\text{-crown-6})(py)_2]_3[Na\{U(dddt)_3\}_2]$ were also obtained. Both tris(dithiolene) compounds exhibit large folding of the dddt ligand and significant interaction between the C=C double bond and the metal center.

The first neutral uranium thiolate compounds have also been studied [104]. Reaction of $[U(NEt_2)_4]$ with HS-2,4,6-^{t}Bu$_3$C$_6$H$_2$ (HSMes*) afforded $[(SMes^*)_3U(NEt_2)(py)]$, while similar treatment of $[U(N(SiMe_3)SiMe_2CH_2)(N(SiMe_3)_2)_2]$ produced $[(SMes^*)U(N(SiMe_3)_2)_3]$. The solid-state structure of $[(SMes^*)_3U(NEt_2)(py)]$ revealed a distorted trigonal bipyramidal configuration where the uranium atom lies 0.3549(7) Å from the basal plane of the three sulfur atoms with an average U–S distance of 2.695(18) Å (Fig. 32). This molecule features a U–H–C β agostic interaction from the coordinated amide. The molecular structure of red crystals of $[(SMes^*)U(N(SiMe_3)_2)_3]$ show U–S distances of 2.6596(8) and 2.696(3) Å. In this case, there is a γ U–H–C interaction from one of the methyls of the trimethylsilyl substitutent. Homoleptic

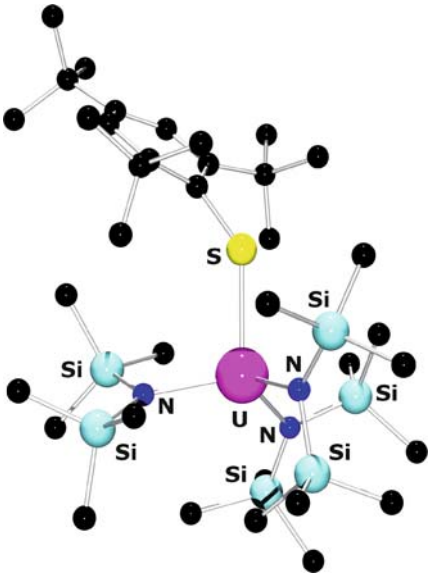

Fig. 32 Molecular structure of $[(SMes^*)U(N(SiMe_3)_2)_3]$. Hydrogen atoms omitted for clarity

$[U(SMes^*)_4]$ can be isolated from the reaction of $[U(BH_4)_4]$ and KSMes* as a black powder. In the molecular structure, the U–S distances of 2.6173(9) and 2.6294(9) Å are similar to those previously observed. There is an agostic interaction between the C–H bond of one of the *tert*-butyl groups and the metal center. The first homoleptic thiolate complex of uranium(III), $[U(SMes^*)_3]$, was synthesized by protonolysis of $[U(N(SiMe_3)_2)_3]$ with HSMes* in cyclohexane to produce dark brown crystals. The crystal structure exhibits the novel η^3 ligation mode for the arylthiolate ligand, and an average U–S distance of 2.720(5) Å. The distance between the trigonal pyramidal uranium and the carbon atoms involved in the U–H–C agostic interaction of each thiolate ligand is shorter, by ~0.05 Å, than that expected from a purely ionic bonding model. DFT reveals that the nature of the U–S bond is ionic and strongly polarized at the sulfur for uranium. The strength of the U–H–C agostic interaction is believed to be controlled by the maximization of the interaction between $U\delta^+$ and $S\delta^-$ under steric constraints. The η^3 ligation mode of the arylthiolate ligand is also obtained from DFT.

The uranium–chalcogenide complexes, $U[N(EPPh_2)_2]_3$ (E=S or Se), were synthesized by treating $[U(N(SiMe_3)_2)_3]$ with three equivalents of the neutral ligand $NH(EPPh_2)_2$ (5) [105]. The electronic absorption spectra of both complexes were acquired as benzene solutions, and display U(III) Laporte-forbidden $5f$–$5f$ transitions with weak absorption bands (750–1300 nm) in the near-IR region and more intense bands (550–700 nm) in the visible region, assigned as Laporte-allowed $5f$–$6d$ transitions [10]. An intense charge-

transfer band can be found below 400 nm. Analysis by infrared spectroscopy shows P–E vibrations at 593 cm^{-1} (E=S) and 536 cm^{-1} (E=Se). Both are lower in energy than the corresponding free ligands, indicating deprotonation and coordination to the uranium center. The structures of both complexes were determined by X-ray diffraction, and showed a nine-coordinate U(III) center in a distorted tricapped trigonal prismatic coordination environment. Each uranium is bound to three $[N(EPPh_2)_2]_2$ anions. In the sulfur compound, the U–S distance is 2.9956(5) Å, the U–N distance is 2.632(2) Å, the S–U–S bite angle is 122.82(2)°, and the P–N–P angle is 147.43(16)°. The U–Se distance in the selenium compound is 3.0869(4) Å, the U–N distance is 2.701(3) Å, the Se–U–Se bite angle is 124.594(12)°, and the P–N–P angle is 144.5(2)°. Because of the steric demands of the ligand, only three molecules fit around the uranium center, dictating the trivalent oxidation state.

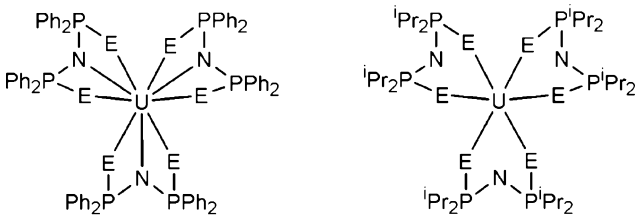

(5)

The tellurium analogues of these ligands have been prepared in a similar manner, but use stabilizing ^{i}Pr substitutents instead of phenyl groups. Treating $[UI_3(py)_4]$ with three equivalents of $[Na(tmeda)\{N(TeP^{i}Pr_2)_2\}]$ produced $[U(N(TeP^{i}Pr_2)_2\text{-}Te,Te')_3]$ as a blue-gray solid (Fig. 33) [106]. Unlike the sulfur and selenium analogues, in the case of the tellurium ligand the central nitrogen atom of the ring is not coordinated (U–N: ~5 Å), creating a six-coordinate U(III) center in a distorted trigonal prism. This dichotomy in ligand coordination is attributed to the increased steric demand of the ^{i}Pr substituents and the larger size of the tellurium atom. The average U–Te distance is 3.164(2) Å and the average Te–U–Te bite angle is 91.01(3)8°. The UV/vis/NIR spectrum displays absorption bands between 480 and 1300 nm (ε = 380–1269 M^{-1} cm^{-1}) due to Laporte-forbidden 5*f*–5*f* transitions and allowed 5*f*–6*d* transitions.

Treatment of uranium metal with PhEEPh (E=S, Se) in the presence of a catalytic amount of iodine in pyridine affords the monomeric, seven-coordinate U(IV) chalcogenolates, $[U(EPh)_4(py)_3]$, which do not require stabilizing ancillary ligands [107]. Crystallographic characterization of the sulfur derivative showed a distorted pentagonal bipyramidal uranium center, an average U–S distance of 2.734(3) Å, and an average U–N distance of 2.597(9) Å. Spectroscopic comparison of the sulfur and selenium com-

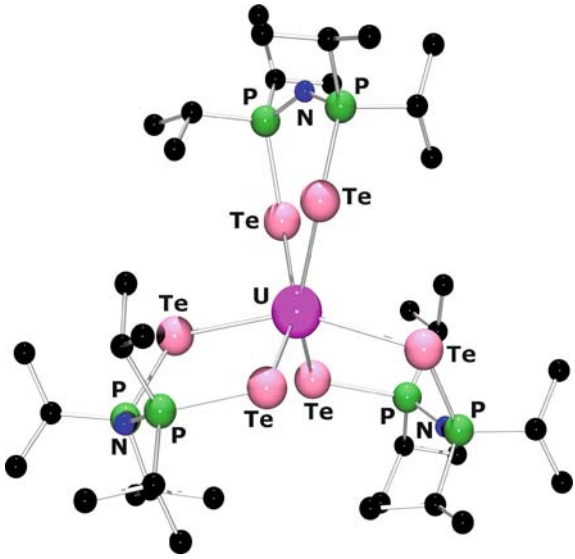

Fig. 33 Molecular structure of $[U(N(TeP^iPr_2)_2\text{-}Te,Te')_3]$. Hydrogen atoms omitted for clarity

pounds suggests that the selenium compound is of similar structure. The dimeric eight-coordinate complexes $[U(EPh)_2(\mu_2\text{-}EPh)_2(CH_3CN)_2]_2$ are obtained by crystallization from solutions of the pyridine complexes dissolved in acetonitrile (Fig. 34). For these complexes, the molecular structures show a uranium center in a triangular dodecahedral geometry. For the sulfur derivative, the U–η^1S distance is 2.813(2) Å while the U–η^2S distances of 2.9378(19) and 2.8667(19) Å are longer. The selenium analogue had a U–η^1Se distance of 2.8491(12) Å and longer U–η^2Se distances of 3.0564(10) and 2.9935(11) Å. Oxidation of U(0) by pySSpy ($C_5H_5NSSC_5H_5N$) and crystallization produced a nine-coordinate compound, $U(Spy)_4(THF)$, as a distorted tricapped trigonal prism, which had average U–S and U–N distances of 2.8299(16) and 2.540(4) Å, respectively. Formation of the distorted cubane cluster $[U(py)_2(SePh)(\mu_3\text{-}Se)(\mu_2\text{-}SePh)]_4 \cdot 4py$ by addition of elemental selenium and diphenyldiselenide produced complexes in which each U(IV) ion is eight-coordinate and the U_4Se_4 core. In this structure, the U–η^1SePh distance is 2.9267(10) Å, the average U–η^2SePh distance is 3.0614(14) Å, the average U–Se^{2-} distance is 2.8681(15) Å, and the average U–N distance is 2.619(10) Å. The electronic absorption spectra of $[U(EPh)_4(py)_3]$, $[U(Spy)_4(THF)]$, and $[U(py)_2(SePh)(\mu_3\text{-}Se)(\mu_2\text{-}SePh)]_4 \cdot 4py$ display bands arising from f–f and f–d transitions. Distinctive bands appear in pyridine between 685 and 687 nm and 1165 and 1170 nm for $[U(EPh)_4(py)_3]$ and $[U(py)_2(SePh)(\mu_3\text{-}Se)(\mu_2\text{-}SePh)]_4 \cdot 4py$ which are indicative of U(IV). The UV/vis/NIR spectrum of $[U(Spy)_4(THF)]$ in benzene has absorptions at 699,

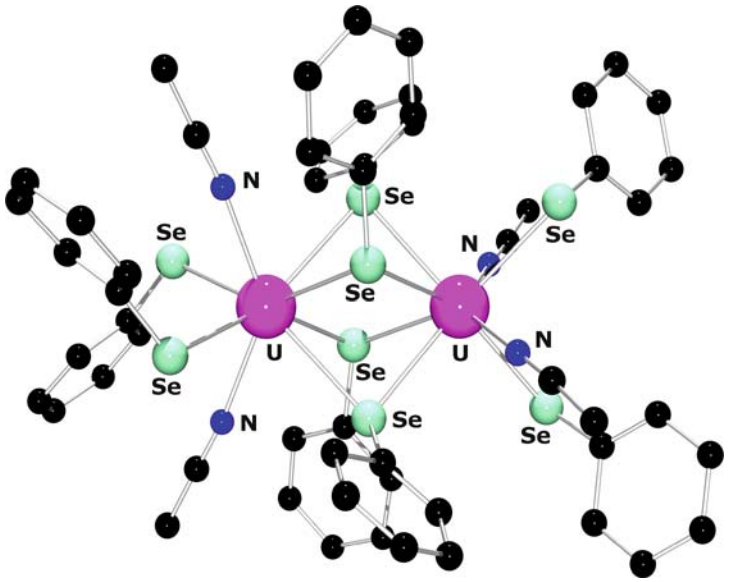

Fig. 34 Molecular structure of $[U(SePh)_2(\mu_2\text{-}SePh)_2(CH_3CN)_2]_2$. Hydrogen atoms omitted for clarity

1130, and 1215 nm. The poor solubility of $[U(EPh)_2(\mu_2\text{-}EPh)_2(CH_3CN)_2]_2$ precluded analysis in benzene, but a UV/vis/NIR spectrum of the compound generated in situ revealed characteristic absorbances at 687 and 1125 nm. All of these complexes also show intense charge-transfer bands below 500 nm. No extinction coefficients were reported.

The first example of a homoleptic actinide complex containing three-membered rings is a thermally stable η^2-sulfenamido complex of uranium, $[U(\eta^2\text{-}^t\text{BuNSPh})_4]$ [108] (Fig. 35). This complex was synthesized by a salt metathesis reaction of $LiN(^t\text{Bu})SPh$ with UCl_4/PMe_3 and isolated as air-sensitive yellow-brown crystals that produce a paramagnetically shifted and broadened ^{1}H NMR spectrum. A diagram of the possible resonance structures for the η^2 forms **A** (sulfenamide) and **B** (iminosulfide, *N*-alkylsulfidimino) is presented below. The molecular structure was determined by X-ray diffraction and confirms the η^2 bonding mode to the uranium center, similar to the bonding of the sulfenamido ligand with the early transition metals Ti, Zr, Mo, and W [109]. The average U–N distance is 2.30 Å and U–S distance is 2.87 Å, similar to the previously discussed chalcogenide compounds.

Reaction of UX_4 (X=Cl, BH_4) and two equivalents of $[Li(Et_2O)][SPS^{Me}]$, the lithium salt of an anionic SPS pincer ligand composed of a central hypervalent λ_4-phosphinine ring bearing two *ortho*-positioned diphenylphosphine sulfide side arms, formed complexes of the type $[UX_2(SPS^{Me})_2]$ (Fig. 36). Crystals of the chloride derivative were obtained as the pyridine adduct, and

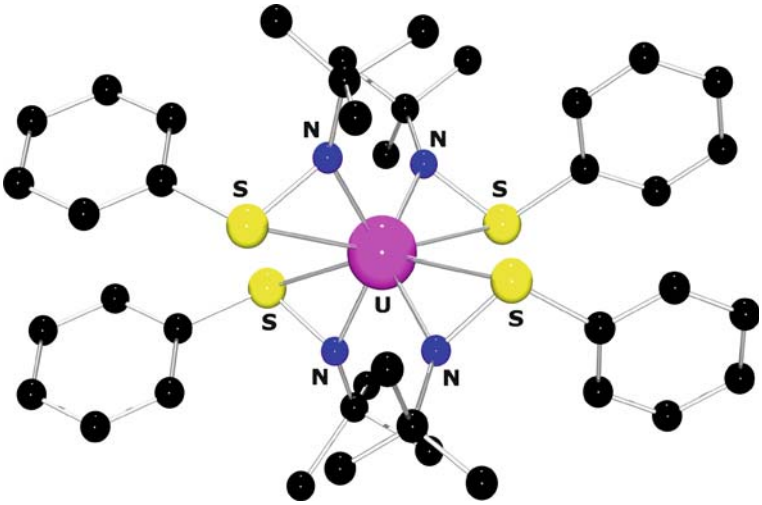

Fig. 35 Molecular structure of $[U(\eta^2\text{-}^t\text{BuNSPh})_4]$. Hydrogen atoms omitted for clarity

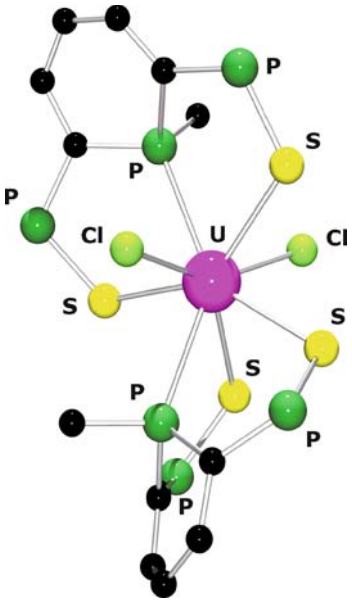

Fig. 36 Molecular structure of $[UCl_2(SPS^{Me})_2]$. Phenyl substituents and hydrogen atoms omitted for clarity

the molecular structure reveals an eight-coordinate uranium in a distorted dodecahedral configuration. The flexible tridentate $[SPS^{Me}]^-$ anion is bound to the metal as a tertiary phosphine with electronic delocalization within the

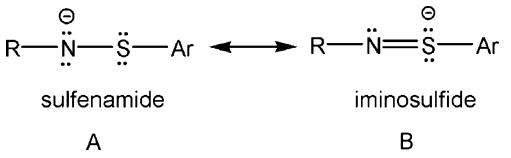

(6)

unsaturated parts of the ligand [99]. The U–S distances vary from 2.7799(10) to 2.9892(12) Å with an average value of 2.88(8) Å. The two U–P distances are 2.9508(11) and 3.0001(12) Å. The SPS^{Me} ligand can adopt two geometric forms based on the resonance structures presented, where **A** adopts a facial coordination mode and **B** is coordinated in a planar fashion. The uranium derivative coordinates one of each type of ligand.

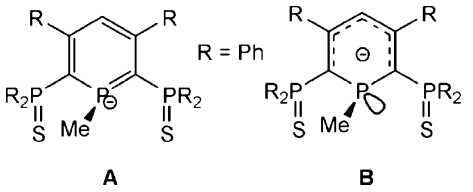

(7)

For ligand **B**, the relatively large P–C bonds in the central ring show that the ligand lost the ylidic structure of the phosphinine upon coordination to the uranium, while the relatively shorter external P–C bonds (P to C in ring) and the longer P–S bonds are consistent with delocalization of electron density in unsaturated parts of the ligand. The variations observed with the neutral SPS species **A** result from the presence of the anionic charge.

6 Multimetallic Systems of Uranium

Over the last 10–12 years, the growth in uranium coordination complexes has included expansion into the field of multimetallic systems. These complexes offer the potential for a molecule with unique magnetic properties, such as magnetic superexchange, since both a *d* and *f* element are held in proximity by a bridging organic ligand framework which provides the magnetic exchange pathway.

One proven way to create these multimetallic molecules is to start with a transition metal (M=Co, Ni, Cu, Zn) salen complex that contains a pendant hydroxyl group in the *ortho* phenyl position [110–113]. This complex is then treated with one/two equivalents of $[U(acac)_4]$ in the presence of pyridine to form the desired mixed metal complexes of the form $[\{LM^{II}(py)_2\}U^{IV}]$ (L = the hexadentate compartmental ligand *N*,*N*′-bis(3-hydroxysalicylidene)-

2,2-dimethyl-1,3-propanediamine) with pyridine also coordinated. Characterization of the red cobalt derivative by X-ray crystallography revealed a dodecahedral uranium center coordinated by eight oxygen atoms (Fig. 37). The nickel and zinc compounds are isostructural. The cobalt ion has a square pyramidal geometry, and is removed slightly from the N_2O_2 plane by 0.38(2) Å. The Co–U–Co angle is near linear, at 171.84(2)°. This family of compounds is the first reported to contain a linear arrangement of three metal atoms.

The copper derivative shows remarkable magnetic properties, in that the orbitals of the uranium(IV) center are able to mediate ferromagnetic coupling between the copper atoms. The $d(x^2 - y^2)$ orbitals of the copper ions are coupled through the $f(x(y^2 - z^2))$ and $f(y(x^2 - z^2))$ of the uranium center. Two possibilities for this triplet state are the presence of two degenerate molecular orbitals which contain two unpaired electrons from copper, or the transfer of an unpaired Cu^{II} electron toward an empty $5f$ orbital of uranium, forcing the d and f electrons to align in a parallel arrangement. The magnetic susceptibility ($\chi_M T$) of this complex is 1.7 $cm^3\ Kmol^{-1}$ between 300 and 100 K, which then decreases to 0.8 $cm^3\ Kmol^{-1}$ at 2 K. Analogues of this compound, LCu_2Zr and LCu_2Th, were synthesized, and showed magnetic moments of $\chi_M T = 0.77\ cm^3\ Kmol^{-1}$ over the temperature range, consistent with two noninteracting copper centers, confirming that this ferromagnetic coupling is due to the presence of the uranium center. Due to the lack of coupling of a similar Th derivative, the initial hypothesis about coupling through an empty f or-

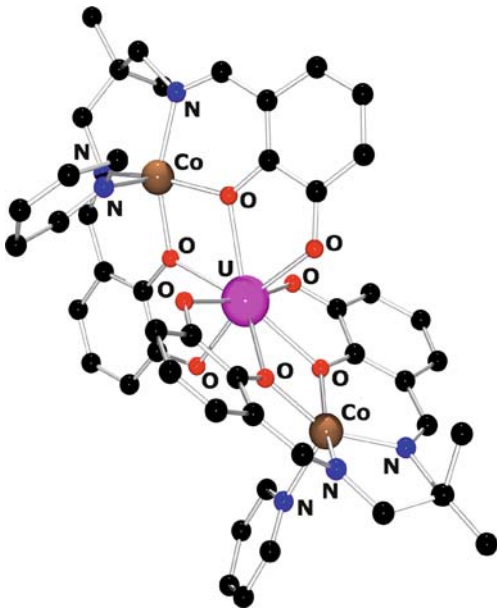

Fig. 37 Molecular structure of $[LCo^{II}(py)_2U^{IV}]$. Hydrogen atoms omitted for clarity

bital is disproved. Thus, the conclusion is drawn that the observed coupling is between the 3*d* unpaired Cu electron and the U 5*f* electrons. At low *T*, the uranium(IV) becomes diamagnetic, so the copper species are magnetically isolated from one another. The nickel analogue, Ni_2U, displays antiferromagnetic coupling, with $\chi_M T = 2\ cm^3\ Kmol^{-1}$, consistent with two Ni^{2+} centers. Subsequent to these findings, the diimino chain length and functionality were varied to determine how the coupling of the copper centers is affected by changing the distance between the copper and uranium atoms. For complexes with short Cu–U distances, antiferromagnetic coupling is reported. However, the authors state that ferromagnetic coupling is observed in those complexes that have a long Cu–U interaction, and no interaction between the copper centers is noted [113].

The polydentate monoanionic $[Zr_2(O^iPr)_9]^-$ (dzni) produces arene-soluble, mixed-metal Zr/U complexes achieved by treating $K[Zr_2(O^iPr)_9]$ with $[UI_3(THF)_4]$, forming $[Zr_2(O^iPr)_9][UI_2(THF)]$ in high yields (Fig. 38) [114]. The ^1H NMR spectrum in C_6D_6 displays five chemical shifts in a 2 : 2 : 2 : 2 : 1 ratio assigned as the methyl groups of the isopropoxide ligands. Only four of the five expected methane resonances were visible. No fluxionality in this molecule was detected, even at 110 °C. The cyclic voltammogram of $[Zr_2(O^iPr)_9][UI_2(THF)]$ recorded in THF displays an irreversible oxidation wave at –0.8 V. Electronic absorption spectroscopy of this complex was performed, and showed strong absorption bands at 436, 501, 612, and 644 nm (ε = 600–900 $M^{-1}\ cm^{-1}$). The NIR region appeared similar to

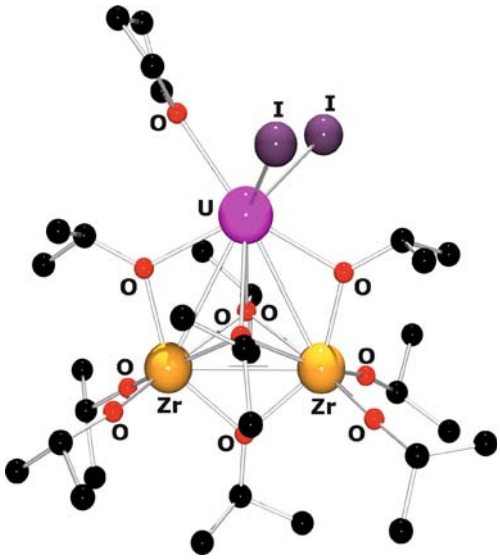

Fig. 38 Molecular structure of $[Zr_2(O^iPr)_9][UI_2(THF)]$. Hydrogen atoms omitted for clarity

$[UI_3(THF)_4]$, showing Laporte-forbidden f–f transitions. The integrity of the $[\{Zr_2(O^iPr)_9\}U]^{2+}$ unit was examined by the reaction with $K_2C_8H_8$ which produces the organometallic complex $[Zr_2(O^iPr)_9][U(C_8H_8)]$. ^{1}H NMR again showed the expected pattern for the methyl groups of the isopropoxide ligands, as well as a resonace at δ –39.8 ppm for the $C_8H_8^{2-}$ ligand. This molecule is fluxional on the NMR timescale. The two isopropyl signals in the ^{1}H NMR spectrum coalesce at 55 °C. In addition, the ^{1}H NMR shifts are temperature dependent, and linear with respect to T_{-1}. Analysis by electrochemistry revealed an irreversible oxidation at –1.5 V. Absorption bands were observed at 447 nm (ε = 950 M^{-1} cm^{-1}) and between 540 and 830 nm (ε = 300–420 M^{-1} cm^{-1}). The NIR region had bands that were more intense and shifted compared to the starting complex. Both of these complexes contain the $[Zr_2(O^iPr)_9]^-$ unit, which coordinates to U(III) as a tetradentate ligand via two triply bridging and two double bridging isopropoxide oxygen atoms. The reaction of $K[Zr_2(O^iPr)_9]$ with UCl_4 did not form U(IV)-dzni complexes, and only the ligand exchange product, $[UCl_2(O^iPr)_2(dme)]_2$ was isolated [114].

The first tris(1,1′-ferrocenylene) metal compound and the sole homoleptic metal-bridged [1]ferrocenophane was recently reported and crystallographically characterized [115]. Reaction of UCl_4 with $Li_2fc \cdot tmeda$ (fc = 1,1′-ferrocenylene, tmeda = tetramethylethylenediamine) gave the tris(1,1′-ferrocenylene) uranium complex $[Li_2(py)_3U(fc)_3]$ (py = pyridine) (Fig. 39). The ^{1}H NMR spectrum has two signals of equal intensity at δ –10.8 and –28.5 assigned as the equivalent protons at the α and β positions of the cyclopentadienyl rings; the most shifted resonance corresponds to the α protons due to the proximity to the paramagnetic uranium center. X-ray analysis

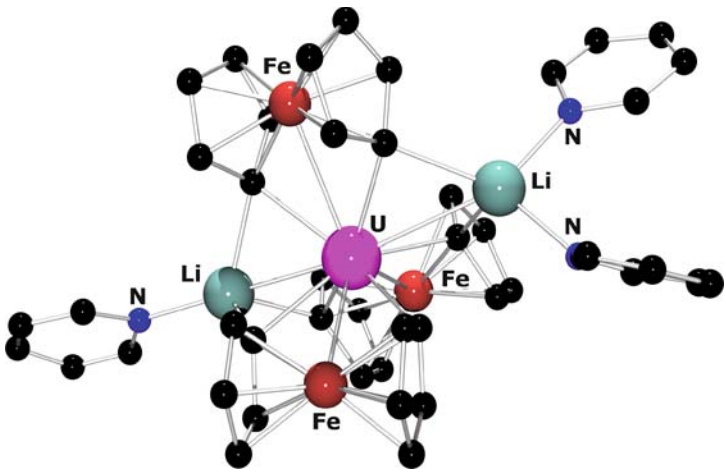

Fig. 39 Molecular structure of $[Li_2(py)_3U(fc)_3]$. Hydrogen atoms omitted for clarity

revealed the propeller type structure of the $[U(fc)_3]$ fragment, with three ferrocenyl units around the uranium center. The planar cyclopentadienyl rings of each fc group are parallel and with U–C and U–Fe bond distances of 2.52(7) and 3.14(2) Å, respectively [115]. The lack of strain between the fc units is responsible for the stability of this molecule. The distances between the U and Fe atoms range from 3.122(2) to 3.165(2) Å (with an average of 3.14(2) Å), consistent with the sum of the atomic radii of 3.15 Å. There are direct U–Fe and U–Li interactions.

Oxidation of a uranium(IV) bis(1,1′-diamidoferrocene) complex produces a mixed-valent bisferrocene complex in which uranium mediates the electronic communication [116]. Treating $[UI_3(THF)_4]$ with $[K_2(OEt_2)_2]fc[NSi\text{-}(t\text{-}Bu)Me_2]_2$ in diethyl ether or toluene led to $[U(fc[NSi(t\text{-}Bu)Me_2]_2)_2]$. A similar trimethylsilyl derivative, $[U(fc[NSiMe_3]_2)_2]$ was also synthesized (Fig. 40). The cyclic voltammogram (CV) of the free *tert*-butyl ligand shows one reversible redox process, at –0.60 V vs $Cp_2Fe^{+/0}$, consistent with the oxidation of Fe(II) to Fe(III). The corresponding uranium compound shows an irreversible reduction, one quasireversible, and two reversible redox processes at –3.26 (ligand-based reduction), –2.54 (U(IV)/U(III) reduction), –0.69 (Fe(II)/Fe(III) oxidation), and 0.56 V (Fe(II)/Fe(III) oxidation) vs $FeCp_2^{+/0}$, respectively. These data support electronic communication between the two iron centers. The low room temperature magnetic moment of 2.50 μB is attributed to an iron–uranium interaction due to orbital overlap. The NIR spectrum of this

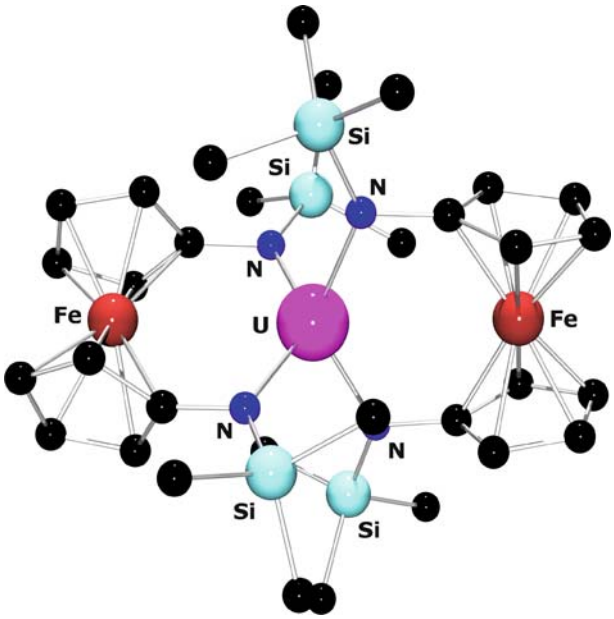

Fig. 40 Molecular structure of $[U(fc[NSiMe_3]_2)_2]$. Hydrogen atoms omitted for clarity

compound displays weak bands consistent with f–f transitions. Chemical oxidation of this compound produced $[U(fc[NSi(t\text{-}Bu)Me_2]_2)_2][BPh_4]$, which reportedly has a similar molecular structure to the starting material. Variable temperature magnetization studies produced a magnetic moment of 2.70 μB at 4 K, which increases to 3.01 μB at 40 K and back down to 2.61 μB at room temperature. The low magnetic moments for the uranium compound are partly due to quenching of the orbital angular momentum. Analysis by EPR spectroscopy reveals that the electron is delocalized over the iron centers. Electronic absorption spectroscopy reveals NIR bands with $\varepsilon \sim 103\ M^{-1}\ cm^{-1}$, consistent with an intervalence charge-transfer transition. The IR spectrum shows two bands indicating that both ferrocene and ferrocenium centers are present [116].

7 Recent Highlights and Perspectives

Because of its large size and accessibility to multiple oxidation states, uranium is capable of unprecedented reactivity and beautiful coordination complexes that cannot be achieved with transition metals or lanthanides. The exciting products highlighted here demonstrate that we have only just begun to learn the capabilities of uranium, and that continuous studies will be needed to determine the full realm of possibilities. From activation of small molecules to unique magnetic properties, uranium offers a synthetic and spectroscopic challenge to coordination chemists of the future.

The first actinide dinitrogen complex was reported in 1998 [117]. Exposure of a benzene-d_6 solution of the trivalent complex $[U(NN'_3)]$ to 1 atm of dinitrogen produced the C_3 symmetric product $[(U(NN'_3))_2\{\mu_2,\eta^2,\eta^2\text{-}N_2\}]$. Analysis of the dark red crystals by X-ray diffraction revealed a side-on bridging mode with trigonal monopyramidal uranium centers that are situated out of the planes of the three ligand amido nitrogen atoms by approximately 0.84 Å (Fig. 41). The N–N bond length of 1.109(7) Å is essentially that of free dinitrogen (1.0975 Å) indicating no activation. The $^{14}N_2$ and $^{15}N_2$ isotopomers have superimposable IR spectra, and the UV/visible electronic absorption spectrum has intense broad bands typical of trivalent uranium complexes [10]. The solution magnetic moment is 3.22 μB (Evans) per uranium atom between 218 and 293 K. It is believed that the preference for side-on over end-on bonding is due to the dinitrogen π_p orbital, which is a better σ donor than the σ_p to trivalent uranium. This dinitrogen binding is reversible as the dinitrogen fragment can be removed during freeze–thaw degassing.

Soon after this initial report, a heteronuclear U–Mo dinitrogen compound was reported by Cummins [30]. A 1 : 1 mixture of $[(N[R]Ar)_3U(THF)]$ (R=*t*–Bu) and $[Mo(N[t\text{–}Bu]Ph)_3]$ in toluene under N_2 (1 atm) afforded the end-on orange $U(\mu_2,\eta^1,\eta^1\text{-}N_2)Mo$ complex. A proposed hypothesis for the observed result is that the putative dinitrogen complex [(N[*t*-

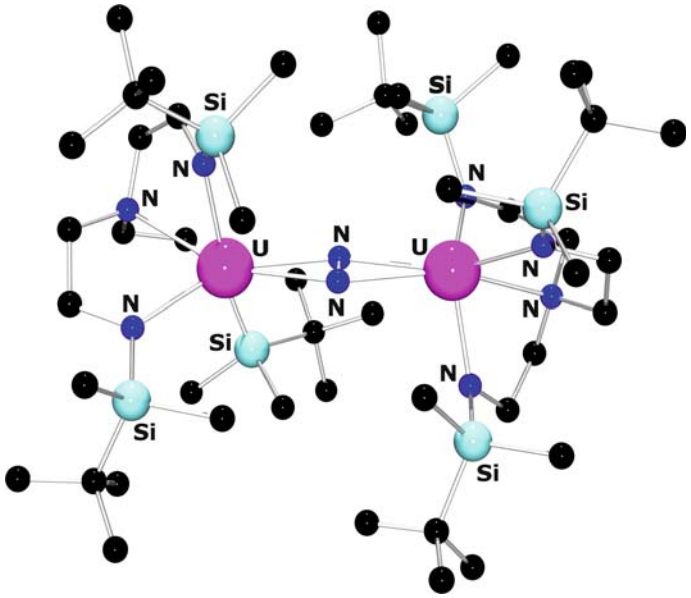

Fig. 41 Molecular structure of $[(U(NN'_3))_2\{\mu_2,\eta^2,\eta^2\text{-}N_2\}]$. Hydrogen atoms omitted for clarity

Bu]Ph)$_3$Mo(N$_2$)] is more efficiently trapped by [(N[R]Ar)$_3$U(THF)] than by another equivalent of [Mo(N[*t*-Bu]Ph)$_3$]. Inspection by infrared spectroscopy did not produce an obvious stretch for the dinitrogen ligand. However, synthesis with $^{15}N_2$ revealed a $\nu_{(NN)}$ stretch at 1547 cm^{-1}. The lack of a band for the $^{14}N_2$ isotopomer was attributed to overlap with prominent amide aryl ring $\nu_{(CC)}$ stretching modes. Crystallographic analysis revealed an N–N distance of 1.232(11) Å (Fig. 42). The shorter distance between the dinitrogen fragment and the uranium center, 2.220(9) Å, is indicative of some degree of multiple bonding between the two, since the three U–N(*amide*) distances are longer, averaging 2.254 Å.

Gambarotta et al. demonstrated dinitrogen cleavage by treating the starting complex [(Et$_8$-calix[4]tetrapyrrole)U(dme)][K(dme)] (dme = 1,2-dimethoxyethane) with an equivalent of potassium naphthalenide in dme [118]. The result is a mixed-valent μ-nitrido U$^{V/IV}$ complex, which is the product of full dinitrogen cleavage (Fig. 43). The formulation of a pentavalent uranium center was supported by the near-IR spectrum, which displays the characteristic absorption at 1247 nm [119], and supports the formulation of two chemically distinct metal centers. Repeating the reaction in the presence of $^{15}N_2$ forms the isotopically labeled complex, which has a distinct hyperfine split EPR spectrum (14 lines) from the ^{14}N congener. The complex is paramagnetic with a magnetic moment of 3.41 μB (23 °C) per dimeric unit, which is lower than expected. The value of the magnetic moment drops with tem-

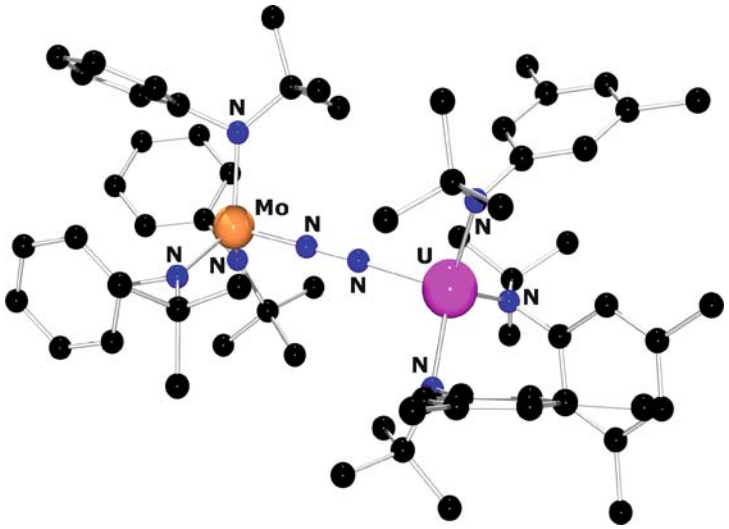

Fig. 42 Molecular structure of $[(N[t\text{-Bu}]Ar)_3U\{\mu_2,\eta^1,\eta^1\text{-}N_2\}Mo(N[t\text{-Bu}]Ph)_3]$. Hydrogen atoms omitted for clarity

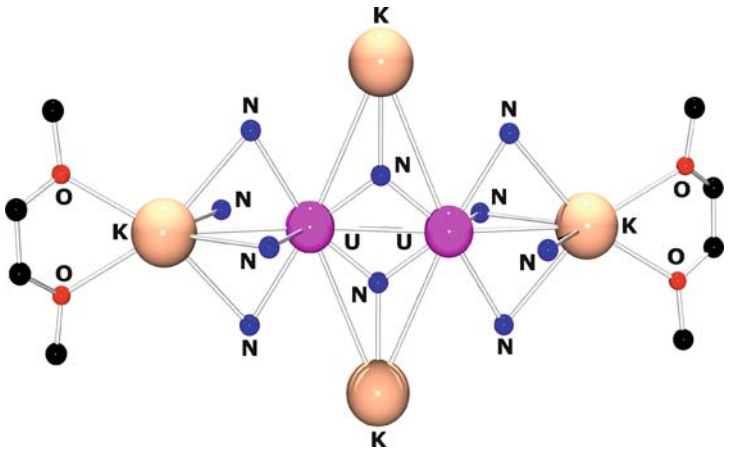

Fig. 43 Molecular structure of $[(Et_8\text{-calix[4]tetrapyrrole})U(dme)]_2(\mu\text{-}N_2)[K(dme)]$. Hydrogen and selected carbon atoms omitted for clarity

perature to 1.91 μB at 2.5 K, with a flex around 10 K that could indicate the presence of substantial antiferromagnetic coupling or superexchange.

A previously discussed uranium pentalene complex, $[(\eta^5\text{-Cp}^*)(\eta^8\text{-}C_8H_4(Si^iPr_3\text{-}1,4)_2)U]$, activates dinitrogen to form the side-on coordinated dinitrogen compound $[(\eta^5\text{-Cp}^*)(\eta^8\text{-}C_8H_4(Si^iPr_3\text{-}1,4)_2)U]_2\{\mu_2,\eta^2,\eta^2\text{-}N_2\}$. Crystallography of the green-black crystals reveals an N1–N2 bond length of 1.232(10) Å, consistent with an N–N double bond (Fig. 44) [120]. In the for-

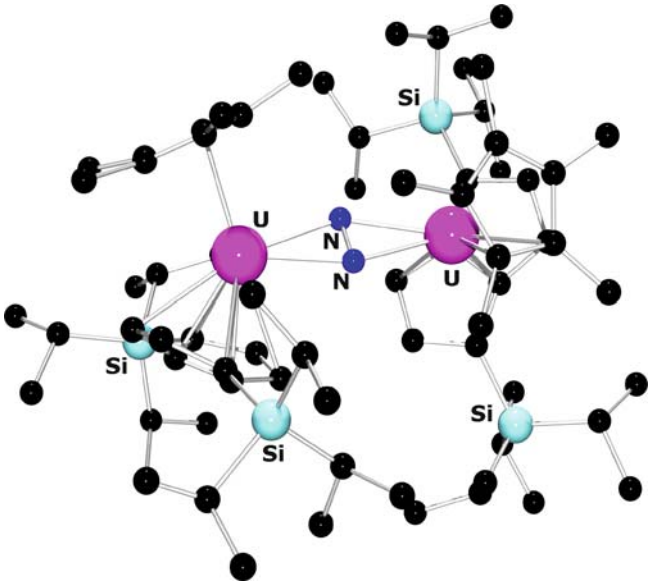

Fig. 44 Molecular structure of $[(\eta^5\text{-Cp}^*)(\eta^8\text{-C}_8\text{H}_4(\text{Si}^i\text{Pr}_3\text{-1,4})_2)\text{U}]_2\{\mu_2,\eta^2,\eta^2\text{-N}_2\}$. Hydrogen atoms omitted for clarity

mation of this molecule, two uranium(III) centers each donate an electron to reduce the dinitrogen ligand. Interestingly, this dinitrogen coordination is reversible, as N_2 is readily lost in both solution and the solid state.

Dinitrogen's isoelectronic counterpart, carbon monoxide, is a polar molecule, and its coordination and activation should be much more facile. However, activation of carbon monoxide has rarely been studied with uranium coordination complexes. Recently, the first example of a CO-bridged diuranium complex was reported. Addition of CO to a pentane solution of $[((^{t\text{Bu}}\text{ArO})_3\text{tacn})\text{U}]$ to CO (1 atm) produced a gradual color change from red-brown to light brown [121]. Evaporation of the solvent and recrystallization from benzene afforded brown hexagonal crystals of the diuranium species $[(((^{t\text{Bu}}\text{ArO})_3\text{tacn})\text{U})_2\{\mu_2,\eta^1,\eta^1\text{-CO}\}]$ (Fig. 45). Infrared spectroscopy reveals a band at 2092 cm^{-1} (Nujol), suggesting a two-coordinate CO molecule. X-ray diffraction revealed the bridging end-on ($\mu^2 : \eta^1, \eta^1$-CO) coordination mode of CO between the uranium centers. The molecule was modeled as an unsymmetrical U–CO–U entity, with one short U–C bond and a longer U–O isocarbonyl interaction, disordered on two positions at the inversion center. The structure is of limited resolution, resulting in unreliable bond distances for the bridging CO ligand. The average U–O(ArO) and U–N(tacn) distances were determined to be 2.185(5) and 2.676(4) Å, respectively, typical for this ligand system. Based on structural parameters, the complex is assigned as a mixed-valent U(III/IV) species, with an average oxidation state of +3.5. The

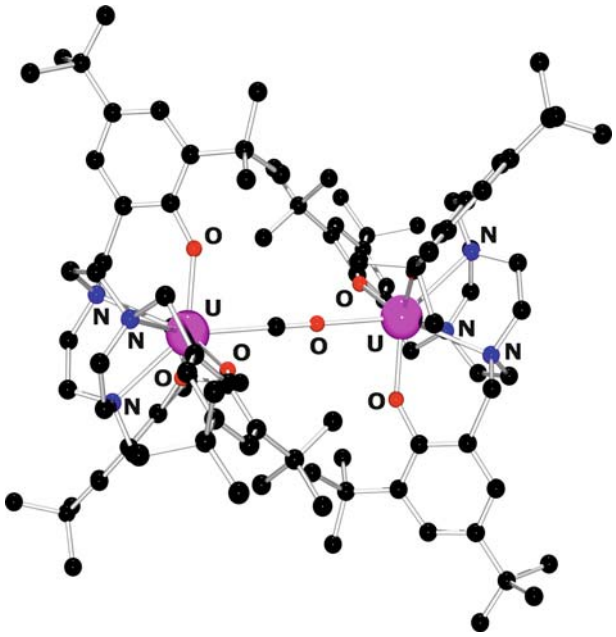

Fig. 45 Molecular structure of $[(((^{tBu}ArO)_3tacn)U)_2\{\mu_2,\eta^1,\eta^1\text{-}CO\}]$. Hydrogen atoms omitted for clarity

formation of this compound is believed to occur via nucleophilic attack of a charge-separated $[((^{tBu}ArO)_3tacn)U(IV)\text{-}CO^{\bullet -}]$ fragment on the coordinatively unsaturated U(III) of $[((^{tBu}ArO)_3tacn)U]$.

Addition of carbon dioxide to the same U(III) starting material produces an interesting reaction as well [121]. In this case, the *tert*-butyl derivatized aryloxide functionalized triazacyclononane uranium(III) complex, $[((^{tBu}ArO)_3tacn)U]$, performs a one-electron reduction of carbon dioxide to release carbon monoxide and produce a bridging μ-oxo species, $[((^{tBu}ArO)_3tacn)U]_2(\mu\text{-}O)$. Additionally, the release of carbon monoxide was confirmed crystallographically, as this small molecule is trapped by the highly reactive uranium(III) starting material to yield the previously mentioned bridging end-on $[(((t\text{BuArO})_3tacn)U)_2\{\mu_2,\eta^1,\eta^1\text{-}CO\}]$. Substituting the *ortho tert*-butyl substituent on the aryloxide ring for a more sterically bulky adamantyl group changes the reactivity drastically.

Using the more bulky ligand set, the U(III) starting material $[((^{Ad}ArO)_3$ tacn)U] was synthesized. Addition of even small amounts of carbon dioxide gas allowed the synthesis and isolation of a uranium–carbon dioxide complex [28]. This compound features an unprecedented η^1-O bound, linear CO_2 ligand. Not only is this the first example of a uranium coordination compound with a linear CO_2 ligand, but it is the first crystallographic evidence for coordination of carbon dioxide to any metal in this way. The

carbon dioxide complex [((^{Ad}ArO)$_3$tacn)U(η^1-OCO)] had a vibrational band at 2188 cm^{-1} in the infrared spectrum, indicative of a coordinated and activated CO_2 ligand. Isotopically labeled $^{13}CO_2$ gas produced a shift in the band to 2128 cm^{-1}. Crystallographic analysis (Fig. 46) of colorless crystals confirmed the linear end-on coordination, and revealed a U–O bond length of 2.351(3) Å. The neighboring C–O bond length is 1.122(4) Å and the terminal C–O bond length is 1.277(4) Å. Both the U–O–C and O–C–O angles (171.1(2)° and 178.0(3)°, respectively) are close to linear. The solid-state magnetic moment of the uranium CO_2 complex is 2.89 μB at 300 K, and slowly decreases with decreasing temperatures to 2.6 μB at 100 K. Below 100 K, μ_{eff} decreases rapidly, reaching a value of 1.51 μB at 5 K. A closed shell U(IV) compound would have a low T moment of approximately 0.5 μB. However, the increased moment of this complex at low temperature supports the formulation of the CO_2 fragment as an open shell radical anion. Electronic absorption spectroscopy of this compound revealed weak absorption bands over the entire visible and NIR region assigned to f–f transitions. Taken together, the crystallographic and spectroscopic analyses of this complex are consistent with a formulation of [((^{Ad}ArO)$_3$tacn)U(η^1-OCO)] as a charge separated uranium(IV) species, [U^+–$L^{\bullet-}$], with a radical anion centered on the carbon dioxide ligand [28]. The ability to form a stable charge separated species is unique to uranium, and indicates that this behavior may be important for stabilizing reactive intermediates in uranium-mediated reactions.

Uranium complexes have also shown unprecedented reactivity with carbon monoxide. Addition of carbon monoxide to [(COT)(Cp*)U(THF)] [122] produced a dimeric $C_3O_3^{2-}$ deltate uranium complex, [{(η^5-Cp*)(η^8-COT)U}$_2$

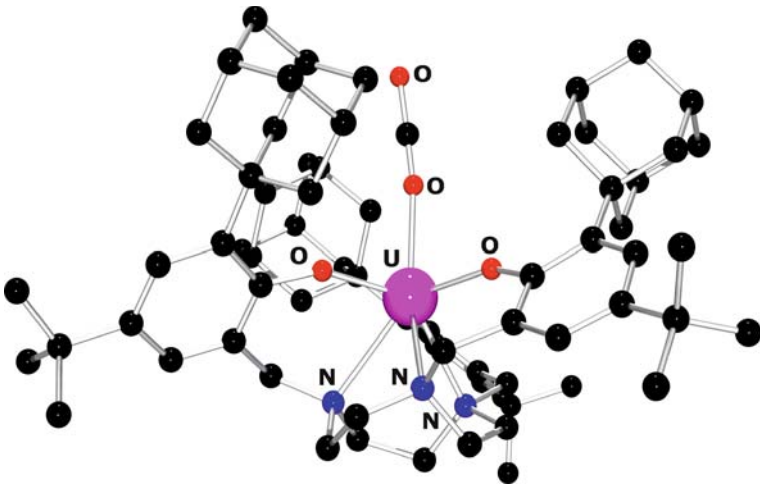

Fig. 46 Molecular structure of [((^{Ad}ArO)$_3$tacn)U](η^1-OCO). Hydrogen atoms omitted for clarity

(μ_2,η^1,η^2-C_3O_3)], made up of two uranium(IV) centers and a planar core. This compound was characterized by X-ray diffraction to confirm the core, and shows that one uranium atom is displaced by 0.0906 Å above the deltate plane, while the other is 0.1747 Å below (Fig. 47). The C–O bond distances in the core are intermediate of single and double bonds, and there are two short C–C distances and one longer one. The longer bond interacts with the uranium via an agostic interaction, which is confirmed by DFT calculations. This interaction rapidly interconverts between the uranium centers on the NMR timescale, causing a C_3 symmetric spectrum at RT. Computation supports that each U is best described as having two electrons localized in 5*f* orbitals, consistent with the U(IV) formulation. The ancillary COT and Cp ligands bind to the U centers as predicted, with a π interaction between U and Cp and a δ interaction between U and COT. Decorating the COT ring with two $^{i}Pr_3Si$ groups and substituting Cp* with Cp^{Me4} provided access to the corresponding red dimeric squarate derivative [29]. This molecule is similar in that the squarate anion is suspended between two U(IV) centers; however, in this case the stabilizing agostic interaction is absent. This is presumably due to the smaller O–C–C angle, which induces bonding to the uranium through only the oxygen atoms. Again, the organic core is planar, but this time the deviation of the uranium centers is much more pronounced; they are situated above and below the core by 0.429 Å.

Because the 5*f* orbitals of actinide ions are more diffuse than the 4*f* orbitals of the lanthanides, actinides have the potential for stronger magnetic coupling via superexchange [123]. Recently, magnetic exchange in uranium complexes has been studied by synthesis of a series of mixed metal halide-bridged 5*f*–3*d* cluster complexes of the form [(cyclam)M[(μ-Cl)U($Me_2Pz)_4]_2$] (M=Ni, Cu, Zn; cyclam = 1,4,8,11-tetraazacyclotetradecane) (Fig. 48). These are the first examples of halide-bridged species involving uranium(IV) and transition metal ions [124]. The central transition metal has

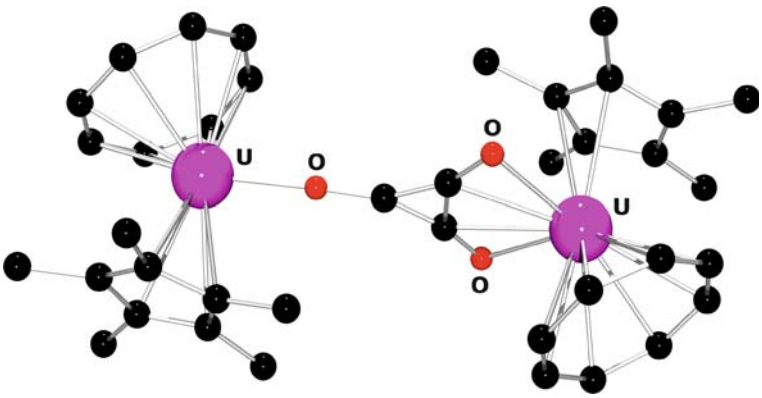

Fig. 47 Molecular structure of [{(η^5-Cp*)(η^8-COT)U}$_2$(μ_2,η^1,η^2-C_3O_3)]. Hydrogen atoms omitted for clarity

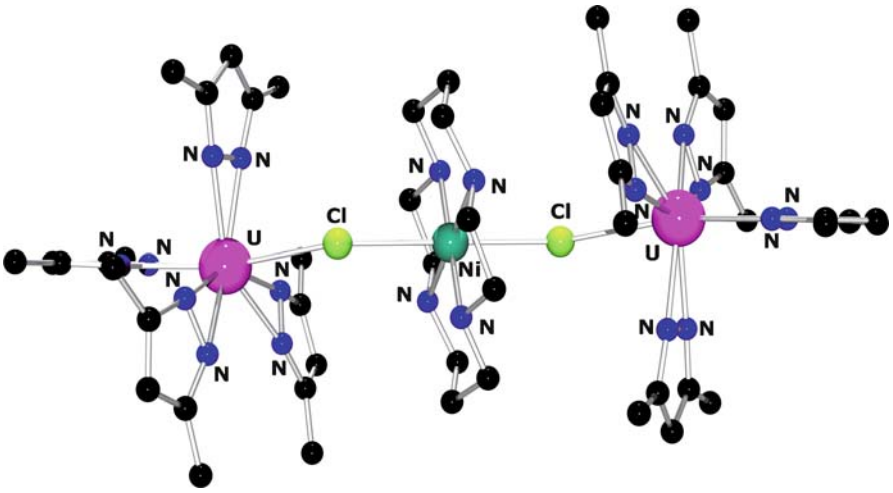

Fig. 48 Molecular structure of [(cyclam)Ni[(μ-Cl)U($Me_2Pz)_4]_2$]. Hydrogen atoms omitted for clarity

a linear coordination geometry, and forms a chloride-bridged cluster with the uranium centers. The U–Cl–M angle and U(IV) coordination environment vary little as M changes. The species containing the diamagnetic Zn(II) ion is used as a model to account for the U(IV) contributions to the magnetism of the other clusters. Subtracting the Zn data from those obtained for the copper cluster, [(cyclam)Cu[(μ-Cl)U($Me_2Pz)_4]_2$], reveals a copper center with no magnetic exchange coupling and a slightly lower than expected magnetic moment (1.70(4) μB). The nickel dimer, however, does show magnetic data consistent with the presence of ferromagnetic exchange interactions, indicated by a dip in magnetic moment at 30 K (1.26 emuK/mol). This is most likely due to the loss of U(IV) spin, but probably also from a zero-field splitting contribution to the ground state. The data above 40 K were then fitted and produced a TIP = 8.25×10^{-4} emu/mol. This represents the first estimate of a $5f$–$3d$ coupling constant within a molecular complex. The spin-containing orbitals were determined by DFT, and found to be $5f(xyz)$ and $5f(z(x^2 - y^2))$, which both exhibit δ symmetry with respect to the U–Cl bond. These are orthogonal to the Ni(II) $3d(z^2)$ spin feeding through σ-type Cl orbitals. Thus, the observed ferromagnetic coupling is consistent with a simple superexchange mechanism [124].

The uranyl ion is the longest known and most thoroughly studied uranium complex. Despite this fact, imido analogues of the uranyl derivative have remained elusive until recently, as the *trans* configuration of the imido ligands is disfavored. In 2005, the first imido derivative was synthesized by addition of *tert*-butylamine and iodine to uranium turnings in the presence of THF, creating the orange *trans*-diimide complex with two *cis*-THFs

and two *cis*-iodide ligands (Fig. 49) [125]. Crystallographic analysis reveals short U=N distances averaging 1.84 Å. A similar complex is created by the addition of aniline to $[UI_3(THF)_4]$. However, in this case, the resulting uranium(VI) complex has one additional THF ligand, which is coordinated in between the two *cis*-iodide ligands. This complex has similar crystallographic parameters, with an average U=N distance of 1.85 Å. The THF molecules in both bis-imido derivatives undergo ligand exchange with neutral donors such as aniline to form $[U(N^tBu)_2I_2(NH_2Ph)_2]$. However, trace amounts of water to this complex resulted in the mixed uranium oxo-imido complex $[U(N^tBu)(O)I_2(THF)(NH_2Ph)_2]$ [126]. The U–O bond length of 1.781(4) Å is comparable to those found in the uranyl ion, and the U=N(imido) bond length of 1.823(4) Å is similar to that of the bis-imido derivatives. The similar compound $[U(N^tBu)(O)I_2(THF)_2]$ was prepared by addition of an equivalent of $B(C_6F_5)_3^*H_2O$ to $[U(N^tBu)_2I_2(THF)_2]$. Infrared spectroscopy of this compound reveals a U–O stretch at 883 cm^{-1}, which shifts to 827 cm^{-1} for the ^{18}O isotopologue. This product undergoes ligand substitution with tppo to form $[U(N^tBu)(O)I_2(Ph_3PO)_2]$. X-ray crystallography of this complex shows similar bond distances to the aniline derivative. The infrared spectrum of a KBr pellet of the tppo derivative exhibits a band at 858 cm^{-1} (U–O), as well as bands at 1128 and 1134 cm^{-1} (U–N vibrations and the assignments were confirmed by calculation). DFT geometry optimizations of both the aniline and tppo derivatives show two π-bonding orbitals involved in the U–O bond which have a larger component of *d* character, while in the U–N bond the uranium *f* orbitals play a larger role. Because the symmetry of the mixed oxo-imido is less than the bis(imido) system, these M–L multiple bonding interactions have been demonstrated to be more ionic in nature.

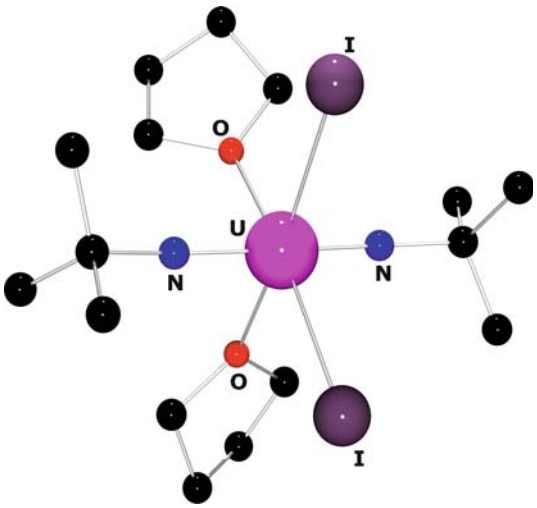

Fig. 49 Molecular structure of $[U(N^tBu)_2I_2(THF)_2]$. Hydrogen atoms omitted for clarity

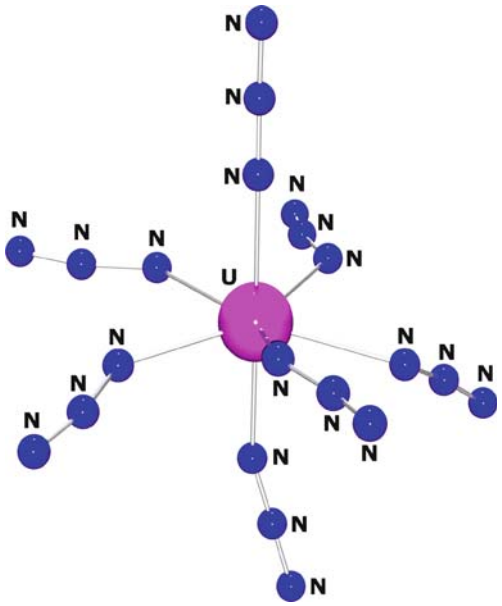

Fig. 50 Molecular structure of $[(Bu_4N)_3][U(N_3)_7]$. Cation omitted for clarity

Recently, a homoleptic uranium azide anion, UN_{21}^{3-}, was reported [127]. Addition of Bu_4NBr and seven equivalents of AgN_3 to $[(Bu_4N)_2][UCl_6]$ in acetonitrile resulted in a color change from pale green to emerald green. Stirring for 12 h followed by isolation produced dark green crystals of the product, $[(Bu_4N)_3][U(N_3)_7]$ (Fig. 50). Analysis by X-ray crystallography showed a seven-coordinate uranium center in a monocapped octahedral geometry. The U–N bond lengths range from 2.32(2) to 2.40(2) Å. A better quality structure was obtained by changing the reaction and crystallization solvents from CH_3CN to CH_3CH_2CN. This structure showed the uranium center has a pentagonal bipyramidal geometry, with U–N bond lengths ranging from 2.323(6) to 2.431(7) Å. The N_α–N_β bond lengths range from 1.162(8) to 1.246(9) Å, and are longer than the corresponding N_β–N_γ bond lengths of 1.055(8)–1.150(7) Å. The angles within the five equatorial azide ligands deviate from linearity, with angles ranging from 164(1) to 168.1(8)°, while those in the apical positions have angles of 179.5(7) and 178.9(9)° [127].

8 Closing Remarks

The work presented here demonstrates the great variety of ligands and coordination modes that have already been studied with uranium. Despite that fact, there is so much still to be learned about the ability of uranium to

coordinate organic ligands, activate small molecules, and perform catalytic chemistry. This review presents just a few examples of the unprecedented chemistry already being studied. The size and highly reducing nature of uranium compared to transition metals promise that this actinide will play an important role in making an impact on modern society.

References

1. Ephritikhine M (2006) Dalton Trans, p 2501
2. Sessler JL, Melfi PJ, Pantos GD (2006) Coord Chem Rev 250:816
3. Szabo Z, Toraishi T, Vallet V, Grenthe I (2006) Coord Chem Rev 250:784
4. Van Horn JD, Huang H (2006) Coord Chem Rev 250:765
5. Cotton SA (2005) Annu Rep Prog Chem Sect A Inorg Chem 101:294
6. Cotton SA (2004) Annu Rep Prog Chem Sect A Inorg Chem 100:303
7. Castro-Rodriguez I, Meyer K (2006) Chem Commun, p 1353
8. Korobkov I, Gambarotta S (2005) Prog Inorg Chem 54:321
9. Clark D, Sattelberger AP, Bott SG, Vrtis RN (1989) Inorg Chem 28:1771
10. Avens LR, Bott SG, Clark DL, Sattelberger AP, Watkin JG, Zwick BD (1994) Inorg Chem 33:2248
11. Clark D, Sattelberger AP, Andersen RA (1997) Inorg Synth 31:307
12. Evans WJ, Kozimor SA, Ziller JW, Fagin AA, Bochkarev MN (2005) Inorg Chem 44:3993
13. Katz JJ, Rabinowitch E (1951) The chemistry of uranium, part 1. McGraw-Hill, New York
14. Berthet J-C, Lance M, Nierlich M, Ephritikhine M (1999) Eur J Inorg Chem, p 2005
15. Andersen R (1979) Inorg Chem 18:1507
16. Stewart JL, Andersen RA (1998) Polyhedron 17:953
17. Enriquez A, Matonic JH, Scott BL, Neu MP (2003) Chem Commun, p 1892
18. Riviere C, Nierlich M, Ephritikhine M, Madic C (2001) Inorg Chem 40:4428
19. Natrajan L, Mazzanti M, Bezombes J-P, Pecaut J (2005) Inorg Chem 44:6115
20. Hermann J, Suttle JF, Hoekstra HR (1957) Inorg Synth 5:143
21. Bagnall K, Brown D, Jones PJ, Du Preesz GH (1965) J Chem Soc, p 350
22. Berthet J-C, Thuery P, Ephritikhine M (2005) Inorg Chem 44:1142
23. Enriquez AE, Scott BL, Neu MP (2005) Inorg Chem 44:7403
24. Schlesinger H, Brown HC (1953) J Am Chem Soc 75:219
25. Berthet J-C, Nierlich M, Ephritikhine M (2002) Eur J Inorg Chem, p 850
26. Berthet J-C, Lance M, Nierlich M, Ephritikhine M (2000) Eur J Inorg Chem, p 1969
27. Pool JA, Lobkovsky E, Chirik PJ (2004) Nature 427:527
28. Castro-Rodriguez I, Nakai H, Zakharov LN, Rheingold AL, Meyer K (2004) Science 305:1757
29. Summerscales OT, Cloke FGN, Hitchcock PB, Green JC, Hazari N (2006) J Am Chem Soc 128:9602
30. Odom AL, Arnold PL, Cummins CC (1998) J Am Chem Soc 120:5836
31. Van der Sluys W, Burns CJ, Huffman JC, Sattelberger AP (1988) J Am Chem Soc 110:5924
32. Hahn JLC, Nasluzov VA, Neyman KM, Roesch N (1997) Inorg Chem 36:3947
33. Stubbert BD, Marks TJ (2007) J Am Chem Soc 129:4253
34. Avdeef A, Raymond KN, Hodgson KO, Zalkin A (1972) Inorg Chem 11:1083

35. Streitwieser A Jr, Müller-Westerhoff U (1968) J Am Chem Soc 90:7364
36. Cloke FGN, Green JC, Jardine CN (1999) Organometallics 18:1080
37. Amoroso AJ, Jeffery JC, Jones PL, McCleverty JA, Rees L, Rheingold AL, Sun Y, Takats J, Trofimenko S et al. (1995) Chem Commun, p 1881
38. Maria L, Domingos A, Santos I (2001) Inorg Chem 40:6863
39. Carvalho A, Domingos A, Gaspar P, Marques N, Pires de Matos A, Santos I (1992) Polyhedron 11:1481–1488
40. Sun Y, Day VW, Eberspacher TA (1995) Inorg Chim Acta 229:315
41. Maria L, Campello MP, Domingos A, Santos I, Andersen R (1999) Dalton Trans, p 2015
42. Castro-Rodriguez I, Olsen K, Gantzel P, Meyer K (2003) J Am Chem Soc 125:4565
43. Castro-Rodriguez I, Olsen K, Gantzel P, Meyer K (2002) Chem Commun, p 2764
44. Castro-Rodriguez I, Meyer K (2003) AIP Conf Proc 673:241
45. Nakai H, Hu X, Zakharov LN, Rheingold AL, Meyer K (2004) Inorg Chem 43:855
46. Monteiro B, Roitershtein D, Ferreira H, Ascenso JR, Martins AM, Domingos A, Marques N (2003) Inorg Chem 42:4223
47. Karmazin l, Mazzanti M, Pecaut J (2002) Chem Commun, p 654
48. Denning RG (1983) In: Gmelin Handbook of Inorganic Chemistry, vol A6. Springer, New York, p 31
49. Zazhogin AA, Lutz HD, Komyak AI (1999) J Mol Struct 482–483:189
50. Berthet J-C, Nierlich M, Ephritikhine M (2003) Angew Chem Int Ed 42:1952
51. Berthet J-C, Nierlich M, Ephritikhine M (2003) Chem Commun, p 1660
52. Berthet J-C, Nierlich M, Ephritikhine M (2004) Dalton Trans, p 2814
53. Caira M, De Wet JF, Du Preez JGH, Busch B, Rohwer HL (1983) Inorg Chim Acta 77:L73
54. Kannan S, Moody MA, Barnes CL, Duval PB (2006) Inorg Chem 45:9206
55. John G, May I, Sarsfield MJ, Steele HM, Collison D, Helliwell M, McKinney JD (2004) Dalton Trans, p 734
56. John GH, May I, Sharrad CA, Sutton AD, Collison D, Helliwell M, Sarsfield MJ (2005) Inorg Chem 44:7606
57. Thuery P (2007) Inorg Chem 46:2307
58. Pasilis SP, Pemberton JE (2003) Inorg Chem 42:6793
59. Thuery P (2006) Chem Commun, p 853
60. Gutowski KE, Cocalia VA, Griffin ST, Bridges NJ, Dixon DA, Rogers RD (2007) J Am Chem Soc 129:526
61. Bradley AE, Hardacre C, Nieuwenhuyzen M, Pitner WR, Sanders D, Seddon KR, Thied RC (2004) Inorg Chem 43:2503
62. Sah A, Rao CP, Saarenketo PK, Wegelius EK, Kolehmainen E, Rissanen K (2001) Eur J Inorg Chem, p 2773
63. Wilkerson M, Burns CJ, Morris DE, Paine RT, Scott BL (2002) Inorg Chem 41:3110
64. Sarsfield M, Steele H, Helliwell M, Teat SJ (2003) Dalton Trans, p 3443
65. Crawford M-J, Mayer P, Noeth H, Suter M (2004) Inorg Chem 43:6860
66. Straka M, Patschke M, Pyykkoe P (2003) Theor Chem Acc 109:332
67. Bombieri G, Forsellini E, De Paoli G, Brown D, Tso TC (1979) Dalton Trans, p 2042
68. Williams VC, Mueller M, Leech MA, Denning RG, Green MLH (2000) Inorg Chem 39:2538
69. Kannan S, Chetty KV, Venugopal V, Drew MGB (2004) Dalton Trans, p 3604
70. Oldham W Jr, Oldham SM, Scott BL, Abney KD, Smith WH, Costa DA (2001) Chem Commun, p 1348
71. Bombieri G, Forsellini E, Day JP, Azeez WI (1978) J Chem Soc Dalton Trans, p 677

72. Akona SB, Fawcett J, Holloway JH, Russell DR (1991) Acta Crystallogr Sect C 47:45
73. Alcock N, de Meester P, Kemp TJ (1979) J Chem Soc Perkin Trans 2, p 921
74. Sarsfield M, Helliwell M, Collison D (2002) Chem Commun, p 2264
75. Mungur S, Liddle ST, Wilson C, Sarsfield MJ, Arnold PL (2004) Chem Commun, p 2738
76. Arnold P, Blake AJ, Wilson C (2005) Chem Eur J 11:6095
77. Rao P, Rao CP, Sreedhara A, Wegelius EK, Rissanen K, Kolehmainen E (2000) Dalton Trans, p 1213
78. Takao K, Ikeda Y (2007) Inorg Chem 46:1550
79. Burdet F, Pecaut J, Mazzanti M (2006) J Am Chem Soc 128:16512
80. Evans WJ, Kozimor SA, Ziller JW (2005) Science 309:1835
81. Meyer K, Mindiola DJ, Baker TA, Davis WM, Cummins CC (2000) Angew Chem Int Ed 39:3063
82. Mindiola DJ, Tsai Y-C, Hara R, Chen Q, Meyer K, Cummins CC (2001) Chem Commun, p 125
83. Rosen R (1989) Report, p 251
84. Cramer RE, Edelmann F, Mori AL, Roth S, Gilje JW, Tatsumi K, Nakamura A (1988) Organometallics 7:841
85. Brennan JG, Andersen RA (1985) J Am Chem Soc 107:514
86. Roussel P, Boaretto R, Kingsley AJ, Alcock NW, Scott P (2002) Dalton Trans, p 1423
87. Castro-Rodriguez I, Nakai H, Meyer K (2006) Angew Chem Int Ed 45:2389
88. Pugh D, Wright JA, Freeman S, Danopoulos AA (2006) Dalton Trans, p 775
89. Evans W, Kozimor SA, Ziller JW (2004) Polyhedron 23:2689
90. Edwards P, Andersen RA, Zalkin A (1984) Organometallics 3:293
91. Edwards P, Andersen RA, Zalkin A (1987) J Chem Soc Chem Commun, p 1846
92. Lukens WW Jr, Beshouri SM, Blosch LL, Stuart AL, Andersen RA (1999) Organometallics 18:1235
93. Jantunen KC, Batchelor RJ, Leznoff DB (2004) Organometallics 23:2186
94. Diaconescu PL, Odom AL, Agapie T, Cummins CC (2001) Organometallics 20:4993
95. Diaconescu PL, Arnold PL, Baker TA, Mindiola DJ, Cummins CC (2000) J Am Chem Soc 122:6108
96. Villiers C, Thuery P, Ephritikhine M (2006) Chem Commun, p 392
97. Mueller M, Williams VC, Doerrer LH, Leech MA, Mason SA, Green MLH, Prout K (1998) Inorg Chem 37:1315
98. Kohlmann H, Beck HP (1997) Z Anorg Allg Chem, p 785
99. Arliguie T, Doux M, Mezailles N, Thuery P, Le Floch P, Ephritikhine M (2006) Inorg Chem 45:9907
100. Arliguie T, Fourmigue M, Ephritikhine M (2000) Organometallics 19:109
101. Belkhiri L, Arliguie T, Thuery P, Fourmigue M, Boucekkine A, Ephritikhine M (2006) Organometallics 25:2782
102. Arliguie T, Thuery P, Fourmigue M, Ephritikhine M (2003) Organometallics 22:3000
103. Roger M, Arliguie T, Thuery P, Fourmigue M, Ephritikhine M (2005) Inorg Chem 44:594
104. Roger M, Barros N, Arliguie T, Thuery P, Maron L, Ephritikhine M (2006) J Am Chem Soc 128:8790
105. Gaunt AJ, Scott BL, Neu MP (2005) Chem Commun, p 3215
106. Gaunt AJ, Scott BL, Neu MP (2006) Angew Chem Int Ed 45:1638
107. Gaunt AJ, Scott BL, Neu MP (2006) Inorg Chem 45:7401
108. Danopoulos A, Hankin DM, Cafferkey SM, Hursthouse MB (2000) Dalton Trans, p 1613

109. Hankin D, Danopoulos AA, Wilkinson G, Sweet TKN, Hursthouse MB (1996) J Chem Soc Dalton Trans, p 1309
110. Le Borgne T, Riviere E, Marrot J, Girerd J-J, Ephritikhine M (2000) Angew Chem Int Ed 39:1647
111. Salmon L, Thuery P, Riviere E, Girerd J-J, Ephritikhine M (2003) Chem Commun, p 762
112. Borgne T, Riviere E, Marrot J, Thuery P, Girerd J-J, Ephritikhine M (2002) Chem Eur J 8:773
113. Salmon L, Thuery P, Riviere E, Ephritikhine M (2006) Inorg Chem 45:83
114. Evans WJ, Nyce GW, Greci MA, Ziller JW (2001) Inorg Chem 40:6725
115. Bucaille A, Le Borgne T, Ephritikhine M, Daran J-C (2000) Organometallics 19:4912
116. Monreal MJ, Carver CT, Diaconescu PL (2007) Inorg Chem 46:7226
117. Roussel P, Scott P (1998) J Am Chem Soc 120:1070
118. Korobkov I, Gambarotta S, Yap GPA (2002) Angew Chem Int Ed 41:3433
119. Arney DSJ, Burns CJ (1993) J Am Chem Soc 115:9840
120. Cloke FGN, Hitchcock PB (2002) J Am Chem Soc 124:9352
121. Castro-Rodriguez I, Meyer K (2005) J Am Chem Soc 127:11242
122. Summerscales OT, Cloke FGN, Hitchcock PB, Green JC, Hazari N (2006) Science 311:829
123. Crosswhite H, Crosswhite H, Carnall WT, Paszek AP (1980) J Chem Phys 72:5103
124. Kozimor SA, Bartlett BM, Rinehart JD, Long JR (2007) J Am Chem Soc 129:10672
125. Hayton TW, Boncella JM, Scott BL, Palmer PD, Batista ER, Hay PJ (2005) Science 310:1941
126. Hayton TW, Boncella JM, Scott BL, Batista ER (2006) J Am Chem Soc 128:12622
127. Crawford M-J, Ellern A, Mayer P (2005) Angew Chem Int Ed 44:7874

Author Index Volumes 101–130

Author Index Vols. 1–100 see Vol. 100

The volume numbers are printed in italics

Subject Index